UNITED STATES DEPARTMENT OF THE INTERIOR

GEOLOGICAL SURVEY

Structural geology and petrology of a part of the Bitterroot lobe of the Idaho batholith, Idaho County, Idaho, and Missoula and Ravalli Counties, Montana

By

Rolland R. Reid[1]

Prepared in cooperation with the Idaho Bureau of Mines and Geology
Open-File Report 84-517

This report is preliminary and has not been reviewed for conformity with U.S. Geological Survey editorial standards and stratigraphic nomenclature.

[1]Present address
University of Idaho
Moscow, Idaho

1984

TABLE OF CONTENTS

	Page
Abstract	1
Introduction	1
Previous work	1
Wall rock southwest of the batholith	2
Structure	2
Calc-silicate gneiss and pelitic metamorphic rock	2
Tonalitic gneiss and associated trondhjemite	14
Petrography of the wall rocks	14
Tonalite of the southwestern batholith	27
Structure	27
Migmatite screens	35
Petrography of the tonalite	43
Joints	44
Granite, granodiorite, and related rocks	44
The western sector	44
Structure	44
Granitic rocks	44
Migmatite	52
Foliation	52
Shear joints	52
Secondary joints	52
Petrography	52
Granite	52
Granodiorite	62
Quartz monzonite	63
Quartz monzodiorite	63
Tonalite	63
Migmatite	63
Xenoliths	64
Pegmatite suite	64
Blastomylonite	65
Microbreccia	65
The central sector	65
Structure	65
Granitic rocks	65
Foliation	65
Quartz diorite	65
Fine-grained dikes	67
Pegmatite suite	67
Blastomylonite	67
Mylonite	67
Mylonitic shear joints	67
Mineralized shear joints	67
Secondary joints	73
Petrography	73
Granite	73
Granodiorite	73
Quartz monzonite	79
Quartz diorite	79
Xenoliths	79
Fine-grained dikes	80
Pegmatite suite	80
Blastomylonite	81
Mylonite	81
Mylonitic shear joints	81
Mineralized shear joints	81
The eastern sector	81
Structure	81
Granitic rocks	81
Foliation	81
Anorthosite I	87
Schlieren	87
Ductile shears	87
Xenoliths	87
Fine-grained dikes	87
Pegmatite suite	87
Blastomylonite	87
Mylonite	89
Mineralized shear joints	89
Secondary fractures	89
Petrography	89

TABLE OF CONTENTS (continued)

	Page
Granite	89
Granodiorite	98
Tonalite	99
Quartz diorite	99
Anorthosite I	99
Xenoliths	100
Fine-grained dikes	100
Pegmatite suite	100
Anorthosite II	100
General structure	100
Tertiary hypabyssal rocks	101
Andesite to quartz latite	101
Rhyolite	101
Tertiary(?) granodiorite and quartz diorite	101
Petrology and structure of the wall rocks	101
Petrology and structure of the tonalite	106
Migmatite screens of the southern zone of the western sector	108
Tertiary dikes of the southern zone of the western sector	108
Joints of the southern zone of the western sector	108
Petrology and structure of the granitic rocks	108
Magmatic features	108
Migmatite screens	110
Xenoliths	110
Secondary foliation	111
Origin of unzoned plagioclase	111
Similarity of plagioclase composition in granite and granodiorite	111
Fibrolite inclusions	111
Generation of extension fractures	111
Origin of secondary foliation	111
Migmatite involvement in the flow foliation	112
Development of Subarea B of the eastern sector	112
The Bitterroot gneissic front	112
Origin of the secondary lineation	113
Late-stage foliation	113
Combined flow symmetries	113
Tonalite to quartz diorite intrusions	113
Fine-grained dikes	113
Ductile faults	113
Pegmatite suite	114
Anorthosite II	114
Blastomylonite	114
Mylonite	115
Mineralized joints	115
Tertiary(?) dikes	115
Secondary joints and faults	115
References cited	116

ILLUSTRATIONS

Figure 1.	Poles to foliation and linear structures (minor fold axes and alined prismatic minerals) in calc-silicate gneiss in wall rocks west of the Idaho batholith in the Chimney Peak quadrangle	4
2.	Small passive-flow folds in the calc-silicate gneiss west of the Idaho batholith in the Chimney Peak quadrangle	4
3.	Vertical section and strip geologic map of the metasedimentary rocks along Selway River in the Fog Mountain quadrangle, northeastward (060° az) to the contact with the Idaho batholith	5
4.	Structural data at Stations 282-284 in figure 3, showing relation of plunging minor folds to bedding and foliation; also showing sense of rotation of minor folds close together in the outcrops	6
5.	Pegmatite injected in biotite quartzite near Station 283 of figure 3, along Selway River west of the Idaho batholith in the Fog Mountain quadrangle	6
6.	Poles to schistosity near Station 284 of figure 3, in biotite quartzite along Selway River west of the Idaho batholith in the Fog Mountain quadrangle	7
7.	Mesoscopic folding in biotite quartzite near Station 284 of figure 3, along Selway River west of the Idaho batholith in the Fog Mountain quadrangle	7
8.	Isoclinal folds with axial-plane schistosity at Station 287 of figure 3, in biotite quartzite along Selway River west of the Idaho batholith in the Fog Mountain quadrangle	8

ILLUSTRATIONS (continued)

Page

Figure 9. Helical axes of minor conical folds at Station 290 of figure 3, in biotite quartzite along Selway River west of the Idaho batholith in the Fog Mountain quadrangle..... 8
10. Details of geometry and direction of plunge in minor conical folds at Station 294 of figure 3, in biotite quartzite along Selway River west of the Idaho batholith in the Fog Mountain quadrangle..... 9
11. Details of geometry and direction of plunge of minor concentric folds at Station 295 of figure 3, in biotite quartzite along Selway River west of the Idaho batholith in the Fog Mountain quadrangle..... 10
12. Details of geometry and direction of plunge of minor concentric folds at Station 296 of figure 3, in biotite quartzite along Selway River west of the Idaho batholith in the Fog Mountain quadrangle..... 11
13. Details of geometry and plunge of a steep conical fold at Station 297 of figure 3, in biotite quartzite along Selway River west of the Idaho batholith in the Fog Mountain quadrangle..... 12
14. Poles to foliation in biotite quartzite in the Fog Mountain-Selway River subarea west of the Idaho batholith..... 13
15. Minor fold axes and mineral lineations in biotite quartzite in the Fog Mountain-Selway River subarea west of the Idaho batholith..... 15
16. Minor fold involving pegmatite; the axis is parallel to the strike line of the foliation in biotite quartzite in the Fog Mountain-Selway River subarea west of the Idaho batholith..... 15
17. Two shears in the Vermillion Peak quadrangle, non-parallel, with nearly parallel muscovite lineation and healed quartz slickensides..... 16
18. Poles to bedding and bedding-parallel schistosity and foliation in the Vermillion Peak quadrangle..... 17
19. Poles to foliation in biotite quartzite, schist, and gneiss. Fog Mountain area, south of Selway River..... 18
20. Minor fold axes, probably of both D_1 and D_2 ages (not distinguishable with certainty). Kink and crenulation fold axes of late D_2 or D_3 age, and lineations including stretched micas, hornblende, boudin axes and $\underline{s}_0/\underline{s}_1$ intersections. All from the Vermillion Peak quadrangle..... 19
21. Minor fold axes probably including both D_1 and D_2 folds, boudins and rods parallel to fold axes, mineral lineations, and kink and crenulation fold axes (probably late D_2 or D_3). Fog Mountain area south of Selway River..... 20
22. Poles of axial planes, axial-plane schistosity ($\underline{s}_2$), and axial planes of crenulation folds (probably of late D_2 or D_3 age) in the Vermillion Peak quadrangle..... 21
23. Poles to joints, to a Tertiary dike, to pegmatite dikes, to faults, and to a quartz vein in the Vermillion Peak and Fog Mountain areas south of Selway River..... 22
24. Poles to flow foliation in tonalitic gneiss west of the Idaho batholith in Chimney Peak quadrangle..... 23
25. Lineations (minor fold axes and biotite streaks) in tonalitic gneiss west of the Idaho batholith in the Chimney Peak quadrangle..... 24
26. Poles to axial planes of small folds at one locality in tonalitic gneiss west of the Idaho batholith in the Chimney Peak quadrangle..... 25
27. Small folds plunging nearly vertically, involving alaskitic trondhjemite sheets in the tonalitic gneiss west of the Idaho batholith in the Chimney Peak quadrangle..... 26
28. Varied axial-planar orientation in vertically plunging minor folds in tonalitic gneiss west of the Idaho batholith in the Chimney Peak quadrangle..... 26
29. Varied flow trends and styles in tonalitic gneiss west of the Idaho batholith in the Chimney Peak area..... 26
30. Poles to flow foliation in quartz diorite to tonalite near the western contact of the Idaho batholith in the Chimney Peak quadrangle..... 31
31. Flow lineations consisting of oriented hornblende prisms in quartz diorite to tonalite near the western contact of the Idaho batholith in the Chimney Peak quadrangle..... 32
32. Poles to pegmatite dikes in quartz diorite to tonalite of the western Idaho batholith within the Chimney Peak quadrangle..... 33
33. Poles to alaskite sheets in quartz diorite to tonalite of the western Idaho batholith within the Chimney Peak area..... 34
34. Poles to flow foliation in biotite tonalite in the Fenn Mountain quadrangle..... 36
35. Four attitudes in swirled-folded primary flow foliation at a point in the Fenn Mountain area..... 37
36. Folded flow foliation at a point in the Fenn Mountain area..... 38
37. Minor folds in primary flow foliation in tonalite in the Fenn Mountain area..... 38
38. Poles to shallow-dipping pegmatite and alaskite sheets or dikes cutting biotite tonalite in the Fenn Mountain area of the western sector..... 39

ILLUSTRATIONS (continued)

Page

Figure 39. Orientation of flow lineation in biotite tonalite in the Fenn Mountain quadrangle, western Bitterroot lobe of the Idaho batholith..... 39
40. Poles to steep-dipping pegmatite and alaskite dikes cutting biotite tonalite in the Fenn Mountain area..... 40
41. Orientation of three simultaneous branched-pegmatite dikes cutting biotite tonalite at a point in the Fenn Mountain area..... 40
42. Diagram to show "frozen" or recrystallized slickensides, microrodding, and grooving in different shear planes, one horizontal and one steeply dipping, both cutting pegmatite intruded into biotite tonalite of the Fenn Mountain area..... 41
43. Folded plagioclase-biotite gneiss septum enclosed in biotite tonalite in the Fenn Mountain area, cut by pegmatite of granitic composition..... 43
44. Poles to secondary joints in biotite tonalite of the Crags area, western sector of the Bitterroot lobe of the Idaho batholith..... 45
45. Poles to 15 shear surfaces, and to 12 with slickensides, in the Greenside Butte quadrangle, western sector of the Idaho batholith, west of Hamilton, Mont..... 46
46. Poles to blastomylonite foliation and lineation in granitic rock near the granite-tonalite contact, in the central Crags area, western sector of the Bitterroot lobe of the Idaho batholith, west of Hamilton, Mont..... 47
47. Poles to primary flow foliation and flow lineation in granite and granodiorite in the central Crags area..... 48
48. Poles to pegmatite dikes and sheets in the granitic rocks of the central Crags area, near the granite-tonalite contact..... 49
49. Poles to flow foliation in granite and granodiorite of the Greenside Butte quadrangle and two axes of folds in the flow foliation..... 50
50. Poles to mylonite schistosity and mylonite lineation in the Greenside Butte quadrangle, western sector of the Bitterroot lobe, Idaho batholith west of Hamilton, Mont..... 51
51. Poles to foliation and fold axes and rods in migmatite, near the granitic rock-tonalite contact in the central Crags area..... 53
52. Poles to foliation and mineral lineation, mostly biotite streaks, rods, and minor fold axes, in migmatite screens in the Greenside Butte quadrangle..... 54
53. Poles to flow foliation and lineation in granitic rocks of the northern zone of the western sector, Bitterroot lobe of the Idaho batholith, west of Hamilton, Mont..... 55
54. Poles to shear joints and slickensides in the shear joints in the western sector, Bitterroot lobe of the Idaho batholith, west of Hamilton, Mont..... 56
55. Poles to secondary joints in the western sector, Bitterroot lobe of the Idaho batholith, west of Hamilton, Mont..... 57
56. Poles to primary and secondary flow foliation and flow lineation in granite and granodiorite in the central sector of the Bitterroot lobe of the Idaho batholith, west of Hamilton, Mont..... 66
57. Poles to filled primary fractures, mineralized primary fractures, and poles to tonalite dikes, in the central sector, Bitterroot lobe of the Idaho batholith, west of Hamilton, Mont..... 68
58. Poles to blastomylonite shear zones, lineation in blastomylonite, and two conjugate shear sets, in the central sector of the Bitterroot lobe of the Idaho batholith, west of Hamilton, Mont..... 69
59. Poles to mylonitic shears and lineation therein, central sector, Bitterroot lobe of the Idaho batholith, west of Hamilton, Mont..... 70
60. Poles to mylonitic shear joints and lineation therein, in the central sector, Bitterroot lobe of the Idaho batholith, west of Hamilton, Mont..... 71
61. Poles to chlorite-patterned shear joints and lineations in the McConnell Mountain, Hungry Rock, and Cedar Ridge quadrangles, in the central sector of the Bitterroot lobe of the Idaho batholith, west of Hamilton, Mont..... 72
62. Poles to secondary joints in the central sector, Bitterroot lobe of the Idaho batholith, west of Hamilton, Mont..... 74
63. Poles to flow foliation and linear features in granitic gneiss of the western and southern parts of the eastern sector (Subarea A), Bitterroot lobe of the Idaho batholith, west of Hamilton, Mont..... 82
64. Poles to foliation and a flow fold axis in granitic gneiss in Subarea B, of northeast-trending gneiss in the Bitterroot lobe of the Idaho batholith, west of Hamilton, Mont..... 84
65. Poles to gneissic foliation and mineral lineation in the gneiss of Subarea C of the eastern sector (Bitterroot gneissic front) of the Bitterroot lobe of the Idaho batholith, west of Hamilton, Mont..... 85
66. Late-stage, secondary foliation relations in the eastern sector of the Bitterroot lobe of the Idaho batholith, west of Hamilton, Mont..... 86

ILLUSTRATIONS (continued)

Page

Figure 67. Poles to blastomylonite foliation and fine, streaky biotite lineation in blastomylonite in the eastern sector of the Bitterroot lobe of the Idaho batholith, west of Hamilton, Mont. 88
68. Poles to mylonitic shears and lineation due to fine streaking and grooving in mylonitic shears in the Bitterroot gneissic front in the eastern sector (Subarea C) of the Bitterroot lobe of the Idaho batholith, west of Hamilton, Mont. 90
69. Conjugate pair of mylonite shears measured at a single outcrop in the eastern sector (Printz Ridge quadrangle) of the Bitterroot lobe of the Idaho batholith, west of Hamilton, Mont. 91
70. Poles to chlorite-coated shear joints and lineation defined by chlorite-patterned slickensides in the shear joints, in the eastern sector of the Bitterroot lobe of the Idaho batholith, west of Hamilton, Mont. 92
71. Poles to secondary joints in the eastern sector of the Bitterroot lobe of the Idaho batholith, west of Hamilton, Mont. 92
72. Average flow directions in granitic rocks in several 7 1/2′ quadrangles across the central Bitterroot lobe of the Idaho batholith, west of Hamilton, Mont. 102
73. Foliation trends in Subareas A, B, and C of the eastern sector, Bitterroot lobe of the Idaho batholith. 102
74. Diagrammatic structure cross section 85 km across the Bitterroot lobe of the Idaho batholith, showing the disposition of secondary flow lineation trending about 290°-110° az. 103
75. Generalized geologic map of the Bitterroot lobe of the Idaho batholith, adapted from a project map by M. I. Toth. 103
76. Poles to hypabyssal dikes in the Fenn Mountain area, western sector of the Bitterroot lobe of the Idaho batholith, west of Hamilton, Mont. 104

TABLES

Table 1. Modes in the Vermillion Peak quadrangle (EG1). 28
2. Modes in the Fog Mountain quadrangle (HG8). 29
3. Modes in the Chimney Peak quadrangle (HF7). 30
4. Modes in the Fenn Mountain quadrangle (HG7). 42
5. Modes in the Huckleberry Butte quadrangle (HF6). 58
6. Modes in the Greenside Butte quadrangle (HG6). 59
7. Modes in the Fish Lake quadrangle (HH6). 61
8. Modes in the Bear Mountain, McConnell Mountain, and Shissler Peak quadrangles (H15, H16, H17). 75
9. Modes in the Hungry Rock quadrangle (HJ6). 77
10. Modes in the Cedar Ridge and Grave Peak quadrangles (HK6, HK5). 78
11. Modes in the Jeanette Mountain quadrangle (HL6). 93
12. Modes in the Blodgett Mountain quadrangle (HM6). 94
13. Modes in the Tenmile Lake quadrangle (HM7). 95
14. Modes in the Printz Ridge quadrangle (HN6). 96
15. Modes in the Ward Mountain quadrangle (HN7). 97

ABSTRACT

Mapping of an area about 15 km north-south by 85 km east-west across the north-central part of the Bitterroot lobe of the Idaho batholith west of Hamilton, Montana shows that the lobe is asymmetric; flow foliation along the western margin strikes northwesterly and dips steeply. Within the lobe, migmatite screens dip varying amounts and strike predominantly 090° az, near the primary flow lineation trend. Foliation becomes progressively more intense to the east and drapes over a north-south arch near the Bitterroot mylonite front. Primary flow foliation is strongly overprinted to destroyed by a secondary flow foliation and lineation trending near 290° az in a pie-shaped area that widens to the east. The disposition of secondary flow lineation suggests original batholith thickness in excess of 30 km. Features of gneissic foliation, non-penetrative blastomylonite, and mylonite are consistent in their indication of cover-rock movement toward 110° az throughout three structural phases.

The asymmetric structure began to develop with the rise of tonalite followed by mixed granite/granodiorite with some anorthosite in its deeper parts, along a north- to northwest-trending fracture set near the western margin of the lobe; the magma spread to the east in a sheet perhaps controlled by a low-angle thrust near its base. Primary flow foliation formed, and migmatite screens were brought to an east-west trend. After consolidation, shearing of still-hot rock created secondary foliation, later blastomylonite, and still later mylonite in episodic shearing that continued during arching and rise to higher crustal levels. Some crustal thinning perhaps occurred in conjunction with thrusting.

INTRODUCTION

The Bitterroot lobe rocks of the Idaho batholith described in this paper occur in and about the area of the Selway Crags, whose peaks rise above 2,666 m (8,000 ft), and extend to the Bitterroot front west of Hamilton, in southwestern Montana, where the peaks rise above 3,000 m (9,000 ft). The low point in the area is at about 666 m (2,000 ft) at the Selway River on the west, with local relief thus about 2000 m (6,000 ft). Quartzite and calc-silicate gneiss provisionally correlated to the Belt Supergroup (Ravalli and Wallace units, respectively) are country rocks into which the batholith was intruded. The rocks in the western part of the batholith broadly comprise tonalite cut by later granitic and other rocks, which become major to the east.

Igneous rock nomenclature follows Streckeisen (1973).

This paper stems from work done on the U.S. Geological Survey project (1979-1981) to assess the mineral potential of the Selway-Bitterroot Wilderness Area. The paper is written to be accompanied by the project map published by the U.S. Geological Survey (Toth, 1983), and should be read with a copy of that map at hand.

PREVIOUS WORK

Reconnaissance investigations constituted the early work in the Bitterroot lobe of the Idaho batholith and its environs. Lindgren (1904) was the earliest; he spoke of a Mesozoic quartz monzonite mass with an eastern schistose slope probably due to a great fault. Ross (1928) showed that the Idaho batholith is post-Triassic and pre-Tertiary, cut by younger granitic masses. Langton (1935) studied the northeastern Idaho batholith, showed two deformations in the country rock and thrusts related to the emplacement of the batholith. Following these early studies, the work became more detailed.

Anderson (1952) did further work on the concept of multiple emplacement of the batholith, a theme developed in earlier reconnaissance (Ross, 1928). Ross (1952) developed a granitization hypothesis to explain the eastern frontal gneiss of the Bitterroot Mountains, appealing to emanations from the batholith to convert sedimentary rock to gneiss. Larsen and Schmidt (1958) showed a considerable variety of rock types (eleven) in reconnaissance modal and chemical studies. Reid (1959) studied wall rocks west of the batholith, and discovered three sets of synmetamorphic folds pre-dating emplacement of the batholith. Leischner (1959) studied the batholith in the vicinity of Lolo Hot Springs, Montana, and found early diorite to quartz diorite, followed by quartz monzonite. Ross (1965) found that the Idaho batholith main interior mass is largely granodiorite and quartz monzonite, surrounded by a narrow discontinuous roof and border zone of quartz diorite and quartz diorite gneiss. Thrusting occurred away from the batholith interior on the eastern and western margins, in part preceding and in part following batholith emplacement. Chase (1968) studied country rock in the northeast contact zone of the Idaho batholith and found metasedimentary units regionally metamorphosed in three phases of synmetamorphic penetrative deformation, prior to emplacement of the Idaho batholith, perhaps comparable to those discovered by Reid (1959). Morrison (1968) found similar relations in the Lochsa area northwest of the batholith--three pre-batholithic metamorphic episodes and a fourth synchronous with batholith emplacement. Further study in the country rock northeast of the batholith (Berg, 1969) disclosed twenty concordant anorthosite bodies in the gneiss, dominantly of labradorite.

Beginning broader work, the State of Idaho studied the reconnaissance geology and mineral potential of the Selway-Bitterroot Wilderness Area, covering much of the Bitterroot lobe of the Idaho batholith (Greenwood and Morrison, 1973). In a regional study, Ryder and Scholten (1973) showed that thick accumulations of syntectonic conglomerate of the Beaverhead Formation in Montana were derived from the northeast margin of the Idaho batholith in late Cretaceous-Paleocene and probably early Eocene. Armstrong (1974) discussed relations between tectonic activity and magmatism of the Cordillera; this work shows the broad temporal and structural framework within which the batholith was emplaced. Nold (1974) showed that the Belt Supergroup rocks and associated orthoamphibolite and orthogneiss units were deformed at least four times prior to injection by quartz-diorite-to-granite of the Idaho batholith. This corresponds well to results obtained northwest of the batholith by Morrison (1968) and earlier by Reid (1959) west of the batholith. In a detailed structural analysis, Cheney (1975) showed that anorthosite bodies in the country rock near the northeast margin of the batholith have experienced three structural

events. Thus, they are closer to the age of the country rock than to that of the batholith. Armstrong (1975a) suggested the name "Bitterroot lobe" for the northern part of the Idaho batholith. Williams (1977) showed that the northern Bitterroot lobe consists largely of foliated, medium- to coarse-grained, megacrystic, two-mica granite, intruded by granodiorite. Wiswall (1979) suggested that exposures near Paradise, Idaho, constitute the base of the Bitterroot lobe, where gneiss and migmatite are overlain horizontally by granitic rock of the batholith, with the contact steepening to the west. Bradley (1981) studied a gneissic tonalitic phase of the Bitterroot lobe along its northeastern border. This is a part of the quartz-diorite gneiss roof and border zone of Ross (1965). Bradley showed the gneissic tonalite to be earlier than the granitic phase of the Bitterroot lobe. Toth (1981) showed that the main Bitterroot lobe comprises two major plutons: the Bear Creek and the younger Cub Creek units. The Bear Creek pluton is a medium-grained granite with varying amounts of poorly defined potassium feldspar phenocrysts and 3-5 percent biotite. The Cub Creek pluton is a finer-grained granodiorite with well-defined potassium feldspar phenocrysts, 3-5 percent biotite, 3-5 percent hornblende, and up to 3 percent sphene. These units may correspond to those described by Williams (1977). During 1977-1981, the U.S. Geological Survey and the U.S. Bureau of Mines evaluated the mineral potential of the Selway-Bitterroot Wilderness Area (Toth and others, 1983); the study covered much of the Bitterroot lobe. The results of the geologic mapping were given by Toth (1983).

As a part of the continuing more detailed study of the Bitterroot lobe, work has been done on extensive migmatite within and peripheral to the lobe. Johnson (1975) showed that migmatite formed by injection, metamorphic differentiation, and anatexis. Bittner-Gaber (1983) showed that the migmatite screens within the lobe are oriented largely east-west (1983, p. 22) and were derived from the wall and (or) roof rocks (1983, p. 114). Their east-west orientation is due to magma flow postulated to be from west to east. The migmatite protolith has been strongly injected by magma of several types, and the resulting migmatite has in many places been intricately folded.

The continuing detailed studies have resulted in the interpretation of a portion of the Bitterroot lobe as a metamorphic core complex (Hyndman, 1980). Many workers too numerous to list here have concentrated on the eastern mylonitic detachment zone (hearken back to Lindgren's 1904 idea of a major fault zone). Core complex effects extend to some distance west within the lobe. Toth (1981) for example, showed that both the Bear Creek and the Cub Creek plutons have moderate to well-developed flow foliation that decreases in dip upward, suggesting proximity to the roof of the batholith. Primary mineral lineations and small fold axes trend 290° and plunge at shallow angles. Secondary mineral lineations trend 290° and 110° and also plunge at shallow angles, with the 110° element increasing in abundance toward the eastern bordering mylonite front. Garmezy and Sutter (1983) have done the most detailed work on the mylonite zone. Mylonitization began at about 45.5 m.y. ago at a depth of probably greater than 9 to 10 km and continued for about 2 m.y. during a period of rapid uplift of the dome (0.1 to 0.3 cm/yr). Mylonitic fabric indicates eastward tectonic transport of the hanging wall throughout the 500-1000 m thick mylonite zone. The presence of ductile normal faults in this zone, which have a sense of displacement parallel to the mylonitic lineation, suggests that mylonitization occurred in an extensional environment in which a principal extension direction is aligned 110°.

Questions of movement direction of the cover rock above the detachment zone have been controversial, but the weight of evidence is coming to support eastward transport. This view for the Okanogan dome was presented early by Hyndman (1980) and lately with convincing evidence by Goodge (1983).

Considerable radiometric dating has been done on the Bitterroot lobe and its country rock. Armstrong (1975b) compiled voluminous data. At page 32 (1975b) he noted that the compiled dates for the Bitterroot lobe are all less than 70 m.y. Chase and others (1978) arrived at an age of 66 m.y. for the main-stage batholithic emplacement and at an age of 39-46 m.y. for a late thermal-plutonic event. Bickford and others (1981), in a very detailed study, showed the following history, based on lower-intercept ages (1981, p. 453): quartz-diorite gneiss at about 73 m.y., medium-grained granite at about 55 m.y., and cataclastic granite at 49-46 m.y. The age for cataclastic granite is close to the time of beginning of mylonitization, given by Garmezy and Sutter (1983) at 45.5 m.y. ago. Upper intercept ages are given by Bickford and others (1981, p. 454) in the range 1,700 to 2,300 m.y. These ages are interpreted as due to country rock zircon contributions either in partial melting or in contamination.

WALLROCK SOUTHWEST OF THE BATHOLITH

Structure

The Chimney Peak area contains the southwestern contact of the Idaho batholith with metasedimentary and metaigneous rock marginal to quartz diorite and tonalite of the batholith. The northern part of this map area contains granite/granodiorite injected into the tonalite.

Calc-silicate gneiss and pelitic metamorphic rock

Calc-silicate gneiss is the principal country rock exposed in the Crags area, whereas biotite quartzite is abundant in migmatite screens inside the batholith. Calc-silicate gneiss is deformed in steep but variably plunging folds. Figure 1 shows varied trends of foliation in calc-silicate gneiss and steep plunges of minor folds and other linear features in the gneiss. Figure 2 shows the style and character of steeply plunging folds in the calc-silicate gneiss. A schistosity lies parallel or sub-parallel to original bedding of the calc-silicate gneiss. This schistosity has been deformed in passive-flow folds of the sort illustrated in figure 2. The small folds show both clockwise and counterclockwise rotation somewhat randomly through the outcrops; no evidence was found to show that they are related as minor folds to larger folds in the common way. The axial planes of the small folds are parallel to the foliation of the enclosing rocks at all points seen, regardless of the orientation of the major foliation. Mineral lineation parallels the minor fold axes, whatever their local plunge, and consists of elongate biotite clots, diopside and hornblende prisms, and quartz rods.

Sillimanite occurs as a minor constituent in schist interbeds in the calc-silicate gneiss. In the schist, sillimanite plunges steeply, parallel to minor fold axes.

The Fog Mountain-Selway River area, largely of quartzitic rocks, presents the best exposed section of metasedimentary rock within the map area, even though that exposure consists of just 17 outcrops in a 5-mile traverse along the Selway River. The description of the structural geology is based upon a compiled cross-section and strip plan map (fig. 3), with sketches and stereograms in succeeding figures, in addition to the field data.

A problem in compiling the cross section is that the folds plunge from horizontally to vertically; although the section cuts across the regional strike at a high angle, some folds yet plunge in the plane of the cross-section. Thus, no single section, even a profile section or a strip plan view, can portray the structure adequately.

Data at Stations 282-284 are shown in stereogram (fig. 4). Fold axes plunge 45° to 60° northeasterly in the approximate plane of the batholith. Two minor folds in this part show opposite directions of rotation; they are close together and both in vertical layers.

Pegmatite, alaskite, or aplite variously are injected along the foliation and folded with it; in places, the igneous material crosscuts both foliation and minor folds and is itself yet folded (fig. 5). The pegmatite is partly also in lozenge boudins, which display separations along the layering up to 1.5 m (4.5 ft).

The structure at Station 284 is simplified into a single attitude (310° az, 55° NE) in figure 3. This is, however, an oversimplification, as can be seen in figure 6. This figure shows 16 poles to foliation in biotite quartzite. The structure is further illustrated in figure 7, a sketched plan view prepared in the field. No vertical section is given here since the folds plunge steeply along the line of the strip plan (fig. 3).

The poles to foliation near Station 284 are so scattered as to give no clue to the character of the folding (fig. 6). Such a clue does come from three measurements made on a single minor fold at Station 284; these are portrayed on figure 6 as planes A, B, and C. Poles to these planes lie in a small-circle girdle indicative of a conical fold. Thus it appears that the small folds mapped at Station 284 are all conical, as are those at the prior stations 282 and 283. The axial plane for the minor conical folds at Station 284 is oriented approximately 360°, 70° E, close to the one shown in figure 1 at Stations 282 and 283. Fold axes are from field measurements. Mineral lineation in the form of stretched muscovite parallels these axes. Considerable variation in the bearing and plunge of minor conical folds is shown in figure 7 at Stations 282-284.

At Station 284, pegmatite injects the axial planes of the minor conical folds. Also cropping out at Station 284 is a set of small isoclinal folds with axial-plane foliation. These folds clearly pre-date the conical folds, as the conical folds deform the foliation. The isoclinal fold foliation stands vertical, and the fold axes plunge 90° down the dip.

Station 287 has a set of small, knife-sharp isoclinal folds (fig. 8) like those at Station 284, with axial-plane foliation. The fold axes here plunge 15°, 360°. These isoclinal folds clearly pre-date the conical folds; again, their axial-plane foliation is the structural element folded in the conical set. The isoclinal folds, oldest recognized in the rock, are assigned to a deformation phase D_1, and the conical folds are assigned to D_2. Station 289 has both D_1 and D_2 minor folds; pegmatite is involved in the D_1 fold set here, injected along and folded with the bedding of the metaquartzite.

Station 290 gives further information on the character of the conical folds; too complex to portray in the cross-section, the data have been placed in a stereogram (fig. 9). This figure shows sequential measurements of the orientation of two small folds downward along their axes; the bearing and plunge change along their axes. Thus, the axes may be characterized as helical or screw-like. This screw-like character is demonstrated on a larger scale in figure 3 at Stations 282-284, in the variation in bearing and plunge of three conical-fold axes measured at adjacent stations.

Station 294 brings out a feature related to a reversal in dip that occurs beyond the vertical dip at Station 291. West of Station 291, the foliation dips generally northeastward, and the D_2 folds plunge generally northeastward, near the dip of the foliation. East of Station 291, as shown at Station 294, the foliation dips southwestward, and the D_2 folds plunge southwestward near the dip of the foliation. A small D_2 fold was measured at Station 294, its features are shown in figure 10.

A small fold at Station 295 cannot be shown at the scale of the cross-section; yet its generally synformal character is suggested therein (fig. 3). The concentric fold style and low-angle plunge of this fold suggest that it be assigned a D_3 age. A low-angle crinkle lineation in the rock is probably related to this fold set, the character of which is shown in figure 11.

A small fold at Station 296 repeats the fold style seen at Station 295. Figure 12 illustrates this fold, showing poles to fold surfaces in a crumpled zone taken to lie in the hinge of a large fold. These poles lie along a great circle of the stereonet, indicating a concentric style of folding which is assigned to D_3. Representative attitudes at this station are shown in figure 3. A crinkle lineation parallels the D_3 fold axes. Note the reversal of plunge direction of the D_3 folds within a short distance, perhaps due to the interference effects of older folds. Figure 12 also gives data on the general orientation of the foliation in the eastern half of the cross-section in figure 3.

A small, near-vertical, conical fold occurs at Station 297; its form is shown diagrammatically in figure 3. See also figure 13.

Generally, poles to foliation for rock in and near the cross-section show a wide scatter, with an approximation to axial symmetry (fig. 14). Mineral lineations and minor fold axes, particularly D_2 fold axes, do not appear to be systematic in any way (fig. 15), although their gross distribution is also suggestive of an axial symmetry.

Muscovite lineation (fig. 15) plunges steeply wherever it is exposed; in a few places, such as at Station 283, it parallels the axes of D_2 folds. Sillimanite lineation also plunges steeply, generally along or near the dip of the foliation. In places, like muscovite, it parallels D_2 fold axes. At Station 283, where mica lineation and fold axes are oriented 60°, 075° az, sillimanite plunges vertically in late, steeply dipping shear fractures.

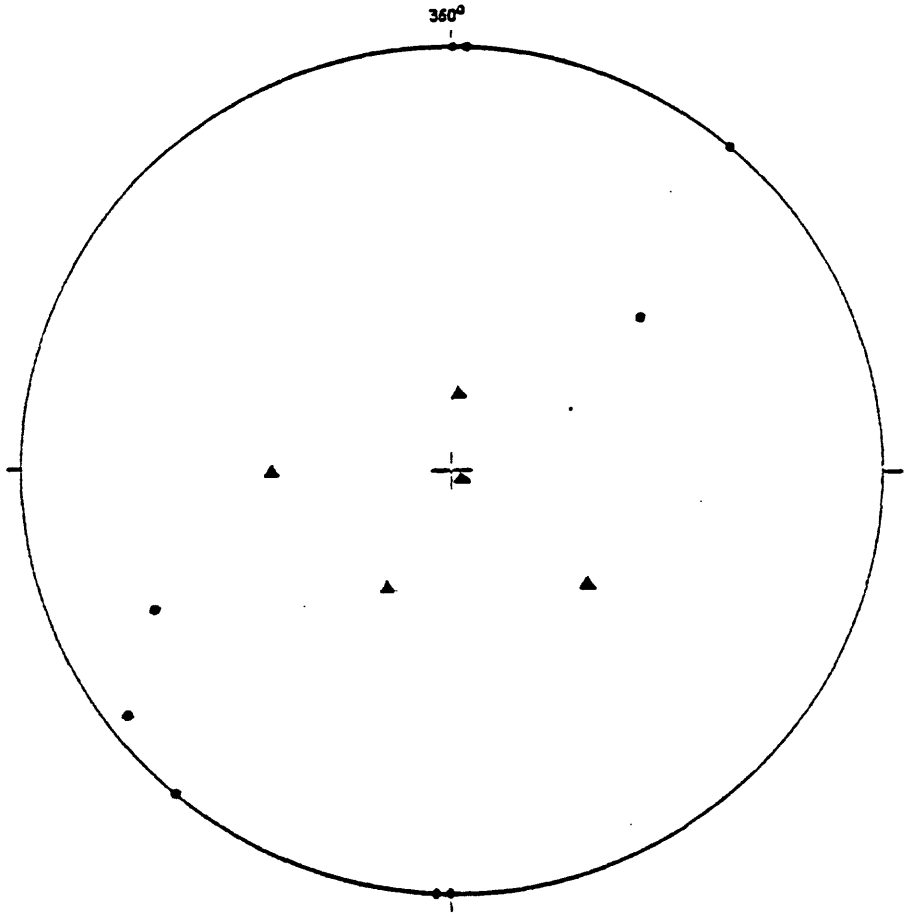

Figure 1.--Poles to foliation (●) and linear structures (▲) (minor fold axes and alined prismatic minerals) in calc-silicate gneiss in wall rocks west of the Idaho batholith in the Chimney Peak quadrangle.

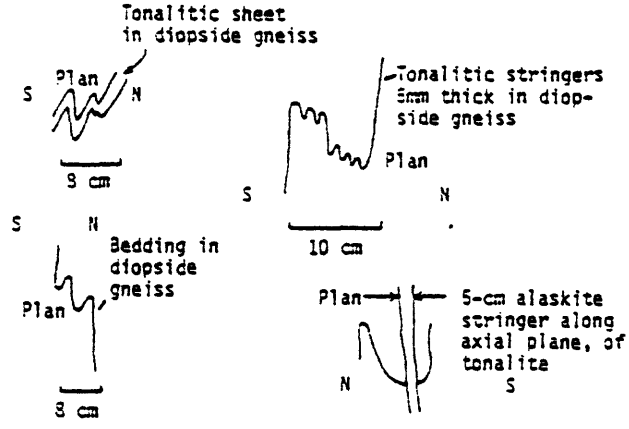

Figure 2.--Small passive-flow folds in the calc-silicate gneiss west of the Idaho batholith in the Chimney Peak quadrangle. Trondhjemite has been injected along the foliation (which is parallel to bedding) and deformed with it to produce some of these small folds. In places, alaskite tonalite has been injected along the axial planes of the small folds parallel to a younger schistosity.

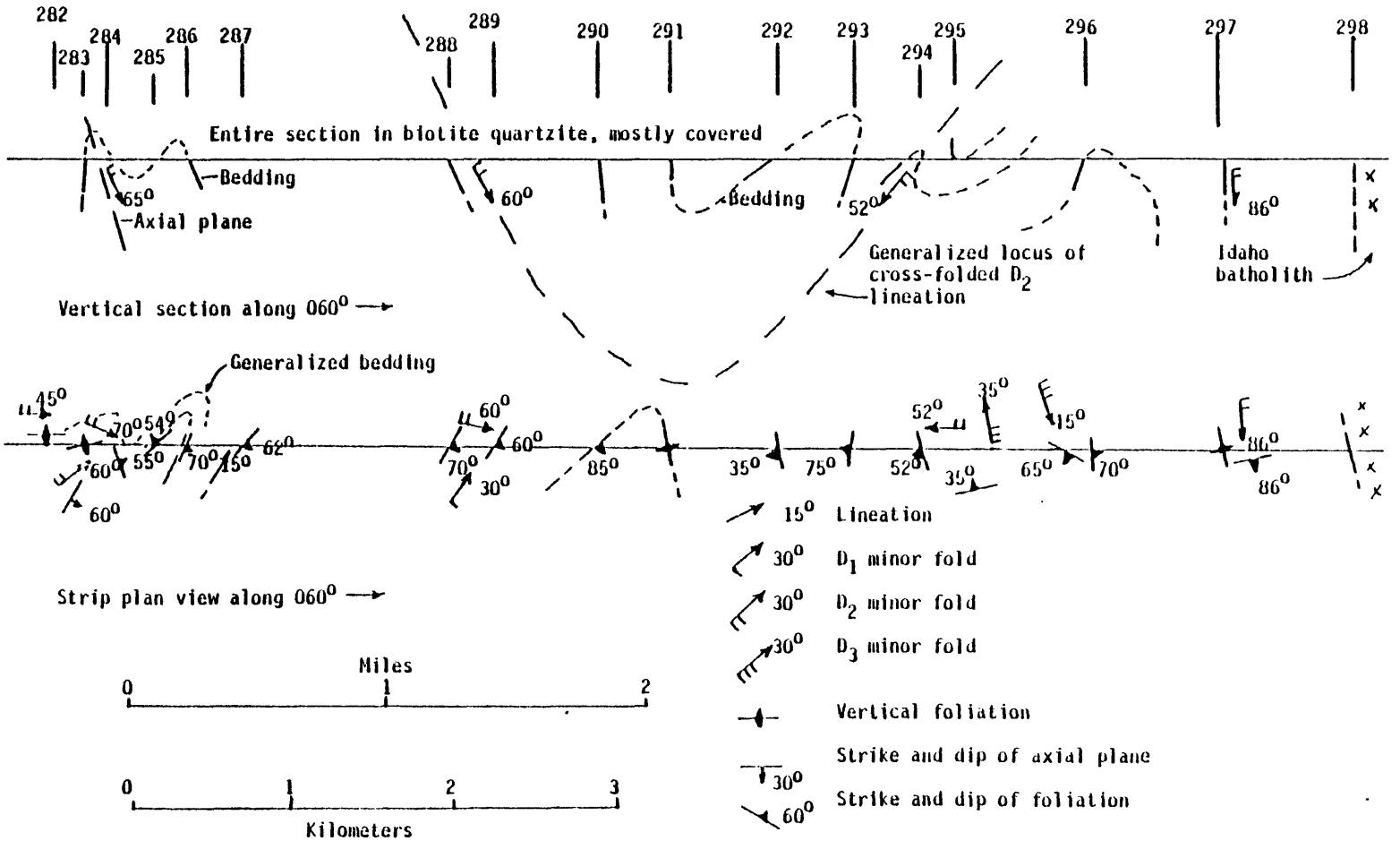

Figure 3.--Vertical section and strip geologic map of the metasedimentary rocks along the Selway River in the Fog Mountain quadrangle, northeastward (060° az) to the contact with the Idaho batholith.

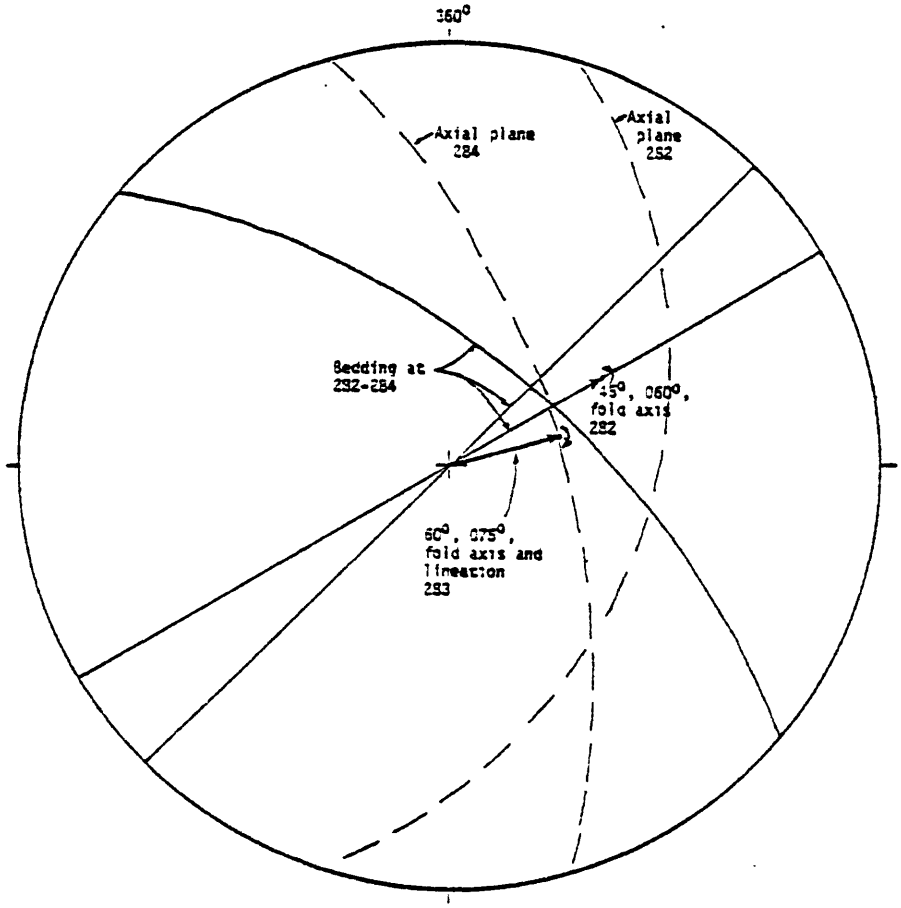

Figure 4.--Structural data at Stations 282-284 in Figure 3, showing relation of plunging minor folds to bedding and foliation; also showing sense of rotation of minor folds close together in the outcrops. The stations are along the Selway River in biotite quartzite west of the Idaho batholith, in the Fog Mountain quadrangle. Data are plotted on the lower hemisphere of the Wulff stereonet.

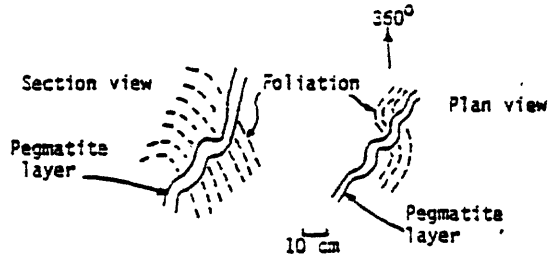

Figure 5.--Pegmatite injected in biotite quartzite near Station 283 of Figure 3, along Selway River west of the Idaho batholith in the Fog Mountain quadrangle.

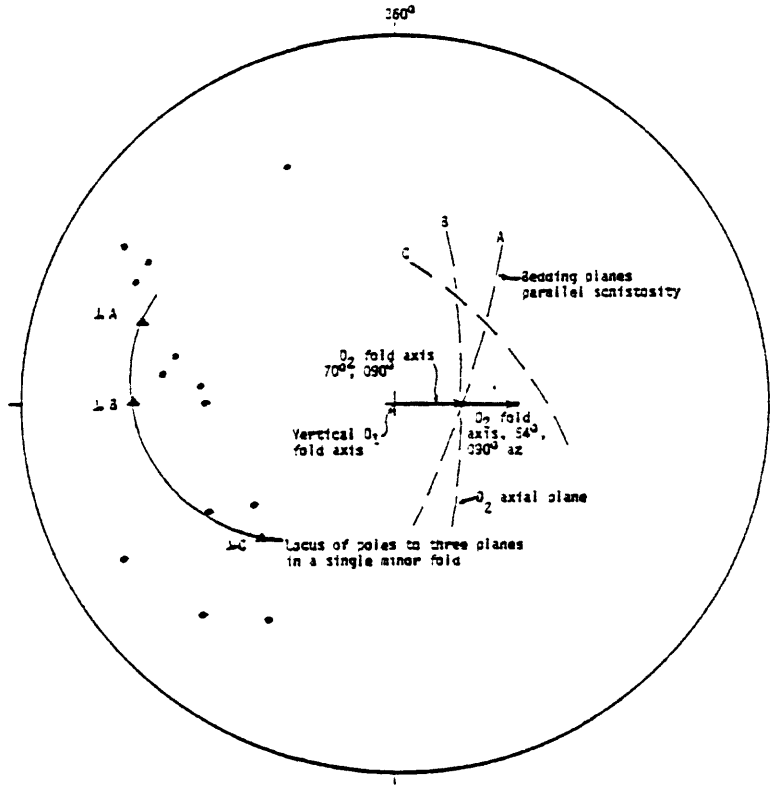

Figure 6.--Poles (•) to schistosity near Station 284 of Figure 3 in biotite quartzite along the Selway River west of the Idaho batholith, in the Fog Mountain quadrangle. Poles on lower hemisphere of Wulff stereonet.

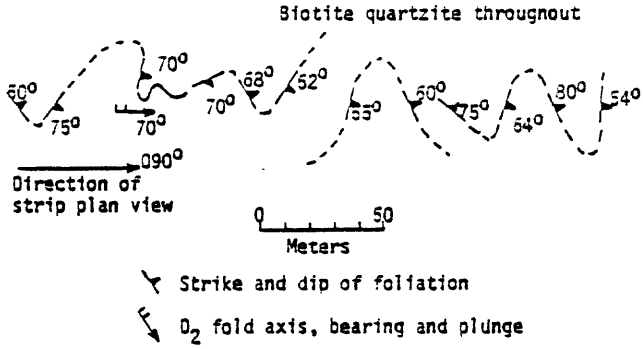

Figure 7.--Mesoscopic folding in biotite quartzite near Station 284 of Figure 3 along Selway River west of the Idaho batholith, in the Fog Mountain quadrangle.

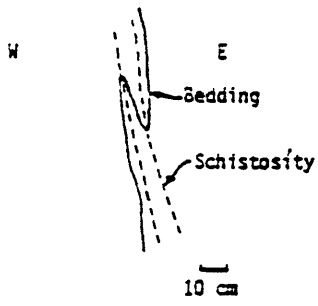

Figure 8.--Isoclinal folds with axial-plane schistosity at Station 287 of Figure 3 in biotite quartzite along Selway River west of the Idaho batholith, in the Fog Mountain quadrangle.

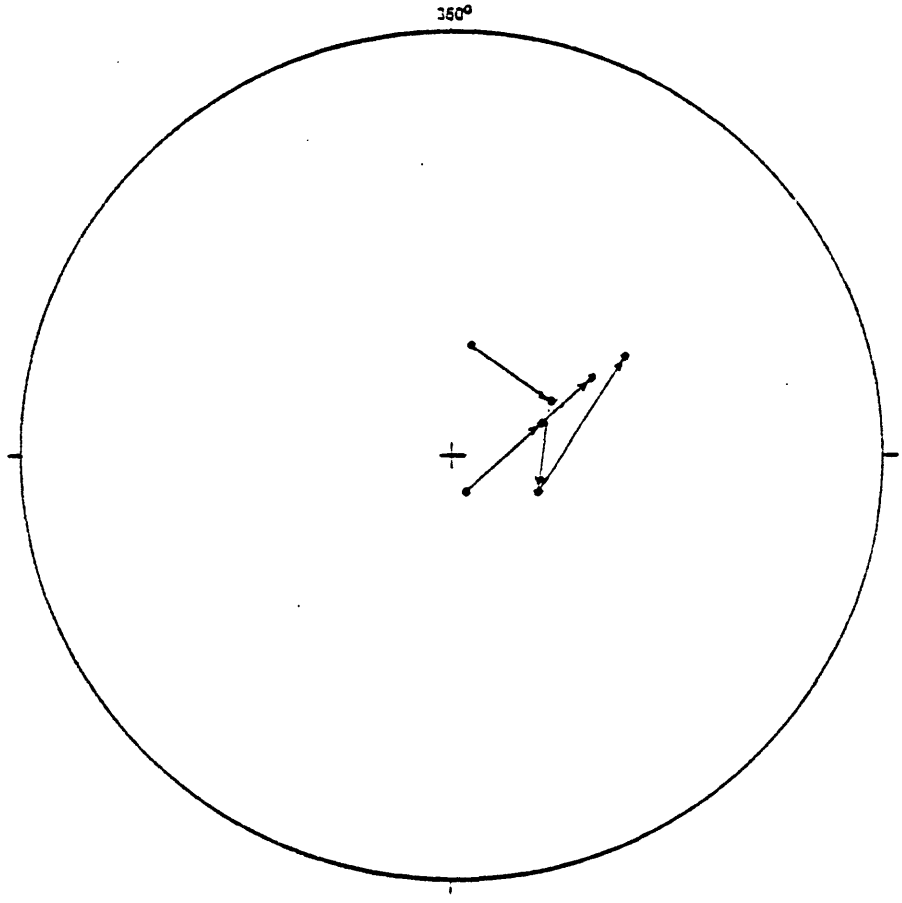

Figure 9.--Helical axes of minor conical folds (•) at Station 290 of Figure 3 in biotite quartzite along Selway River west of the Idaho batholith, in the Fog Mountain quadrangle. Arrows in the diagram connect sequential points downward along each of two fold axes. Data are plotted on lower hemisphere of Wulff stereonet.

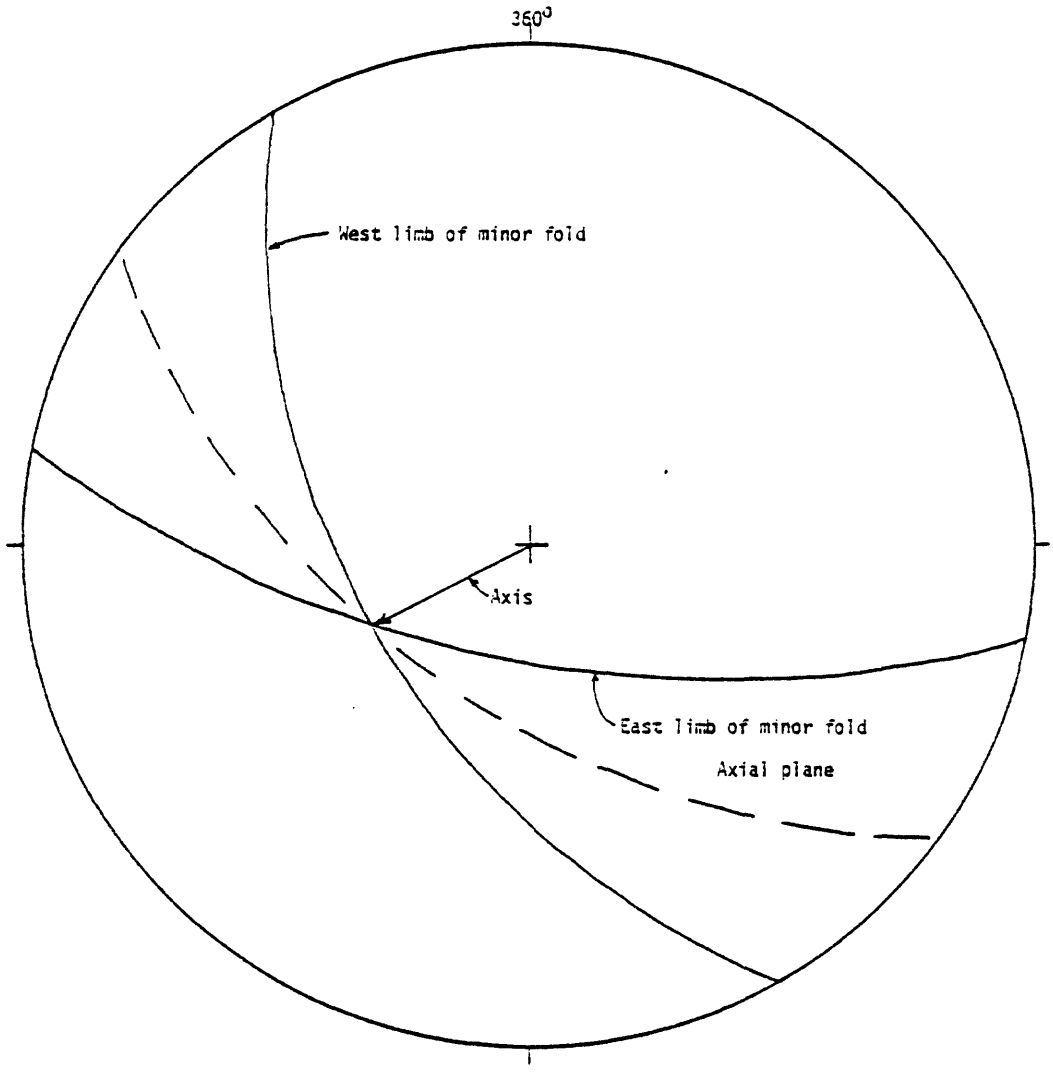

Figure 10.--Details of geometry and direction of plunge in minor conical folds at Station 294 of Figure 3 in biotite quartzite along Selway River west of the Idaho batholith, in the Fog Mountain quadrangle. Data are plotted on lower hemisphere of Wulff stereonet.

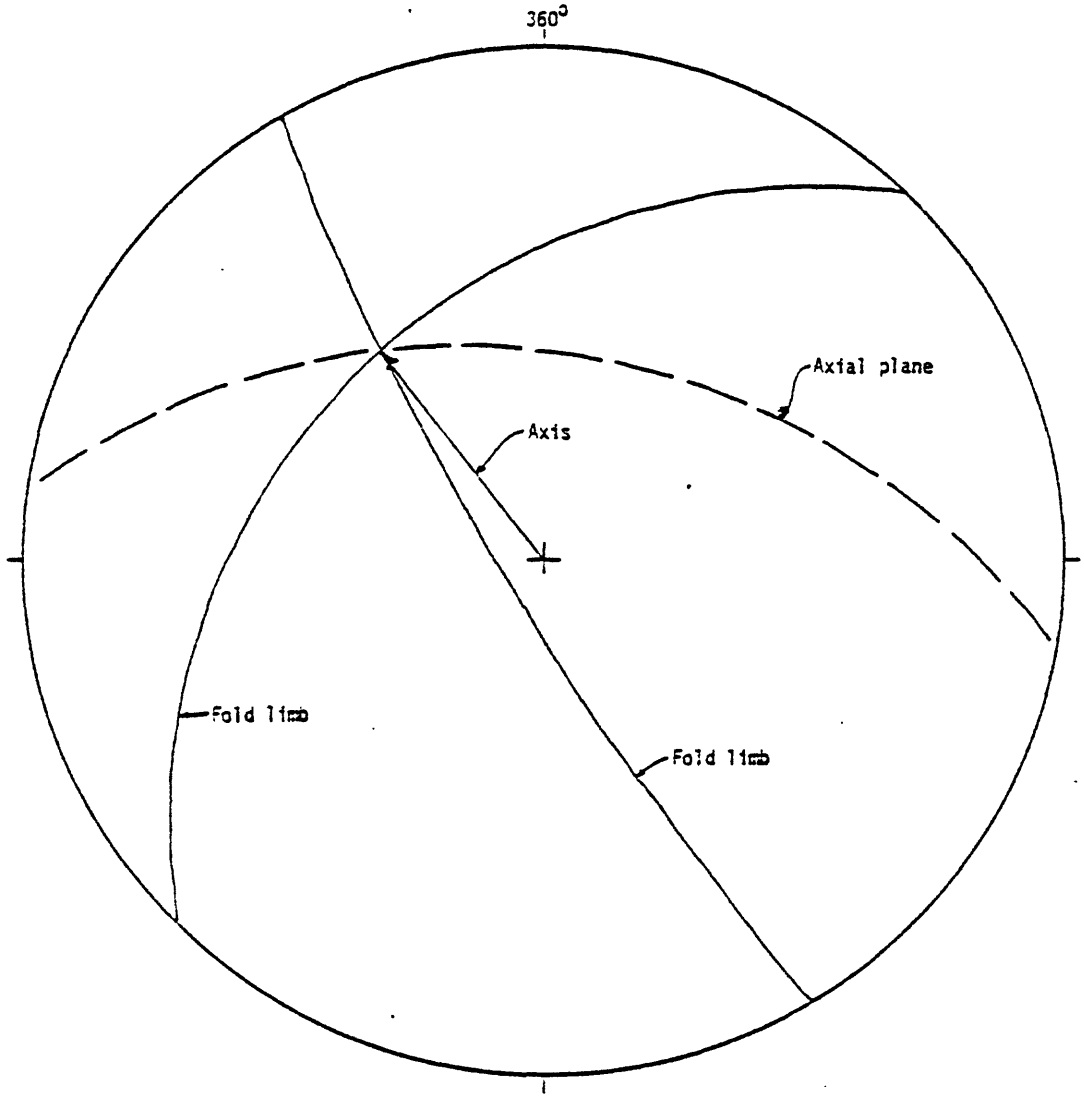

Figure 11.--Details of geometry and direction of plunge of minor concentric folds at Station 295 of Figure 3, in biotite quartzite along Selway River west of the Idaho batholith, in the Fog Mountain quadrangle. Data are plotted on lower hemisphere of Wulff stereonet.

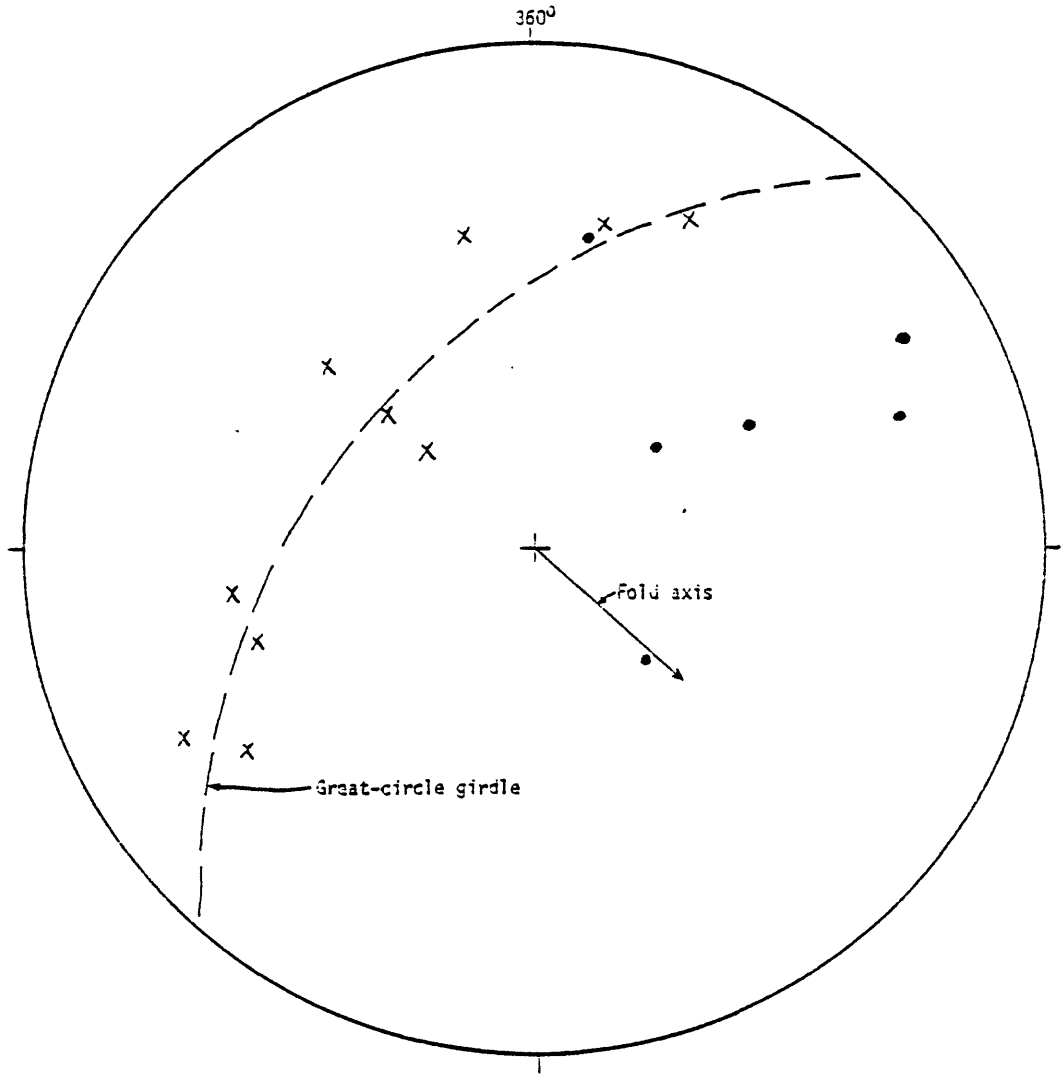

Figure 12.--Details of geometry and direction of plunge of minor concentric folds at Station 296 of Figure 3, in biotite quartzite along Selway River west of the Idaho batholith, in the Fog Mountain quadrangle. (•) Poles to general foliation. (X) Poles to foliation in a single concentric fold set. Data are plotted on lower hemisphere of Wulff stereonet.

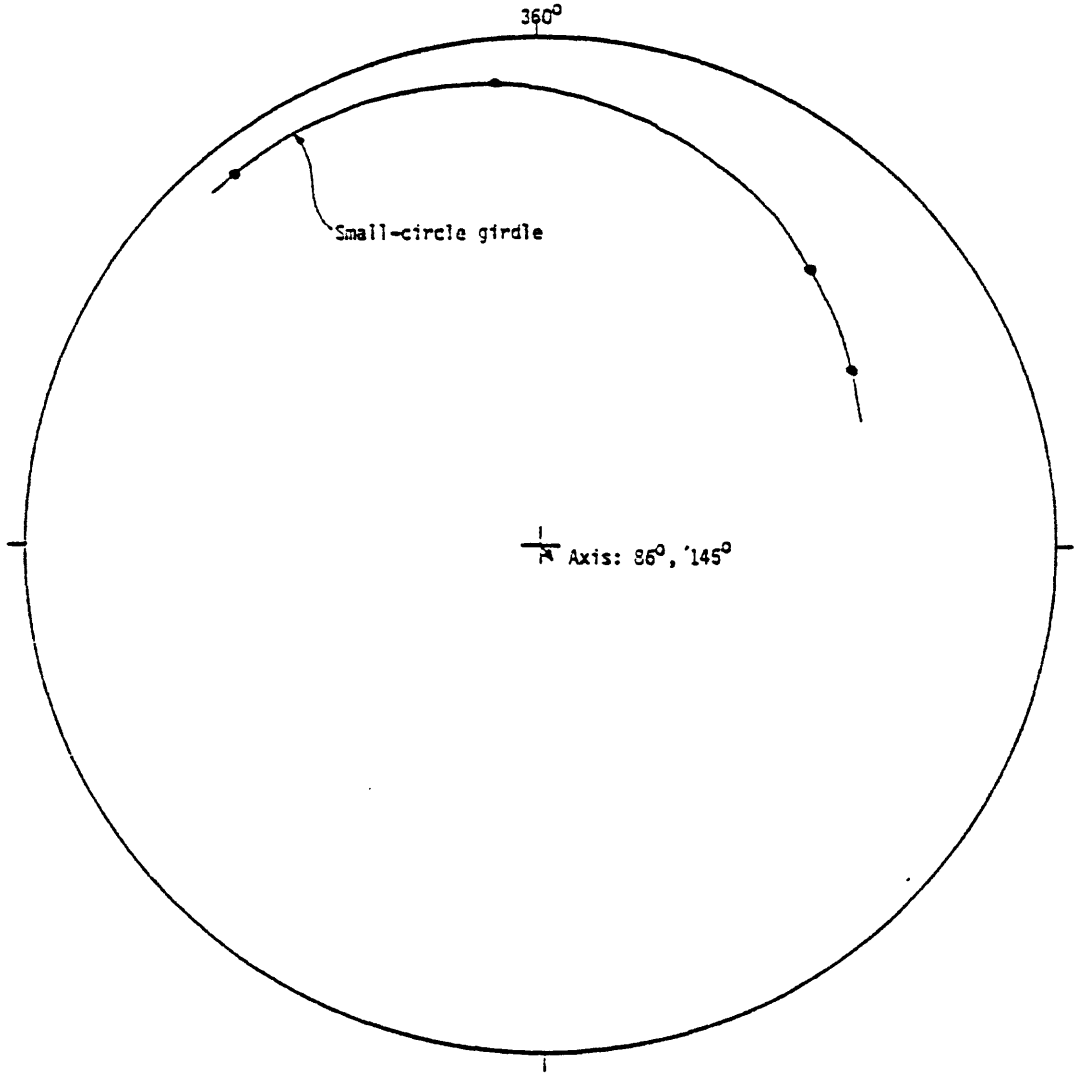

Figure 13.--Details of geometry and plunge of a steep conical fold at Station 297 of Figure 3, in biotite quartzite along Selway River west of the Idaho batholith in the Fog Mountain quadrangle. (•) Poles to foliation. Data are plotted on lower hemisphere of Wulff stereonet.

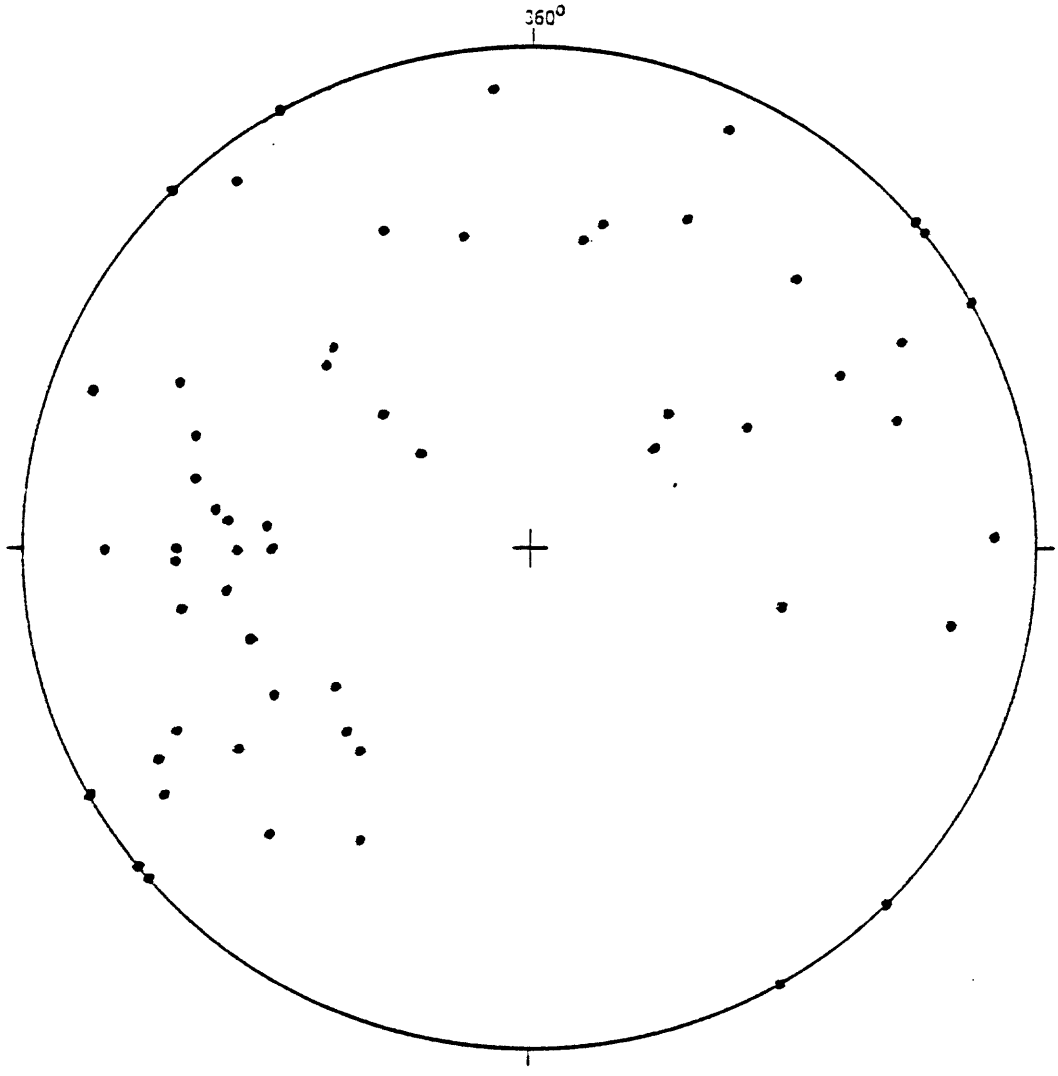

Figure 14.--Poles to foliation (•) in biotite quartzite in the Fog Mountain-Selway River subarea west of the Idaho batholith. Data are plotted on lower hemisphere of Wulff stereonet.

Not all the small folds plunge steeply (fig. 15). One small fold of apparent D_2 style in this subarea (fig. 16) trends parallel to the strike of the foliation; similar relations are also seen in the rocks along the Lochsa River, outside the map area.

Continuing this description farther to the south, three principal rock types occur south of the Selway River and in the Vermillion Peak area; biotite quartzite (predominant), biotite gneiss, and biotite-muscovite schist (least abundant). The rocks were analyzed in profile section perpendicular to the 30° southeast plunge. Rare, thin, calc-silicate layers up to 65 m thick occur. The data are scanty for more than a very tentative interpretation. A schist-quartzite contact on the southwest is occupied partly by biotite gneiss, and the overall structure for this part may be that of a nearly recumbent, somewhat refolded isoclinal fold. Biotite quartzite predominates in the center of the section, deformed in open upright folds. Biotite gneiss in the northeastern parts is involved in this folding. Minor folds in the rocks are generally consistent with this interpretation.

The rocks are generally schistose and foliated. Early folds (D_1) are isoclinal and have axial-plane schistosity. Quartz-rich layers are boudined, and lineated muscovite and biotite parallel minor fold axes. Amphibolite and tonalite sheets occur along the schistosity and are deformed by the early fold set. The rocks are injected both by concordant and discordant pegmatite, folded and schistose parallel to the external schistosity. Some folded pegmatite extends apophyses into the external schistosity in a way suggestive of fluidity during folding and therefore synkinematic intrusion. Orbicules are flattened in the plane of the schistosity ($\underline{s}_2$). Fold hinges are scarce; on the limbs of the folds, quartzite bedding and schistosity appear to be parallel.

Later folds (D_2) developed a secondary axial-plane schistosity largely restricted to their hinges ($\underline{s}_2$). Lineated biotite and muscovite extend parallel to the D_2 fold axes. Lineated biotite in such rock parallels both $\underline{s}_1$ and $\underline{s}_2$. Boudins produced by stretching in D_1 are locally folded in D_2. Crenulation folds (late D_2 or D_3) kink earlier schistosity and igneous rock sheets along the schistosity. Biotite and muscovite are lineated parallel to kink fold axes. Shears of the age ($\underline{s}_3$) are partly filled with quartz, and similar quartz veins along the schistosity cut off intrafolial folds, making a kind of rodding. Late shears of diverse orientations contain sheared-out, streaked muscovite and slickenside-like features that are nearly parallel, nearly of due east trend (fig. 17).

For purposes of structural geometric analysis, the biotite quartzite and other rocks have been subdivided into areas of relative homogeneity. Poles to foliation/bedding in the northern Vermillion Peak area show a diffuse girdle (fig. 18) indicative of folding about an axis oriented 30°, 146° az, and this is the basis for selection of the profile-section orientation used. Poles to foliation in the Fog Mountain area south of the Selway River are rather scattered, suggesting some complexity (fig. 19). The rocks can be further analyzed through consideration of their linear features.

Lineation in the Vermillion Peak area is shown in figure 20. Early fold axes are of scattered orientations. Crenulation fold axes average a 30° plunge along 146° az, but are also widely scattered. Mineral lineations are of trends quite as diverse as those of the several fold sets. Lineation of the Fog Mountain area south of the Selway River is shown in figure 21. The diversity of trend is remarkable. Axial planes measured are few (fig. 22), but their geometry is similar to that of the foliation in the Vermillion Peak area (fig. 18), and therefore they have been folded in the same way. The scatter of the axial planes of crenulation folds shown in figure 22 is probably due to interference effects.

Only a few fractures were exposed for measuring in the Vermillion Peak area, including pegmatite dikes, a Tertiary dike, a quartz vein, faults, and joints (fig. 23). The paucity and scatter of the data make interpretation unreliable.

Tonalitic gneiss and associated trondhjemite

Tonalitic gneiss occurs as concordant sheets in the country rock southwest of the Idaho batholith. A few attitudes on foliation in the gneiss indicate a considerable range of strikes in steeply dipping rocks (fig. 24). Minor fold axes in the gneiss plunge vertically or nearly so, with a broad range of bearings (fig. 25). The axial planes of these folds also display widely varied trends (fig. 26). Mineral lineation consisting of elongate biotite streaks and clots commonly parallels the axes of the minor folds. The minor folds have both clockwise and counterclockwise rotation more or less randomly through the outcrops.

The minor folds are developed through the folding of schistosity, and their axial planes partly parallel the foliation in the gneiss. Concordant veins of trondhjemite (5-40 cm, 1.9-15.7 in. thick) are injected along the foliation and folded with the gneiss. Figure 27 illustrates the style of these folds. The axial planes are commonly rotated out of parallelism with the local foliation planes, although in many places the two structural elements are parallel (fig. 28).

Varied flow directions are expressed in yet a different way in some places (fig. 29). Flow at the place portrayed in figure 29 was first along a 035° az trend. Later flow folds distort those of the 035° az trend in a 010° az trend; both sets show right-lateral ductile shear later than the minor folds described above. Both trends are crossed by shear joints of more brittle character along a 325° az trend in which the gneissic flow foliation is bent only in the vicinity of the shear joints; movement on these shear joints was also of right-lateral character. Thus, the two joint sets are not related as in a conjugate joint set.

One shallow-dipping alaskite sheet cutting the tonalitic gneiss is of granite; most such sheets are of trondhjemite.

Petrography of the wall rocks

The wall rocks comprise (a) pelitic quartzite and schist and (b) calc-silicate quartzite and gneiss. The quartzite and schist are major in the Fog Mountain Area and to the south, and the calc-silicate rocks dominate in the Chimney Peak area. Petrography for these rocks follows. Procedures used over the whole map area for modal determination are given below. Modes were measured in the thin sections on rocks whose grain size is 2 mm or smaller. For medium-grained rocks coarser than 2 mm, modes were measured both in thin section and on stained slabs, and the results combined. For coarsely

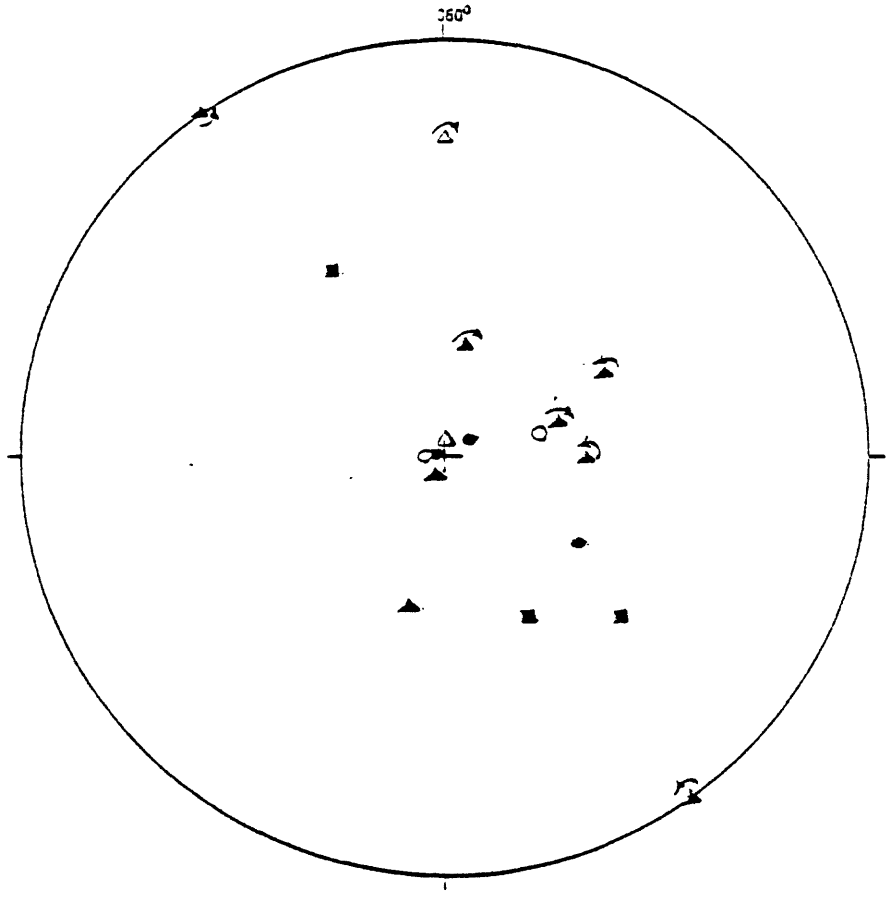

Figure 15.--Minor fold axes and mineral lineations in biotite quartzite in the Fog Mountain-Selway River subarea west of the Idaho batholith. (△) D_1 fold axis with sense of rotation shown by small arrow. (▲) D_2 fold axis with sense of rotation. (■) D_3 fold axis. (○) Muscovite streaks. (●) Sillimanite prisms. Data are plotted on lower hemisphere of Wulff stereonet.

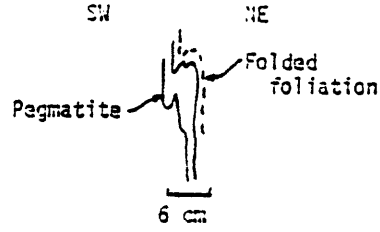

Figure 16.--Minor fold involving pegmatite; the axis is parallel to the strike of the foliation in biotite quartzite in the Fog Mountain-Selway River subarea west of the Idaho batholith.

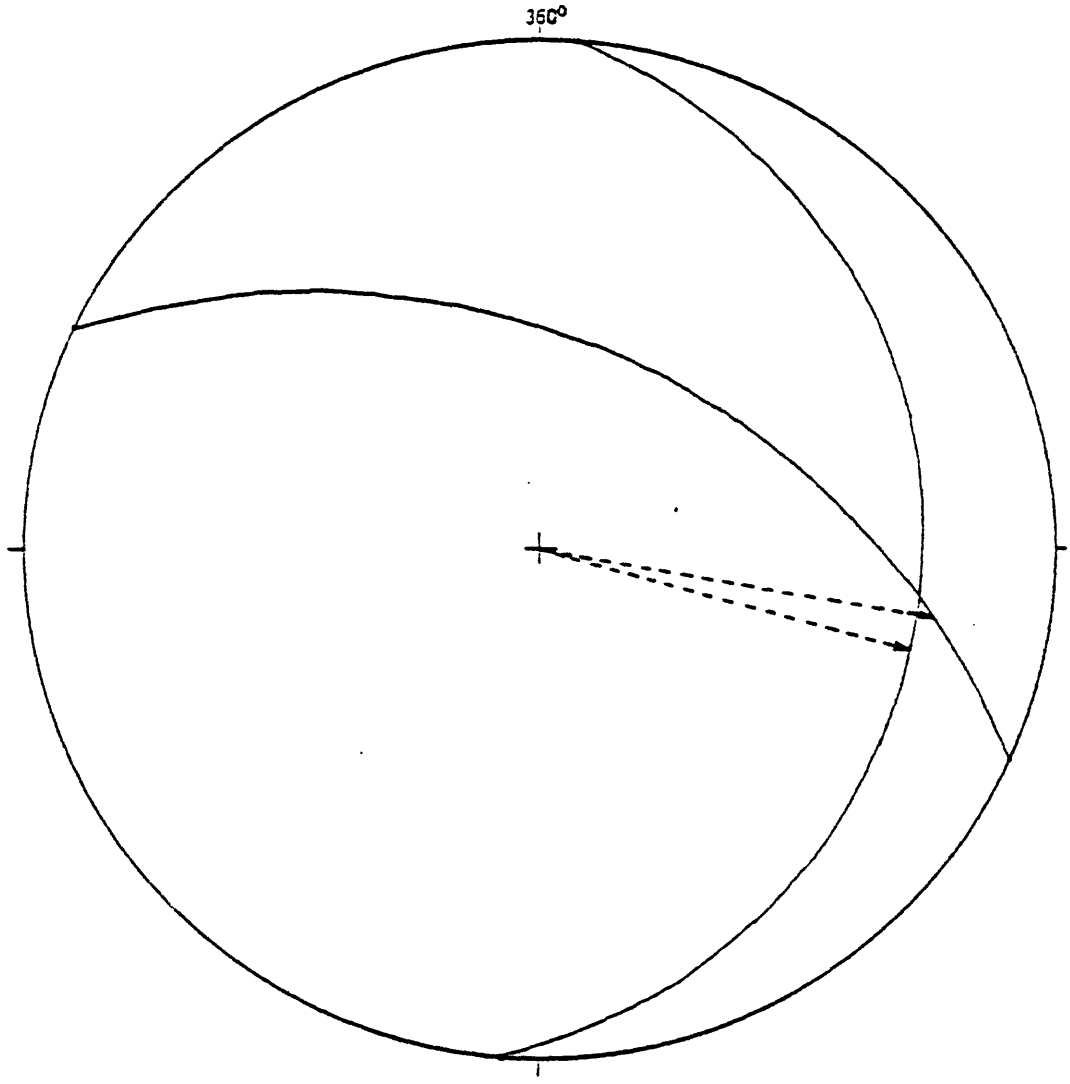

Figure 17.--Two shears in the Vermillion Peak quadrangle, non-parallel, with nearly parallel muscovite lineation and healed quartz slickensides, shown by the dashed lines. Data are plotted on lower hemisphere of Wulff stereonet.

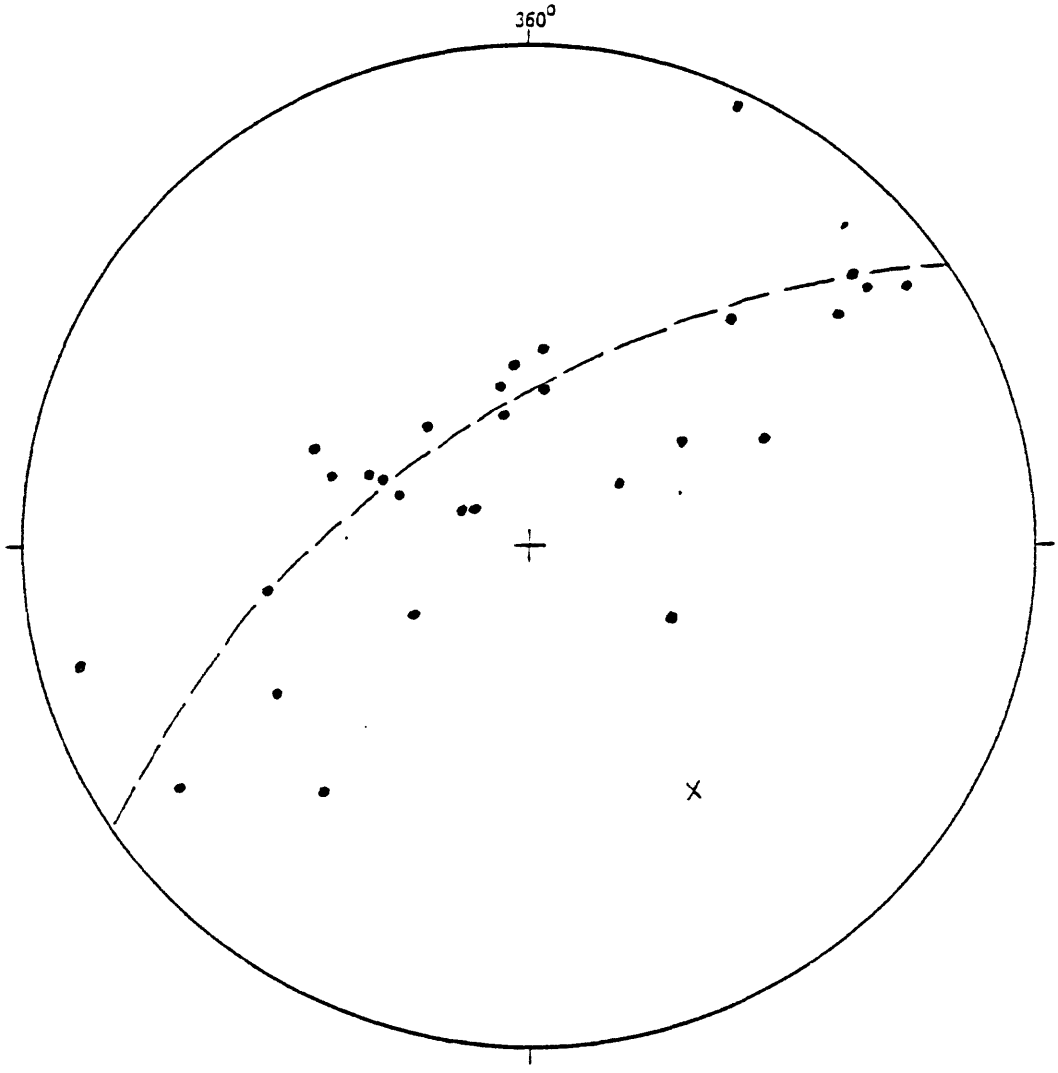

Figure 18.--Poles (•) to bedding and bedding-parallel schistosity and foliation in biotite quartzite in the Vermillion Peak quadrangle, just west of the Bitterroot lobe of the Idaho batholith. The pole (X) to the large-circle girdle defined by bedding/schistosity poles defines the average fold axis, oriented 30° 146° az. Data are plotted on lower hemisphere of Wulff stereonet.

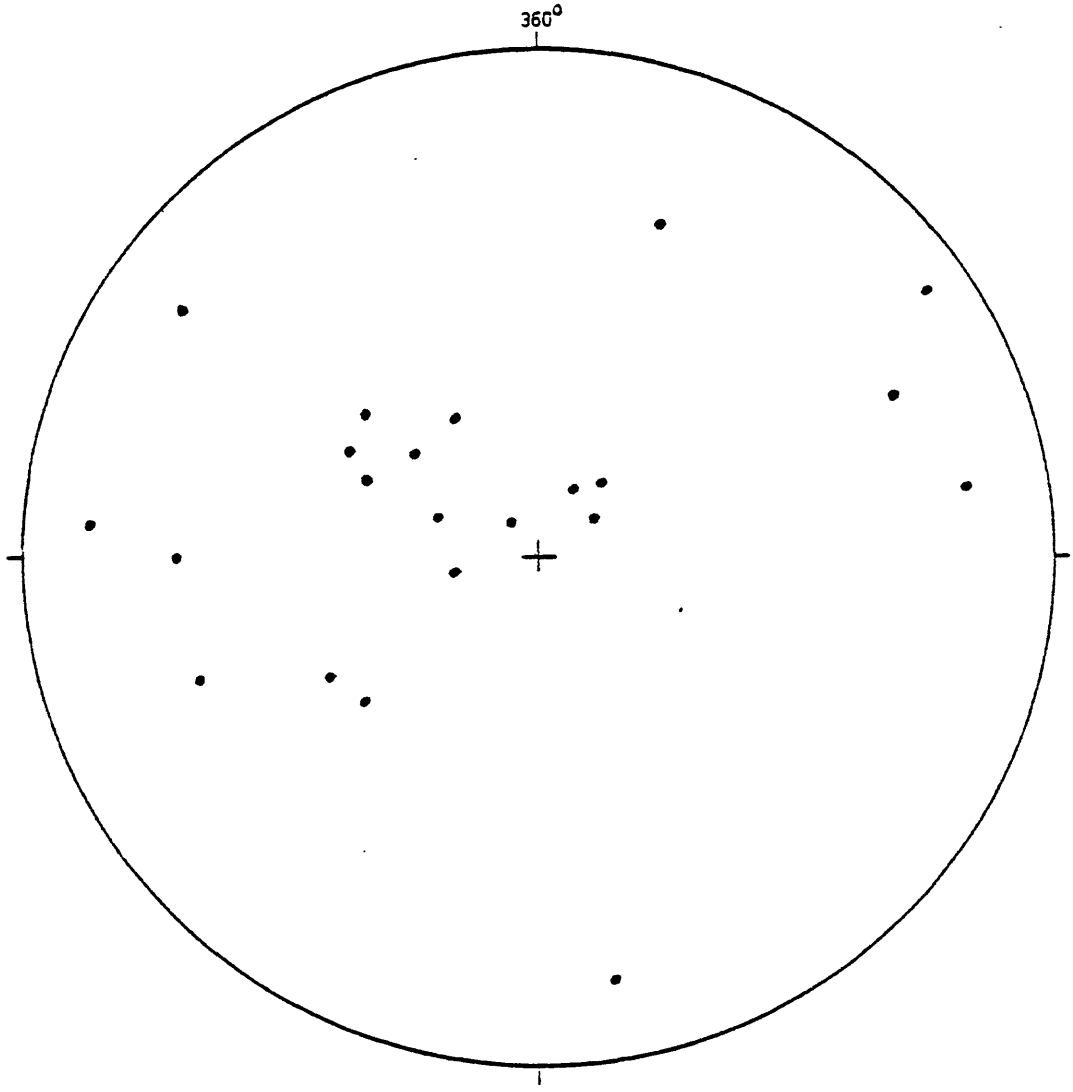

Figure 19.--Poles (•) to foliation in biotite quartzite, schist, and gneiss, plotted on lower hemisphere of Wulff stereonet. Fog Mountain area, south of Selway River.

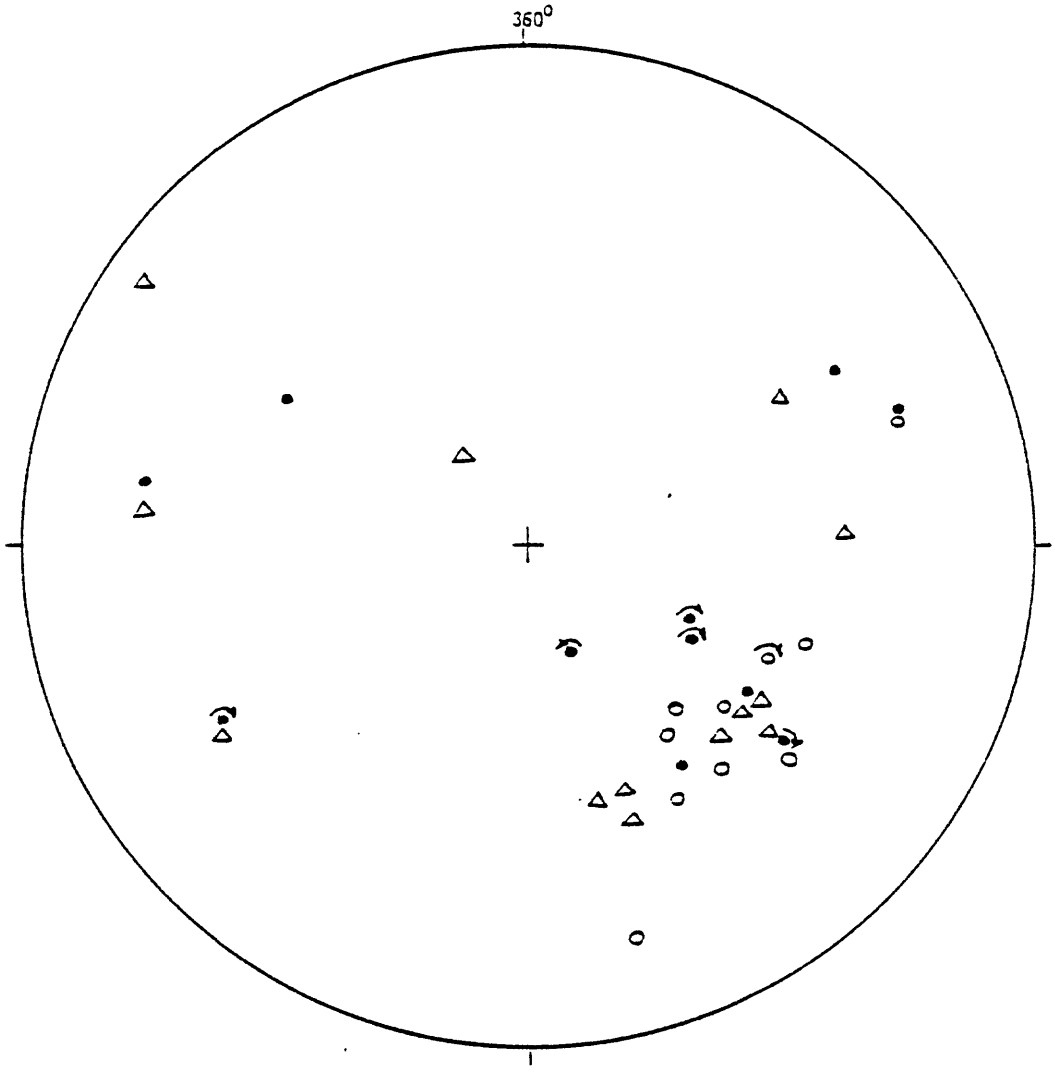

Figure 20.--Minor fold axes (•), probably of both D_1 and D_2 ages (not distinguishable with certainty); small arrows show sense of rotation. Kink and crenulation fold axes (O) of late D_2 or D_3 age and lineations (Δ) including stretched mica, hornblende, boudin axes, and $\underline{s}_0/\underline{s}_1$ intersections. All from the Vermillion Peak quadrangle. Data are plotted on lower hemisphere of Wulff stereonet.

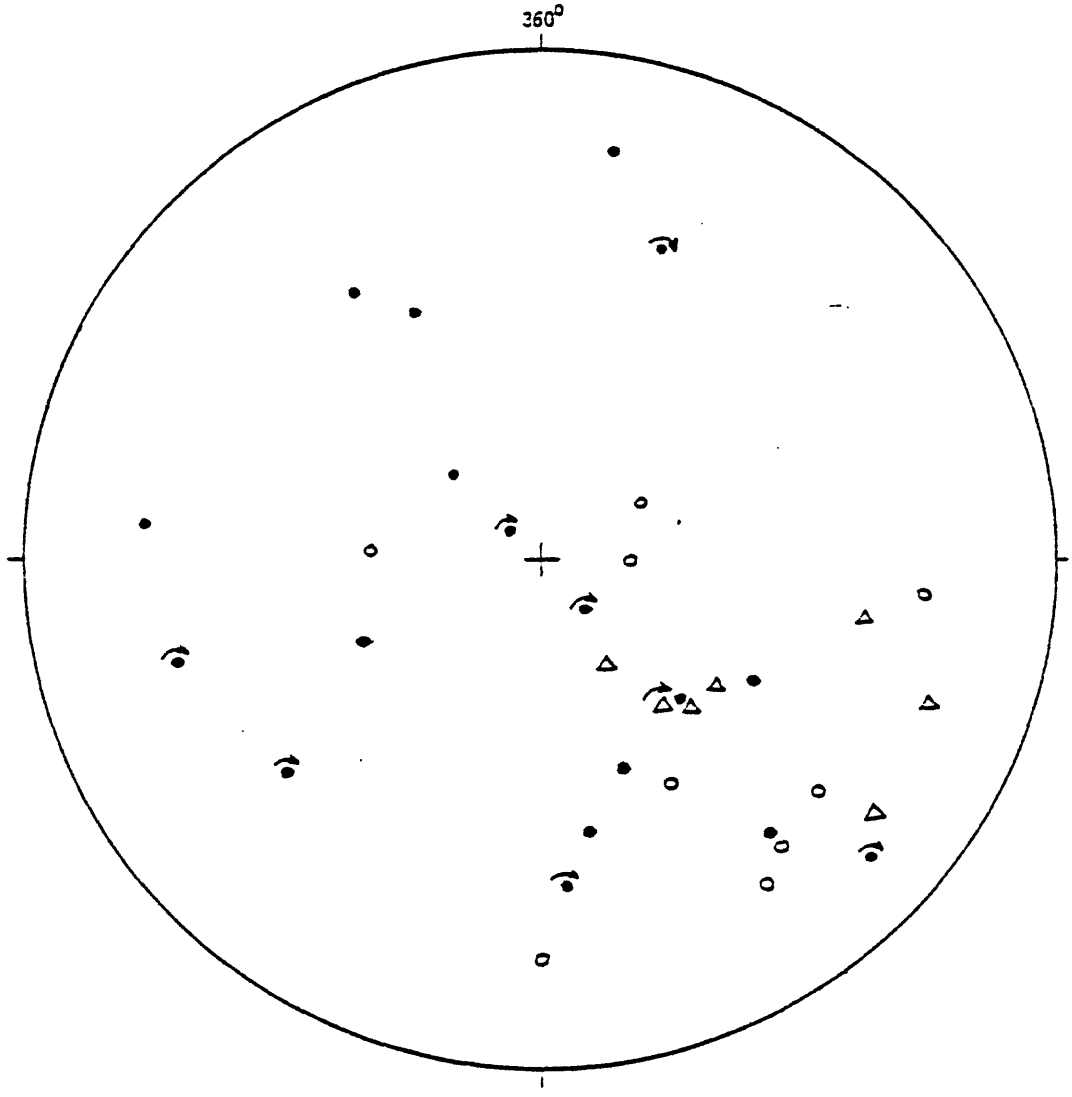

Figure 21.--Minor fold axes (●), probably including both D_1 and D_2 folds; small arrows show the sense of rotation. Some boudins and rods parallel to fold axes are included. Mineral lineations (○). Kink and crenulation fold axes (△) are probably late D_2 or D_3. Fog Mountain area south of Selway River. Data are plotted on lower hemisphere of Wulff stereonet.

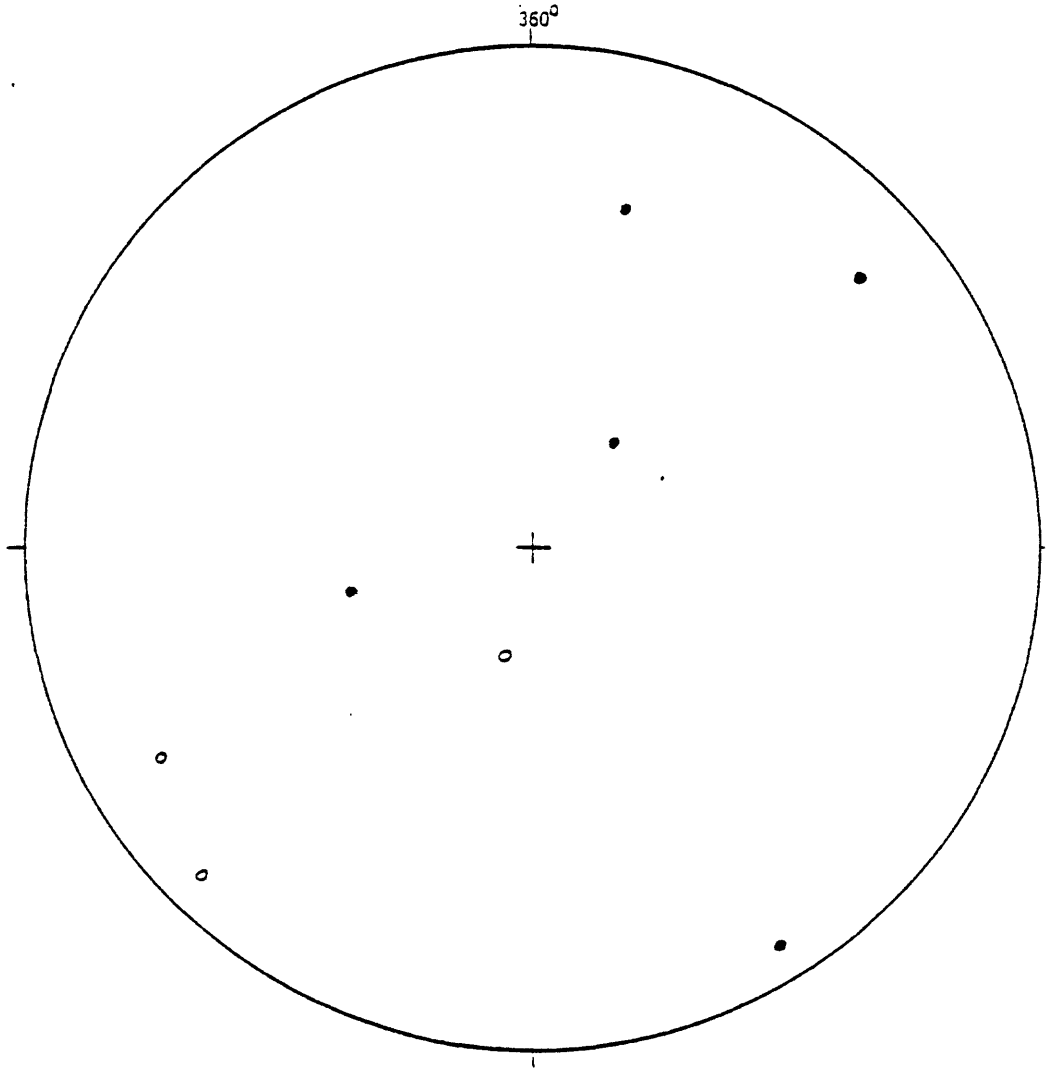

Figure 22.--Poles (●) to axial planes and axial-plane schistosity $\underline{s}_2$ and poles (O) to axial planes of crenulation folds (probably of late D_2 or D_3 age) in the Vermillion Peak quadrangle. Data are plotted on lower hemisphere of Wulff stereonet.

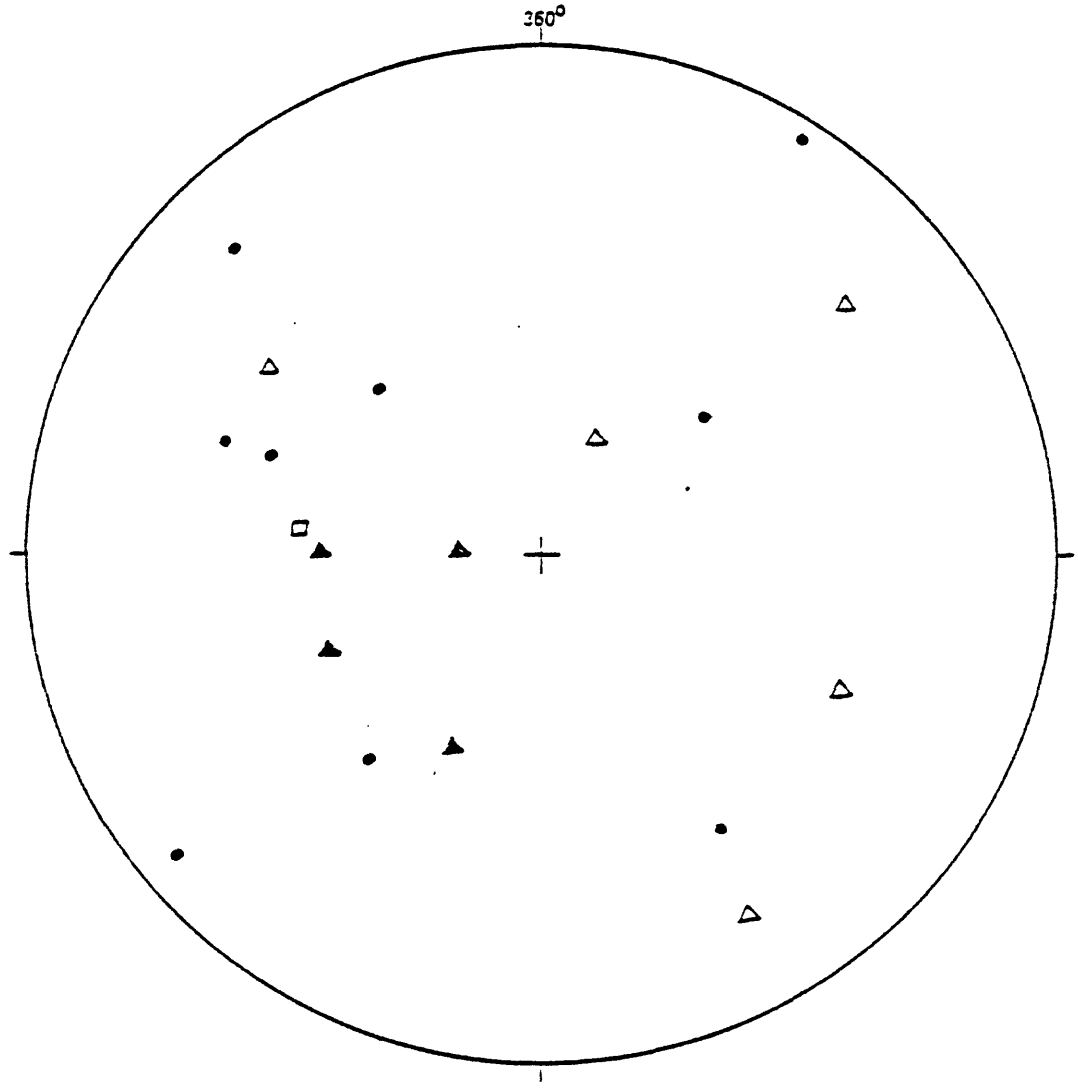

Figure 23.--Poles to joints (●), to a Tertiary dike (○), to pegmatite dikes (△), to faults (▲), and to a quartz vein (□) in the Vermillion Peak and Fog Mountain areas south of Selway River, west of the Bitterroot lobe of the Idaho batholith. Data are plotted on lower hemisphere of Wulff stereonet.

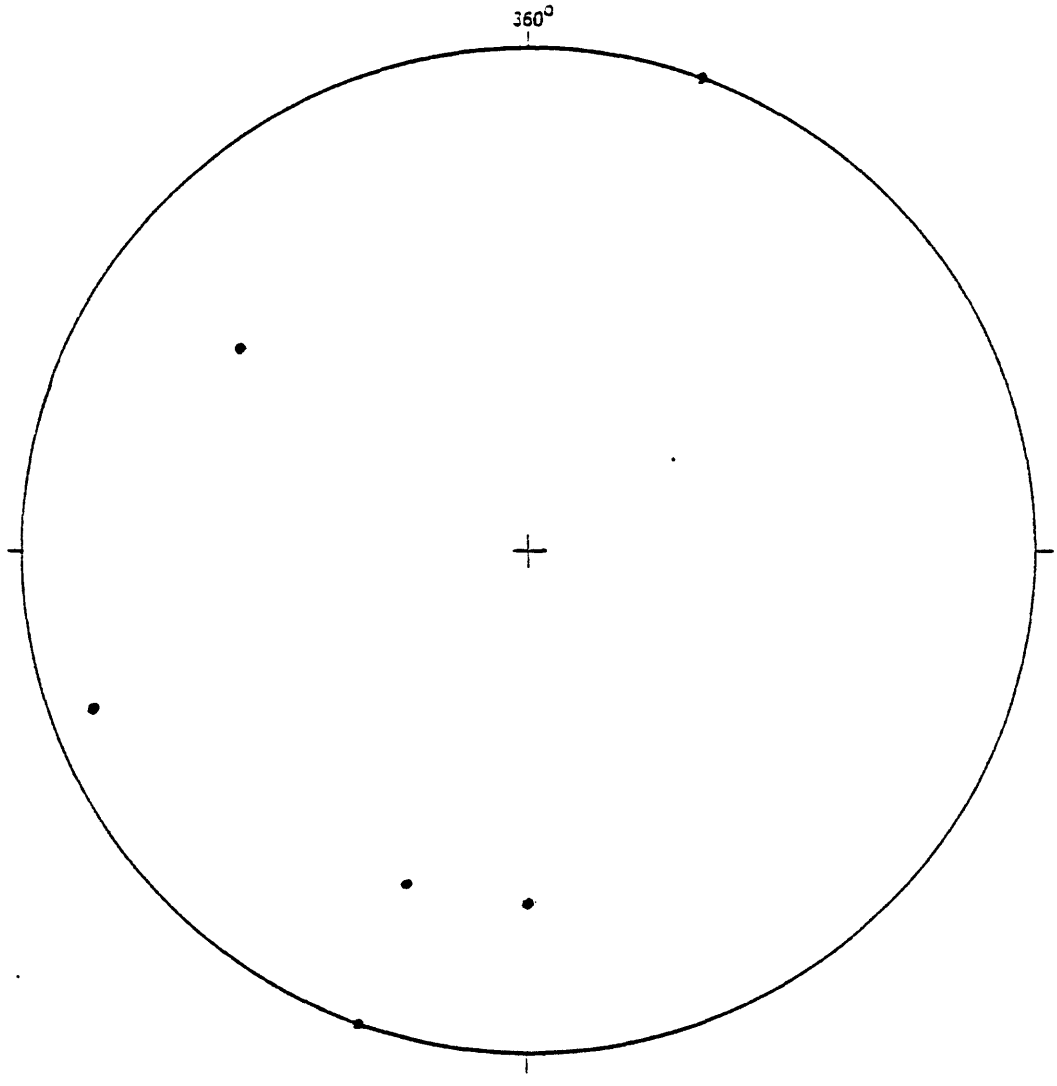

Figure 24.--Poles to flow foliation (•) in tonalitic gneiss west of the Idaho batholith in the Chimney Peak quadrangle. Data are plotted on lower hemisphere of Wulff stereonet.

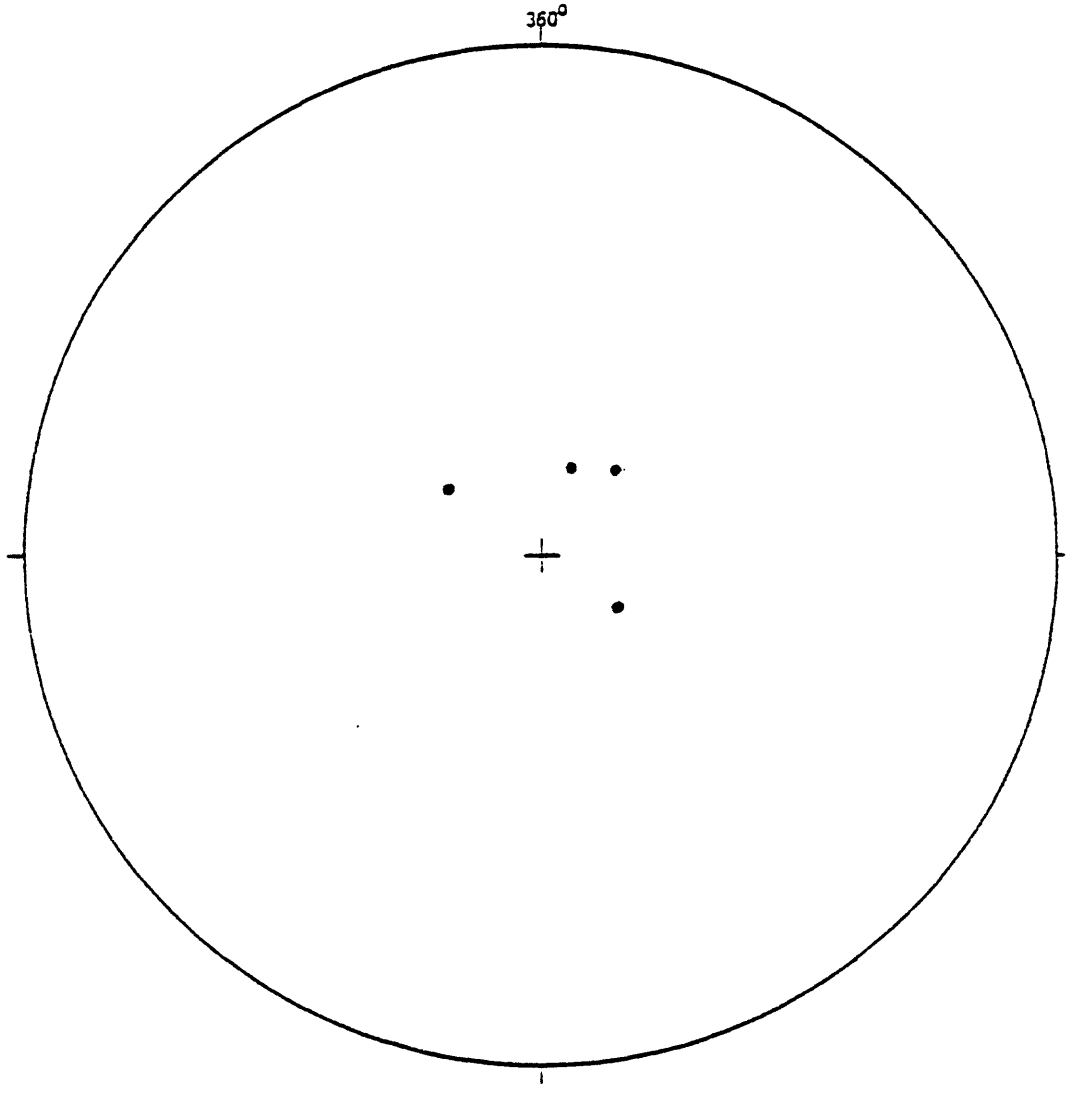

Figure 25.--Lineations (●) (minor fold axes and biotite streaks) in tonalitic gneiss west of the Idaho batholith in the Chimney Peak quadrangle. Data are plotted on lower Hemisphere of Wulff stereonet.

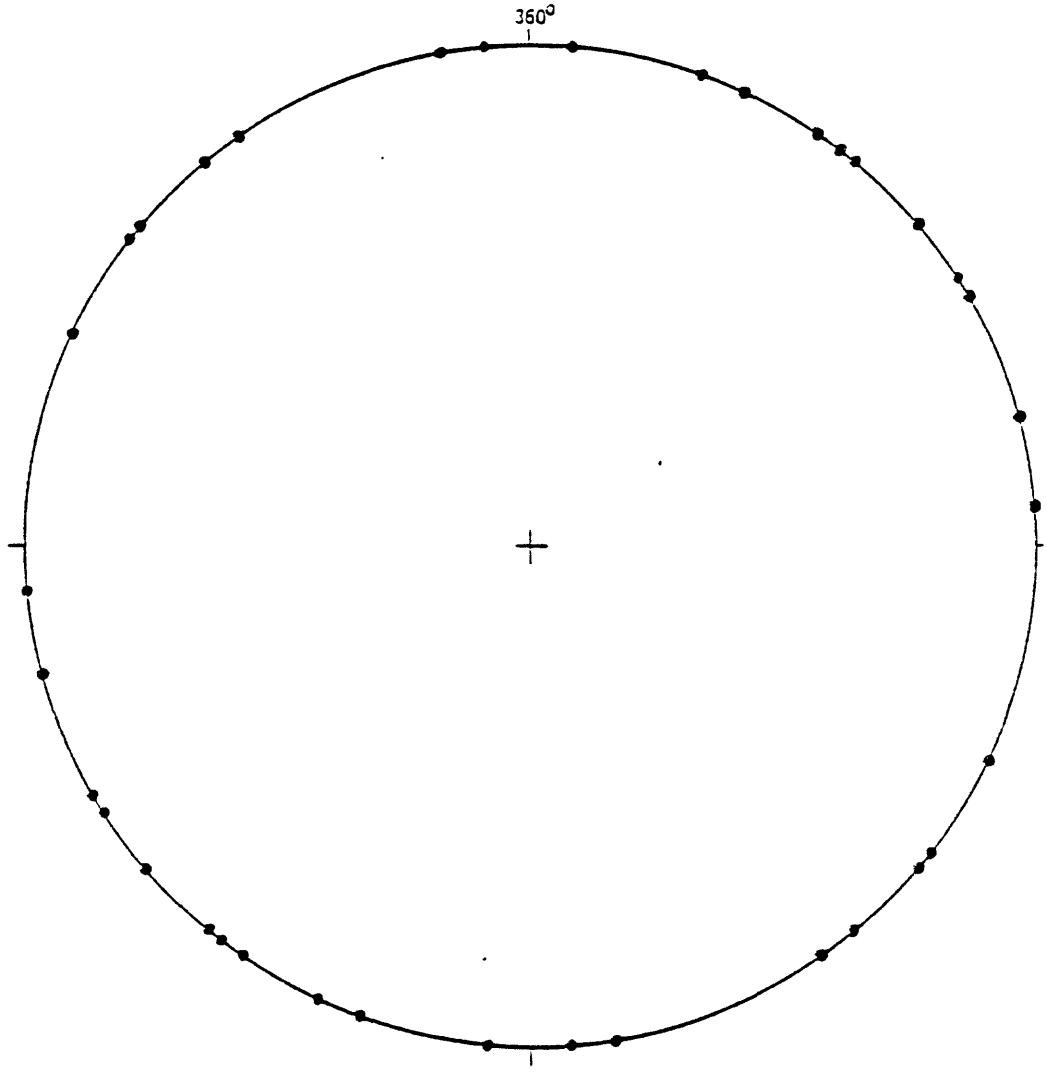

Figure 26.--Poles to axial planes of small folds (●) at one locality in tonalitic gneiss west of the Idaho batholith in the Chimney Peak quadrangle Data are plotted on lower hemisphere of Wulff stereonet.

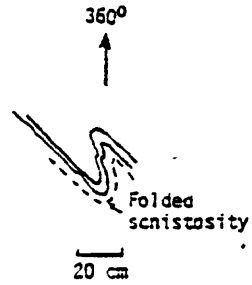

Figure 27.—Small folds plunging nearly vertically, involving alaskitic trondhjemite sheets in the tonalitic gneiss west of the Idaho batholith in the Chimney Peak quadrangle.

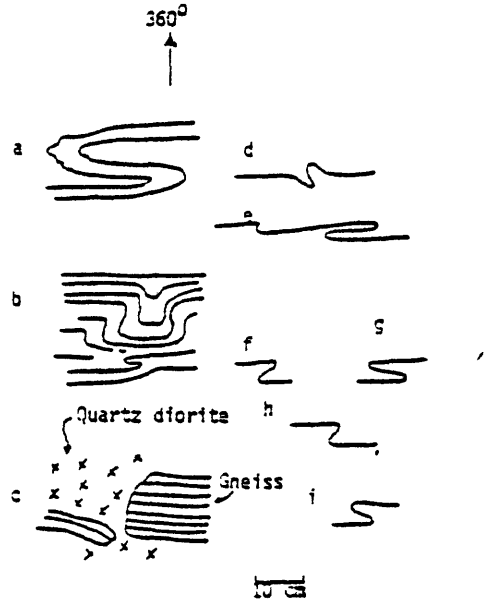

Figure 28.--Varied axial-planar orientation in vertically plunging minor folds in tonalitic gneiss west of the Idaho batholith in the Chimney Peak quadrangle. Fold a is a folded trondhjemitic layer in the gneiss. Folds b, d, e, f, g, h, and i all show variations of folded foliation in the tonalitic gneiss. Sketch c shows partial disruption of the tonalitic gneiss by intrusive quartz diorite or tonalite.

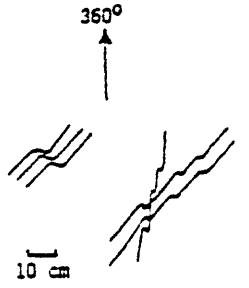

Figure 29.--Varied flow trends and styles in tonalitic gneiss west of the Idaho batholith in the Chimney Peak area. The small structures shown occur close together in the same outcrop and plunge nearly vertically.

porphyritic rocks, the percentage of phenocrysts was measured at the outcrop and the results combined with thin section and stained slab measures of the matrix. Anywhere from 200 to 1,600 points per specimen were counted depending on grain size and inhomogeneity of the rocks.

The rocks of category (a) comprise biotite-plagioclase schist and quartzite, muscovite-biotite plagioclase schist, and biotite-muscovite schist and quartzite. Modes are given in table 1 (modes 1-14 and 16-20) and table 2. The modal content of quartz in the rocks of category (a) ranges from 31 to 60 percent. Quartz occurs in granoblastic grains in two populations. First is in 2 to 4 mm platy grains parallel to the schistosity and elongate within the schistosity parallel to other mineral lineations. These grains enclose oriented biotite, muscovite, and fibrolite, and are cut by a-c extension fractures spaced at 0.3 to 0.7 mm intervals. Second is in 0.3 to 0.5 mm irregular grains. Most grains show undulatory extinction.

The modal content of plagioclase in the rocks of category (a) ranges from zero to 25%. Plagioclase is unzoned in granoblastic grains and ranges from An_{20} to An_{30} in 0.5 to 1 mm grains. Clay alteration is minor but pervasive.

The modal content of biotite in rocks of category (a) ranges from 1 to 19%. Biotite is lepidoblastic in 0.3 to 2 mm grains. Most biotite is in stretched, elongate grains or clusters of grains streaked out in a lineation. Pennine alteration is varied, weak to strong. Some biotite is in vermiform intergrowths with quartz.

The modal content of muscovite in the rocks of category (a) ranges from zero to 39%. Muscovite is in 0.1 to 0.3 mm flakes replacing biotite, and the grains are mostly of random orientation. Some muscovite is in vermiform intergrowths with quartz.

The modal content of sillimanite in rocks of category (a) ranges from 2 to 13%; sillimanite occurs in only a few of the rocks. Representative prisms are 0.03x0.15 mm and oriented parallel to other mineral lineations in the rock. Prisms are commonly broken and stretched parallel to their length.

Microcline makes from 0.7 to 22% of those rocks in which it occurs; it is absent in several. Where biotite abuts microcline, biotite is commonly replaced by a rind of muscovite. Microcline grains are platy parallel to the foliation and are elongate in the foliation parallel to other mineral lineations (e.g., 1.5x4 mm as seen in an a-b section). Sillimanite is mostly absent in microcline grains where they are found in the same rock, and the few grains that are found in microcline are mere shreds that appear to be undergoing replacement. Microcline encloses small, oriented biotite flakes. It is cut by a-c extension fractures spaced at 0.1 to 0.2 mm intervals. The stained slabs show microcline to be concentrated in certain folia.

Garnet (1%) occurs in 0.3 mm grains in a single thin section and is partly altered to chlorite.

Accessory minerals include magnetite (elongate grains parallel to other mineral lineation), zircon, baddeleyite, thorite, apatite, epidote (tr), and schorlite (minor, in one thin section).

The modal content of quartz in category (b), calc-silicate gneiss and quartzite, ranges from none to 52%. Modes are given in table 1 (modes 21 to 23) and table 3 (modes 34 to 38). Quartz occurs in irregularly granoblastic 0.5 mm grains, or partly in elongate, flattened blebs parallel to the other mineral lineation.

The modal content of plagioclase in the calc-silicate rock is 26 to 28%. Plagioclase occurs in granoblastic, non-zoned 1 mm grains, partly as elongate plates parallel to other mineral lineation. Plagioclase composition ranges from An_{25} to An_{43} in different rocks.

Biotite (24%) occurs in one rock studied, in elongate grains and grain clusters parallel to other mineral lineation. Grains average 1 mm diameter. Microcline is minor in 0.5 mm interstitial grains.

Hornblende (11% to 16%) occurs in lineated prisms lying in the foliation. Diopside prisms are similarly alined, partly to strongly replaced by hornblende. Scapolite occurs in one rock (29%), in granoblastic 0.5 mm grains.

TONALITE OF THE SOUTHWESTERN BATHOLITH

Structure

The country rock of quartzite, calc-silicate gneiss, and tonalitic gneiss is invaded by quartz diorite to tonalite. The intrusive unit has strong flow foliation of varied attitudes (fig. 30) that averages a northerly trend, a 70° westerly dip, and is yet rather swirled. Flow lineation consisting of oriented hornblende prisms plunges down the dip of the flow foliation (fig. 31). Dark inclusions are drawn out in elongate spindles parallel to the hornblende lineation and are also flattened in the plane of the flow foliation; such inclusions are rare.

Pegmatite, alaskite, and aplite occur in dikes in the quartz diorite to tonalite unit, displaying no particular orientation in the steeply dipping ones (fig. 32) but a marked preferred orientation in the shallow-dipping dikes or sheets (fig. 33). The shallow-dipping sheets, mostly trondhjemitic, trend in a northerly direction and dip about 20° easterly in a somewhat en echelon manner. Pegmatite dikes are up to 4 m thick, and some of them have central zones up to 3 m thick of massive white quartz. Massive white quartz also cores some of the alaskite and aplite sheets. Some shallow-dipping sheets are entirely of massive white quartz.

Fenn Mountain area farther into the batholith is underlain principally by biotite tonalite, which extends from the south edge of the map to the migmatite zone of Old Man Creek and partly beyond nearly to Stanley Butte. Granite injects the tonalite-migmatite complex irregularly (Toth, 1983). It is not clear whether this biotite tonalite is a separate pluton from the hornblende-to-hornblende-biotite tonalite and quartz diorite of the Chimney Peak area. No sharp contact between the two rock types was seen, and the two rocks are lumped in a single unit on the geologic map.

Migmatite screens trend 280° to 290° az through the tonalite and quartz diorite of the Crags area. The southerly migmatite screens are zones of intermixed tonalite to quartz diorite with sheets of metasedimentary and metaigneous rock up to aggregate thicknesses of a kilometer or so. The northerly ones also contain granite and granodiorite in addition to tonalite; their thicknesses are also about one kilometer. Four such screens are major in the Crags area.

Table 1.--Modes in the Vermillion Peak quadrangle (EG1)

(1) Orthoclase-biotite-plagioclase quartzite 79RR131A. (2) K-feldspar quartzite 79RR131B. (3) Quartzite 79RR133A. (4) Plagioclase quartzite 79RR135A. (5) Biotite-plagioclase quartzite 79RR136A. (6) Quartzite 79RR139A. (7) Muscovite quartzite 79RR141A. (8) Muscovite quartzite 79RR142A. (9) Plagioclase-biotite-muscovite quartzite 79RR143A. (10) Plagioclase quartzite 79RR144A. (11) Plagioclase-biotite-muscovite quartzite 79RR145A. (12) Biotite-muscovite quartzite 79RR147A. (13) Microcline quartzite 79RR160A. (14) Plagioclase-biotite quartzite 79RR165A. (15) Quartz diorite sheet in plagioclase-biotite quartzite 79RR165A. (16) Biotite quartzite 79RR167A. (17) Biotite-plagioclase quartzite 79RR169A. (18) Plagioclase-biotite quartzite 79RR224A. (20) Plagioclase quartzite 79RR226A. (21) Calc-silicate schist 79RR138A. (22) Calc-silicate granofels 79RR165B. (23) Calc-silicate gneiss 79RR167B. (24) Granodiorite sheet in quartzite 79RR165A.

	1	2	3	4	5	6	7	8	9	10	11	12	13	14	15	16	17	18	19	20	21	22	23	24
Plagioclase	13.5	2.8	6.0	18.3	24.0	9.4	0.7	5.8	10.0	16.0	16.0	5.7	9.5	14.0	53.0	5.3	23.8	10.8	30.9	6.3		47.6	9.9	43.8
Quartz	56.0	65.6	85.3	74.9	53.4	79.8	82.9	68.3	49.6	65.9	46.8	67.0	48.7	64.5	3.6	71.0	56.1	72.8	61.8	36.5		19.2	35.2	30.1
K-spar	11.3	26.6				0.7			1.8				22.2				8.6	3.9			10.0		1.6	20.3
Biotite	12.4			3.6	22.0	3.8		8.3	12.4	8.4	16.7	11.7	11.1	20.9	24.4	16.9	10.6	12.2	4.4	16.8				4.6
Muscovite	6.4	3.9	8.7	0.5		5.6	16.3	17.6	25.8	9.5	20.4	15.2	3.8		18.4	1.8	0.9	0.2	1.1	40.3				
Andalusite													1.8											
Hornblende																						14.0		
Diopside																					10.0	13.4	0.3	
Scapolite																					29.1			
Sillimanite																4.5								
Actinolite																					49.8		38.1	
Epidote																						1.7	11.8	
Garnet																							0.3	
Accessories	0.4	1.2	tr	2.7	0.6	0.7	tr	tr	0.4	0.2	tr	0.4	3.0	0.6	0.5	0.5	tr	tr	1.7	0.2	1.0	4.1	2.6	1.3
	100.0	100.0	100.0	100.0	100.0	100.0	99.9	100.0	100.0	100.0	99.9	100.0	100.1	100.0	99.9	100.0	100.0	99.9	99.9	100.1	99.9	100.0	99.8	100.1

Table 2.--Modes in the Fog Mountain quadrangle (HG8)

(1) Tonalitic gneiss 78RR044B. (2) Tonalite 78RR225B. (3) Tonalite 78RR298A. (4) Trondhjemite (alaskite) 78RR283G. (5) Granite 79RR159A. (6) Sillimanite-biotite-plagioclase-microcline quartzite 78RR016A. (7) Plagioclase-muscovite-biotite quartzite 78RR277B. (8) Plagioclase quartzite 78RR282B. (9) Biotite-muscovite-sillimanite quartzite 78RR283B. (10) Muscovite quartzite 78RR286A. (11) Muscovite-biotite quartzite 78RR293B. (12) Plagioclase quartzite 78RR196A. (13) Plagioclase-biotite-muscovite quartzite 79RR148A. (14) Muscovite quartzite 79RR148B. (15) Sillimanite-biotite-plagioclase quartzite 79RR149A. (16) Plagioclase quartzite 79RR150A. (17) Biotite-muscovite quartzite 79RR151A. (18) Plagioclase-biotite-muscovite quartzite 79RR152A. (19) Plagioclase-muscovite quartzite 79RR153A. (20) Microcline quartzite 79RR155A. (21) Biotite-muscovite-plagioclase quartzite 79RR156A. (22) Biotite-muscovite quartzite 79RR228A. (23) Muscovite quartzite 79RR229A. (24) Biotite-muscovite quartzite 79RR232. (25) Muscovite quartzite 79RR232A. (26) Biotite-plagioclase quartzite 79RR235A. (27) Plagioclase quartzite 79RR238A. (28) Muscovite-plagioclase-biotite quartzite 79RR300A. (29) Sillimanite mica schist 79RR230.

	1	2	3	4	5	6	7	8	9	10	11	12	13	14	15	16	17	18	19	20	21	22	23	24	25	26	27	28	29
Plagioclase	49.6	29.1	63.4	55.4	26.0	13.4	18.2	22.5	6.2	0.4		25.1	10.0	8.3	30.6	12.3	9.2	11.0	10.4	2.8	22.0	2.7	0.9	7.5	3.9	26.4	17.3	12.7	1.9
Quartz	22.5	63.2	20.0	37.8	26.0	57.4	57.7	57.8	57.3	59.3	51.1	60.0	56.7	53.2	32.1	69.0	52.1	61.8	69.1	63.4	44.7	52.7	66.8	52.6	67.2	55.6	74.3	60.9	39.1
K-spar			5.5		46.3	15.9						1.1	2.8				1.1	1.4		18.7				6.2					
Biotite	13.9	6.4	9.8	1.4	1.4	6.6	10.2	5.9	10.7	9.8	26.1	6.7	11.0	8.6	16.2	7.2	11.2	12.4	3.9	3.7	10.3	15.7	3.0	12.1	7.2	10.0	3.5	15.4	27.5
Muscovite				5.4		1.7	12.7	8.8	11.6	28.2	20.4	6.3	19.2	28.3	3.7	9.9	25.9	12.5	15.0	5.7	21.0	28.7	28.9	20.5	21.7	7.4	4.4	10.4	20.5
Hornblende					tr																								
Diopside																													
Scapolite																													
Sillimanite						4.6			13.1		2.4				15.7			0.3		3.9	1.0			0.3				0.6	10.5
Epidote																													
Garnet										1.6																			
Accessories	9.8	1.2	1.4	tr	0.2	0.4	1.2	4.9	1.2	0.8	tr	0.7	0.2	1.4	1.7	1.5	0.5	0.5	1.6	1.8	1.0	0.2	0.2	0.8	tr	0.7	0.4	tr	0.4
	99.9	99.9	100.1	100.0	99.9	100.0	100.0	99.9	100.1	100.1	100.0	99.9	99.9	99.8	100.0	99.9	100.0	99.9	100.0	100.0	100.0	100.0	99.8	100.0	100.0	100.1	99.9	100.0	99.9

Table 3.--Modes in the Chimney Peak quadrangle (HF7)

(1) Tonalitic gneiss 78RR055A. (2) Trondhjemite veinlets in tonalitic gneiss of (1) 78RR055A. (3) Tonalitic gneiss 78RR078B. (4) Foliated tonalite injected in tonalitic gneiss 78RR078F. (5) Tonalitic gneiss 79RR198A. (6) Tonalitic gneiss 79RR199A. (7) Tonalitic gneiss 79RR201A. (8) Tonalite 78RR078B. (9) Tonalite 78RR086B. (10) Tonalite 79RR191A1. (11) Tonalite 79RR192A. (12) Blastomylonite after tonalite 79RR193A. (13) Tonalite 78RR092B. (14) Tonalite 78RR157A. (15) Tonalite 78RR174B. (16) Tonalite 78RR227A. (17) Spindled diorite xenoliths in tonalite 78RR086F. (18) Tonalite xenolith in tonalite 79RR191A2. (19) Granitic gneiss 79RR194A. (20) Alaskite sheet folded in granitic gneiss 79RR204E. (21) Granitic gneiss 79RR205. (22) Granitic gneiss 79RR205A. (23) Granite 78RR240B. (24) Granite 78RR203B. (25) Granite 78RR202B. (26) Granite 78RR164B. (27) Granite 78RR090B. (28) Leucogranodiorite 78RR228B. (29) Granodiorite 79RR206A. (30) Granitic alaskite 78RR064B. (31) Trondhjemite 78RR064F. (32) Trondhjemite 78RR076E. (33) Quartz diorite gneiss or amphibolite 79RR202B. (34) Calc-silicate gneiss 78RR050B. (35) Calc-silicate gneiss 78RR091A. (36) Calc-silicate quartzite 78RR176B. (37) Calc-silicate gneiss 78RR228F. (38) Plagioclase-muscovite-biotite schist 78RR240E. (39) Mica schist 78RR213A. (40) Plagioclase-bearing biotite quartzite 78RR064G. (41) Fine-grained, late biotite diorite 79RR191E.

	1.	2	3	4	5	6	7	8	9	10	11	12	13	14	15	16	17	18	19	20	21
Plagioclase	44.1	46.8	24.9	53.7	53.5	50.8	45.8	51.4	43.8	47.1	47.3	51.7	47.6	51.3	47.0	59.8	54.1	56.3	13.4	31.2	25.3
Quartz	25.6	46.3	56.8	24.7	22.1	31.2	25.8	21.7	18.7	21.2	19.3	30.6	20.9	29.7	27.6	22.9	2.1	20.1	39.4	29.6	30.5
K-spar										0.7		0.2			4.7			0.2	37.3	31.7	32.2
Biotite	15.6	5.4	18.2	21.2	13.6	16.8	19.3	17.1	21.3	15.0	24.4	16.7	25.8	17.7	13.6	15.6	19.4	15.3	7.0	5.4	11.2
Muscovite																			2.1	1.2	0.7
Hornblende	5.2				8.3		0.1	6.6	15.7	13.8	7.8		2.3		5.2		22.9	5.2			
Diopside																					
Scapolite																					
Accessories	9.4	1.5	0.1	0.4	2.5	1.2	1.0	3.1	0.5	2.1	1.1	0.8	3.3	1.4	1.9	1.7	1.6	2.9	0.7	0.9	tr
	99.9	100.0	100.0	100.0	100.0	100.0	100.0	99.9	100.0	99.9	99.9	100.0	99.9	100.1	100.0	100.0	100.1	100.0	99.9	100.0	99.9

	22	23	24	25	26	27	28	29	30	31	32	33	34	35	36	37	38	39	40	41
Plagioclase	28.8	42.1	18.2	33.1	15.9	34.6	54.2	44.9	28.3	49.7	57.6	47.4	28.6	8.1	28.1	25.8	16.4		18.8	75.1
Quartz	27.2	33.0	48.9	28.2	51.3	32.3	34.4	31.1	35.1	37.6	37.6	5.2	30.6	12.3	52.4			46.9	41.1	0.6
K-spar	35.9	23.4	16.8	32.0	18.6	26.7	11.4	20.2	23.5		1.0		1.2		1.1					1.8
Biotite	6.0	1.1	15.6	4.4	11.1	4.5		2.7		2.2	3.3	12.5	23.9		1.2		57.2	14.5	18.8	20.0
Muscovite	1.5							0.9	13.1	10.4							25.1	36.1	21.2	
Hornblende												34.9	10.9		15.5					
Diopside													4.0	59.5	0.1	42.6				
Scapolite														11.6		29.3				
Sillimanite																		0.3		
Accessories	0.6	0.4	0.6	2.2	3.1	1.9	tr	0.2	tr	tr	0.4	tr	0.6	8.4	1.4	2.4	1.3	2.2	0.2	2.5
	100.0	100.0	100.1	99.9	100.0	100.0	100.0	100.0	100.0	99.9	99.9	100.0	99.8	99.9	99.8	100.1	100.0	100.0	100.1	100.0

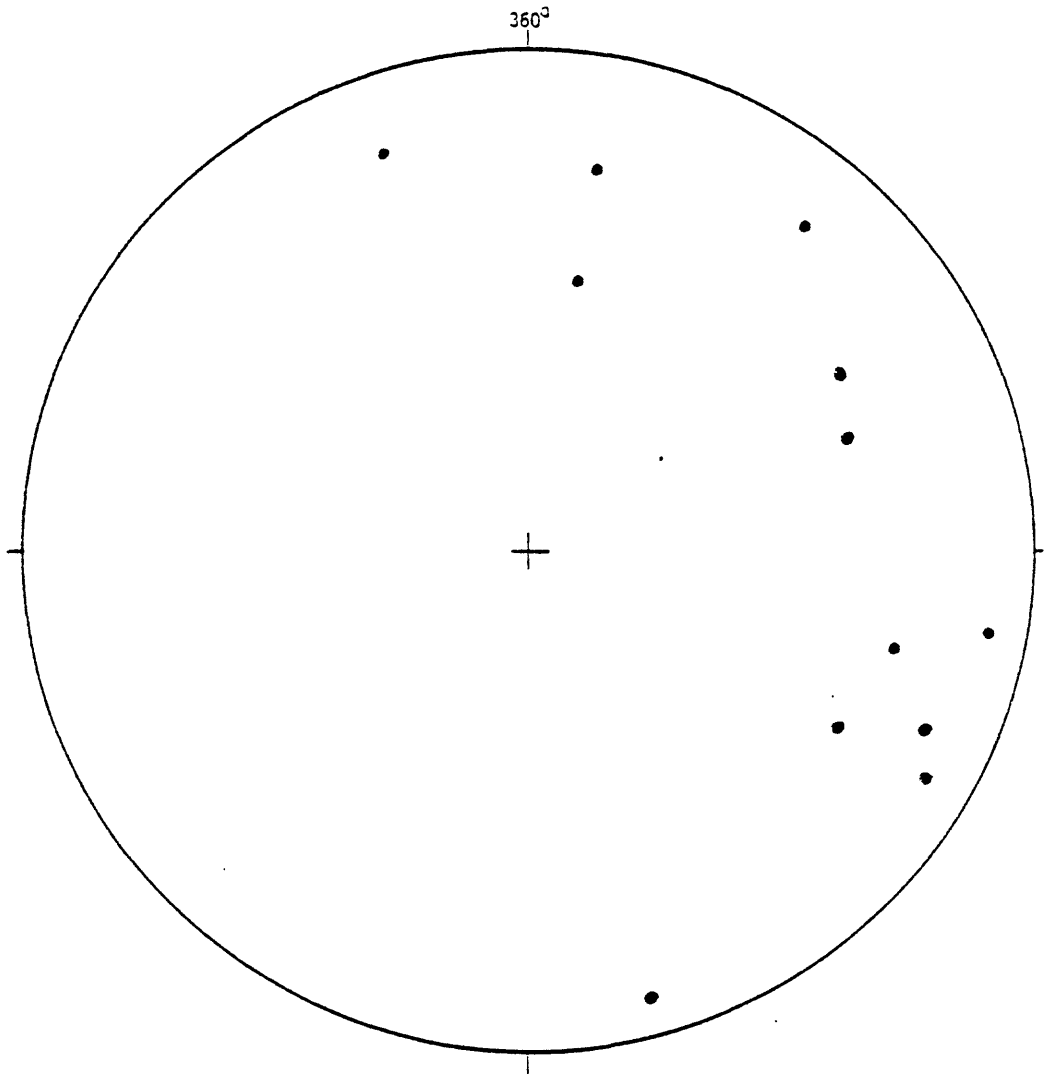

Figure 30.--Poles to flow foliation (●) in quartz diorite to tonalite near the western contact of the Idaho batholith in the Chimney Peak quadrangle. Poles plotted on lower hemisphere of Wullf stereonet.

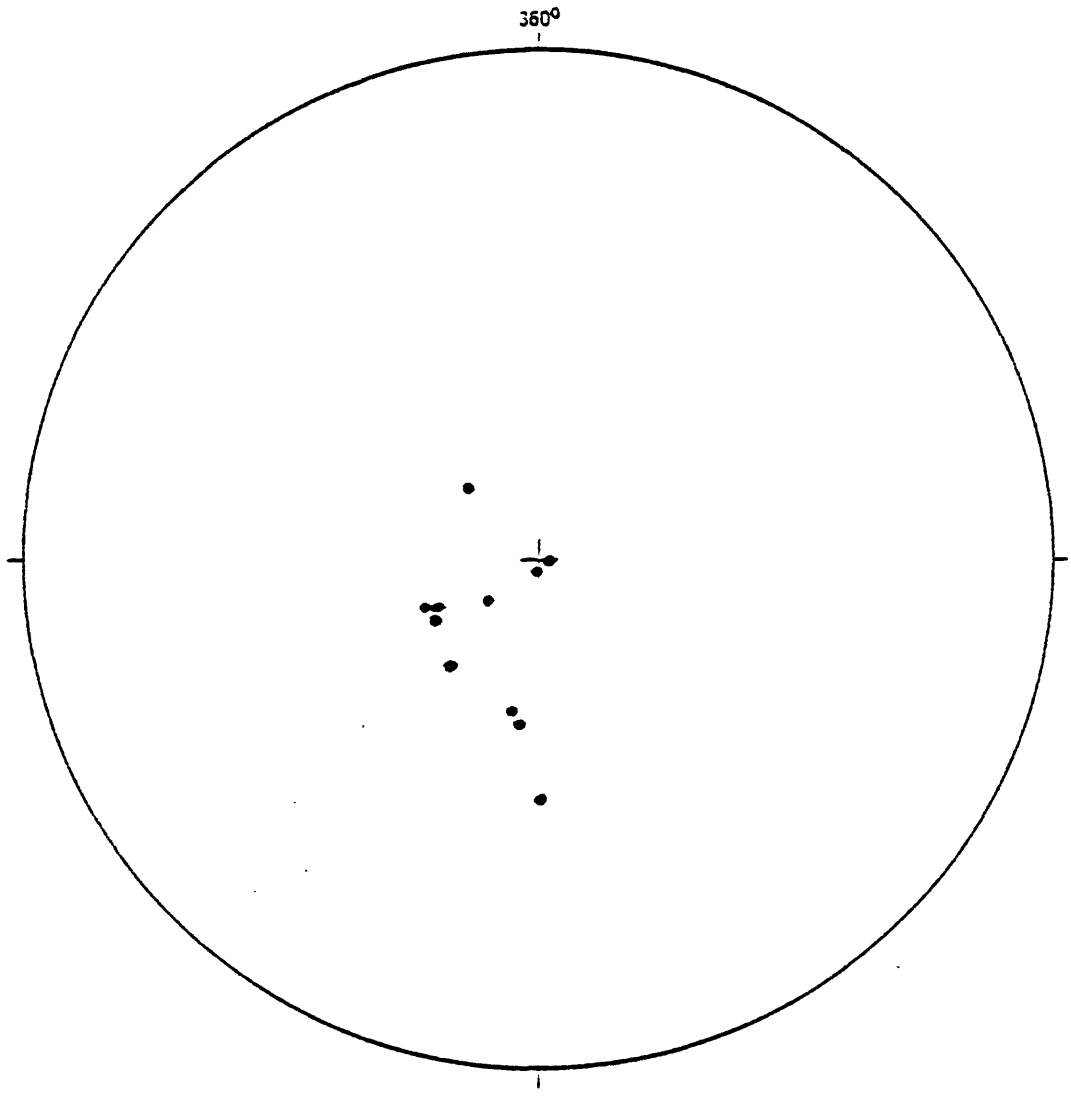

Figure 31.--Flow lineations (●) consisting of oriented hornblende prisms in quartz diorite to tonalite near the western contact of the Idaho batholith in the Chimney Peak quadrangle. Data are plotted on lower hemisphere of Wulff stereonet.

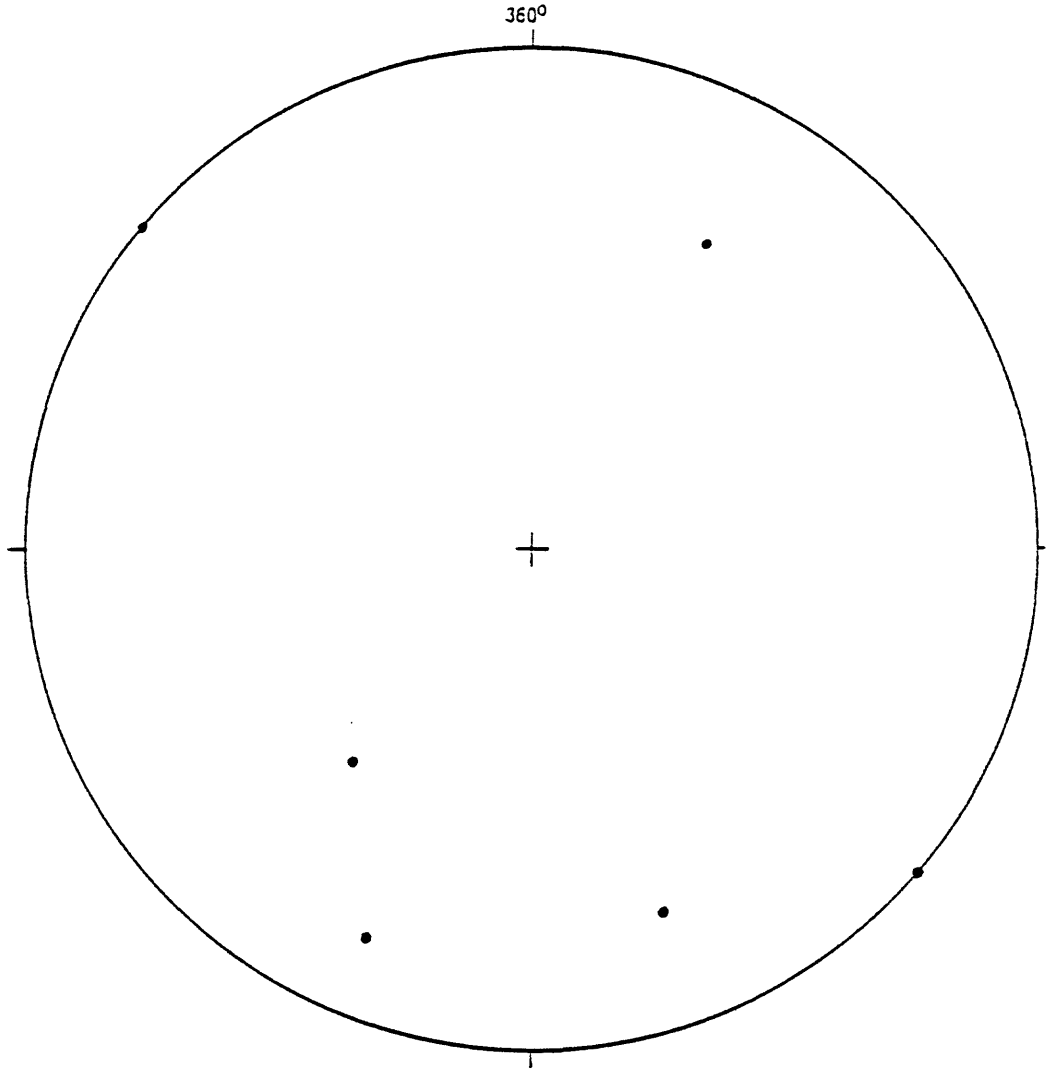

Figure 32.--Poles to pegmatite dikes (●) in quartz diorite to tonalite of the western Idaho batholith in the Chimney Peak quadrangle. The poles show steep dips and a wide range of strikes. Data are plotted on lower hemisphere of Wulff stereonet.

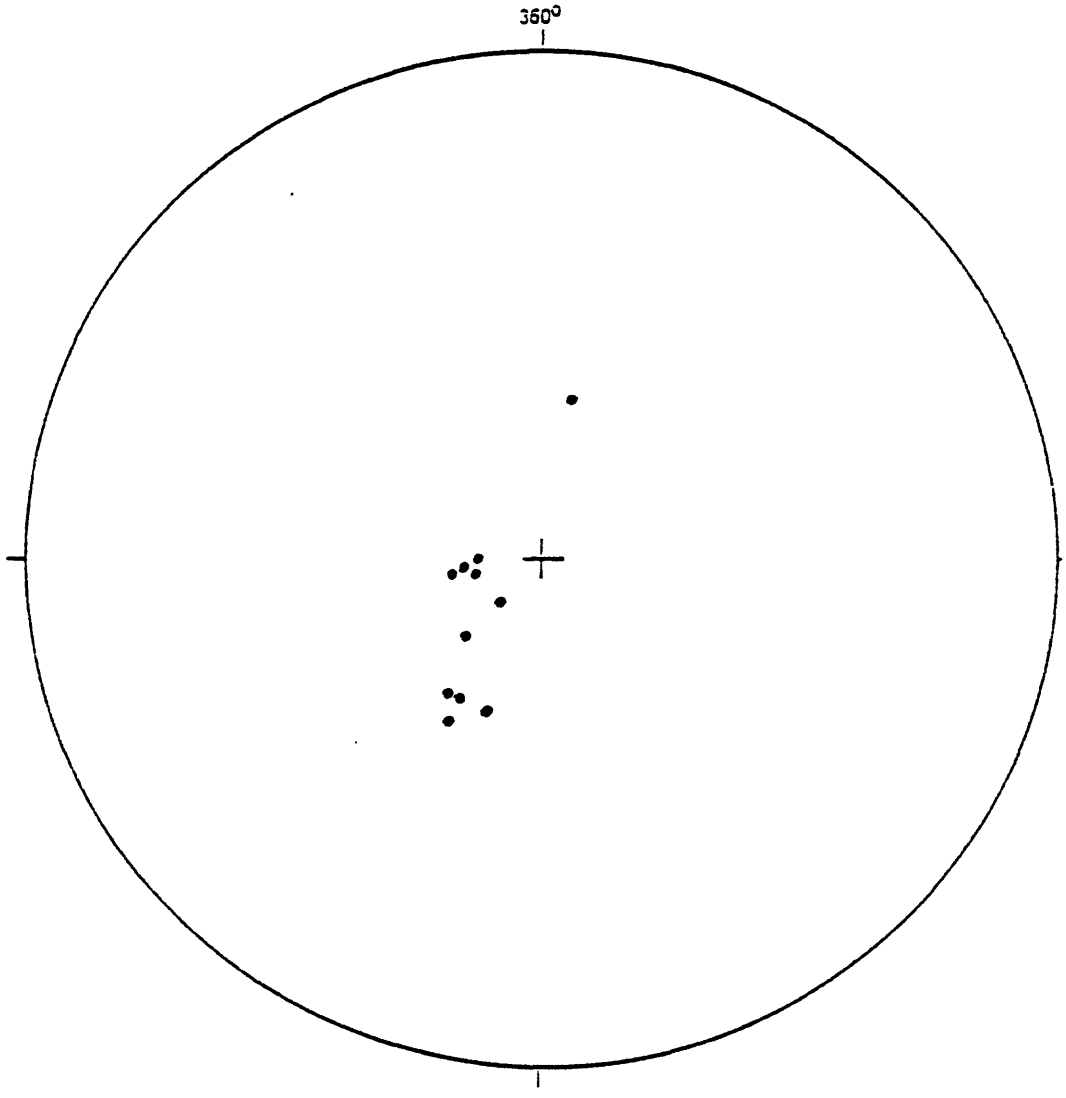

Figure 33.--Poles to alaskite sheets (●) in quartz diorite to tonalite of the western Idaho batholith in the Chimney Peak quadrangle. Data are plotted on lower hemisphere of Wulff stereonet.

The foliation in the biotite tonalite largely parallels that in the enclosed migmatite screens as seen on the outcrop scale. However, as shown in figure 34, the orientation of the flow foliation is complex in detail, whereas the migmatite screens are fairly continuous in their easterly trend. Figure 34 shows steeply dipping flow foliation striking in all points of the compass, with a generally axial symmetry about a near-vertical axis. Further complexities emerge on the outcrop scale. At one point (see table 3, sample 78RR230E), the flow foliation is complexly swirled in small folds. Figure 35 gives data on one such fold in which a curved axis of folding plunges steeply in an easterly direction. Figure 36 gives data on a fold set in which a rectilinear axis of folding is involved, plunging steeply to the southwest. Minor folds in this flow-folded primary gneiss show both clockwise and counterclockwise rotation randomly through the outcrop. Figure 37 shows the appearance of minor folds.

Flow lineation in the biotite tonalite consists largely of streaked-out biotite grains and grain clusters and axes of minor flow folds. Figure 38 shows the orientation of flow lineation in the Fenn Mountain area, not abundant, with a steep average plunge to the southwest.

In places in the tonalite, as in the cirque headwall west of Florence Lake (head of Old Man Creek), vertical, leucocratic trondhjemite dikes (striking 320° az) cut the tonalite, and grade into "mylonite" which is in turn injected by pegmatite. The "mylonite" is seen in thin section to be a fine-grained (0.5 mm) schist or blastomylonite derived from the trondhjemite of the dikes.

Alaskite and pegmatite occur in two ways in the biotite tonalite; first in shallow-dipping sheets 10 cm to 2 m thick, and second in steeply dipping dikes 5 cm to 2 m thick. In a few places, pegmatite injects the flow foliation of the primary gneiss in 0.5 mm-thick sheets.

The average trend of the sheet alaskite and pegmatite is about 300° az, and the average dip is about 30° NE (fig. 38), nearly perpendicular to the average flow lineation (fig. 39). Alaskite and pegmatite dikes dip steeply and strike in all directions (fig. 40). Pegmatite and alaskite dikes may simultaneously fill fractures of more than one orientation at a particular place (fig. 41).

Tonalitic rocks including pegmatite and alaskite are cut in places by cataclastic shear in which slickensides are "frozen" or recrystallized, resulting in microrodding and grooving. These features are commonly best shown in the pegmatite and alaskite, both on near-horizontal surfaces and on steeply dipping ones (fig. 42).

Migmatite screens

The general orientation of migmatite screens in the tonalite has been described in the foregoing material. The folding of the metamorphic component of the migmatites is rather complex as shown by data from a representative outcrop (fig. 43). Two fold sets exist, both of which are cut by post-kinematic granite pegmatite. Study of the rock discloses a conical fold style like that seen in the wall rocks. The minor folds and associated mineral lineation parallel the fold axes, which plunge steeply more or less parallel to primary flow lineation in the surrounding tonalite.

The migmatite screens are composed of continuous sheets of country rock near the contact of the tonalite and become progressively more broken up farther inside. As the screens become more broken, the fragments are rotated out of alinement with the original trend of the screens. In intermediate stages, the minor folds tend to disappear, destroyed perhaps by passive flow generated in the flow of the enclosing magma, and the metamorphic elements in the migmatite units retain only a crude planar banding. Foliation of the screens broadly parallels flow foliation of the enclosing primary gneiss. In places the foliation bends over to near-horizontal attitudes. Vugs in the screen rock are partly filled with quartz in places, suggesting some late-stage silicification.

Migmatite screens up to 1 km thick in the tonalite extend for several kilometers in a 090° to 290° az trend. They consist of varied mixtures of igneous and metamorphic rock. Metamorphic rock in the screens in the Fenn Mountain area is principally andesine-biotite quartzite, although small amounts of amphibolite, calc-silicate gneiss, and tonalitic gneiss are seen. Igneous rock injected along the migmatite foliation includes varieties ranging from diorite to granite; some of this material has granoblastic texture and has therefore been metamorphosed.

The andesine-biotite quartzite of the migmatite screens resembles closely that in the wall rock, more or less feldspathic and therefore of gneissic aspect, not easily separated in the field from tonalitic gneiss. Relict small isoclinal folds are complexly refolded. A streaky mica lineation commonly plunges steeply, near or along the dip line in steeply dipping foliation. One occurrence of quartzite is of a white color; the rock is 25% microcline and has no plagioclase.

Representative mineral modes for biotite quartzite of the migmatite screens are given in table 4. Considerable variation in feldspar content exists; some rock contains only plagioclase, some only microcline, and some both.

Petrographic study shows that biotite quartzite in the migmatite screens retains its metamorphic features: Crystalloblastic texture and crystallization foliation in which biotite is strongly lepidoblastic. Quartz is major. It occurs in irregular grains 1 to 4 mm in diameter. Most grains show undulatory extinction in blocky sub-domains 0.1 to 0.5 mm in diameter, and many quartz-quartz boundaries are sutured.

Plagioclase occurs in most but not all of the biotite quartzite in xenoblastic grains 1 to 4 mm in diameter. Plagioclase composition in various quartzites ranges from An_7 to An_{45} in unzoned, locally myrmekitic grains. Sericite and clay alteration are common. Some cataclastically bent twin lamellae are seen. The plagioclase grains appear to be of the same age in the fabric as the quartz grains.

Microcline occurs as the sole feldspar (25%) in one rock studied and in an amount equal to plagioclase in one other rock; it is not present even in trace amounts in the others. It occurs in xenoblastic grains 1 to 2 mm in diameter and appears to be of the same age in the fabric as the other minerals.

Biotite is lepidoblastic in grains 0.2 to 2 mm in diameter. In several rocks, elongate grains or trains of grains occur in linear array; biotite is partly altered to various mixtures of muscovite, epidote, and pennine.

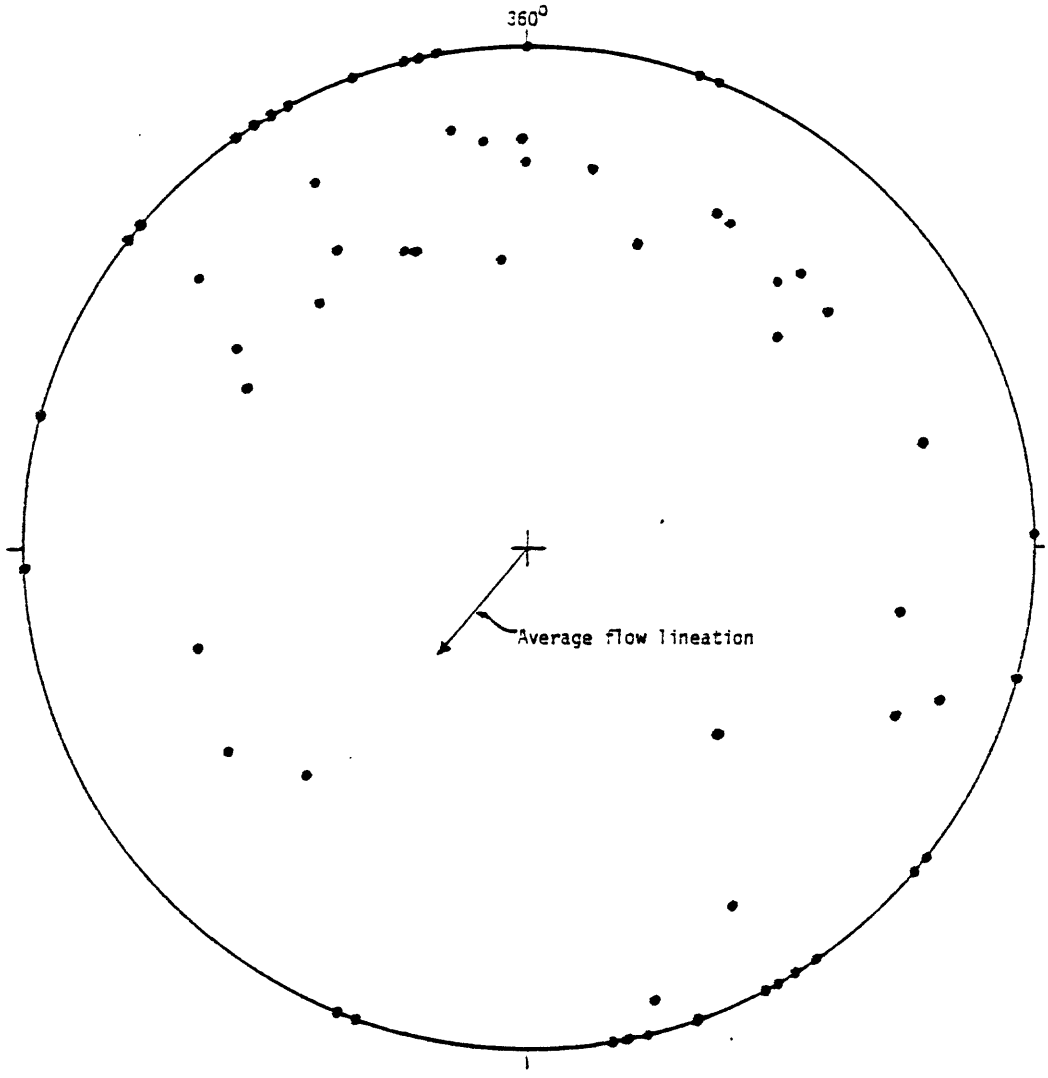

Figure 34.--Poles to flow foliation (●) in biotite tonalite in the Fenn Mountain quadrangle. Poles are plotted on lower hemisphere of Wulff stereonet.

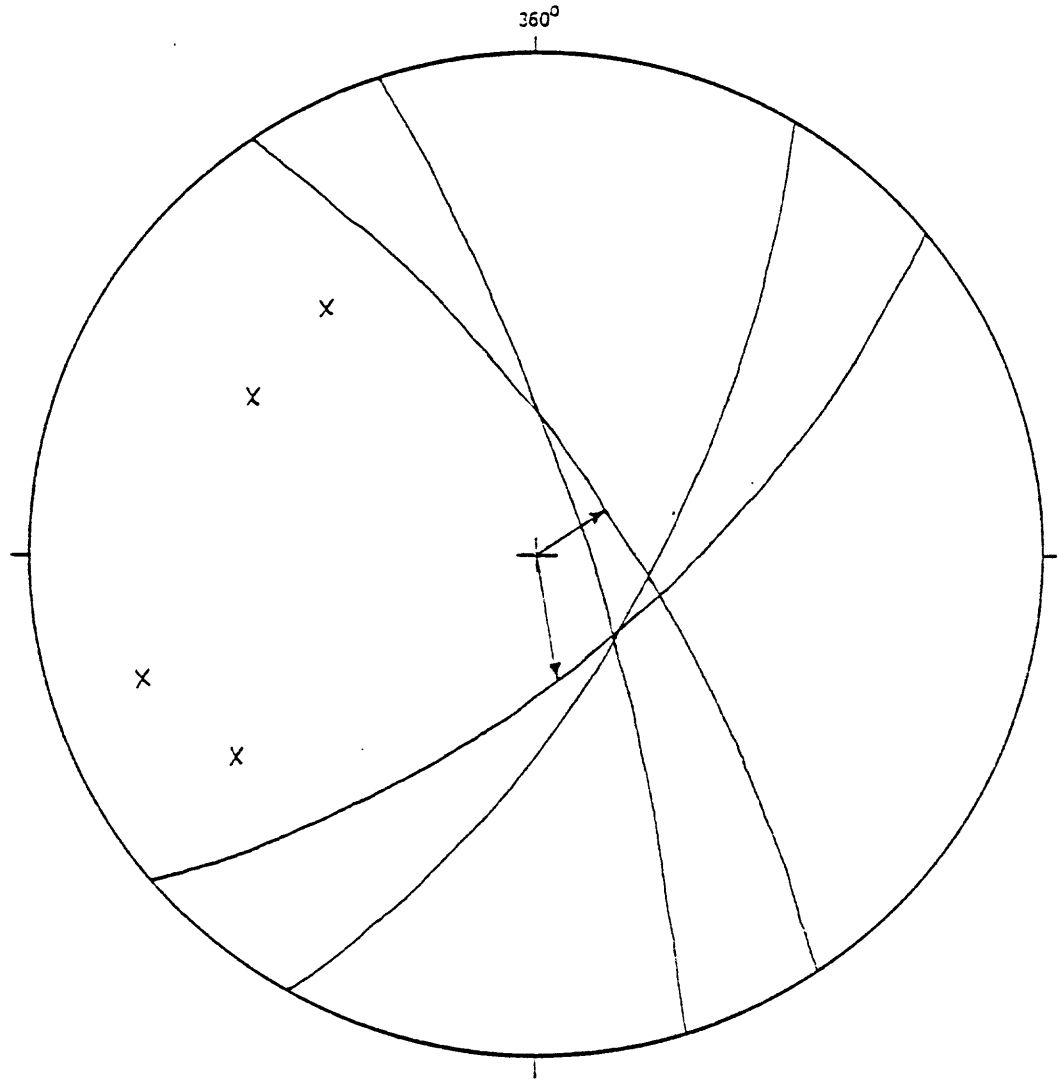

Figure 35.--Four attitudes in swirled-folded primary flow foliation at a point in the Fenn Mountain area. No rectilinear axis of folding exists, although the generally curved axis of folding averages a steep easterly plunge. The poles to the folded layers (X) lie in neither a great-circle nor a small-circle girdle. Streaky flow lineation (arrows in diagram) lies in two of the planes measured, distorted in the folding. Data are plotted on lower hemisphere of Wulff stereonet.

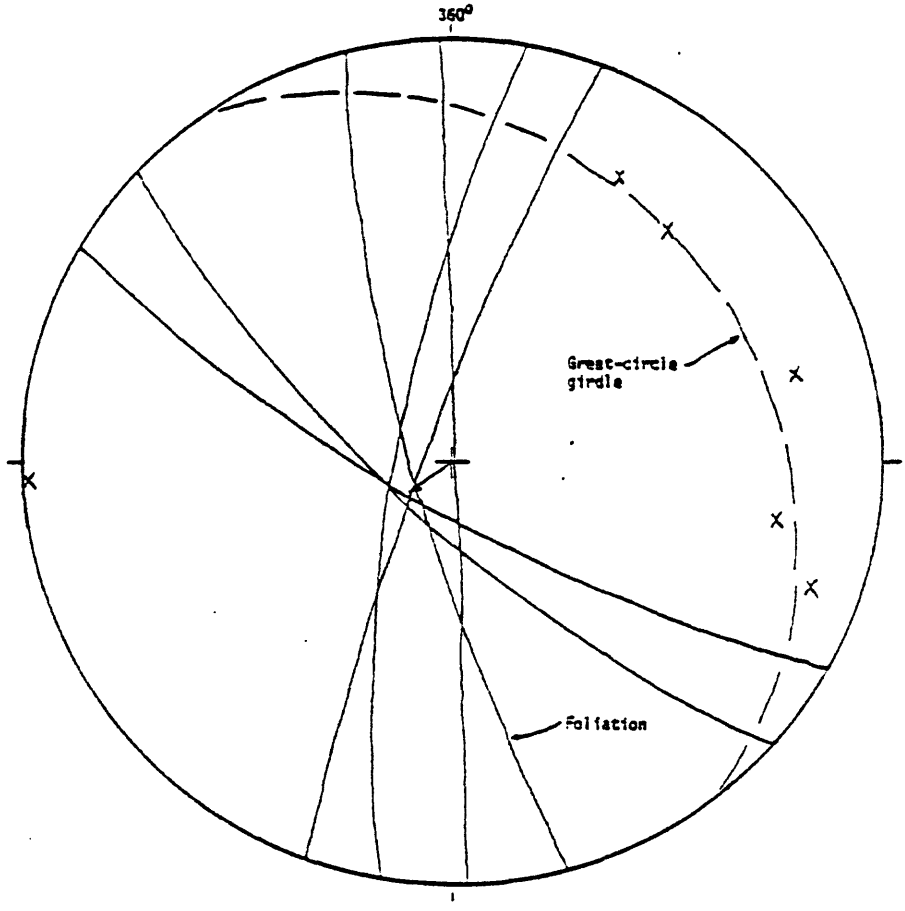

Figure 36.--Folded flow foliation at a point in the Fenn Mountain quadrangle. The axis of folding approximates that of a rectilinear cylindrical fold (the poles to the folded layers (X) approximate to a great-circle girdle), although even here one measurement in the fold set gives a plane whose pole lies well outside the girdle. The fold axis averages an orientation of 72°, 234° az. Data are plotted on lower hemisphere of Wulff stereonet.

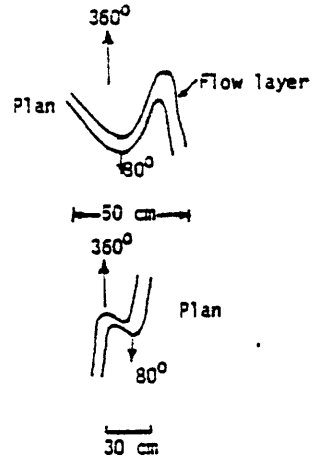

Figure 37.--Minor folds in flow foliation in tonalite in the Fenn Mountain quadrangle. These folds resemble those seen in the metamorphic components of the migmatite screens. The small folds show both clockwise and counterclockwise rotation.

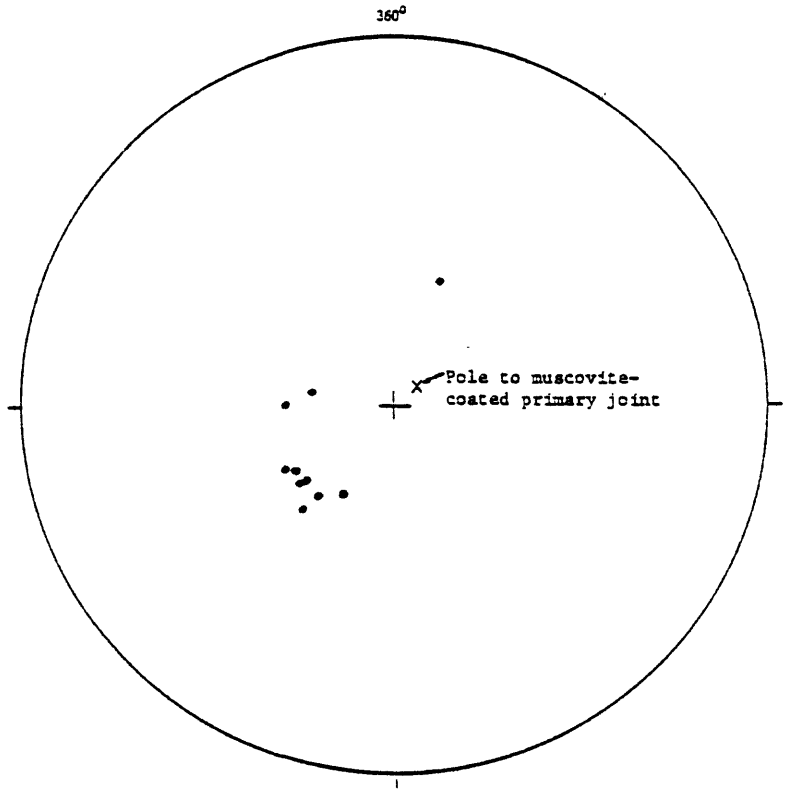

Figure 38.--Poles (●) to shallow-dipping pegmatite and alaskite sheets or dikes cutting biotite tonalite in the Fenn Mountain area of the western sector. One muscovite-coated primary joint was measured. Poles are plotted on lower hemisphere of Wulff stereonet. Location is in the Bitterroot lobe of the Idaho batholith, west of Hamilton, Mont.

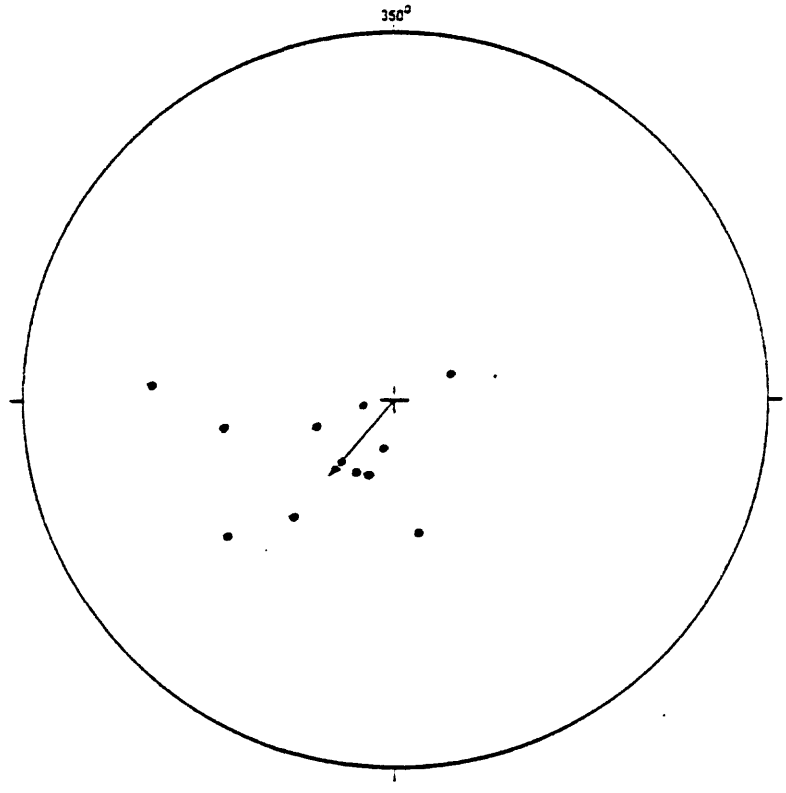

Figure 39.--Orientation of flow lineation (●) in biotite tonalite in the Fenn Mountain quadrangle, western Bitterroot lobe of the Idaho batholith. The arrow shows the average orientation. Data are plotted on lower hemisphere of Wulff stereonet.

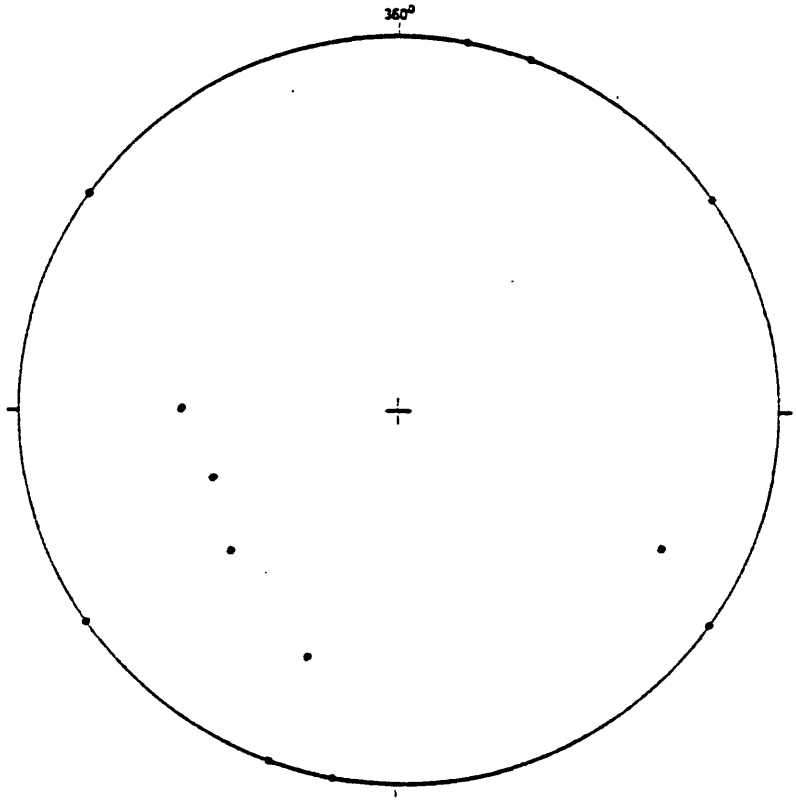

Figure 40.--Poles (●) to steep-dipping pegmatite and alaskite dikes cutting biotite tonalite in the Fenn Mountain area of the western sector of the Bitterroot lobe, west of Hamilton, Mont.

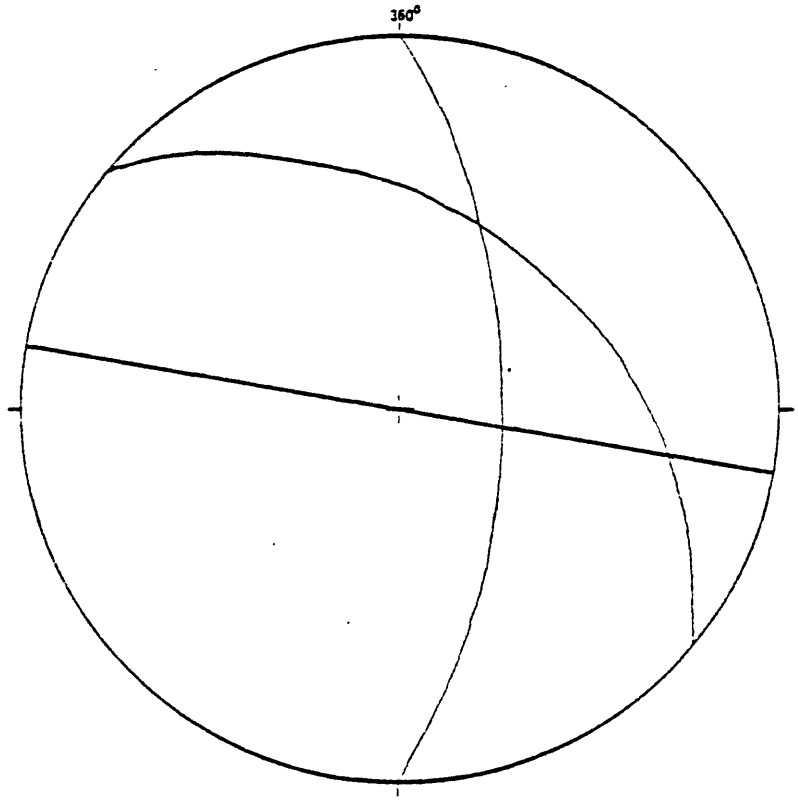

Figure 41.--Orientation of three simultaneous branched pegmatite dikes cutting biotite tonalite at a point in the Fenn Mountain area. The shallow-dipping dike belongs to the shallow-dipping set; the other two belong to the steep-dipping set. Data are plotted on lower hemisphere of Wulff stereonet.

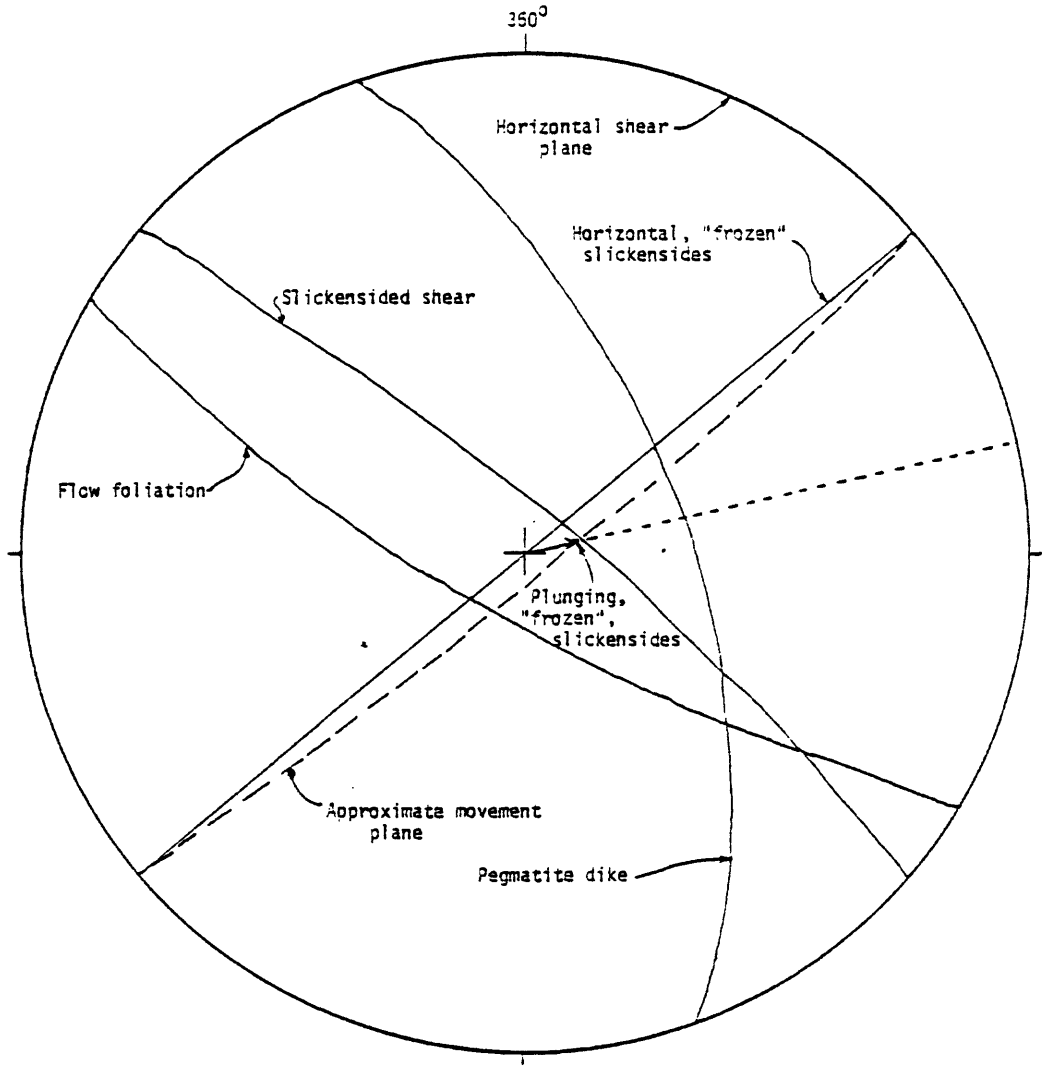

Figure 42.--Diagram to show "frozen" or recrystallized slickensides, micro-rodding, and grooving in different shear planes, one horizontal and one steeply dipping, both cutting pegmatite intruded into biotite tonalite in the Fenn Mountain area. The so-called movement plane is the constructed plane containing slickensides from both shear planes, which also contains the aveage slip line for the movement. Data are plotted on lower hemisphere of Wulff stereonet.

Table 4.--Modes in the Fenn Mountain quadrangle (HG7)

(1) Tonalite 78RR095B. (2) Tonalite 78RR107B. (3) Tonalite 78RR138B. (4) Tonalite xenoliths or cognate inclusions in tonalite 78RR143F. (5) Tonalite 78RR177B. (6) Blastomylonitic tonalite 78RR230E. (7) Tonalite 78RR235A. (8) Tonalite 78RR266B. (9) Quartz diorite 78RR125B. (10) Quartz diorite 78RR132B. (11) Quartz diorite 78RR232B. (12) Trondhjemite 78RR230B. (13) Granodiorite 78RR141B. (14) Granodiorite 78RR269B. (15) Granite 78RR143A. (16) Granite 78RR178B. (17) Granite 78RR234B. (18) Granite 78RR268B. (19) Granitic alaskite 78RR096B. (20) Granitic alaskite 78RR179B. (21) Biotite-oligoclase quartzite 78RR096E. (22) Biotite-oligoclase quartzite 78RR105B. (23) Microcline quartzite 78RR128A. (24) Biotite-oligoclase quartzite 78RR131B. (25) Oligoclase-biotite quartzite 78RR133B. (26) Biotite-microcline-oligoclase quartzite 78RR137B. (27) Biotite-andesine quartzite 78RR143E. (28) Biotite-oligoclase-muscovite-microcline quartzite 78RR233A. (29) Amphibolite 78RR130E.

	1	2	3	4	5	6	7	8	9	10	11	12	13	14	15	16	17	18	19	20	21	22	23	24	25	26	27	28	29
Plagioclase	45.3	50.7	58.8	54.2	47.1	48.3	59.0	34.4	65.0	50.8	55.8	10.4	41.9	21.8	38.3	32.7	29.8	26.0	33.6	6.3	27.9	33.2	0.5	18.2	16.9	17.4	21.9	5.9	27.6
Quartz	16.3	29.6	28.2	25.2	24.4	25.7	25.0	46.9	14.0	2.7	10.2	75.7	29.6	67.2	31.2	30.0	26.2	42.0	33.2	25.6	52.4	52.5	73.8	64.9	63.6	46.9	60.5	70.1	5.1
K-spar			3.3				5.7						19.8	3.3	26.2	33.0	29.5	15.6	33.2	68.1	6.3		24.6			14.3		11.8	
Biotite	34.5	18.4	8.6	19.8	14.0	23.5	8.8	0.1	17.0	42.2	9.8	3.9	7.0	6.5	3.1	3.3	12.6	11.6			9.2	12.7		16.4	19.1	11.8	17.4	4.2	0.7
Muscovite							0.9	11.8				0.9		0.1			1.9	2.8										7.6	
Hornblende	3.3				13.0						20.9																		63.4
Diopside																													
Scapolite																													
Sillimanite																													
Accessories	0.6	1.2	1.2	0.7	1.4	2.5	0.5	6.8	4.0	4.2	3.3	0.1	1.7	1.1	1.2	1.0	0.1	1.8	tr.	tr	4.1	1.6	1.1	0.4	0.4	9.6	0.2	0.4	3.0
	100.0	99.9	100.1	99.9	99.9	100.0	99.9	100.0	100.0	99.9	100.0	100.0	100.0	100.0	100.0	100.0	100.1	99.8	100.0	100.0	99.9	100.0	100.0	99.9	100.0	100.0	100.0	100.0	99.8

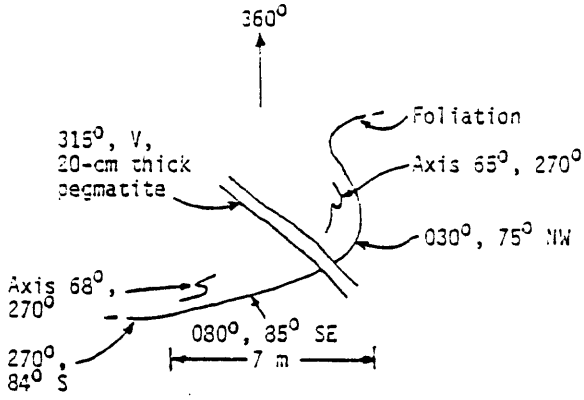

Figure 43.--Folded plagioclase-biotite gneiss septum enclosed in biotite tonalite in the Fenn Mountain area, cut by pegmatite of granitic composition.

Accessory minerals include apatite, baddeleyite, corundum, ilmenite? (leucoxene altered), magnetite (red iron oxide altered), monazite, sphene, thorite, and zircon.

The metamorphism produced one fabric age of minerals, with a bit of late alteration and some cataclasis.

Petrography of the tonalite

Tonalite occurs in major amounts in the Crags area of the western Bitterroot lobe of the Idaho batholith, in the Fog Mountain, Chimney Peak, and Fenn quadrangles, and in lesser amounts in the Greenside Butte and Fish Lake quadrangles. Petrography for the tonalite follows; measured modes are given in table 3 (modes 1 to 18) and table 4 (modes 1 to 22).

Biotite tonalite is coarsely foliated, medium-grained rock with varied amounts of flow lineation, stronger near the margin of the intrusion and weaker to the east away from the contact. The flow lineation consists mostly of hornblende prisms plunging steeply down the dip of the foliation.

Hornblende occurs in varied amounts in some of the rocks, larger in amount in the western part of the intrusion, and in lesser amounts to none toward the eastern part. It occurs in 2 mm prisms, partly altered to biotite.

Biotite occurs in 0.5 to 2 mm flakes in crude lepidoblastic array in the flow foliation. Grains display olive-brown to strong reddish brown pleochroism, and minor pennine-epidote-sericite alteration. Some grains are bent cataclastically.

Plagioclase (An_{27-37}) is euhedral to subhedral in 2 to 3 mm grains which have albite twinning and are mostly unzoned. Anorthite content of the plagioclase shows no systematic area variation. A small amount of plagioclase has normal zoning from cores of An_{28} to rims of An_{25}. Alteration products are minor sericite and epidote, and a few grains have bent albite twin lamellae.

Quartz occurs in 0.5 to 2 mm grains. Most grains show undulatory extinction and many of them have sutured grain boundaries (quartz-quartz). Minor amounts of microcline occur in a few of the rocks, from trace amounts to 5%. Accessory minerals include allanite, baddeleyite, magnetite, sphene, thorite, and zircon.

Rare, dark, spindled and lineated xenoliths in the tonalite are of diorite (table 3, mode 17), perhaps cognate inclusions. They consist of hornblende in 0.5 mm grains, biotite in 0.5 mm grains, and plagioclase in 0.5 mm, unzoned, granoblastic grains of composition An_{37}. Accessory minerals are apatite, baddeleyite, magnetite, and zircon.

Tonalitic gneiss injects the country rocks near the batholith in concordant sheets more than a few hundred meters thick. The mineralogy is like that of tonalite in the batholith; the rock differs from the batholithic tonalite only in its gneissic structure. A mode is given in table 3 (mode 1).

Tonalitic gneiss is rich in leucocratic veinlets parallel to the foliation. Quartz occurs partly in small, equant grains and partly in large, flattened, elongate platelets typically 1x3x6 mm, oriented with their long direction parallel to the other lineation in the rock. Hornblende and plagioclase (An_{37}) prisms 4 to 6 mm long also parallel the lineation. In quartz-rich varieties, minor sillimanite occurs in fibers parallel to the lineation, and plagioclase is more sodic (An_{27}) than in high-plagioclase varieties. Muscovite also occurs in some of the rocks. Accessory minerals include apatite, baddeleyite, magnetite, sphene, thorite, and zircon.

Trondhjemite occurs as lit-par-lit veinlets in the tonalitic gneiss, parallel to its foliation. Modes are given in table 3 (modes 31 to 32) and table 4 (mode 12). Quartz occurs as elongate platelets 4 to 6 mm long in a crude linear array and has mild undulatory extinction. Biotite occurs in elongate grains and grain aggregates in a linear array parallel to quartz platelets. Plagioclase (An_{25-30}) in 2 to 3 mm grains is more sodic than plagioclase in the enclosing tonalitic gneiss. Grains are mostly granoblastic and unzoned, but some patchy, irregular, relict(?) zoning occurs. A trace of muscovite occurs together with chlorite, magnetite, thorite, and zircon.

The tonalite and neighboring rocks are cut by dikes and sheets of pegmatite, alaskite, and aplite. Alaskite sheets are most common and are representative of the mineralogy of the pegmatite suite; they are mostly trondhjemitic. Three sheets of granitic alaskite were found (table 4, modes 19 and 20; and table 4, mode 30). Trondhjemitic plagioclase (An_{31}) occurs in 2 mm, mostly unzoned prisms, but a few

grains show some oscillatory normal zoning. Quartz and biotite are in 1 to 2 mm grains, and accessories include apatite, epidote, muscovite, pennine, and thorite.

In the granitic alaskite, microcline occurs in grains more than 8 mm in diameter. Plagioclase (An_{20}) is in grains up to 6 mm diameter, unzoned, and partly myrmekitic where in contact with microcline grains. Plagioclase is somewhat altered to muscovite. Quartz shows some undulatory extinction and sutured grain boundaries.

In both the trondhjemite and the granitic alaskite, some shear reduction of quartz and feldspar occurs in cataclastic zones with partial strain recovery. Grain size in the cataclastic zones averages 0.3 mm. Many cataclastically reduced grains are free of undulatory extinction, and the sutured grain boundaries are annealed.

JOINTS

Joints in the Crags area are well weathered and not certainly classifiable into extension and shear joint categories. Poles to 76 joints are given in figure 44. The array has somewhat random appearance. Those joints that are slickensided and therefore clearly shear joints are given in figure 45. The slickensides are somewhat varied in their trends but average to lie in a generally easterly direction. These joints may be in part older extension joints that have been utilized in younger shear movement.

GRANITE, GRANODIORITE AND RELATED ROCKS

Granite, granodiorite, and smaller amounts of quartz monzonite, quartz monzodiorite, tonalite, diorite and anorthosite occur in a continuous transect across the Bitterroot lobe of the Idaho batholith from west to east, in a row of nine 7 1/2 " quadrangles along about 46°15′ North Latitude, approximately from the Crags area to Hamilton, Mont. No significant modal variations in the main rock types occur over the transect; granite and granodiorite occur mixed in about equal amounts. Because of structural variations, and for convenience, the rocks are discussed in western, central and eastern sectors. All of these rocks, in all three sectors, belong to the Bear Creek pluton defined by Toth (1981).

The western sector

Structure.

Granitic rocks.

The western sector covers all or parts of the following 7 1/2′ quadrangles: Fenn Mountain, Chimney Peak, Huckleberry Butte, Greenside Butte, and Fish Lake, Idaho. The western sector is discussed in terms of two zones: a northern one and a southern one, as structures are different in the two.

Granite/granodiorite cuts the tonalite and occupies the northern part of the Crags area, which is the southern part of the western sector; contact relations are well exposed north of Louse Point. The first approach to the contact is expressed by a zone of non-parallel shears in tonalite and bounding migmatite, injected synkinematically by fine-grained granite in the form of blastomylonite; the granite-filled shears are cut by aplite and pegmatite. Microcline megacrysts up to several cm in diameter and spindled during deformation grew in the host tonalite near the fine-grained granite. All the shears have a steep-plunging biotite lineation, but the microcline spindles have horizontal axes. Orientation data for blastomylonite foliation and lineation are given in figure 46. Xenoliths of tonalite occur in the granite, showing further that it is younger than the tonalite.

The granite has a marked development of primary flow foliation near the contact with tonalite and its bounding migmatite. Representative attitudes are given in figure 47. Considerably swirled, the steep-dipping flow foliation does not conform in detail to the 080° az contact. Yet the near-vertical orientation of the flow lineation is comparable to that of the lineation in the bounding migmatite screen and tonalite. Thus, a degree of fluid-flow viscous flow coupling may have existed between the magma and its wall rock during the emplacement of the granite. The flow trends in the granite are somewhat different from those of the earlier tonalite, guided, of course, by a differently oriented contact.

Pegmatite dike and sheet orientations in the granite are given in figure 48. These are different from the ones in the tonalite, indicative of a different flow and stretching system. The data are sparse for interpretation. Some pegmatite in the granite is trondhjemite probably of tonalite derivation, younger than the tonalite of the area to the south and perhaps coeval with the granite.

Farther into the granite pluton and across a subtle but major zone of structural transition, the representative Greenside Butte area (northern zone of the western sector) is underlain principally by granite/granodiorite, with local flow foliation shown mostly by biotite or microcline bands and less commonly by biotite-rich schlieren. The character of the flow foliation is shown in figure 49. Poles to the flow foliation lie in a very diffuse girdle whose axis is near horizontal along a trend of about 320° az.

Several exposures of blastomylonite were found in the Greenside Butte area. Their average attitude is 320° az, 40° SW (fig. 50), and the lineation in them trends 30°, 290° az.

Reconnaissance mapping suggests that the various igneous rocks are rather thoroughly intermixed. In a representative traverse along a ridge in well-exposed rocks for 11 km, the following rocks were encountered in the order listed: granite - granite (again) - granodiorite and foliated tonalite at the same outcrop - granite - migmatite - granite - migmatite - granite and granodiorite at the same outcrop - granodiorite - porphyritic granodiorite - tonalite - foliated, porphyritic granodiorite - granite - migmatite - granodiorite - granodiorite (again). The rocks are all medium grained and gray colored, looking much alike and not recognized as separate varieties in the field; no unit contacts were discerned beyond those of the migmatite zones. This traverse is judged to be indicative of the degree of mixing of rock types in the entire sector as shown by the mixed distribution of samples from less well exposed parts of the area.

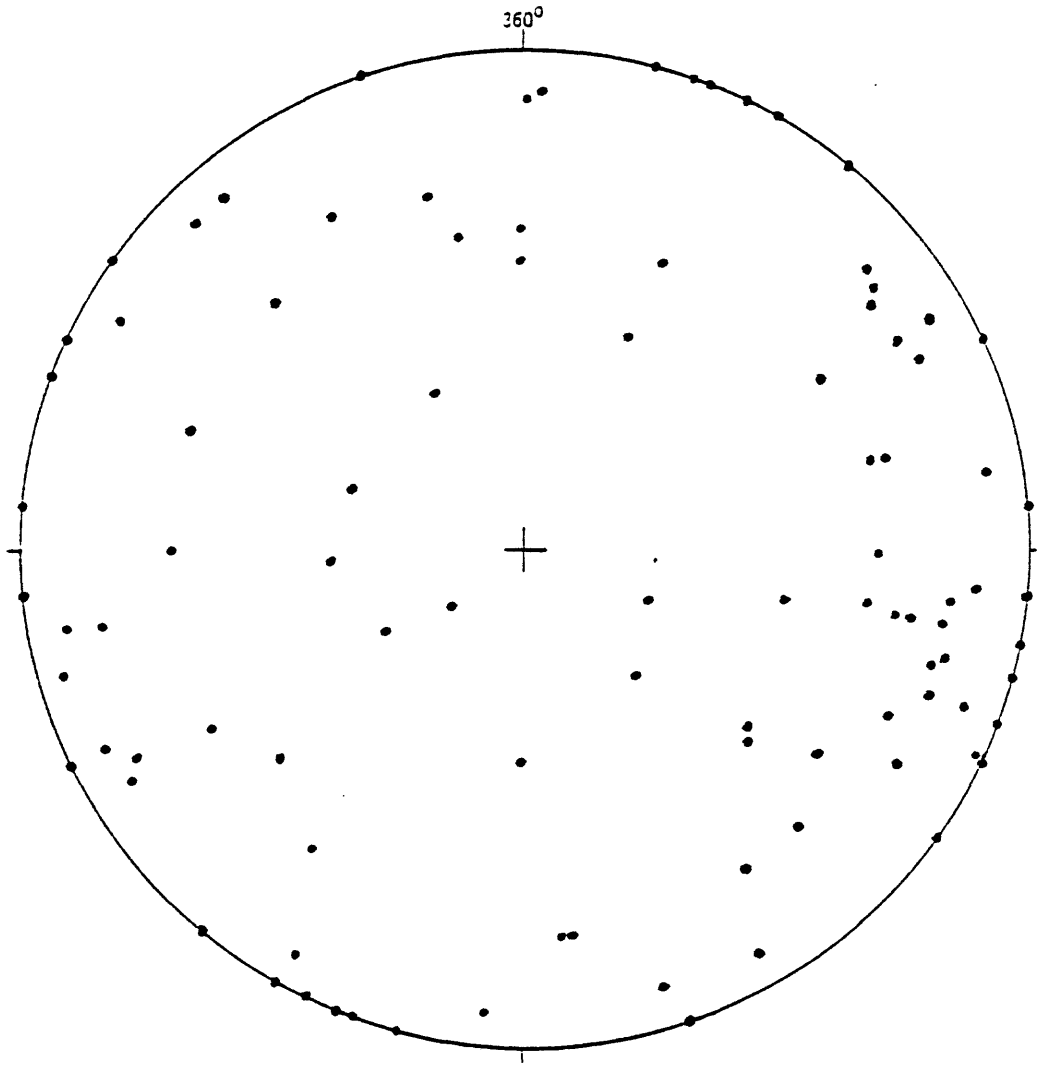

Figure 44.--Poles (●) to secondary joints in biotite tonalite of the Crags area, western sector of the Bitterroot lobe of the Idaho batholith, west of Hamilton, Mont. Data are plotted on lower hemisphere of Wulff stereonet.

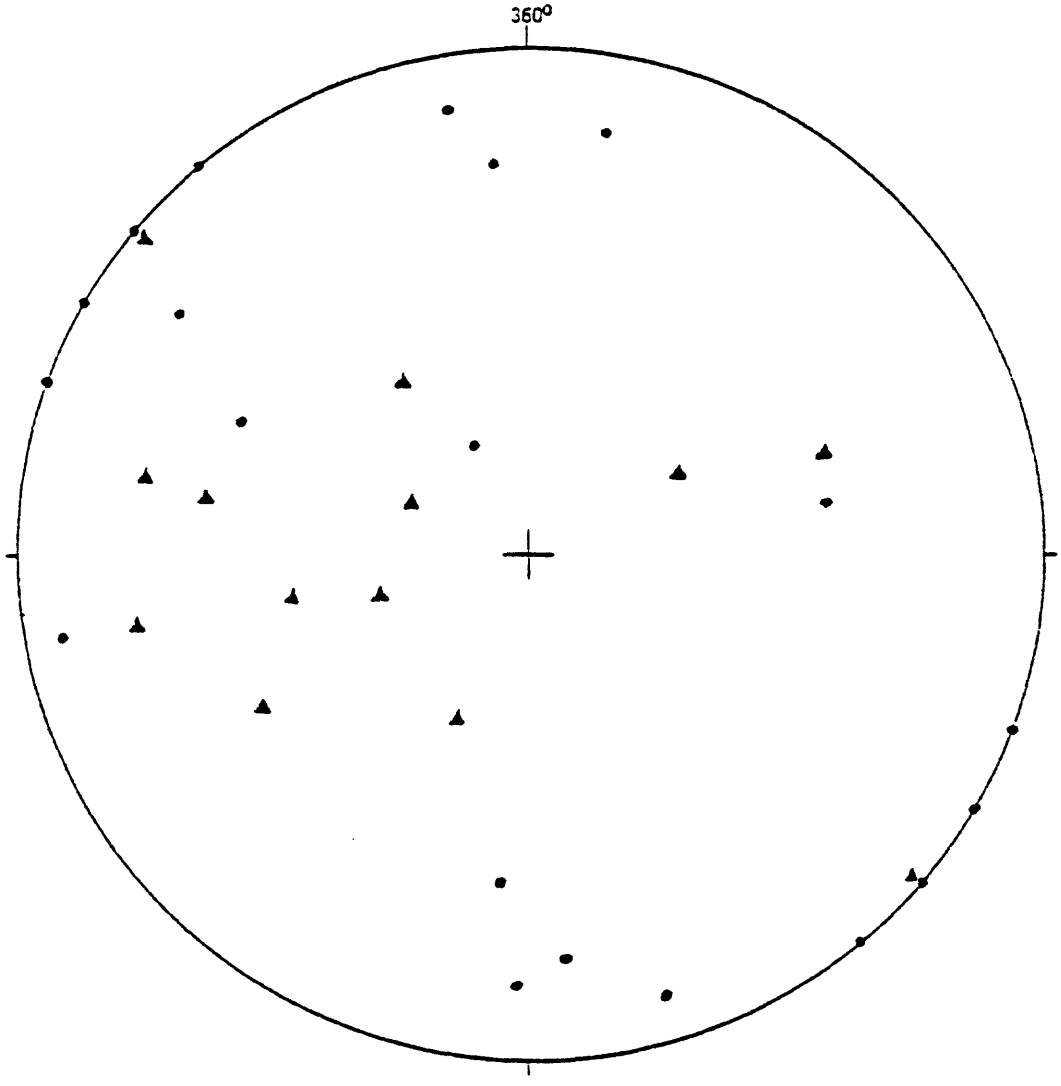

Figure 45.--Poles to 15 shear surfaces (●) and to 12 with slickensides (▲), in the Greenside Butte quadrangle, western sector of the Idaho batholith, west of Hamilton, Mont. Data are plotted on lower hemisphere of Wulff stereonet.

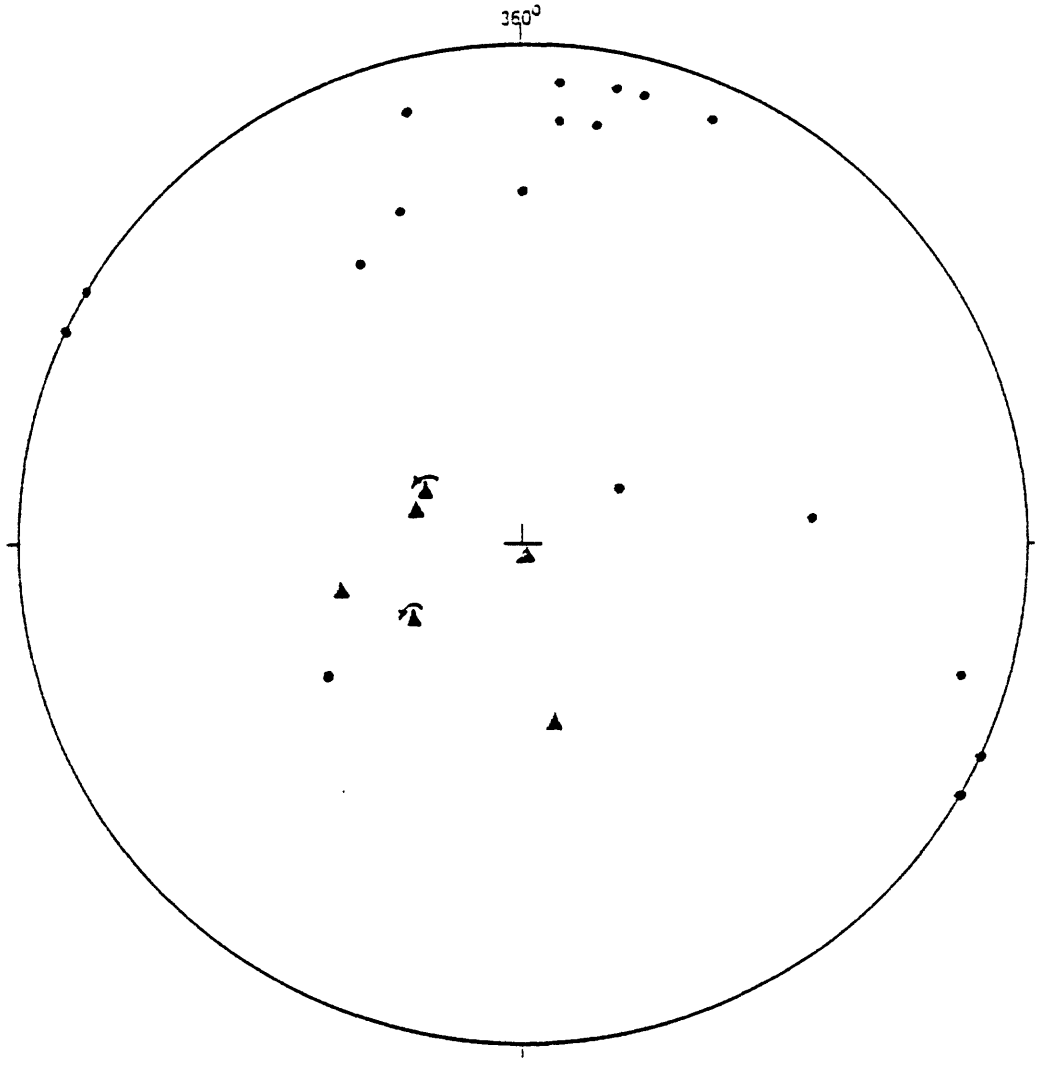

Figure 46.--Poles to blastomylonite foliation (●) and lineation (▲) in granitic rock near the granite-tonalite contact, in the central Crags area, western sector of the Bitterroot lobe of the Idaho batholith, west of Hamilton, Mont. Small arrows show the sense of rotation on small folds whose axes parallel the blastomylonite foliation. Data are plotted on lower hemisphere of Wulff stereonet.

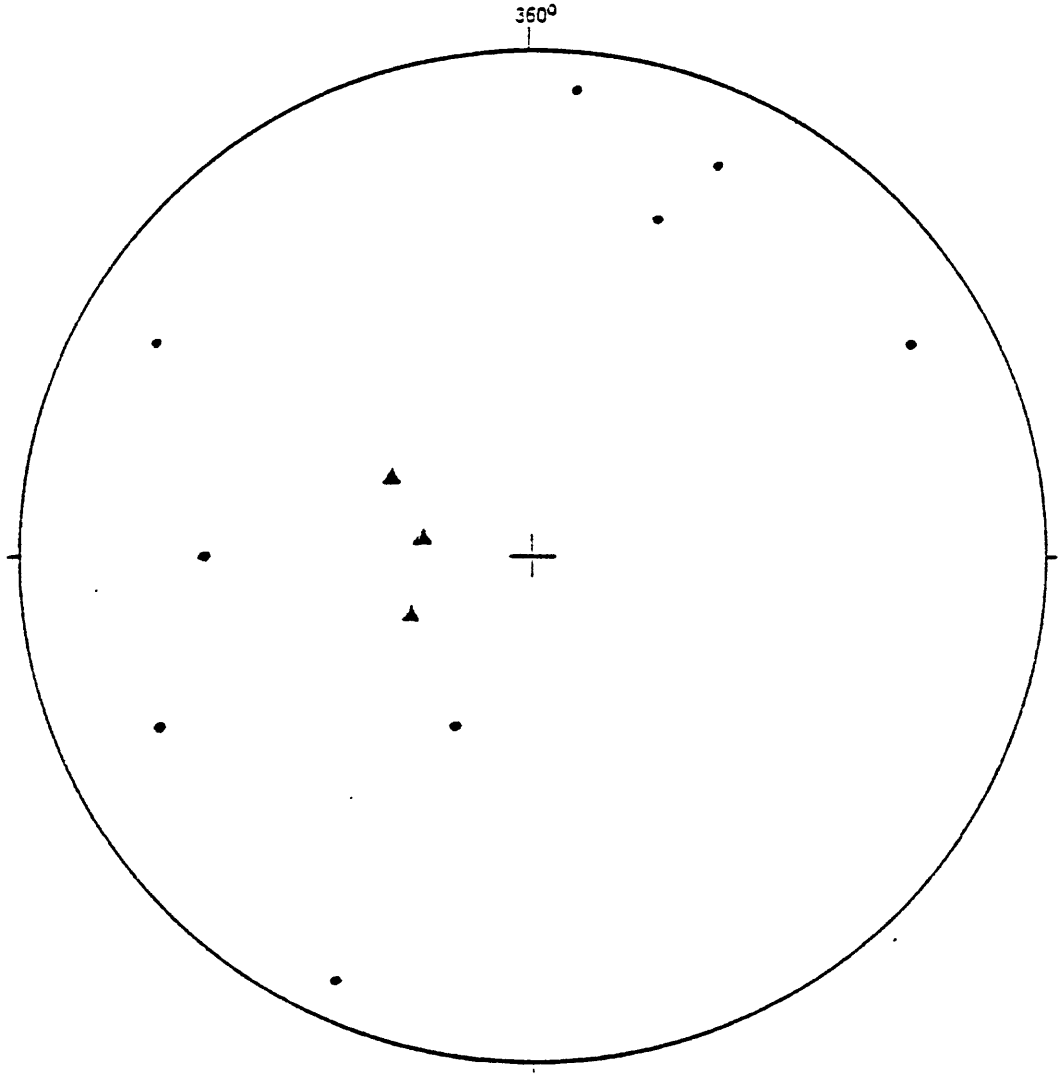

Figure 47.--Poles to primary flow foliation (●) and flow lineation (▲) in granite/granodiorite near the granite-tonalite contact, in the central Crags area, southern zone of the western sector of the Bitterroot lobe of the Idaho batholith, west of Hamilton, Mont. Poles are plotted on lower hemisphere of Wulff stereonet.

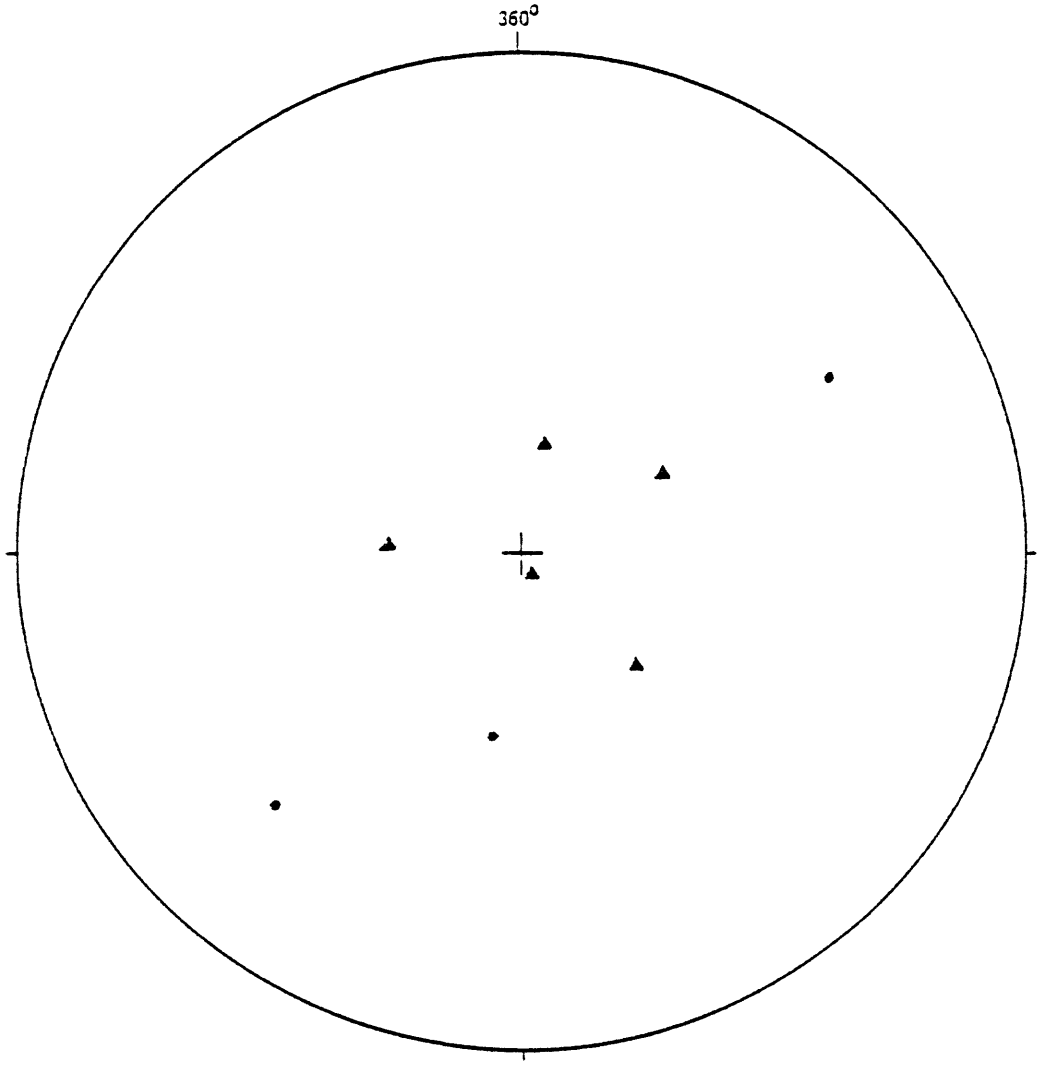

Figure 48.-- Poles to pegmatite dikes (●) and sheets (▲) in the granitic rock of the central Crags area, near the granite-tonalite contact. Western sector of the Bitterroot lobe of the Idaho batholith, west of Hamilton, Mont. Data are plotted on lower hemisphere of Wulff stereonet.

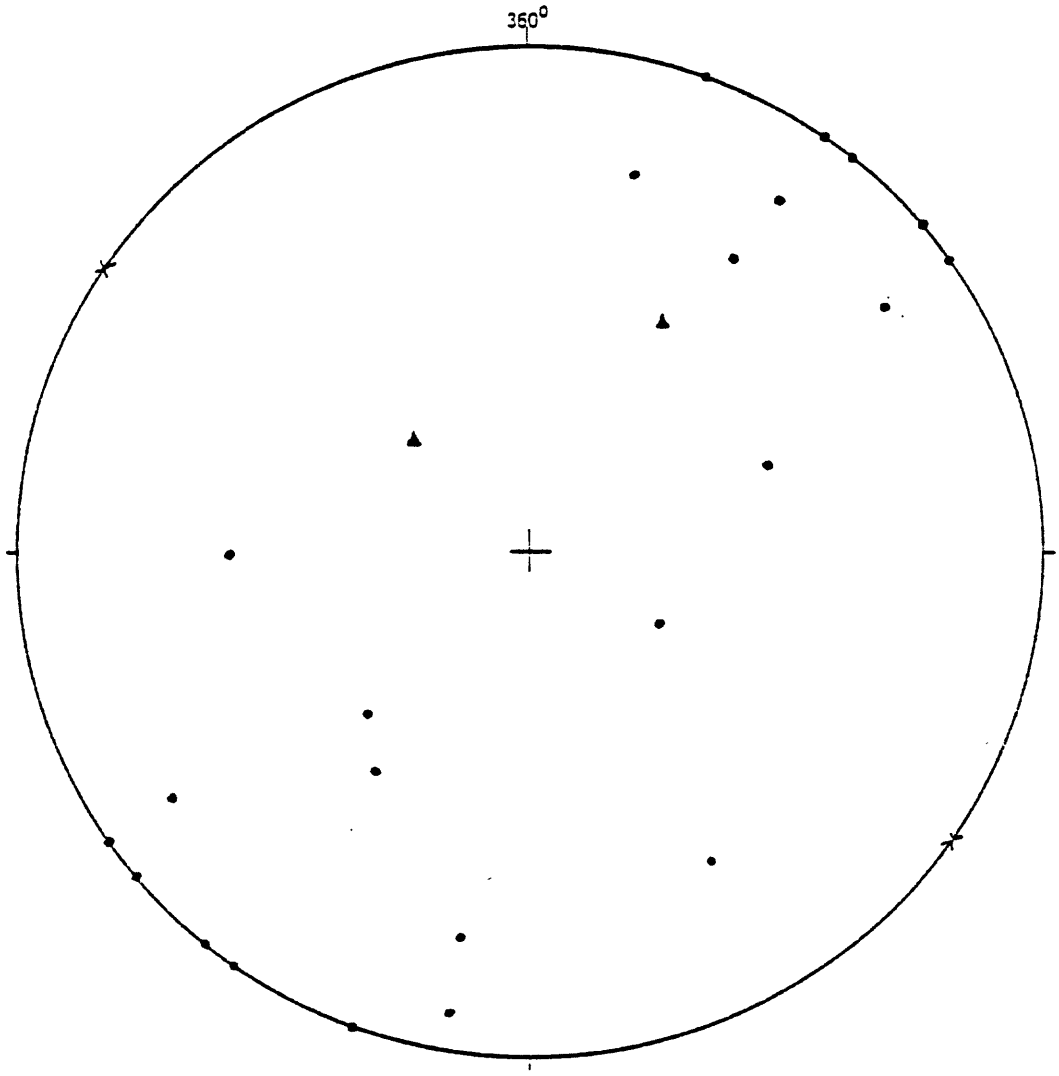

Figure 49.--Poles to flow foliation (●) in granite/granodiorite of the Greenside Butte quadrangle, and two axes of folds (▲) in the flow foliation. X= axis of diffuse girdle oriented 00°, 305° az. Northern zone of the western sector, Bitterroot lobe of the Idaho batholith, west of Hamilton, Mont.

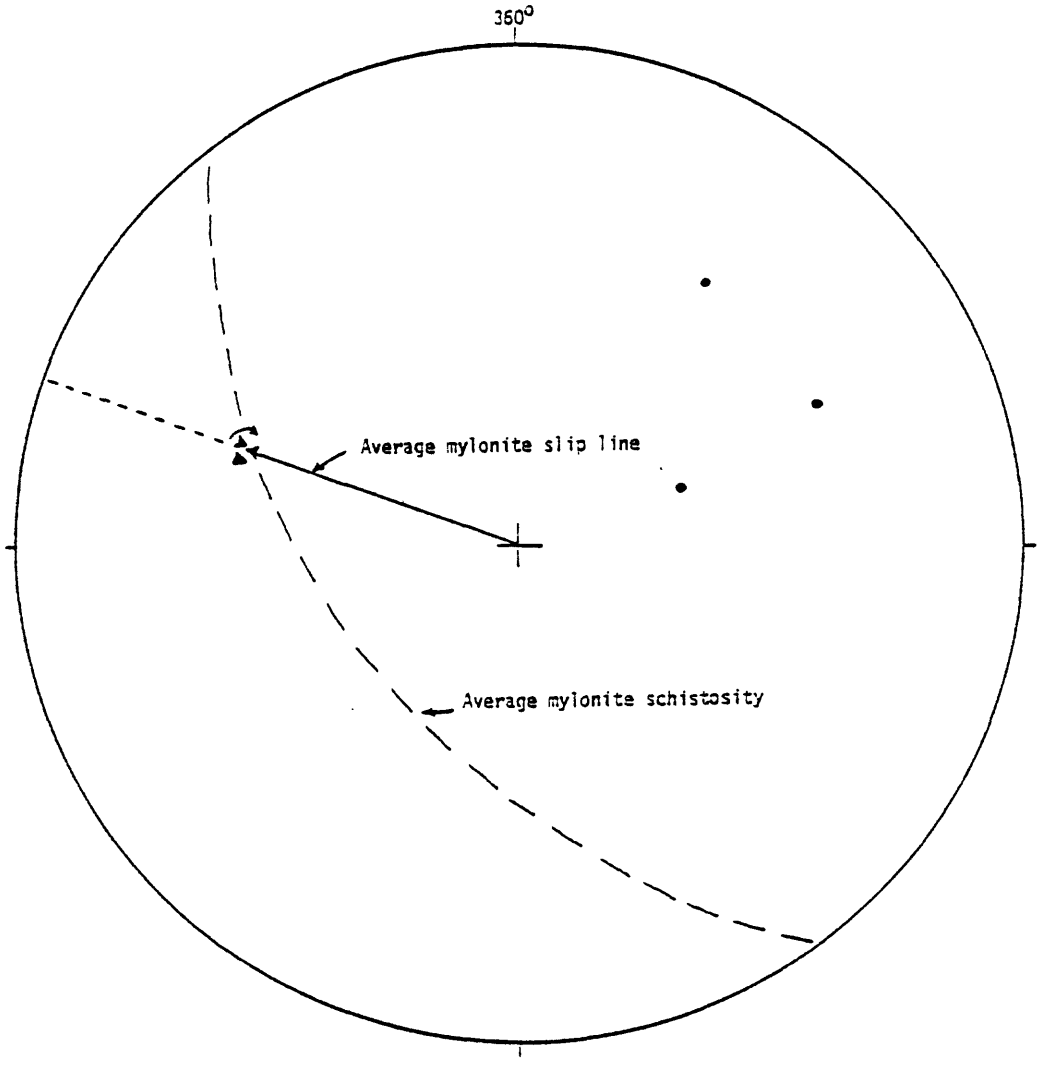

Figure 50.--Poles to mylonite schistosity (●) and mylonite lineation (▲) in the Greenside Butte quadrangle, western sector of the Bitterroot lobe of the Idaho batholith, west of Hamilton, Mont. Data are plotted on lower hemisphere of Wulff stereonet.

Migmatite.

In the southern zone of the western sector, a considerable amount of migmatite occurs in sheets of westerly to west-northwesterly trends. Migmatite screens seem to have trends from 270° to 060° az, based on interpolation of sketchy map data. Some granitic rocks are injected in sheets along the foliation of the migmatite screens. Granite and granodiorite predominate and appear to be intermingled with each other and with subordinate plutonic rock types. One sawed slab shows tonalite grading into granite. At one outcrop, granite and granodiorite were collected a few feet apart; they look identical in hand specimen. The migmatite protolith is of quartzite and calc-silicate rock.

A zone or screen of granite-migmatized metamorphic rock about 3 km thick intervenes between the tonalite and the granite north of Louse Point. The few available data show that foliation attitudes within the migmatite screen vary widely, but that lineation plunges steeply along a trend of 250° az (fig. 51). Map data suggest that the screen as a whole trends about 080° az. It is likely coextensive with a comparable screen that passes south of Old Man Lake in the Fenn Mountain quadrangle and continues east into the East Peak area where it has been mapped by Bittner-Gaber (1983). In the Chimney Peak area and Fenn Mountain quadrangle, it has a strike length of more than 23 km. Both granite and tonalite are injected into the migmatite screen.

Poles to foliation (fig. 52) in the migmatite screens of the northern zone of the western sector lie in an ill-defined girdle whose axis plunges 50°, 290° az. Minor folds and mineral lineations are of scattered trend, but an average orientation of 30°, 320° az may be estimated. Granite/granodiorite sheets are in places folded with the migmatite.

Foliation.

Flow foliation occurs in part of the rocks in the northern zone of the western sector; about one-third of the samples collected are foliated and two-thirds are massive. The two types are irregularly intermixed over the area among all the rock types present. Poles to flow foliation in the zone are plotted in figure 53; it will be seen that the poles occupy a crude girdle whose pole plunges about 30° to the northwest, not far in orientation from the lineation points due to the axes of folded schlieren, minor folds in migmatite, and other linear elements such as alined microcline phenocrysts in the foliation. The rocks are coarsely foliated and the foliation is visible for the most part at the outcrop only; it cannot be seen at the scale of many hand specimens, most sawed slabs, and virtually all the thin sections. The flow foliation is judged to be mostly primary flow foliation, expressed not only by rather coarse banding but also by alined schlieren and platy xenoliths.

Certain fabric elements in the northern zone of the western sector impart a subtle foliation to some of the plutonic rocks, expressed principally by flattened quartz and feldspar grains. This subtle foliation is called "secondary foliation", generally too weakly developed to be recognized in the weathered outcrops, it has been seen principally in the stained slabs. In several plutonic rock samples, secondary foliation is present in rocks for which a foliation was measured at the outcrop. This may be solely secondary foliation or it may be primary foliation paralleled by secondary foliation. In any case, all the poles to foliation lie in the same crude girdle (fig. 53). Secondary foliation was measured locally in the field and recognized in slabs in several rocks of the pegmatite suite. Poles to dikes of the pegmatite suite and to the foliation in them lie generally in the girdle of figure 53, and rodding in them also trends at a shallow angle to the northwest. At one outcrop, pegmatite sheets were injected along the foliation. At another, foliation of uncertain affinity oriented 340° az, 37° SW, containing biotite lineated along 30°, 290° az, proved to be of secondary character upon thin section study.

Shear joints.

Shear joints of ENE trend occur in the western sector. They are generally slickensided and a little bit chloritized. Slickensides rake both to the northeast and to the southwest (fig. 54).

Secondary joints.

Secondary joints in the western sector have a random pattern widely varied both in strike and in dip (fig. 55).

Petrography.

Granite.

Granite studied from the western sector is listed in table 3 (modes 22 to 25), table 4 (modes 15 to 18), table 5 (modes 1 to 7), table 6 (modes 1 to 25), and table 7 (modes 1 to 16). One slab revealed inhomogeneities on the centimeter scale in feldspar distribution. One patch yielded a feldspar ratio of 56% plagioclase and another gave 71%. Thus, one patch would be granite and the other granodiorite, and the one rock grades insensibly into the other.

Plagioclase in the granite (12% to 46% in the mode) occurs in 0.5 to 4 mm grains. Here and in the following material, such measures refer to the range of average grain sizes determined in the several thin sections studied. Plagioclase composition is in the range An_{15} to An_{32}. Both modal amount and plagioclase composition are more or less randomly distributed over the area, and this applies to plagioclase composition and indeed to all mineral modes over the entire map area. Virtually all the plagioclase is unzoned; only in a few rocks were zoned grains (cores An_{26} to An_{28}, rims An_{20} to An_{23}) seen, and even there they are mostly relicts. Grains are equant to prismatic, and euhedral to subhedral; some of the subhedral grains may be crystalloblastic. Some plagioclase is myrmekitic against K-feldspar. In three granites, a considerable part of the plagioclase is in clusters of 0.5 to 0.7 mm grains of irregular granoblastic form with interfacial angles approaching 120° and with some microcline inclusions. These clusters are in part enclosed within K-feldspar. In several granite specimens, plagioclase grains are cut by filled, 0.1 mm thick extension fractures that are perpendicular to foliation (where it is present); filling minerals include K-feldspar, quartz, and pennine. Plagioclase in four granites is in flattened grains which in the stained slabs impart a distinctly foliated aspect to the rock; some of these flattened grains are broken in 0.5 mm, strain-free subgrains. These rocks contain the strongest development of secondary fabric seen in the area; all are

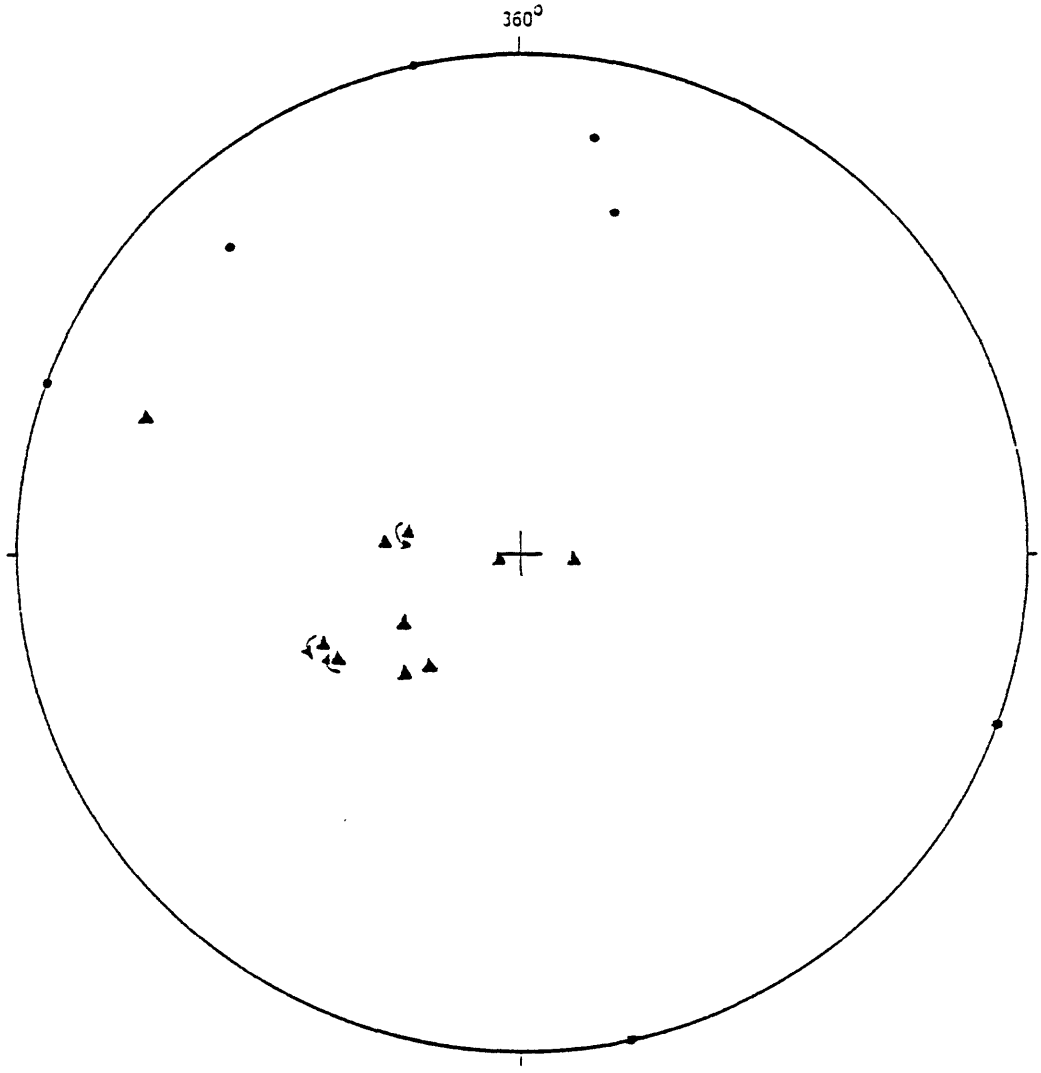

Figure 51.--Poles to foliation (●) and fold axes and rods (▲) in migmatite near the granite-tonalite contact, in the southern zone of the western sector, central Crags area, Bitterroot lobe of the Idaho batholith. Small arrows show the sense of rotation on small folds. Data are plotted on lower hemisphere of Wulff stereonet.

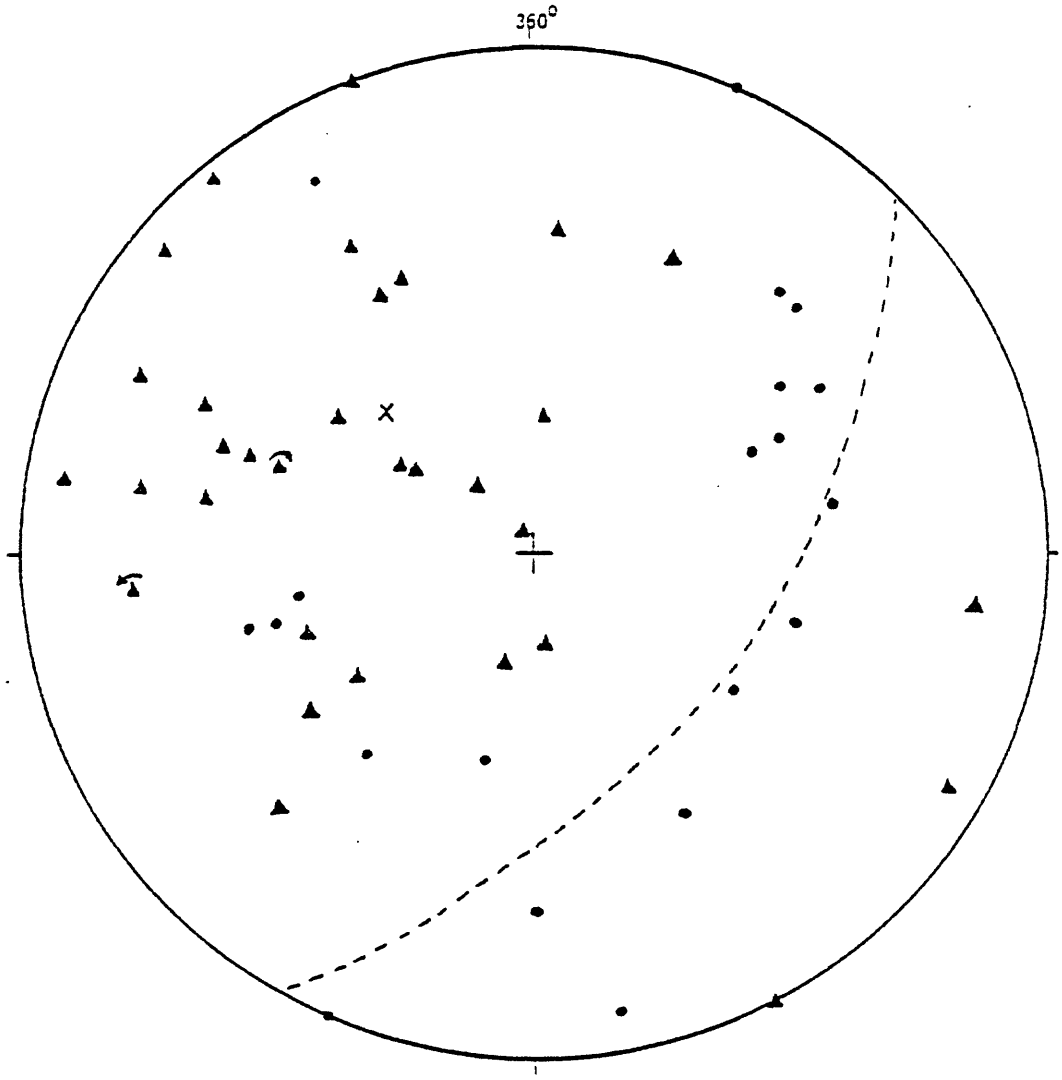

Figure 52.--Poles to foliation (●) and mineral lineation (▲), mostly biotite streaks, rods, and minor fold axes, in migmatite screens in the Greenside Butte quadrangle, northern zone of the western sector, Bitterroot lobe of the Idaho batholith. X= pole to ill-defined girdle. Small arrows show the sense of rotation in small folds. Data are plotted on lower hemisphere of Wulff stereonet.

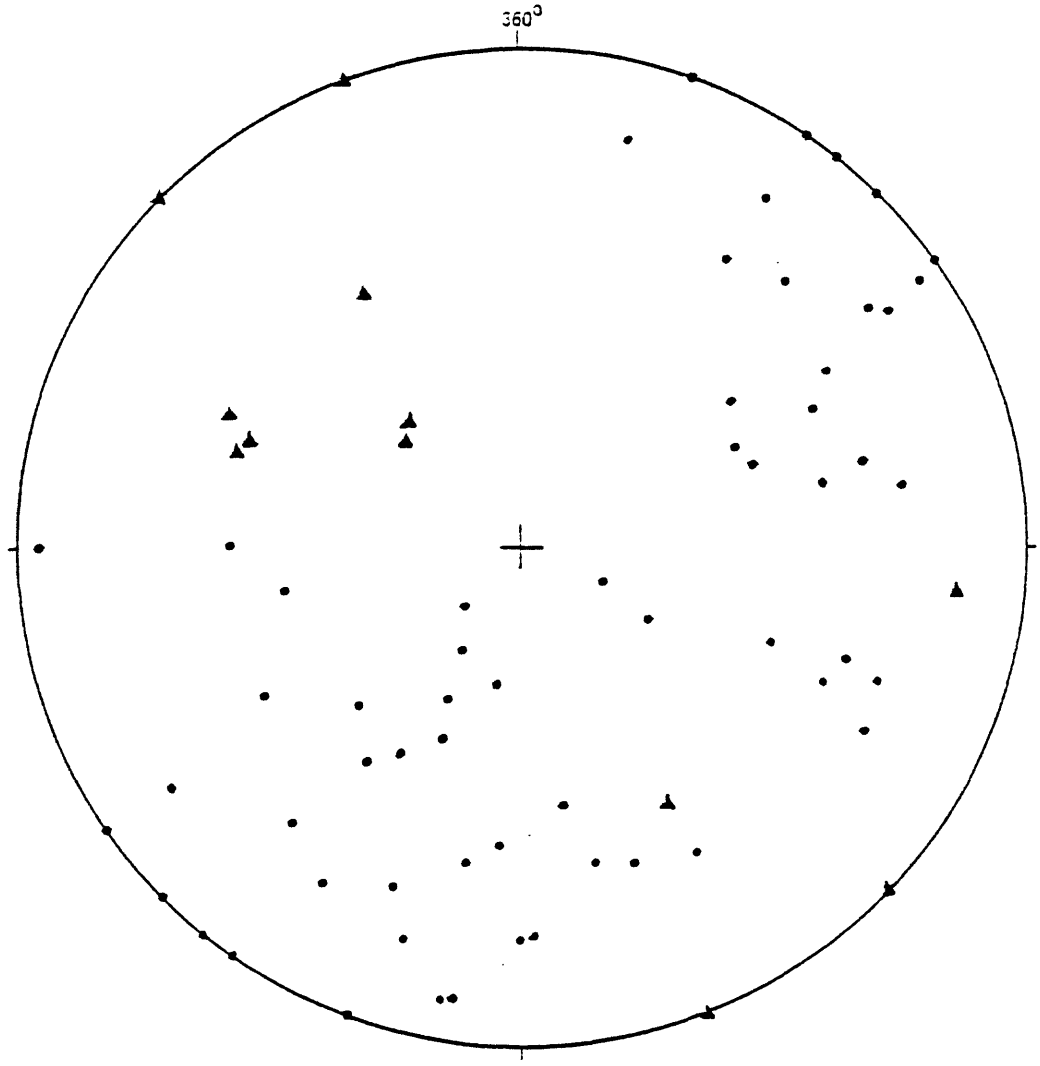

Figure 53.--Poles to flow foliation (●) and lineation (▲) in granitic rocks of the northern zone of the western sector, Bitterroot lobe of the Idaho batholith, west of Hamilton, Mont. Data are plotted on lower hemisphere of Wulff stereonet.

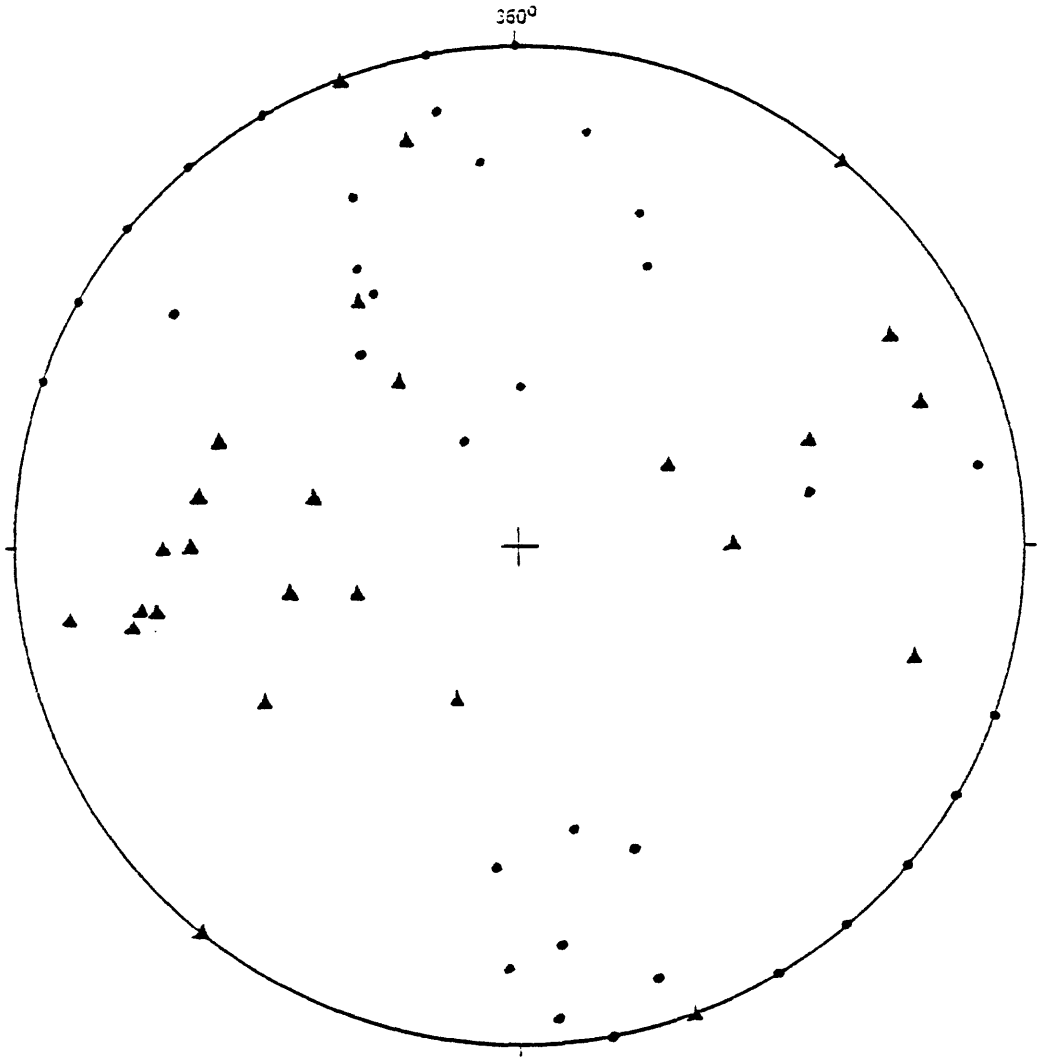

Figure 54.--Poles to shear joints (●) and slickensides in the shear joints (▲) in the western sector, Bitterroot lobe of the Idaho batholith, west of Hamilton, Mont. Data are plotted on lower hemisphere of Wulff stereonet.

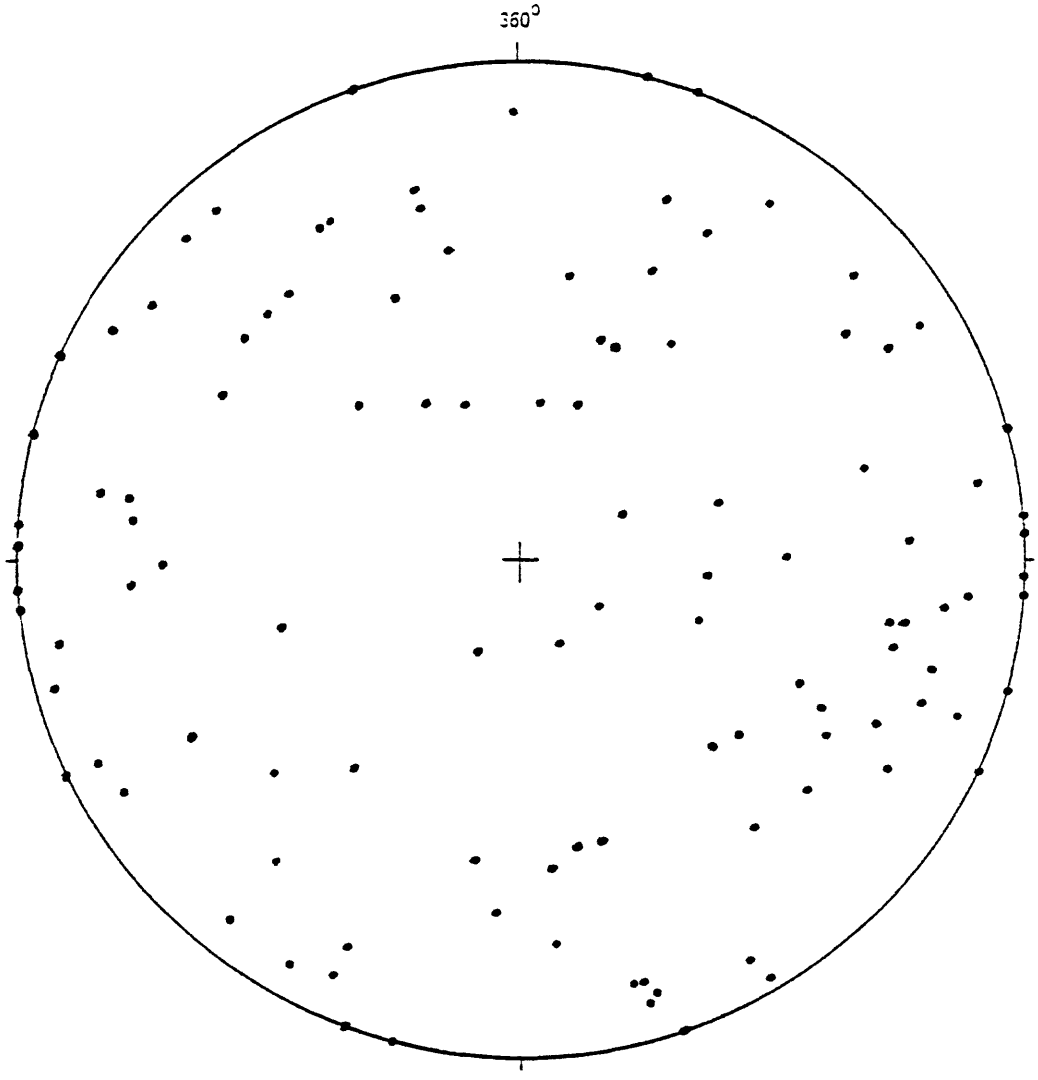

Figure 55.--Poles to secondary joints (●) in the western sector, Bitterroot lobe of the Idaho batholith, west of Hamilton, Mont. Data are plotted on lower hemisphere of Wulff stereonet.

Table 5.--Modes in the Huckleberry Butte quadrangle (HF6)

(1) Granite 78RR212B. (2) Granite 78RR251B. (3) Granite 78RR261B. (4) Granite 79RR271F. (5) Granite 79RR273B. (6) Granite 79RR318A. (7) Granite 79RR337A. (8) Granodiorite 78RR263A. (9) Granodiorite 79RR280A. (10) Granodiorite 79RR281A. (11) Granodiorite 79RR334B. (12) Oligoclase-biotite schist 78RR259B. (13) Microcline quartzite 78RR264B. (14) Microcline-muscovite quartzite 79RR270. (15) Muscovite quartzite 79RR271A1. (16) Microcline-muscovite quartzite 79RR271A2. (17) Muscovite quartzite 79RR271A3. (18) Oligoclase-biotite quartzite 79RR274A. (19) Neosome (granodiorite) in migmatite with oligoclase-biotite quartzite of 79RR274A. (20) Orthoclase quartzite 79RR275A. (21) Muscovite-oligoclase quartzite 79RR277A. (22) Biotite quartzite 79RR334A. (23) Neosome (alkali-feldspar granite) in migmatite with biotite quartzite of 79RR334A. (24) Biotite-muscovite-oligoclase quartzite 79RR336. (25) Microcline quartzite 78RR339A. (26) Hornblende-labradorite-quartz granofels 79RR272A. (27) Meta-tonalite(?) 79RR341A.

	1	2	3	4	5	6	7	8	9	10	11	12	13	14	15	16	17	18	19	20	21	22	23	24	25	26	27
Plagioclase	41.6	43.0	21.4	22.3	38.2	32.0	36.1	47.6	44.3	42.5	35.0	20.6	2.7	7.6		8.4	4.8	7.5	45.2	1.8	16.3	6.5	2.4	24.4	3.3	28.4	42.8
Quartz	25.4	23.1	34.9	54.2	24.6	33.1	33.2	25.3	33.9	34.8	41.2	35.0	73.4	61.4	61.5	46.4	56.3	77.1	28.2	80.2	65.4	70.6	48.6	53.2	78.4	46.5	33.7
K-spar	26.1	25.6	28.2	19.9	29.6	25.5	25.5	21.4	19.7	19.6	17.8		13.6	10.5		19.1			17.2	10.7		2.7	42.3		12.0		
Biotite	5.0	7.0	12.8	1.8	7.5	4.1	3.8	3.9	1.8	2.7	2.1	32.8	4.5	5.6		0.2		10.7	4.8	3.3	6.7	14.1	2.4	9.7	4.2		21.9
Muscovite		0.9	2.3	1.6		5.1	1.1	1.7	0.2	0.2	3.9	10.6	5.7	14.5	37.6	23.9	35.1	4.7	4.5	3.6	11.4	6.0	4.2	11.7	2.1		1.3
Hornblende					tr																					23.0	
Diopside																											
Scapolite																											
Sillimanite														0.4		1.3	0.2										
Accessories	1.9	0.3	0.3	0.2	0.2	0.2	0.2	0.1	tr	0.2	tr	0.8	0.1	tr	0.8	0.6	3.6	tr	tr	0.4	0.2	tr	tr	0.9	tr	2.0	0.3
	100.0	99.9	99.9	100.0	100.1	100.0	99.9	100.0	99.9	100.0	100.0	99.8	100.0	100.0	99.9	99.9	100.0	100.0	99.9	99.9	100.0	99.9	99.9	99.9	100.0	99.9	100.0

Table 6.--Modes in the Greenside Butte quadrangle (HG6)

(1) Granite 78RR206B. (2) Granite 79RR185A. (3) Granite 79RR186A. (4) Granite 79RR188A. (5) Granite 79RR208E. (6) Granite 79RR209A. (7) Granite 79RR213A. (8) Granite 79RR220B. (9) Granite 79RR223A. (10) Granite 79RR257B. (11) Granite 79RR263A. (12) Granite 79RR266A. (13) Granite 79RR306A. (14) Granite 79RR313A. (15) Granite 79RR314A. (16) Granite 79RR315A. (17) Granite 79RR316A. (18) Granite 79RR317A. (19) Granite 79RR319A. (20) and (21) Granite 79RR323A. (22) Granite 79RR325I. (23) Granite 79RR328A. (24) Granite 79RR331A. (25) Granite 79RR332A. (26) Granodiorite 78RR150A. (27) Granodiorite 78RR196B. (28) Granodiorite 79RR179A. (29) Granodiorite 79RR180A. (30) Granodiorite 79RR181A. (31) Granodiorite 79RR222A. (32) Granodiorite 79RR254A. (33) Granodiorite 79RR256A. (34) Granodiorite 79RR261A. (35) Granodiorite 79RR262A. (36) Granodiorite 79RR264A. (37) Granodiorite 79RR269A. (38) Granodiorite 79RR302A. (39) Granodiorite 79RR305E. (40) Granodiorite 79RR305F. (41) Granodiorite 79RR311A. This is the neosome in a quartzite, forming migmatite. (42) Granodiorite 79RR312A. (43) Granodiorite 79RR314B. (44) Granodiorite 79RR322A. (45) Granodiorite 79RR324A. (46) Granodiorite 79RR329A. (47) Granodiorite 79RR330A. (48) Granodioritic alaskite 79RR215B. (49) Quartz monzonite 78RR148B. (50) Quartz monzonite 79RR217A. (51) Quartz monzonite 79RR218A. (52) Quartz monzodiorite 78RR151B. (53) Tonalite 78RR188B. (54) Tonalite 79RR208A, gradational into (55) Granodiorite 79RR208A, in the outcrop and in the stained slab. (56) Tonalite 79RR215A. (57) Tonalite 79RR260B. (58) Tonalite 79RR326B. (59) Tonalite xenolith 79RR217E. (60) Trondhjemite 79RR325A. (61) Biotite metagabbro xenolith in granite 79RR217B. (62) Sillimanite-microcline quartzite 79RR208B. (63) Plagioclase quartzite 79RR219E. (64) Biotite-microcline quartzite 79RR255A. (65) Biotite-muscovite quartzite 79RR303A. (66) Quartz-pebble conglomerate 79RR305A. (67) Plagioclase-biotite quartzite 79RR307A. (68) Plagioclase-muscovite-quartzite 79RR311A. (69) Biotite-muscovite quartzite 79RR312B. (70) Lit-par-lit felsic material in schist 79RR312B. (71) Microcline quartzite 79RR326A. (72) Diopside-hornblende gneiss 79RR184A. (73) Calc-silicate granulite 79RR267A. (74) Plagioclase quartzite 79RR308A. (75) Hornblende-plagioclase quartzite 79RR310A. (76) Calc-silicate schist 79RR314E. (77) Amphibolite 79RR256B. (78) Amphibolite 79RR256G.

	1	2	3	4	5	6	7	8	9	10	11	12	13	14	15	16	17	18	19	20	21	22	23	24	25	26	27	28
Plagioclase	44.4	45.1	36.6	36.4	31.4	30.6	24.7	33.9	39.4	32.2	44.4	24.0	40.4	25.7	12.4	32.7	40.2	35.6	27.6	39.6	39.6	41.7	41.1	41.2	34.4	53.2	46.6	43.7
Quartz	19.4	20.2	21.6	24.9	36.7	20.2	19.6	25.5	22.3	37.6	23.3	54.1	28.0	49.0	63.5	29.7	30.1	31.5	30.6	30.9	30.9	27.2	31.2	28.0	31.1	19.4	25.2	32.7
K-spar	26.3	23.0	34.8	27.9	23.7	43.1	52.1	35.1	32.8	23.6	28.6	14.2	26.2	16.6	13.5	31.6	23.6	24.5	36.8	22.2	22.2	26.8	23.0	22.8	29.3	16.6	22.7	18.7
Biotite	7.4	9.5	4.6	9.9	3.8	4.7	3.3	4.3	4.8	3.6	2.4	6.1	2.0	4.5	6.4	5.9	6.0	7.5	2.4	4.6	4.6	2.6	2.9	3.8	3.4	10.0	2.7	3.8
Muscovite		0.9	1.5	0.7	3.8	0.6	0.6	1.1	0.7	2.9		1.5	2.5	4.0	2.6				1.8	2.4	2.4	1.0	1.8	3.6	1.6		1.2	0.8
Hornblende																		0.6										
Accessories	2.3	0.9	0.9	0.2	0.8	tr	tr	tr	tr	1.4	tr	tr	0.8	0.2	1.5	tr	tr	0.3	0.9	0.2	0.2	0.8	tr	0.7	0.2	0.8	1.6	0.2
	99.8	99.8	100.0	100.0	100.0	100.0	100.1	99.9	100.0	99.9	100.1	99.9	99.9	100.0	99.9	99.9	99.9	100.0	100.1	99.9	99.9	100.1	100.0	100.1	100.0	100.0	100.0	99.9

Table 6.--Modes in the Greenside Butte quadrangle (HG6) (continued)

	29	30	31	32	33	34	35	36	37	38	39	40	41	42	43	44	45	46	47	48	49	50	51	52	53	54	55	56
Plagioclase	41.8	50.9	37.2	43.2	48.7	48.8	49.4	38.0	47.6	50.6	45.8	44.6	32.5	37.2	41.9	46.4	40.8	43.8	42.1	39.4	43.1	40.2	36.9	61.5	42.3	52.6	42.0	43.2
Quartz	31.4	24.9	39.0	33.2	20.0	22.4	22.5	34.1	29.4	31.2	28.0	28.2	38.7	39.9	39.9	28.8	36.5	29.2	31.7	43.0	16.8	18.1	15.8	12.8	43.7	31.5	25.2	25.0
K-spar	19.2	16.5	6.5	20.4	24.3	18.9	21.8	17.5	18.2	6.0	22.0	22.5	16.1	18.2	15.8	15.7	16.5	20.2	21.3	17.1	33.1	34.9	41.2	21.8		1.5	21.4	
Biotite	2.8	6.2	11.7	2.0	5.5	8.6	5.5	4.4	4.1	12.0	2.8	3.2	7.3	3.8	2.0	6.3	4.0	4.6	1.8	0.2	6.9	3.2	4.6	3.2	13.2	13.1	10.5	14.7
Muscovite	3.0	0.6	4.7	0.3	0.6	0.6		5.9	0.6		0.8	0.7	5.4	0.6	0.5	2.3	1.1	1.4	2.6			2.8	0.9					
Hornblende																												16.8
Sillimanite																												
Epidote																												
Accessories	1.6	1.0	0.9	0.9	0.9	0.6	0.8	tr	0.2	0.2	0.6	0.7	tr	0.3	tr	0.4	1.1	0.9	0.5		tr	0.8	0.5	0.8	0.8	1.2	1.0	0.3
	99.8	100.1	100.0	100.0	100.0	99.9	100.0	99.9	100.1	100.0	100.0	99.9	100.0	100.0	100.1	99.9	100.0	100.1	100.1	100.0	99.9	100.0	99.9	100.1	100.0	99.9	100.1	100.0

	57	58	59	60	61	62	63	64	65	66	67	68	69	70	71	72	73	74	75	76	77	78
Plagioclase	52.7	56.2	52.6	26.0	57.6	6.0	34.4	3.6	6.7	3.2	22.7	12.2	2.0	16.2	2.7	17.0	34.8	27.5	31.9	36.4	53.4	44.7
Quartz	27.6	31.1	22.9	55.6	0.6	71.9	51.6	66.7	62.2	70.4	44.0	53.8	45.9	51.4	75.2	27.3	36.1	61.6	46.8	47.4	2.7	0.5
K-spar	4.2	2.3				8.8		17.8	4.0	17.4		0.7	0.3		16.9							
Biotite	12.0	9.1	22.2	6.3	36.8	3.7	13.7	11.9	11.6	8.1	31.0	18.1	25.3	4.6	2.4			3.1	3.0	12.8	4.3	
Muscovite	1.3	0.9	0.7	12.0		2.6	0.2		15.2	0.3		15.3	25.9	27.4	2.7							
Hornblende											tr					41.8	27.9	2.6	11.9	0.2	39.3	51.9
Diopside						7.1										12.2						
Sillimanite					2.1				0.3	0.3												
Epidote											1.4							2.6	4.6			
Garnet											0.6							0.5	0.8	1.7		
Accessories	2.1	0.4	1.6	tr	3.0	tr	tr	tr	tr	0.3	0.3	tr	0.6	0.4	tr	1.8	1.3	2.0	1.1	1.4	0.3	3.0
	99.9	100.0	100.0	99.9	100.1	100.1	99.9	100.0	100.0	100.0	100.0	100.0	100.0	100.0	99.9	100.1	100.1	99.9	100.1	99.9	100.0	100.1

Table 7. Modes in the Fish Lake quadrangle (1116)

(1) Granite 78RR155F. (2) Granite 79RR014A. (3) Granite 79RR113A. (4) Granite 79RR114A. (5) Granite 79RR121A. (6) Granite 79RR127B. (7) Granite 79RR128A. (8) Granite 79RR189E. (9) Granite 79RR190A1. (10) Granite 79RR240A. (11) Granite 79RR243A. (12) Granite 79RR248A1. (13) Granite 79RR250A. (14) Granite 79RR253A. (15) Granite 79RR282A. (16) Granite 79RR289A. (17) Granodiorite 78RR153A. (18) Granodiorite 78RR153B. (19) Granodiorite 79RR032B. (20) Granodiorite 79RR111B. (21) Granodiorite 79RR122B. (22) Granodiorite 79RR124A. (23) Granodiorite 79RR126A. (24) Granodiorite 79RR129A. (25) Granodiorite 79RR189A. (26) Granodiorite 79RR189B. (27) Granodiorite 79RR246A. (28) Granodiorite 79RR246B. (29) Granodiorite 79RR247A. (30) Granodiorite 79RR248A. (31) Granodiorite 79RR251A. (32) Granodiorite 79RR284A. (33) Granodiorite 79RR287A. (34) Granodiorite 79RR320A. (35) Granodiorite 79RR321A. (36) Tonalite 79RR111E. (37) Tonalite 79RR111F. (38) Tonalite 78RR156A. (39) Tonalite 79RR249A. (40) Tonalite gneiss 79RR253B. (41) Granitic aplite 79RR121F. (42) Granitic alaskite 79RR123G. (43) Granitic aplite 79RR128B. (44) Granitic aplite 79RR189F. (45) Calc-silicate quartzite 79RR034A. (46) Calc-silicate gneiss 79RR242A. (47) Calc-silicate hornfels 79RR250. (48) Microcline-biotite quartzite 78RR154A. (49) Plagioclase quartzite 79RR035B. (50) Plagioclase-microcline quartzite 79RR123B. (51) Microcline-plagioclase quartzite 79RR123E. (52) Biotite quartzite 79RR248B. (53) Microgranite 79RR240B.

	1	2	3	4	5	6	7	8	9	10	11	12	13	14	15	16	17	18	19	20	21	22	23	24	25	26	27	28
Plagioclase	40.7	19.6	37.9	24.7	45.7	36.4	33.4	36.4	39.9	41.6	25.3	44.8	31.3	40.6	33.6	41.5	47.4	43.9	48.3	46.9	43.4	43.6	45.9	43.0	46.0	46.5	48.4	50.8
Quartz	22.7	50.0	36.9	33.9	21.2	29.2	25.7	24.3	27.2	24.8	30.8	22.7	27.7	32.3	27.2	24.6	21.6	25.6	21.6	26.5	30.8	28.0	25.2	32.2	30.5	29.0	35.3	25.4
K-spar	29.4	23.3	22.9	35.6	27.8	25.3	32.8	31.0	26.5	27.4	34.3	25.8	28.4	24.0	37.0	28.4	24.3	23.6	22.8	22.0	20.2	22.2	21.6	14.4	13.3	18.4	9.9	15.1
Biotite	5.9	6.7	1.3	3.4	3.6	3.7	2.7	5.3	4.3	4.4	6.7	5.3	5.9	2.0	1.8	3.7	5.2	5.7	6.2	2.8	3.2	3.2	5.2	6.0	5.9	4.5	5.7	6.6
Muscovite		0.4	0.6	2.0	1.2	5.2	5.3	1.9	1.6	1.1	2.1	1.0	6.1	1.1	0.4	1.4			0.2	1.1	1.4	2.0	1.0	4.4	2.9	1.1	0.7	0.9
Accessories	1.3	tr	0.3	0.3	0.5	0.2	tr	1.0	0.4	0.7	0.7	0.4	0.5	tr	tr	0.4	1.6	1.2	0.7	0.6	0.9	1.0	1.0	tr	1.4	0.4	tr	1.2
	100.0	100.0	99.9	99.9	99.9	100.0	99.9	99.9	99.9	100.0	99.9	99.9	99.9	100.0	100.0	100.0	100.1	100.0	99.8	99.9	99.9	100.0	99.9	100.0	100.0	99.9	100.0	100.0

	29	30	31	32	33	34	35	36	37	38	39	40	41	42	43	44	45	46	47	48	49	50	51	52	53
Plagioclase	34.6	41.6	56.2	55.2	36.7	40.6	41.6	52.9	63.1	48.0	55.6	46.8	29.2	20.5	33.7	14.8	5.3	32.6	47.6	4.9	12.5	12.2	16.3	0.9	33.2
Quartz	34.0	31.7	26.4	26.2	40.0	34.0	33.0	29.9	33.8	38.3	26.8	28.3	35.2	38.0	33.0	35.1	41.4	11.3	46.0	66.7	80.7	67.0	64.8	80.9	26.0
K-spar	20.6	17.2	11.4	12.7	16.6	14.3	18.4	4.9		4.9			27.8	25.7	27.2	38.6		0.4		11.7		12.2	10.3	0.5	24.9
Biotite	5.7	6.9	2.7	4.8	5.2	3.2	4.9	11.5	3.1	4.7	14.4	23.0	0.6						5.5	14.1	6.7	7.5	6.0	14.8	15.1
Muscovite	4.8	2.1	2.9	0.2	0.9	6.7	1.8	0.7			1.0		6.6	15.8	5.8	11.3				2.5		0.3	2.6	2.0	0.5
Garnet																	21.5		0.4						
Epidote																	29.2								
Diopside																	1.4	43.1							
Calcite																	tr								
Actinolite																		11.1							
Accessories	0.3	0.5	0.4	0.9	0.6	1.1	0.2	tr	tr	4.0	2.1	1.8	0.6	tr	0.2	tr	1.2	1.4	0.4	tr	tr	0.7	tr	0.9	0.3
	100.0	100.0	100.0	100.0	100.0	99.9	99.9	99.9	100.0	99.9	99.9	99.9	100.0	100.0	99.9	99.8	100.0	99.9	99.9	99.9	99.9	99.9	100.0	100.0	100.0

in the northern zone of the western sector. In one granite, plagioclase is locally broken and recrystallized in 0.3 mm, strain-free, granoblastic subgrains together with quartz and microcline of comparable size in zones up to 0.5 mm across. This is a blastomylonitic texture; it is overprinted by microbreccia presumably related to steep shears of 280° az trend seen in outcrop. Cataclastic effects due to microbrecciation along narrow shears include bending of plagioclase twin lamellae, undulatory extinction, and breaking of light-colored minerals. Associated with the cataclasis are sericite and clay alteration.

Quartz content ranges from 19% to 63% in the granite, in 1.5 to 4 mm grains. The habit of the quartz is different in the northern zone from that in the southern zone. Specifically, a subtle but major zone of structural transition of easterly trend crosses through the south half of the Huckleberry Butte and Greenside Butte quadrangles and continues east near the southern boundary of the Fish Lake quadrangle, well within the area of granitic rocks. Beyond the Fish Lake quadrangle, this zone passes southeasterly into the area mapped by Bittner-Gaber (1983). Quartz of the northern zone is altogether broken in 0.5 to 0.7 mm subgrains, free of strain effects where not overprinted by younger cataclastic features. Five rocks contain flattened grains from 2x4 to 2x6 mm in size, also broken in strain-free subgrains. Where affected by cataclastic processes, the subgrains show sutured quartz-quartz boundaries and varied degrees of undulatory extinction. Quartz of the southern zone is largely free of subgrains, the development of which dies out to the south over a zone a kilometer or so wide. The quartz of the southern zone is therefore in single, optically continuous grains. Cataclastic effects are much the same here as in the northern zone except that the undulatory extinction in large grains has a blocky appearance. Four rocks show blastomylonitic shear zones up to 1 mm thick along which granoblastic or strain-free quartz grains of 0.2 mm occur; these are northern-zone rocks. Quartz in about a third of the rocks studied shows the effects of cataclasis in varied degree. Some is partly broken in 0.05 mm or larger strained fragments in cataclastic shears up to 0.3 mm thick; these cut and overprint the blastomylonitic arrays described above.

K-feldspar in the granite of the western sector (14% to 52% in the mode) occurs entirely as microcline (except for orthoclase in one rock) in 1 to 8 mm, irregular grains; some of the microcline is submicroscopically twinned and therefore masquerades as orthoclase. In a few porphyritic granites, microcline phenocrysts are 1 to 2 cm in diameter. Larger matrix grains include plagioclase, biotite, and quartz. Some plagioclase inclusions are myrmekitic and some are oriented parallel to crystal planes of the host. Microcline in two granites encloses 0.5 to 0.7 mm clusters of 0.2 to 0.4 mm, granoblastic, unzoned plagioclase grains (An_{22}) with 120° interfacial angles of distinctly crystalloblastic aspect. The microcline of one granite is cut by extension fractures filled with quartz and muscovite. In several granites of the northern zone, microcline occurs in flattened grains ((2:1) lenses), and these grains contain 1 mm, strain-free subgrains; the long axes of the ovoids are subparallel to one another and to flattened plagioclase and quartz grains. Moderate clay alteration is fairly common in microcline.

Biotite (2% to 10% in the mode) occurs in 0.4 to 1 mm grains, generally a little altered to pennine and to varied but minor amounts of sericite, epidote, and rutile needles; in one rock, it is partly altered to green biotite. Most biotite appears to be randomly oriented, but two granites have biotite in crude lepidoblastic array. Some shearing-out and recrystallization to finer grains occurs along blastomylonitic shears. Biotite is kinked or bent by cataclasis in several rocks and partly reduced to smaller sizes along cataclastic shears. Muscovite (0.4% to 6.1% in the mode) occurs in 0.4 to 2 mm flakes. It occurs as primary grains in the larger part of the rocks and as secondary sericite in a smaller part; six granites contain no muscovite at all. In two rocks, it has been sheared and recrystallized to finer grain size along with biotite and quartz in blastomylonitic shears. Where sericite is developed, it occurs principally along late cataclastic shears, partly formed through shear reduction of primary muscovite. Accessory minerals listed in their approximate order of abundance include magnetite, zircon, apatite, thorite, baddeleyite, allanite, epidote, sphene, leucoxene, and hematite. Of these, magnetite is more abundant than all the others taken together. Some ilmenite may be lumped in with the magnetite.

Granodiorite.

Granodiorite studied in the western sector is listed in table 3 (modes 28 to 29), table 4 (modes 13 and 14), table 5 (modes 8 to 11), table 6 (modes 26 to 47), and table 7 (modes 17 to 35). Plagioclase in the granodiorite (32% to 56% in the mode) occurs in 1.5 to 4 mm grains. Plagioclase composition is in the range An_{15} to An_{33}, about the same as in the granite. In a few rocks, a few plagioclase grains show normal zoning (e.g., An_{33} cores to An_{25} rims) and prismatic form, but most of the grains are unzoned, partly equant, and euhedral to subhedral. Some subhedral grains may be crystalloblastic in part, as they have a rounded appearance where sheared-around. In one rock, plagioclase is partly in 2 mm clusters of smaller granoblastic grains with 120° interfacial angles; some of these clusters are enclosed by microcline grains. Three rocks show flattened feldspar grains, imparting a weak foliation best shown in the stained slabs. In three rocks, plagioclase grains are cut by extension fractures perpendicular to secondary foliation, filled with quartz, microcline, muscovite, and pennine, or combinations thereof. Plagioclase in eight granodiorites is partly broken in strain-free, 0.5 to 1.5 mm subgrains. Sericite alteration occurs in the plagioclase of a few rocks, partly controlled by irregular shears. Plagioclase twin lamellae in two granodiorites show some cataclastic bending.

Quartz in the granodiorite (19% to 40% in the mode) occurs in irregular 1 to 4 mm grains. Quartz habit is controlled by the same zone that controls it in the subgrains free of strain effects where not overprinted by younger cataclasis. With strong subgrain development, a crude fluxion structure develops, with subgrain flattening. Quartz of the southern zone is largely free of subgrains, and the quartz is therefore in large, single grains. In three granodiorites of the northern zone, quartz subgrain arrays are overprinted by irregular, shear-controlled arrays of granoblastic, strain-free, 0.1 mm quartz grains due to younger blastomylonite development. Cutting both structures are younger zones of cataclastic shear and associated undulatory extinction; thus, the late cataclastic shear was widespread.

K-feldspar in granodiorite of the western sector (6% to 29% in the mode) occurs mostly as microcline, except for orthoclase in three rocks along Wounded Doe Ridge (also the site of orthoclase occurrence in one granite). K-feldspar occurs in 1 to 6 mm grains and generally encloses plagioclase, biotite, and quartz. Five granodiorites are porphyritic with 1 to 2 cm K-feldspar phenocrysts. Some plagioclase inclusions (An_{25}) are oriented along crystalloblastic planes in microcline; matrix plagioclase has a composition of An_{20} in the same rock. Deformed K-feldspar described below belongs to the northern zone. In four rocks, K-feldspar grains are cut by 0.1 mm-thick extension fractures filled with quartz, muscovite, and pennine. In one granodiorite, the K-feldspar shows a crude alinement of flattened grains best seen in the stained slab. In six rocks, K-feldspar occurs in flattened or rodded grains in crudely developed foliation. One has some 1 mm, strain-free subgrains developed at the expense of originally larger grains. In one rock, the microcline is broken in 0.02 mm fragments in a 0.5 mm-thick shear zone with quartz, plagioclase, and mica of like size. This may be due to sericite-coated shears oriented 085° az, 75° SE seen at the outcrop.

Biotite (2% to 12% in the mode) occurs in 0.4 to 1 mm grains, generally a little altered to pennine, minor sericite, or green biotite (in one rock). Most biotite appears to be randomly oriented; two granodiorites of the northern zone have biotite in crude lepidoblastic array. These two also contain flattened quartz and feldspar grains. Muscovite content ranges from 0.2 to 7%. Muscovite occurs as primary grains in most of the rocks and as secondary sericite in a few of them; it is absent in two rocks. Mica is a little kinked by cataclasis in some rocks. Accessory minerals listed in their approximate order of abundance include magnetite, zircon, apatite, thorite, allanite, baddeleyite, epidote, pyrite, and leucoxene. Some ilmenite (opaque grains with leucoxene rims) may be lumped with magnetite (partly altered to hematite). Sphene, noted in granite, was not found in granodiorite. The black opaques are more abundant among the accessories than all the other accessories taken together.

Quartz monzonite.

Quartz monzonite, found only in small amounts in the Greenside Butte quadrangle and mostly porphyritic, is listed in table 6 (modes 49 to 52). Plagioclase (40% to 62% in the mode) occurs in 2 to 3 mm, unzoned, subhedral, prismatic grains (An_{20} to An_{22}). Quartz (13% to 18% in the mode) in 2 mm grains contains few to no subgrains; all the quartz monzonite lies in the southern zone. Microcline (22% to 41% in the mode) in 3 to 6 mm grains includes plagioclase and biotite. Biotite (3% to 7% in the mode) occurs in 0.5 to 1 mm grains and is a bit altered to pennine. Muscovite, absent in two rocks, occurs in 0.9% and 2.8% amounts in the other two. Accessory minerals in their approximate order of abundance include magnetite, zircon, apatite, thorite, baddeleyite, and rutile.

Quartz monzodiorite.

One quartz monzodiorite was found (table 6, mode 52) in the southern zone in the Greenside Butte quadrangle, among outcrops of granite and granodiorite and seemingly gradational into them. Plagioclase is antiperthitic, partly normally zoned (cores An_{28}, rims An_{20}) in relicts, but mostly unzoned (An_{20}). In places, it is myrmekitic against K-feldspar. Quartz is in 2 mm grains largely free of subgrains, with a little undulatory extinction. Microcline in 6 mm grains is poikilitic with quartz and plagioclase and is string perthitic. Biotite occurs in 1 mm flakes altered to pennine, sphene, epidote, and sericite. Accessories include magnetite, zircon, apatite, sphene, and baddeleyite.

Tonalite.

Tonalite studied in the western sector within the area of granitic rocks is listed in table 6 (modes 53 and 54 and 56 to 59) and table 7 (modes 36 to 40); it is mixed more or less randomly with the other plutonic rocks. Plagioclase (42% to 63% in the mode) occurs in 1 to 3 mm, euhedral to subhedral, unzoned prismatic grains (An_{25} to An_{32}). Relicts of normal zoning in the plagioclase of one rock have cores of An_{25} and rims of An_{20}. In two rocks, some plagioclase grains are cut by extension fractures filled with quartz, muscovite, microcline, sericite, and pennine. Grains in two rocks are bent or broken by cataclasis.

Quartz (23% to 44% in the mode) occurs in 2 to 4 mm grains, with subgrains in some rocks and none in others, depending on whether the rocks occur in the northern or southern zone. One rock is cut by blastomylonitic shears 0.5 mm thick, within which quartz occurs in 0.2 mm, strain-free, granoblastic grains. K-feldspar and plagioclase occur also in these shears, as 0.2 mm grains, associated with sericite, chlorite, and leucoxene. One rocks is strongly cataclastically sheared with 0.02 mm to 0.07 mm grains in pervasive, 1 mm-thick shear zones. All the deformed rocks occur in the northern zone.

Microcline occurs in small amounts in about half the tonalite (1.5% to 5% in the mode) in 0.2 to 6 mm grains. Biotite occurs in 1 mm flakes (3% to 23% in the mode), subparallel in one rock altered a bit to pennine in several, and bent cataclastically and reduced to smaller grain size in cataclastic shear zones. Muscovite or sericite are present in trace amounts or absent. Accessory minerals in their approximate order of abundance include magnetite, apatite, zircon, thorite, allanite, sphene, baddeleyite, and pyrite (elongate blebs in cataclastic shear zones).

Migmatite.

Migmatite in west- to northwest-trending sheets is relatively abundant in the northern zone of the western sector. Poles to migmatite foliation lie close to the girdle for flow foliation shown in figure 53. Axes of many small folds, and mineral lineations in the migmatite trend at shallow angles to the northwest, similar to linear trends in the enclosing igneous rock. A major migmatite unit occurs in the southwestern part of the Greenside Butte quadrangle (Lottie Lake-Rock Lake area); smaller amounts of migmatite occur scattered in other parts of the northern zone. Granite to tonalite, massive to gneissic, is complexly intermixed with quartzite, mica schist, calc-silicate rock, granitic gneiss, and amphibolite. Three granodiorites (table 6, modes 31, 38, and 41) were injected as sheets and partly infolded in migmatite. The petrographic description given above for granodiorite is applicable. The muscovite in three specimens contains a little fibrolitic sillimanite.

Several quartzites from the migmatite were studied (table 3, mode 40; table 5, modes 12 to 14; table 6, modes 62 to 71; and table 7, modes 48 to 52). Quartz ranges from 44% to 81% in the mode and is in grains 0.3 to 4 mm in diameter. Quartz in rocks from the northern zone is broken in 0.4 to 0.7 mm, strain-free subgrains, variously deformed in younger cataclasis. Plagioclase (1% to 34% in the mode)

ranges in composition from An_{15} to An_{28} in equant, unzoned grains from 0.2 to 4 mm in diameter. Extension fractures filled with quartz cut some grains. K-feldspar is mostly microcline (orthoclase in one rock) in amounts ranging from 0.5% to 18% of the mode, in grains from 0.2 to 1.5 mm in diameter. Biotite (2% to 31% in the mode) occurs in 0.5 to 2 mm grains, partly altered to pennine. Biotite lineation in the northern zone trends northwest at shallow angles, parallel to linear features in the enclosing granitic rocks. In one rock, it is partly sheared-out in strong cataclasis parallel to older schistosity and much reduced in grain size. Muscovite (zero to 27%; absent in three rocks) occurs in grains from 0.2 to 2 mm in diameter, crudely lepidoblastic. Accessory minerals seen are zircon, apatite, rutile, baddeleyite, magnetite, ilmenite?, fibrolite (found in three rocks, 0.3% to 7.1% in the mode), and pyrite (in one rock). A quartz-pebble conglomerate contains the largest amount of sillimanite, present only in the pebbles. The pebbles have been stretched in greater than 13:1 ratio in the fold axis direction (50°, 110° az) in the same trend as linear features in the surrounding rock.

Several calc-silicate rocks from the migmatite were studied (table 3, modes 35 and 36; table 5, mode 26; table 6, modes 72 to 76; and table 7, modes 45 to 47). Their mineralogy is rather diverse; average grains size is about 0.3 mm. Minerals include hornblende (0.2% to 42%), plagioclase (5% to 47%) ranging from An_{54} to An_{95} in composition, quartz (11% to 62%), biotite (zero to 12%), and diopside (zero to 12%). Minor to accessory minerals include K-feldspar, garnet, epidote, calcite, actinolite, apatite, sphene, magnetite, and allanite.

Petrography of the mica schist is shown by two specimens (table 4, modes 38 and 39). One of these is of biotite, muscovite, and plagioclase (An_{32}). Plagioclase is granoblastic in 0.5 mm grains. Trace amounts of epidote and fibrolite occur; as well as skeletal crystals of corundum in the biotite, in 0.1 mm grains. Accessories include zircon, magnetite, and thorite. The other schist is of muscovite, biotite, and quartz, with fibrolite enclosed in muscovite. Accessories include thorite, zircon, epidote, and apatite. Much of the muscovite (2 mm flakes) has been shear(?) reduced or hydrothermally(?) recrystallized to very fine-grained sericite mats which still display bulk extinction indicative of preferred orientation.

The petrography of the granitic gneiss in the migmatite screens, seen only in the southern zone in the Chimney Peak quadrangle, is shown by four specimens (table 3, modes 19 to 22). The granitic gneiss occurs as concordant sheets along the foliation in the migmatite screens; e.g., in a 6-m band, and is locally folded in the foliation. Plagioclase (13% to 31% in the mode) ranges in composition from An_{20} to An_{33}, in unzoned, generally granoblastic grains 0.7 to 3 mm in diameter. In one gneiss, 3-mm, stubby prismatic grains are partly recrystallized in 0.5 mm, sub-granoblastic grain arrays. Quartz (27% to 39% in the mode) occurs in 1 to 2 mm, irregular grains. Orthoclase (37%) occurs as 0.5 mm, granoblastic grains in one gneiss; in the others, microcline occurs in 2 to 4 mm grains, 32% to 36% of the mode. Biotite (5% to 11% in the mode), more or less lepidoblastic, occurs in 0.5 to 1.5 mm grains. Muscovite (1% to 2% in the mode) occurs in 0.5 mm grains. Accessories include apatite, magnetite, zircon, and cassiterite?

Three amphibolitic rocks from migmatite were studied (table 3, mode 33; and table 6, modes 77 and 78). Green hornblende and plagioclase ($An_{38\ to\ 47}$) occur in 0.4 mm grains and make up most of the rock. Minor and accessory minerals are biotite, quartz, magnetite, sphene, thorite, and apatite.

Xenoliths.

Xenoliths of several types occur in the granitic rocks and are particularly abundant near the contact with the earlier tonalite intrusion to the south. One near the contact is quartzite injected by tonalite gradational into granodiorite (table 6, modes 54 and 55). In the tonalitic part of the rock, plagioclase (An_{36}) is unzoned in subhedral, prismatic grains up to 3 mm; smaller plagioclase grains have much granoblastic habit and approach 120° triplets. Quartz is in 1.5 mm, platy grains parallel to biotite schistosity. A little microcline is present. Biotite occurs in 0.5 mm, crudely lepidoblastic flakes. Accessories include magnetite, apatite, and zircon. This tonalite grades into a rock with 20% microcline phenocrysts which has the composition of granodiorite. The quartzite (table 6, mode 62) is injected also by pegmatite which is in boudins whose axes trend 10°, 295° az. Quartz is major in the quartzite, in unstrained, granoblastic 0.5 mm grains. Biotite occurs in scattered, 0.5 mm flakes, crudely lepidoblastic, microcline in 0.3 mm perthitic grains, and plagioclase in 0.3 mm grains of untwinned albite. Scattered through the above as a matrix are 2x6 mm patches of 0.3 mm quartz grains rich in fibrolitic sillimanite. The appearance is of a stretched-pebble conglomerate.

A xenolith about a kilometer from the contact is of tonalite (table 6, mode 59); a number of similar xenoliths occur closer to the contact. Plagioclase (An_{25}) occurs in 3 mm, unzoned prisms. Quartz is in 1 mm, irregular grains, free of any subgrains and thus still in the southern zone. Biotite is in 0.5 mm flakes a little altered to pennine. Muscovite occurs in 0.5 mm flakes. Accessory minerals include zircon, allanite, baddeleyite, sphene, epidote, magnetite, and thorite. At the locale of this tonalite xenolith, a xenolith of metagabbro was found (table 6, mode 61). Plagioclase (An_{55}) occurs in 0.3 mm granoblastic grains. A trace of quartz occurs in 0.2 mm grains. Biotite is in 0.5 mm flakes. Accessories include allanite, epidote, magnetite, and apatite.

Pegmatite suite.

Four granitic pegmatites were studied from the northern zone. The pegmatites, being very coarse-grained, were not counted for modes. Plagioclase (An_{18}) occurs in 1 to 3 cm grains or larger and has been broken into 2 to 6 mm, annealed subgrain aggregates more or less flattened in a crude foliation that transects the dikes. Foliation is not everywhere developed, but all the pegmatites have subgrain development.

Quartz is broken from original large grains into 0.5 to 1 mm, strain-free subgrains, flattened in some of the pegmatite. In two pegmatites, these subgrain aggregates are cut by blastomylonitic shears with 0.05 mm, granoblastic, strain-free grains. Some late cataclasis produced sutured grain boundaries and undulatory extinction.

Microcline occurs in 2 to 12 mm, strain-free subgrains, some of them flattened, developed at the expense of original large grains. Biotite occurs as minor, 4 mm flakes in one pegmatite. Muscovite occurs in all the pegmatite as 1 to 2 mm flakes, locally sheared to 0.3 mm lepidoblastic flakes along late cataclastic shear zones. Accessories include garnet and thorite.

Two granitic alaskites (table 4, modes 19 and 20) and one granodioritic alaskite, all injected in granodiorite and all from the southern zone were studied. The granodioritic alaskite is listed in table 6, mode 48. Plagioclase (An_{18}) occurs in 2 mm, unzoned, subhedral, equant grains. Some of it is in clusters with 120° triple junctions. Quartz occurs in irregular, interconnected 1 to 2 mm grains in patches from 4 to 8 mm in diameter. It is free of subgrains and shows moderate undulatory extinction. Microcline occurs in 2 mm grains. Biotite and muscovite occur in 0.3 mm grains; no accessory minerals were seen.

One trondhjemitic alaskite was found, intruding granite of the northern zone. It consists of plagioclase (An_{22}), quartz and muscovite. Its fabric consists of 4 mm, strain-free subgrains developed at the expense of earlier, large grains. This rock was a pegmatite initially and now has an alaskitic fabric due to secondary strain and recrystallization involving reduction in grain size.

Blastomylonite.

Blastomylonite occurs at one place in the northern zone, in a 1 m-thick, finely schistose sheet lineated 20°, 335° az. The bulk composition, as shown by an estimate from the stained thin section, is in the granite to granodiorite range. This is the megascopic analog of the 0.5 mm thick blastomylonitic shears seen in many thin sections of the plutonic rocks. Average grains size is 0.05 mm for all the blastomylonite constituents of the blastomylonite. Plagioclase, near An_{20}, is in unzoned, granoblastic grains, with a tendency for somewhat platy grains to be oriented parallel to the rather strong schistosity. Quartz is in granoblastic, slightly platy grains, free of any undulatory extinction, parallel to the schistosity. K-feldspar is submicroscopically twinned microcline, in grains a bit platy and parallel to the schistosity. Biotite is strongly lepidoblastic, mostly brown but partly green. Accessories seen are zircon, allanite, and magnetite.

Microbreccia.

A shear zone a meter or so wide, oriented 020° az, 90°, occurs in granite in the headwaters area of Heath Creek (southeastern corner of the Greenside Butte quadrangle). Larger tectonic clasts, with undulatory extinction, in the microbreccia of this shear zone average 0.5 mm in diameter and are of quartz, microcline, and plagioclase (with strong clay-calcite alteration). The matrix is a finely crushed mass of the same minerals with some sericite aggregates, pennine and leucoxene.

The central sector

Structure.

Granitic rocks.

The central sector covers all or parts of the following 7 1/2′ quadrangle sheets: McConnell Mountain, Bear Mountain, Shissler Peak, Hungry Rock, Cedar Ridge, and Grave Peak, Idaho. This area is underlain almost entirely by intermixed granite and granodiorite in roughly equal amounts, lying entirely within the zone of secondary fabric. The boundary zone for transition into non-secondary fabric within the granitic rocks passes to the south of this sector.

Some outcrops contain both granite and granodiorite. Contacts between any major units were not found, as the rocks look much alike in the field. In the western part of this area (McConnell Mountain quadrangle), the plutonic rock is about two-thirds massive and one third foliated/lineated. In the central part (Hungry Rock quadrangle), massive rock makes up only about half the area. In the eastern part (Cedar Ridge quadrangle), massive rock makes up only about one-third of the area, and the remaining two-thirds is foliated/lineated. Foliated granite and granodiorite are distributed more or less randomly through the massive granite and granodiorite. Both massive and foliated granite and granodiorite are locally porphyritic, with K-feldspar phenocrysts making from 1% to 20% of the rock.

Foliation.

Where foliation has developed (fig. 56), it is expressed in various ways. Where weak, a few zones up to half a meter thick of oriented biotite may be the sole expression of foliation in otherwise massive rock. Foliation may also be expressed by parallel biotite grains, biotite streaks, biotite-rich bands or schlieren, or by platy xenoliths oriented parallel in flow. Foliation is also expressed by parallel K-feldspar phenocrysts in a number of places, where the resultant foliation plane dips more steeply than biotite foliation in the same outcrops. These resemble strongly the C and S surfaces of the South Armorican Shear Zone (Berthé and others, 1979, p. 33). Rarely, feldspar phenocrysts can be seen to form a lineation in the foliation. At one point near the center of the area, they plunge vertically down the dip of a vertical flow foliation. At another point near the center of the area, two orthogonal flow bands 5 to 20 cm thick are oriented vertically, with E-W and N-S trends; the appearance of their intersection suggests that they developed simultaneously. Pegmatite parallels the E-W band. In many places, the primary foliation is crossed and even destroyed, except for some schlieren along its former trace, and is supplanted by a northwest-trending, secondary, medium- to fine-grained foliation expressed principally by flattened quartz and feldspar grains. Secondary lineation in the secondary foliation is expressed by linear biotite streaks in schlieren and by minor fold axes and linear biotite arrays in xenoliths of biotite quartzite and schist. Both primary and secondary flow foliation are plotted in figure 56, as it is not generally possible to decide in the field which one is present if only one is developed. Cutting the flow foliation(s) are a few pre-pegmatite ductile shear zones 1 to 50 cm thick, of northeast trend (e.g., 055°, 60° NW) and lineation, that concentrate medium-grained biotite within them. Poles to foliation lie near a partial girdle whose pole is oriented near a 330° az trend; secondary flow lineation is oriented near 330° az, near the girdle pole.

Quartz diorite.

In the Elk Summit area of the Cedar Ridge quadrangle, a concordant sheet of biotite-hornblende quartz diorite up to several hundred meters thick has been injected more or less along the gneissic foliation and extends for several kilometers along the strike. It is foliated and metamorphosed in its outer parts in about the same degree as the enclosing gneissic granite; in its central parts it is more massive, although its fabric is still predominantly metamorphic.

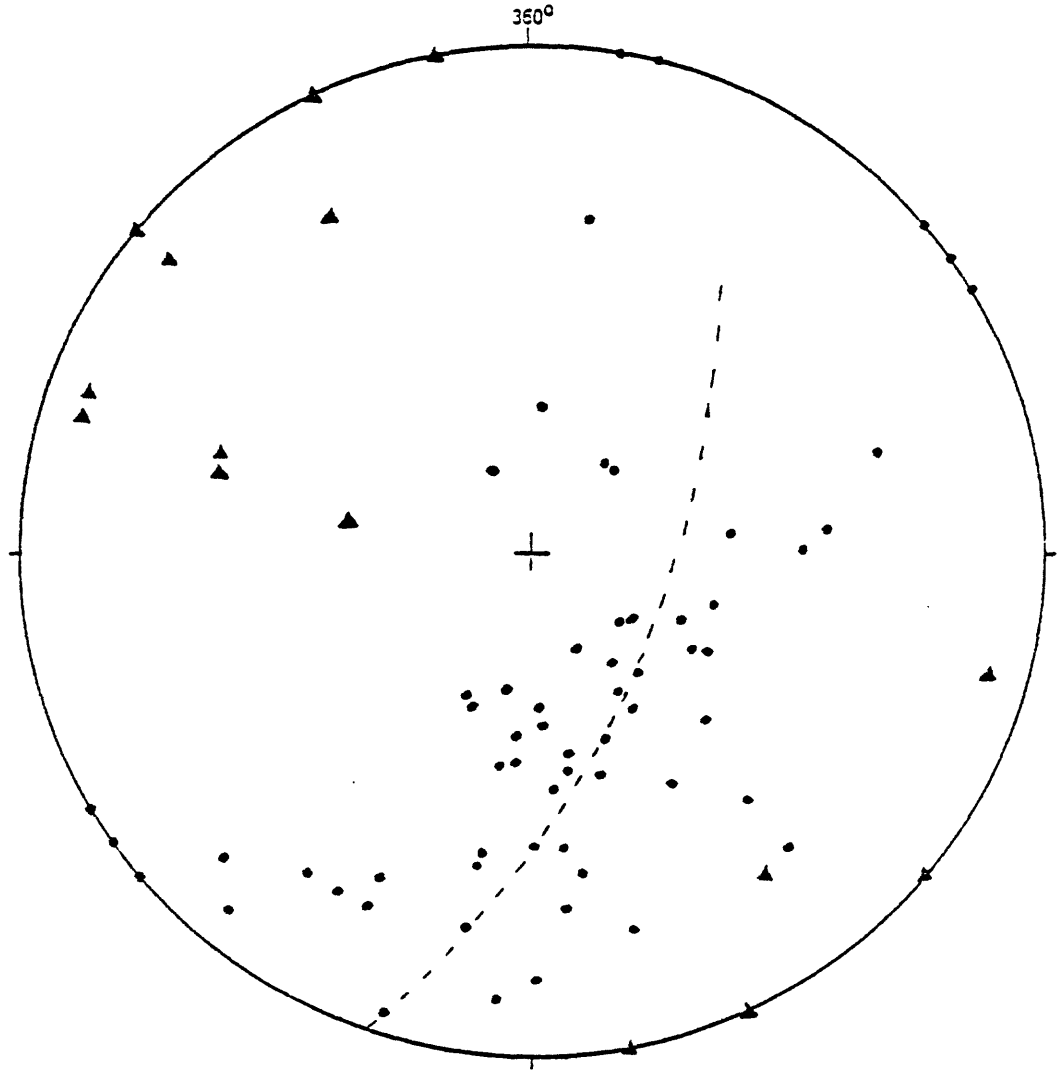

Figure 56.-- Poles to primary and secondary flow foliation (●) and flow foliation (▲) in granite/granodiorite in the central sector of the Bitterroot lobe of the Idaho batholith, west of Hamilton, Mont. The dashed line represents a partial girdle consistent with average pole distribution. Data are plotted on lower hemisphere of Wulff stereonet.

Fine-grained dikes.

Foliation in gneissic granitic rocks is injected parallel to or crosscut by 10 to 70-cm-thick, fine-grained biotite granite, granodiorite, and tonalite sheets and dikes. These are cut in turn by pegmatite and later tonalite, seen in only a few places.

Pegmatite suite.

Pegmatite tends to be earlier than aplite, where they show clear age relations. Ductile shears up to 1 m thick, oriented 080° az, cut pegmatite but are injected by aplite. A typical one of these shears concentrates biotite in more than a dozen closely spaced, 0.5 to 1 cm shear zones. Schlieren in the shears are lineated along the strike line, and passive-flow folds of biotite laminae within the shears indicate left-lateral, strike-slip, ductile fault movement. Still later than aplite are dikes of pegmatitic quartz containing minor feldspar or none at all. All these pegmatite-stage dikes fill primary fractures in the batholith, up to 30 cm thick. Two pegmatite-stage dikes are schistose parallel to their walls, in massive granite. Some pegmatite contains garnet and tourmaline as accessories. Later, mineral-coated primary fractures also occur, variously coated with feldspar phenocrysts, feldspar-quartz-muscovite, quartz-muscovite-tourmaline (with muscovite and tourmaline lineated along the dip line), or with medium-grained tourmaline both lineated and non-lineated on different fractures, or with mixtures of mylonitized quartz and lineated tourmaline. Other linear elements in the pegmatite-suite dikes include rodded quartz and feldspar, streaky biotite, and slickensides. Orientations given in figure 57 are considerably scattered. The mineral-coated fractures are not oriented in quite the same way as the filled primary fractures. Further evidence from that in figure 57 comes from a sheared 1-cm pegmatite dike with tourmaline in it, lineated 18°, 325° az. A contemporaneous release joint containing rosettes of non-lineated tourmaline is oriented 032° az, 45° SE. Analysis shows an oblique, left-lateral, strike-slip fault with the top moving west. But the matter is still more complicated as shown by the orientation of the primary fractures and mineral lineations in figure 57; the matter defies analysis. Perhaps some more or less random cooling fractures define blocks jostled in complicated ways by an oblique stress.

Blastomylonite.

The granitic rocks, the plutonic, fine-grained sheet and dike sequences, and the pegmatite suite and mineral-lined primary fractures are cut in places by fine-grained, blastomylonitic schistosity or by zones of blastomylonite up to 35 cm thick. Bell and Etheridge (1973) suggested that mylonite is generally the result of ductile rather than brittle strain. Their suggestion seems applicable to the mylonitic rocks of the Bitterroot lobe. However, their definition of "mylonite" seems too general for discrimination of several rocks encountered in this study. For instance, both the rock termed "blastomylonite" and "mylonite" in our study would qualify as "mylonite" under their definition. Accordingly, definitions in the Glossary of Geology (1972) are adopted. "Blastomylonite" is thus "a mylonitic rock in which some recrystallization and/or neomineralization has taken place." In the blastomylonite described here, a great lot of recrystallization has occurred, so that the small grains of the fabric are entirely free of strain effects; i.e., no undulatory extinction is seen.

The blastomylonitic schistosity partly parallels and partly crosscuts flow foliation or is developed independently in massive granitic rock. Most blastomylonite is foliated, with fine-grained, streaky biotite lineation, but some is non-foliated and contains only fine-grained, streaky biotite lineation. Blastomylonite is also developed in pegmatite-suite and other, earlier dikes, where it may parallel their walls or cross at various angles. At one point, pegmatite dikes are offset left-laterally along a 20-cm blastomylonitic shear oriented 275° az, 50° NE. The blastomylonitic shears vary widely in their orientation, but their poles lie near an inclined girdle whose axis plunges westerly toward about 330° az (fig. 58). At one place, a 2-cm pegmatite sheet oriented 087° az, 30° NW is split by a blastomylonitic shear parallel to its walls. Streaky biotite is oriented 18°, 320° az in the shear surface. Two large phenocrysts were split by the shear and their top halves transported 5 cm to the southeast. Shear steps on the shear surface suggest the same sense of shear as that shown by the offset phenocrysts.

Mylonite.

Late-stage, mylonitic shears were found in several places, cutting earlier structures, including blastomylonite. Mylonite (Glossary of Geology, 1972), "may.....be described as a microbreccia with fluxion structure." Implicit in the definition is the presence of deformation features such as strong undulatory extinction in the mineral particles, and the absence of recrystallization. Mylonitic shears are all relatively thin, mostly less than 0.5 mm thick, although one 8 cm thick was found. They are strongly lineated due to fine-developed grooving and streaky sericite. The shears are all low angle, and their lineations trend in the 120° az to 300° az sector (depending on the plunge direction). Shear steps suggest that the tops moved to the east on these low-angle shears. Orientation data are given in figure 59.

Mylonitic shear joints.

Later than the low-angle mylonite, a number of non-mineralized shear joints with thin, lineated mylonite zones (mostly less than a few mm thick) were mapped (fig. 60). The data suggest complex movement in a conjugate shear system; the axial symmetry of these shears of northeast trend, with mostly dip-slip movement, attests to some complexity in the movement.

Mineralized shear joints

Next youngest are shear joints with slickensides patterned by chlorite and minor epidote (fig. 61). These shear joints trend NNE in the eastern part of the central sector and swing to an ENE trend as they cross to the western part. Slickensides rake both to the SW and to the NE in different fractures. The data are sparse, but permit the tentative observation that northeast rakes prevail in the eastern part and that southwest rakes prevail in the western part. In a few places, the joints developed by reactivation of earlier fractures, as shown by chlorite overprinting older mullions of different rake, or lineated tourmaline of rake different from that expressed by the streaked-out chlorite. Thin-section study shows that very fine-grained microbreccia formed along these joints.

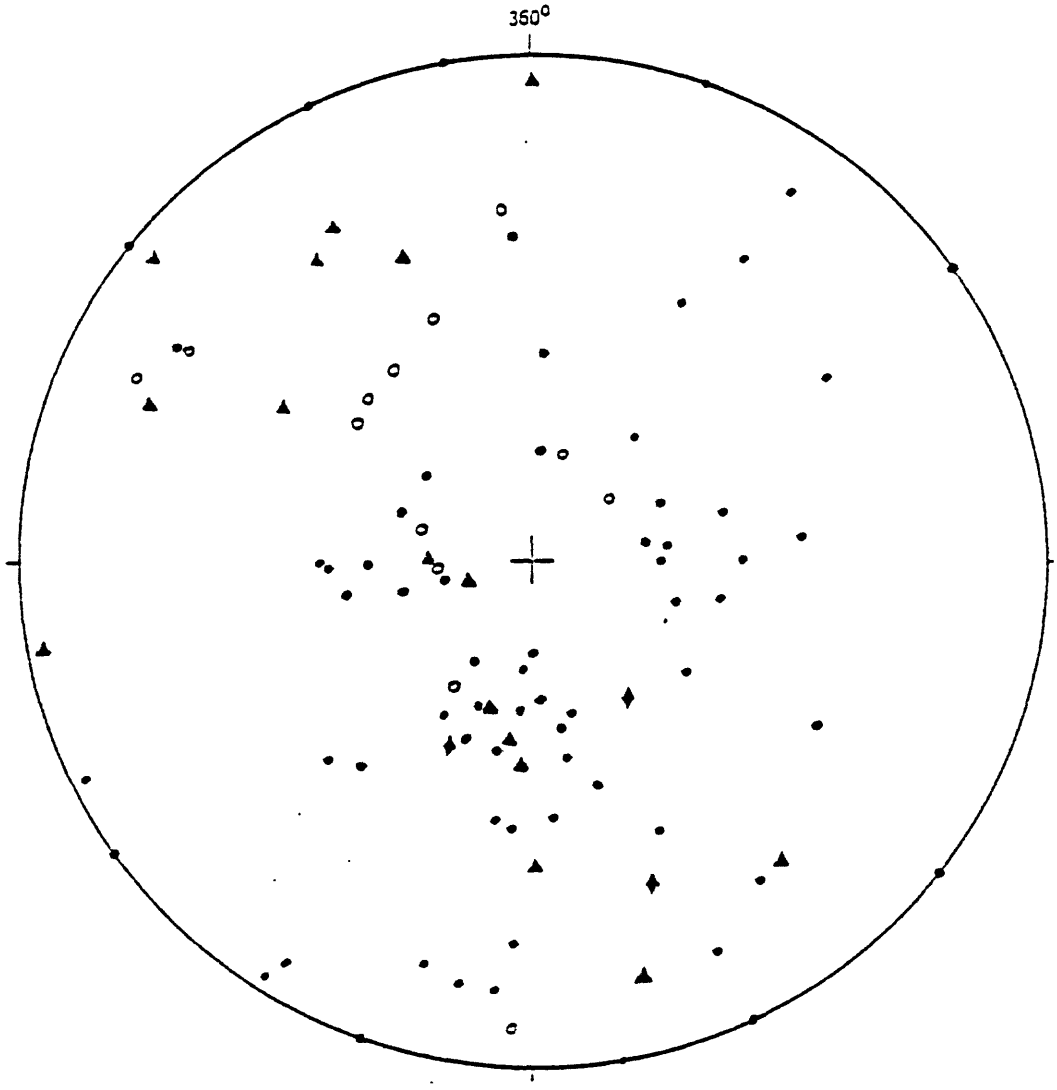

Figure 57.--Poles to filled primary fractures (●), including pegmatite, alaskite, aplite, and pegmatitic quartz dikes; poles to mineralized primary fractures (○); lineation in the primary fractures (▲); and poles to tonalite dikes (♦) that cut pegmatite dikes and are in turn cut by aplite dikes. Central sector, Bitterroot lobe of the Idaho batholith, west of Hamilton, Mont. Data are plotted on lower hemisphere of Wulff stereonet.

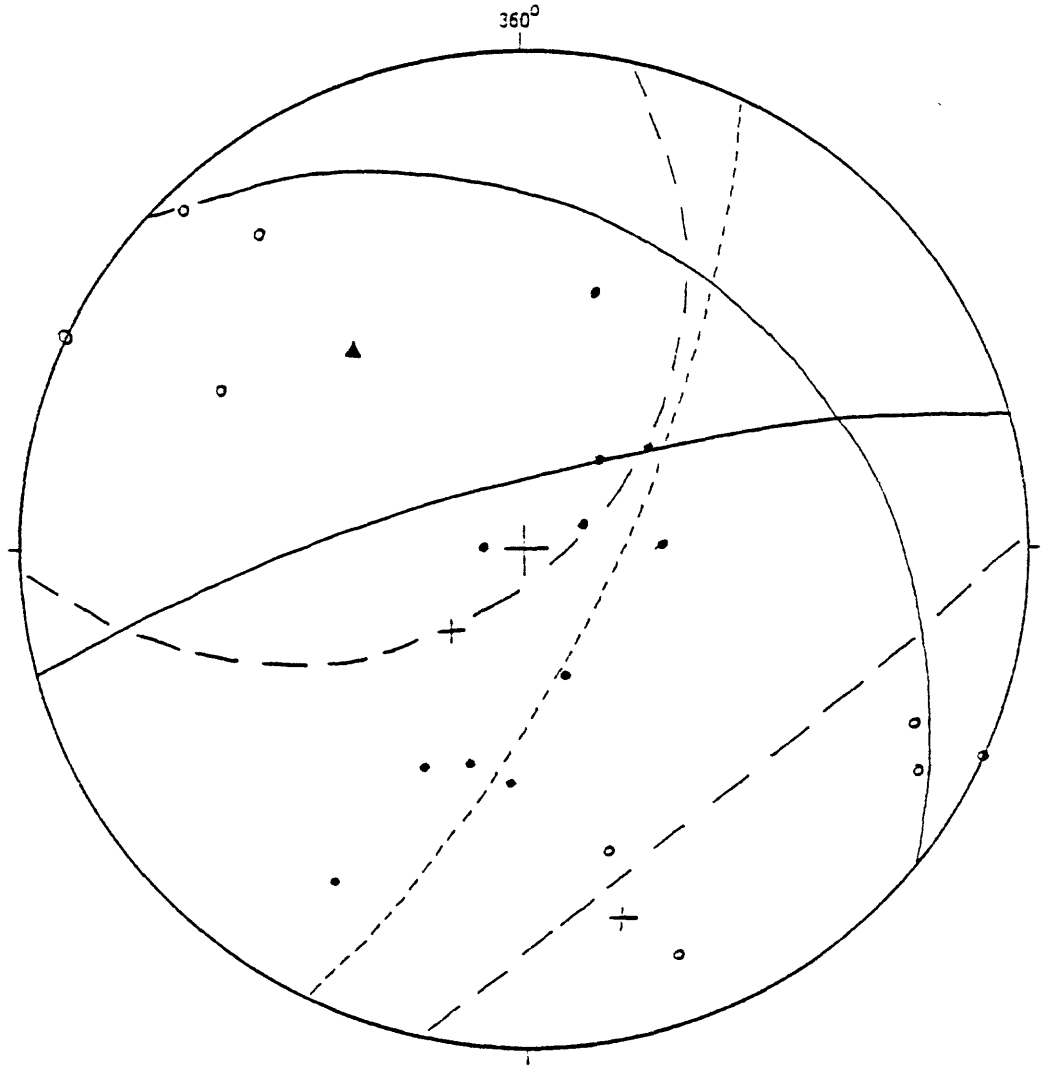

Figure 58.--Poles to blastomylonite shear zones (●), and lineation in blastomylonite (○) (defined by fine-grained, streaky biotite) in the central sector, Bitterroot lobe of the Idaho batholith, west of Hamilton, Mont. The fine-dashed arc is a girdle perpendicular to the 290°-110° az trend. Solid arcs represent two conjugate shear sets 65° apart measured at one station. The apparent axis of maximum principal stress that generated the two conjugate shears is shown by (▲). Its approximate orientation is 35°, 320° az. Crosses (+) are drawn on poles to the two conjugate shear planes. The coarse-dashed arcs represent the locus of poles to theoretical shear planes tangent to a 60° cone, 120° from the maximum principal stress taken as a cone axis. Data are plotted on lower hemisphere of Wulff stereonet.

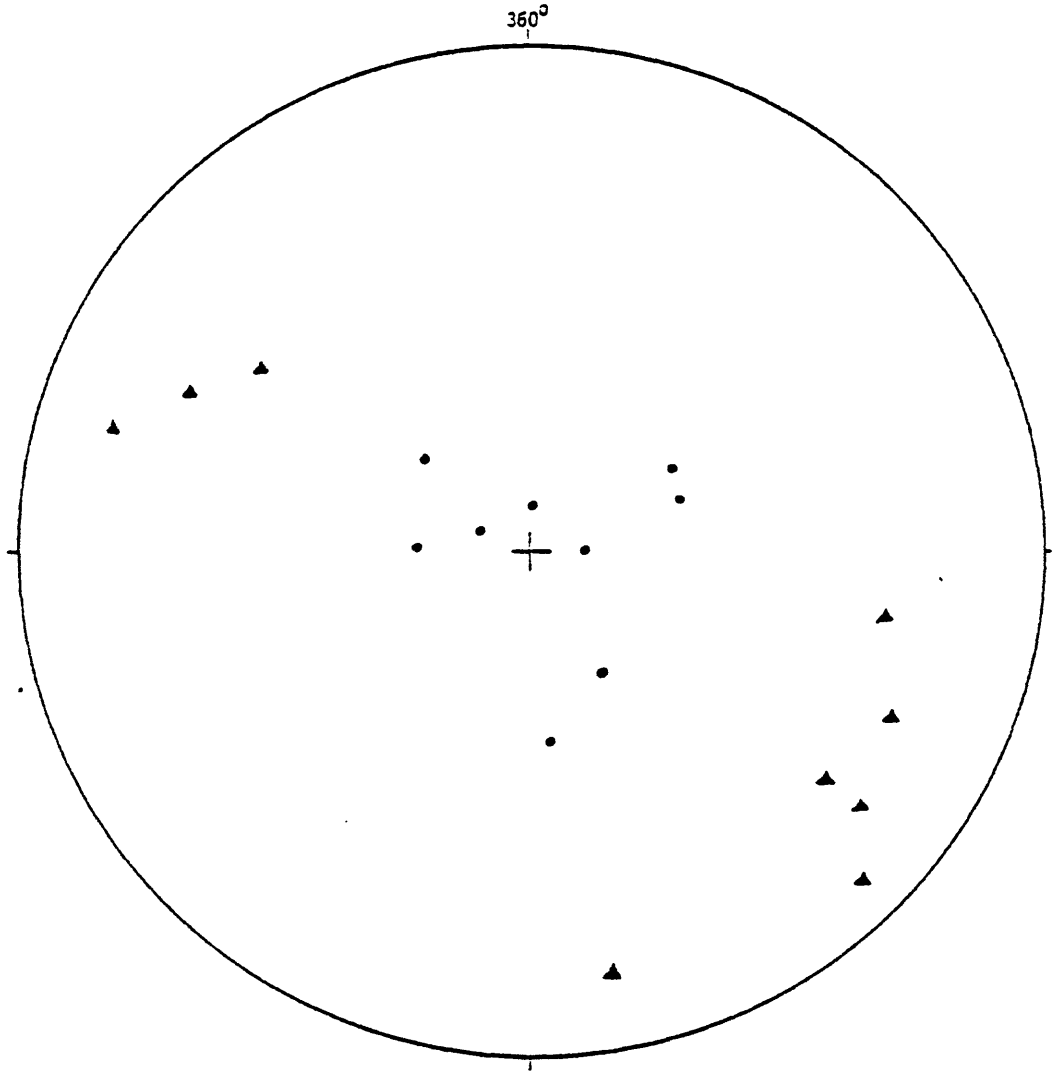

Figure 59.--Poles to mylonitic shears (●) and lineation therein (▲), central sector, Bitterroot lobe of the Idaho batholith, west of Hamilton, Mont. Data are plotted on lower hemisphere of Wulff stereonet.

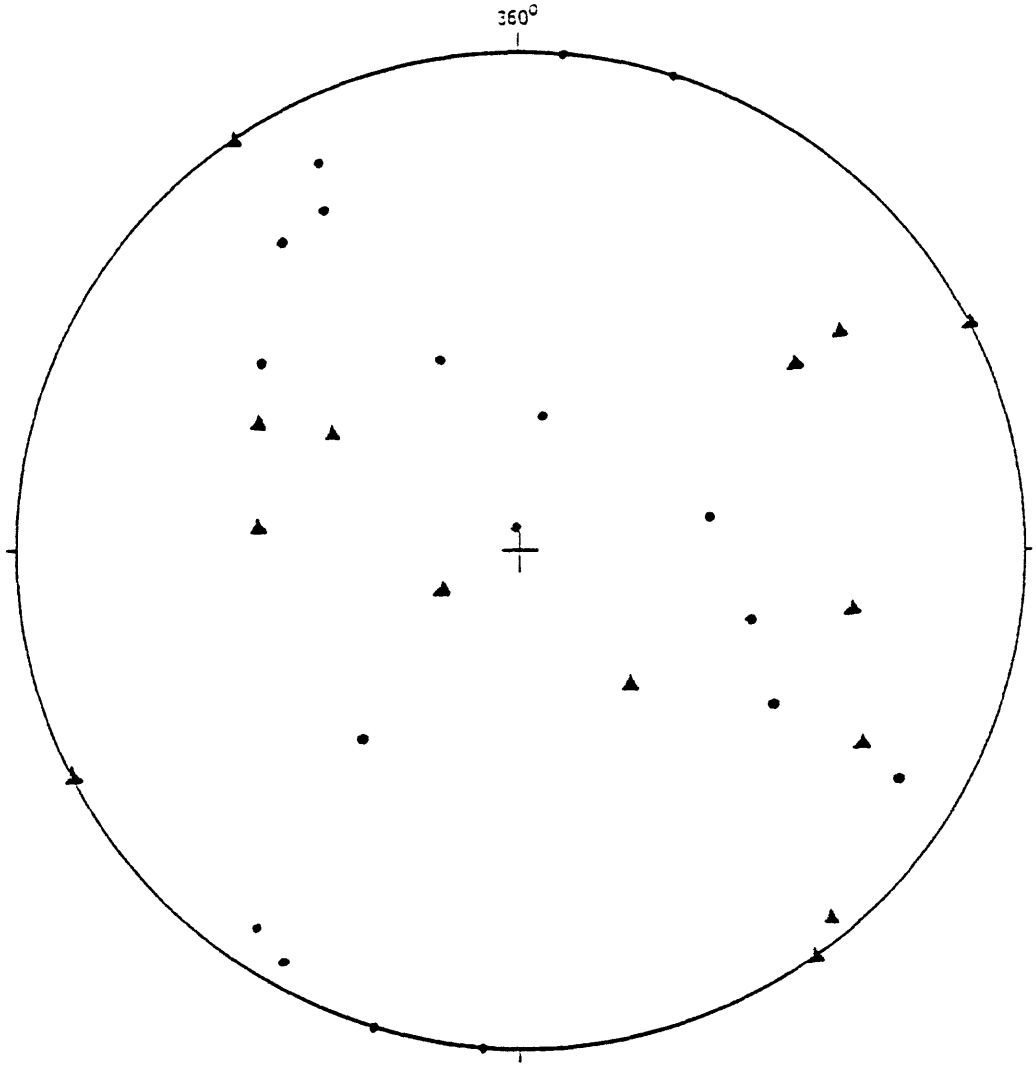

Figure 60.--Poles to mylonitic shear joints (●) and lineation therein (▲), in the central sectore, Bitterroot lobe of the Idaho batholith, west of Hamilton, Mont. Data plotted on lower hemisphere of Wulff stereonet.

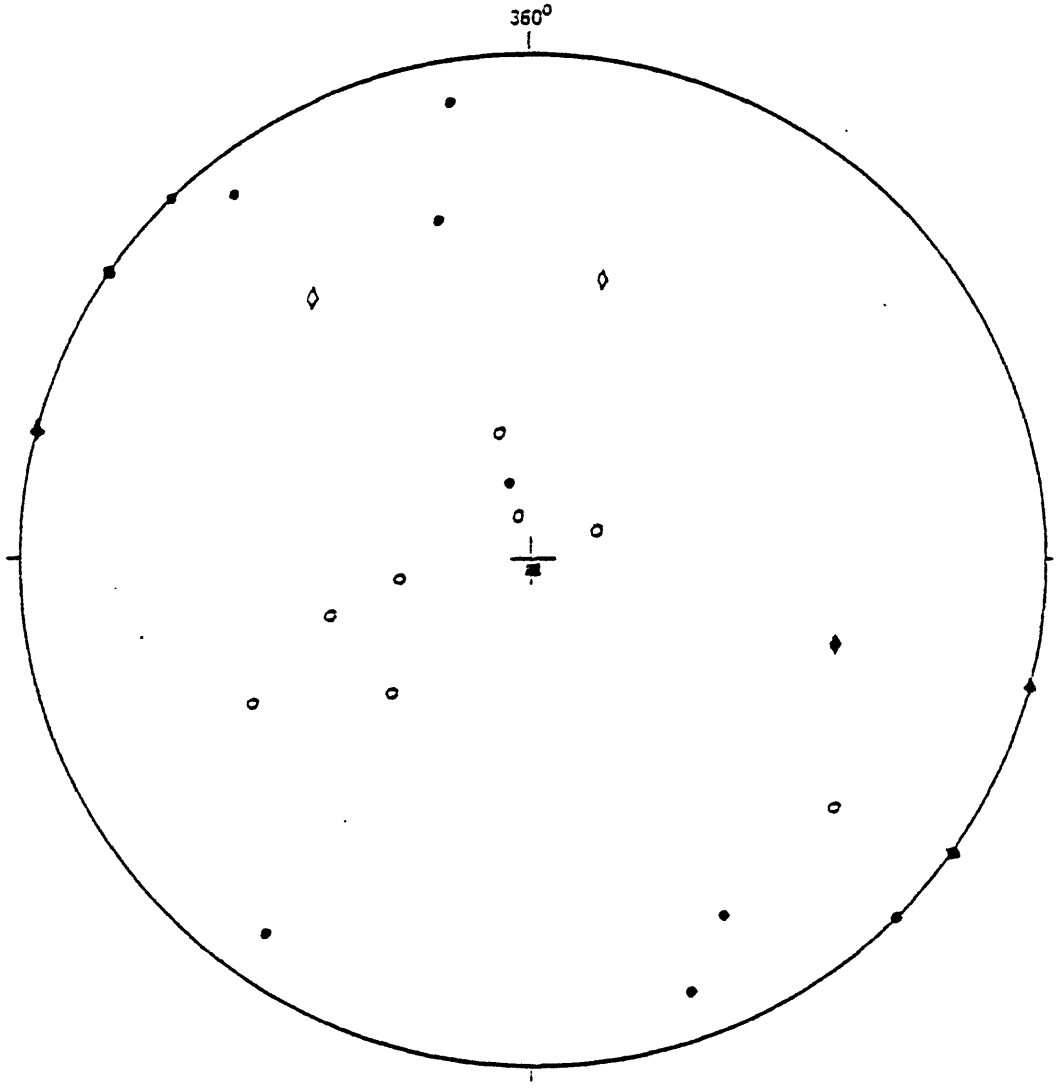

Figure 61.--Poles to chlorite-patterned shear joints (●) and lineation therein (○) in the McConnell Mountain quadrangle, central sector of the Bitterroot lobe of the Idaho batholith, west of Hamilton, Mont. One pole to a chlorite-patterned shear joint (■) and one lineation therein (□) are in the Hungry Rock quadrangle, next east. Two poles to chlorite-patterned shear joints (♦) and two lineations therein (◊) are in the Cedar Ridge quadrangle, next east. Data are plotted on lower hemisphere of Wulff stereonet.

Secondary joints.

Secondary joints in the central sector are shown in figure 62. Because of weathered surfaces, most joints are placed in this group, and it is possible that shear and extension joints of more than one age are included. Trends and dips are scattered.

Petrography.

Granite.

Modes for granite in the central sector are given in tables 8 (modes 1 to 35), table 9 (modes 1 to 27), and table 10 (modes 1 to 13). Plagioclase (20% to 51% in the mode) ranges in composition for An_{15} to An_{30}. Most plagioclase is unzoned in equant to prismatic, subhedral grains. Average grain size ranges from 1.6 to 4 mm. Only a few grains show relicts of normal zoning (e.g., cores An_{28}, rims An_{18}). One granite specimen has mostly prismatic plagioclase, normally zoned (cores An_{35}, rims An_{27}). Plagioclase is generally a bit myrmekitic against K-feldspar. In a few granites, much of the plagioclase is untwinned. In two granites, some plagioclase grains are cut by 0.2mm-thick extension fractures perpendicular to the foliation, filled variously with biotite, K-feldspar, quartz, and muscovite. Strain-free subgrains (0.7 mm) developed in plagioclase in a few rocks, some foliated and some not. In the foliated rocks, some of the plagioclase grains are elongate (up to 2x6 mm) parallel to the foliation. In one foliated rock, equant grains of plagioclase are strung out in such a way as to yield the appearance of drawn-out plagioclase rods in the sawed slab (evidently, some metamorphic segregation process is responsible for this effect). The various deformation effects are due to secondary strain; the secondary fabric is cut in a few granites by blastomylonitic shears up to 0.5 mm thick, seen in thin section. Within these shears, plagioclase, quartz, microcline, and biotite are in 0.2 mm, granoblastic, strain-free grains. In thicker blastomylonite zones, up to 8 cm thick, grains are coarser, up to 0.5 mm in diameter, and partly flattened (e.g., 2:1 ratio), but otherwise resemble the finer grains of the thin blastomylonites seen in many thin sections. One granite was strongly mylonitized, and plagioclase and other grains in it form a cataclastic schistosity or fluxion structure. This fabric is cut by 0.1 to 0.2 mm-wide, pyrite-bearing microbreccia zones with 0.02 mm plagioclase and other grains.

Quartz (20% to 44% in the mode) occurs in 1.5 to 4 mm grains, broken to 0.3 to 0.7 mm, strain-free subgrains in all but five rocks. These five contain quartz in large, uniform grains virtually free of subgrain development (one of these rocks also contains much normally zoned plagioclase). The boundaries between the subgrains are generally of smooth, curviform character; in a few rocks, the boundaries are more or less intricately sutured (strain-induced boundary migration) and the subgrains have some undulatory extinction all due to later cataclasis. In thirteen granites, the quartz grains are flattened (from 0.7x1.5 mm to 1x7 mm) parallel to foliation, all with strain-free subgrains. Quartz in two rocks is cut by blastomylonitic shear zones up to 0.5 mm thick, in which the quartz is in 0.2 mm, strain-free subgrains. Twenty-one rocks show more or less the effects of cataclastic deformation in quartz, ranging from mild to severe. The milder effects include undulatory extinction and subgrain boundary suturing in strain-induced boundary migration. Stronger effects include breaking in 0.03 to 0.3 mm cataclastic subgrains, with undulatory extinction and more or less intricate microsuturing of subgrain boundaries. Some of these stronger effects can be related to shear zones or shear joints mapped at the outcrop; one, for instance, oriented 050° az, 75° SE, with slickensides down the dip, and another oriented 325° az, 66° SW, with slickensides parallel to its strike. Two rocks have relatively severe cataclasis shown in the quartz and other minerals by the development of cataclastic schistosity in zones up to 0.5 mm wide. The light and dark minerals are reduced to 0.1 to 0.2 mm in size in the cataclastic schistosity and segregated therein. Biotite is altered to pennine in these zones, suggesting that they might be equivalent to the chlorite-coated shears of NE trend mapped at the outcrop.

K-feldspar (18% to 40% in the mode) occurs in 1 to 8 mm grains, and in 1 to 4 cm phenocrysts in the porphyritic granite. The K-feldspar is microcline in one-third of the rocks, submicroscopically twinned microcline in one-third of the rocks, and orthoclase in one-third of the rocks. In a few granites, both orthoclase and submicroscopically twinned microcline are present. The larger grains contain many inclusions of plagioclase, biotite, and quartz. K-feldspar is cut by quartz-muscovite-filled extension fractures in several granites. In the foliated granite, K-feldspar occurs in lenticular grains from 1x3 to 3x8 mm parallel to the foliation. These grains are all broken to strain-free subgrains (0.5 mm). In one rock, the K-feldspar grains occur in 0.3 mm size with undulatory extinction, in a cataclastic schistosity (mylonite). Locally, microbrecciation occurs along shear joints which cut across cataclastic schistosity.

Biotite (0.2% to 10.2% in the mode) occurs in 0.5 to 2 mm flakes in the massive granite, with some pennine-epidote-sphene alteration. It is somewhat lepidoblastic in the foliated granite, mostly in 0.5 mm grains. In blastomylonitic shears, biotite is reduced to 0.2 mm, lepidoblastic flakes. One mylonitic granite contains 0.3 mm biotite, lepidoblastic in a cataclastic schistosity, crossed by microbreccia zones 2 mm wide, in which green biotite occurs in 0.01 mm grains. Many biotite grains are bent by cataclastic shear. Muscovite (zero to 10% in the mode, absent in three rocks) occurs in 0.5 to 4 mm grains. In the gneissic granite, it occurs as 0.5 to 1 mm, more or less lepidoblastic flakes. Muscovite is converted to 0.3 mm flakes in blastomylonitic shear zones. It is further reduced in grain size along cataclastic shears. Accessory minerals in the granite listed in their approximate order of abundance include magnetite, zircon, apatite, thorite, baddeleyite, allanite, epidote, sphene, garnet, and pyrite (on late shear joints of NE trend in which microbreccia formed).

Granodiorite.

Modes for granodiorite in the central sector are given in table 8 (modes 36 to 59), table 9 (modes 28 to 47), and table 10 (modes 15 to 32). Plagioclase (32% to 59% in the mode) occurs in 1.5 to 4 mm grains in the massive granodiorite. Composition ranges from An_{15} to An_{38}; most grains are unzoned, subhedral, and equant to prismatic. Only a few grains show relicts of normal zoning (e.g., cores An_{29} to rims of An_{20}). Some of the plagioclase is myrmekitic in thin zones where it abuts K-feldspar. Plagioclase in three rocks is cut by extension fractures filled variously with quartz and K-feldspar, with biotite and muscovite, singly or in various mixtures. In a few rocks, the plagioclase is mostly

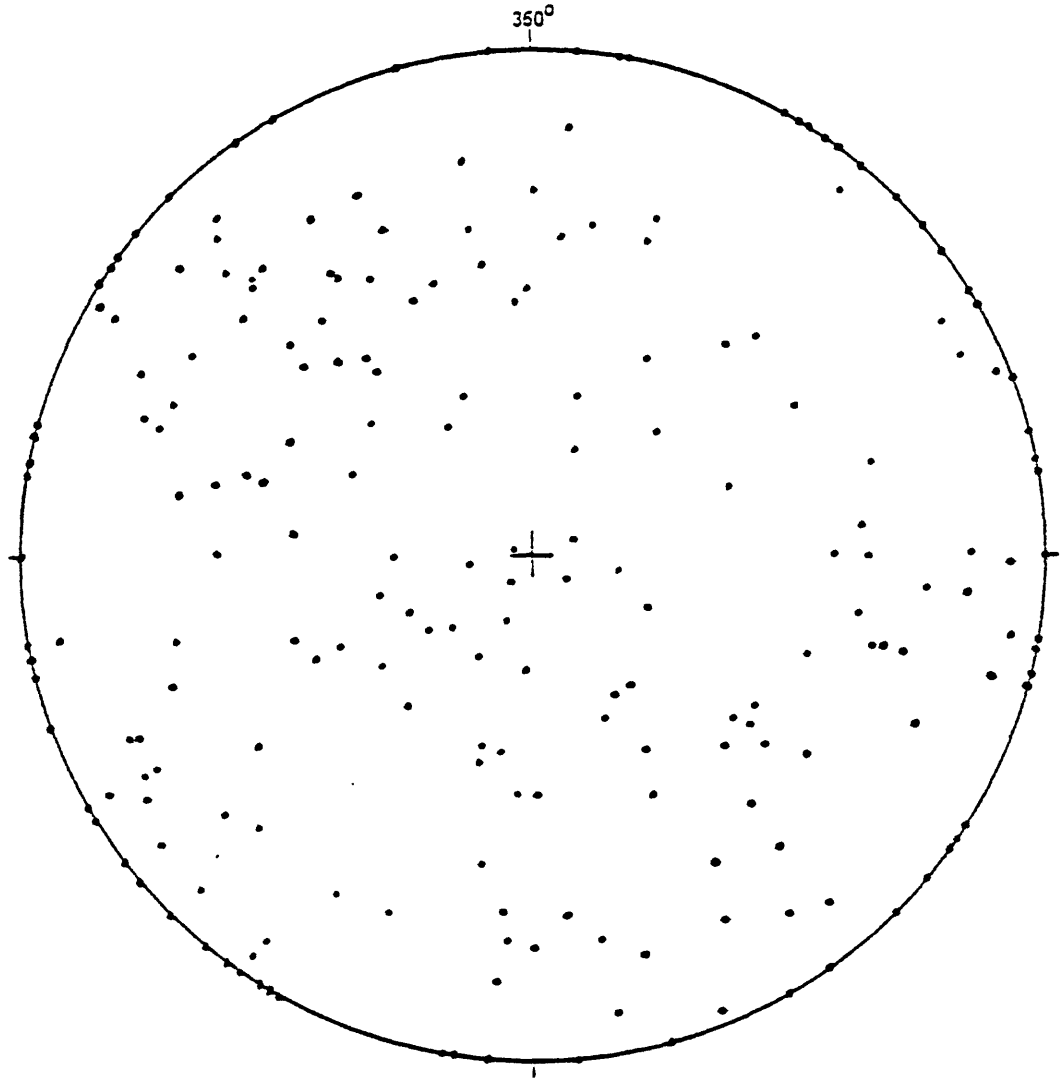

Figure 62.--Poles to secondary joints (●) in the central sector, Bitterroot lobe of the Idaho batholith, west of Hamilton, Mont. Data are plotted on lower hemisphere of Wulff stereonet.

Table 8.--Modes in the Bear Mountain, McConnell Mountain and Shissler Peak quadrangles (H15, H16, H17)
(1) Granite 79RR060B. (2) Granite 79RR175A. (3) Granite 79RR063B. (4) Granite 79RR065B. (5) Granite 79RR066A. (6) Granite 79RR096B. (7) Granite 79RR096E. (8) Granite 79RR130F. (9) Granite 79RR292A. (10) Granite 79RR298A. (11) Granite 80RR195A. (12) Granite 80RR196A. (13) Granite 80RR197A. (14) Granite 80RR198A. (15) Granite 80RR202A. (16) Granite 80RR203A. (17) Granite 80RR209A. (18) Granite 80RR210A. (19) Granite 80RR211A. (20) Granite 80RR212A. (21) Granite 80RR215A. (22) Granite 80RR217A. (23) Granite 80RR221B. (24) Granite 80RR273A. (25) Granite 80RR276A. (26) Granite 80RR278A. (27) Granite 80RR293A. (28) Granite 80RR294A. (29) Granite 80RR296A. (30) Granite 80RR297A. (31) Granite 80RR301A. (32) Granite 80RR302A. (33) Granite 80RR303A. (34) Granite 80RR304A. (35) Granite 80RR305A. (36) Granodiorite 79RR060E. (37) Granodiorite 79RR060F. (38) Granodiorite 79RR065E. (39) Granodiorite 79RR065F. (40) Granodiorite 79RR086B. (41) Granodiorite 79RR086E. (42) Granodiorite 79RR088B. (43) Granodiorite 79RR088E. (44) Granodiorite 79RR130E. (45) Granodiorite 79RR173A1. (46) Granodiorite 79RR176A. (47) Granodiorite 79RR177A. (48) Granodiorite 79RR291A. (49) Granodiorite 80RR201A. (50) Granodiorite 80RR204A. (51) Granodiorite 80RR213A. (52) Granodiorite 80RR218A. (53) Granodiorite 80RR219A. (54) Granodiorite 80RR220A. (55) Granodiorite 80RR269A. (56) Granodiorite 80RR270A. (57) Granodiorite 80RR277A. (58) Granodiorite 80RR279A. (59) Granodiorite 80RR291A. (60) Quartz monzonite 80RR300A. (61) Fine-grained granite 80RR294E. (62) Fine-grained granodiorite 80RR211B. (63) Fine-grained granodiorite 80RR214A. (64) Granitic aplite 80RR211E. (65) Granodioritic aplite 80RR304B. (66) Tonalite xenolith in granite 80RR217B. (67) Quartz gabbro xenolith 80RR217E in tonalite xenolith. (68) Calc-silicate hornfels xenolith in granite 80RR199A. (69) Calc-silicate hornfels xenolith in granite 80RR292A. (70) Para-amphibolite xenolith in granodiorite 80RR221A.

	1	2	3	4	5	6	7	8	9	10	11	12	13	14	15	16	17	18	19	20	21	22	23	24	25	26	27	28
Plagioclase	40.2	43.5	38.6	35.0	35.5	38.5	29.6	34.2	36.2	44.7	41.6	38.3	39.9	40.9	28.0	38.0	36.3	32.9	41.2	28.4	41.9	42.9	44.8	38.2	37.8	41.2	38.9	37.0
Quartz	25.8	24.3	20.8	28.6	32.2	28.3	25.5	27.8	32.5	21.3	32.8	27.2	31.4	22.6	39.2	33.9	26.7	30.4	25.0	28.4	28.3	26.8	23.6	26.9	30.5	24.5	28.4	31.2
K-spar	27.8	26.1	26.6	31.8	29.6	30.2	41.8	33.3	25.8	26.2	19.6	25.6	21.9	31.4	24.6	22.0	30.0	33.7	30.1	40.9	26.3	26.3	24.4	28.3	24.7	30.5	26.7	27.2
Biotite	4.0	4.3	10.4	2.3	2.1	2.1	3.0	3.2	3.3	6.8	3.2	3.5	5.0	3.2	4.3	3.5	4.1	1.7	3.7	1.1	2.2	2.8	5.0	4.3	1.3	3.2	3.1	3.7
Muscovite	2.1	1.4	2.7	2.3	0.6	0.4	0.3	1.3	1.8		2.6	5.4	1.2	1.7	3.8	2.6	2.5	1.1		0.7	0.4	0.2	1.9	1.9	5.4	0.3	2.7	0.5
Accessories	0.2	0.4	0.9	tr	tr	0.4	tr	0.2	0.3	0.9	0.2	tr	0.6	0.2	0.2	tr	0.2	tr	tr	0.4	0.9	1.1	0.2	0.4	0.3	0.3	0.2	0.4
	100.1	100.0	100.0	100.0	100.0	99.9	100.1	100.0	99.9	99.9	100.0	100.0	100.0	100.0	100.1	100.0	99.8	99.8	100.0	99.9	100.0	100.1	99.9	100.0	100.0	100.0	100.0	100.0

	29	30	31	32	33	34	35	36	37	38	39	40	41	42	43	44	45	46	47	48	49	50	51	52	53	54	55	56
Plagioclase	45.4	34.5	40.7	35.1	38.1	36.2	34.2	57.1	50.7	48.9	49.5	42.8	45.6	45.3	40.8	40.6	54.8	48.3	50.7	48.0	37.6	33.2	52.3	44.7	45.4	57.8	51.7	42.3
Quartz	21.2	29.9	26.5	32.4	24.9	25.0	22.9	22.4	20.9	23.2	30.4	29.5	27.0	32.7	21.1	33.7	24.8	21.6	20.6	26.5	37.2	49.6	26.1	27.4	26.0	24.6	10.3	32.9
K-spar	29.2	29.5	22.3	24.2	34.3	33.0	38.0	15.2	22.7	22.1	15.2	20.5	20.8	15.8	12.1	19.0	16.2	25.2	24.6	14.3	19.5	13.9	12.3	22.4	23.2	11.8	23.6	19.8
Biotite	3.3	3.1	4.6	4.2	2.3	3.1	3.3	2.9	3.9	5.3	4.4	5.3	3.6	3.2	10.9	4.9	3.1	3.7	2.9	4.3	3.2	3.0	8.2	3.9	4.0	1.8	4.4	2.2
Muscovite	0.8	2.7	5.7	4.2	tr	1.8	1.1	2.0	1.3	0.4	tr	1.6	2.6	2.9	14.8	1.3	0.6	0.6	0.5	6.7	1.8	0.2	1.0	0.9	0.2	4.0	0.9	2.6
Accessories	tr	0.4	0.2	tr	0.4	0.7	0.4	0.4	0.6	tr	0.4	0.3	0.4	tr	0.2	0.4	0.4	0.6	0.7	tr	0.7	tr	tr	0.6	1.3	tr	tr	0.2
	99.9	100.1	100.0	100.1	100.0	99.8	99.9	100.0	100.1	99.9	99.9	100.0	100.0	99.9	100.0	99.9	99.9	100.0	100.0	99.8	100.0	99.9	99.9	99.9	100.1	100.0	99.9	100.0

Table 8.--Modes in the Bear Mountain, McConnell Mountain and Schissler Peak quadrangles (H15, H16, H17) (continued)

	57	58	59	60	61	62	63	64	65	66	67	68	69	70
Plagioclase	40.5	42.5	42.6	45.7	33.3	53.8	44.1	33.5	35.1	38.5	41.7	37.8	17.6	15.3
Quartz	35.5	30.4	36.4	17.8	27.4	21.5	28.9	33.3	43.6	24.3	8.7	16.7		22.5
K-spar	19.5	22.4	19.8	32.6	34.5	8.4	14.1	21.5	14.8					
Biotite	2.8	2.9		2.9	2.0	11.6	12.9	0.6	1.0	34.0	18.2			
Muscovite	1.5	1.8	0.7	0.2	2.8			11.2	5.2					
Hornblende											31.0			56.5
Diopside												42.3	73.6	
Pargasite?													6.6	
Phlogopite													0.7	
Garnet													0.7	
Accessories	0.2	tr	o.5	0.9	tr	4.8	tr	tr	0.3	3.2	0.4	3.2	0.7	5.7
	100.0	100.0	100.0	100.1	100.0	100.1	100.0	100.1	100.0	100.0	100.0	100.0	99.9	100.0

Table 9.--Modes in the Hungry Rock quadrangle (HJ6)

(1) Granite 79RR071B. (2) Granite 79RR071E. (3) Granite 79RR076E. (4) Granite 79RR076F. (5) Granite 79RR081F. (6) Granite 79RR081G. (7) Granite 79RR083B. (8) Granite 79RR083E. (9) Granite 79RR103B. (10) Granite 79RR104B. (11) Granite 79RR106E. (12) Granite 79RR108A. (13) Granite 79RR109A. (14) Granite 79RR110A. (15) Granite 79RR296A1. (16) Granite 80RR154A. (17) Granite 80RR167A. (18) Granite 80RR171A. (19) Granite 80RR172A. (20) Granite 80RR174A. (21) Granite 80RR182A. (22) Granite 80RR185A. (23) Granite 80RR253A. (24) Granite 80RR255E. (25) Granite 80RR257A. (26) Granite 80RR258A. (27) Granite 80RR263A. (28) Granodiorite 79RR081E. (29) Granodiorite 79RR082F. (30) Granodiorite 79RR104A. (31) Granodiorite 79RR105A. (32) Granodiorite 79RR297A. (33) Granodiorite 80RR173A. (34) Granodiorite 80RR173B. (35) Granodiorite 80RR175A. (36) Granodiorite 80RR176A. (37) Granodiorite 80RR178A. (38) Granodiorite 80RR179A. (39) Granodiorite 80RR180A. (40) Granodiorite 80RR205A. (41) Granodiorite 80RR255A. (42) Granodiorite 80RR256A. (43) Granodiorite 80RR260A. (44) Granodiorite 80RR261A. (45) Granodiorite 80RR265A. (46) Granodiorite 80RR266A. (47) Granodiorite 80RR268A. (48) Fine-grained granodiorite 79RR105A. (49) Tonalite 80RR168A. (50) Tonalite 80RR170A. (51) Granitic aplite 79RR082B. (52) Granitic aplite 79RR105A1. (53) Granitic aplite 80RR178B. (54) Granodioritic aplite 79RR083F. (55) Granodioritic alaskite 79RR106B. (56) Granodioritic aplite 80RR255B. (57) Tonalitic alaskite (trondhjemite) 79RR082E. (58) Biotite-plagioclase-actinolite schist xenolith 79RR104E in granite. (59) Calc-silicate granofels xenolith in granite 80RR181A. (60) Granite gneiss xenolith 79RR071G in granite. (61) Tonalite dike 79RR105B cutting aplite.

	1	2	3	4	5	6	7	8	9	10	11	12	13	14	15	16	17	18	19	20	21	22	23	24	25	26	27	28	29	30	31
Plagioclase	31.9	39.4	39.3	29.0	30.6	29.4	40.8	26.9	42.4	42.0	42.0	23.7	20.8	34.0	41.4	39.3	37.5	32.1	24.7	37.5	42.0	24.7	40.6	42.5	38.3	33.4	39.5	43.3	44.1	39.1	50.4
Quartz	34.5	26.9	28.1	35.4	30.2	20.4	28.2	39.9	23.2	24.3	22.0	23.9	39.5	33.6	30.0	31.3	25.0	40.2	30.2	33.0	26.4	39.6	28.0	27.6	31.2	35.4	32.1	28.8	30.4	34.5	32.8
K-spar	26.0	25.8	23.0	26.9	34.0	36.6	26.0	29.1	29.5	29.4	29.4	42.9	33.0	21.0	24.7	23.0	23.8	22.6	40.4	25.7	24.3	21.7	24.4	23.5	25.4	21.8	22.0	20.6	18.2	19.1	12.0
Biotite	0.7	2.3	3.0	1.6	2.6	8.2	4.3	2.2	4.2	4.0	3.9	4.3	5.1	1.4	2.4	6.6	10.2	3.5	2.2	3.8	6.7	2.7	5.0	5.2	3.9	4.9	3.6	2.3	4.9	6.0	4.8
Muscovite	6.7	5.6	6.5	6.9	2.6	5.3	0.4	1.9	0.5		2.3	4.6	1.5	9.9	1.4	1.1	3.1	1.6	2.4			11.3	2.0	0.9	1.1	4.3	2.8	4.9	2.4	0.4	
Accessories	0.2	tr	tr	0.2	tr	tr	0.2	tr	0.2	0.2	0.4	0.5	tr	tr	0.2	0.4	0.4	tr	tr	tr	0.5	tr	tr	0.2	0.2	0.2	tr	tr	tr	tr	tr
	100.0	100.0	99.9	100.0	100.0	99.9	99.9	100.0	100.0	99.9	100.0	99.9	99.9	99.9	100.1	99.8	100.0	100.0	99.9	100.0	99.9	100.0	100.0	99.9	100.1	100.0	100.0	99.9	100.0	99.9	100.0

	32	33	34	35	36	37	38	39	40	41	42	43	44	45	46	47	48	49	50	51	52	53	54	55	56	57	58	59	60	61
Plagioclase	50.7	50.8	42.9	34.5	49.8	38.4	38.6	46.2	43.1	42.6	37.3	41.6	43.5	43.9	40.2	42.3	47.6	62.4	55.5	29.0	31.1	31.0	41.2	45.1	47.6	53.1	33.5	30.2	10.4	58.2
Quartz	28.9	21.8	26.1	35.2	31.7	34.9	33.8	30.3	30.1	35.3	31.7	32.5	31.3	28.2	35.0	30.1	24.6	22.6	25.6	32.1	35.8	30.1	36.1	28.8	38.4	34.2	2.5	19.0	20.6	28.6
K-spar	13.4	18.7	21.3	18.3	9.4	19.7	19.0	18.3	17.7	14.6	16.7	17.6	19.5	22.7	19.9	18.7	19.8	4.2	4.8	29.8	25.7	30.1	17.6	20.8	10.1	3.0			30.5	0.7
Biotite	6.0	8.0	7.1	4.1	8.1	6.7	3.4	2.3	5.4	4.4	8.2	5.4	5.0	2.6	2.3	3.2	7.5	9.9	14.1	0.5	7.4	4.8	3.4	4.3	2.0	0.2	15.5		6.9	12.5
Muscovite	0.9	0.5	2.6	7.8	1.0	0.2	4.9	2.5	3.5	3.1	6.0	2.6	0.4	2.5	2.5	5.7				8.1		3.7	1.7	1.0	1.7	9.2			31.6	
Actinolite																											46.7			
Hornblende																												39.7		
Diopside																												9.9		
Accessories	tr	0.2	tr	tr	tr	tr	0.3	0.4	0.2	tr	tr	0.2	0.2	tr	tr	tr	0.5	0.8	tr	0.5	tr	0.4	tr	tr	0.2	0.2	1.8	1.2	tr	tr
	99.9	100.0	100.0	99.9	100.0	99.9	100.0	100.0	100.0	100.0	99.9	99.9	99.9	99.9	99.9	100.0	100.0	99.9	100.0	100.0	100.0	100.1	100.0	100.0	100.0	99.9	100.0	100.0	100.0	100.0

Table 10.--Modes in the Cedar Ridge and Grave Peak quadrangles (HK6, HK5)

(1) Granite 80RR079A. (2) Granite 80RR115A. (3) Granite 80RR117A. (4) Granite 80RR123A. (5) Granite 80RR124A. (6) Granite 80RR137A. (7) Granite 80RR138A. (8) Granite 80RR142A. (9) Granite 80RR150A. (10) Granite 80RR153A. (11) Granite 80RR186A. (12) Granite 80RR189A. (13) Granite 80RR242A. (14) Granodiorite 80RR089B. Xenolith in granodiorite. (15) Granodiorite 80RR090A. (16) Granodiorite 80RR111A. (17) Granodiorite 80RR124B. (18) Granodiorite 80RR125A. (19) Granodiorite 80RR134A. (20) Granodiorite 80RR136A. (21) Granodiorite 80RR139A. (22) Granodiorite 80RR143A. (23) Granodiorite 80RR144A. (24) Granodiorite 80RR146A. (25) Granodiorite 80RR183A. (26) Granodiorite 80RR184A. (27) Granodiorite 80RR188A. (28) Granodiorite 80RR191A. (29) Granodiorite 80RR193A. (30) Granodiorite 80RR194A. (31) Granodiorite 80RR245A. (32) Granodiorite 80RR246A. (33) Granodioritic alaskite 80RR122E. (34) Granodioritic alaskite 80RR146B. (35) Quartz diorite 80RR243A. (36) Fine-grained granite 80RR111B. (37) Fine-grained granite 80RR194B. (38) Fine-grained tonalite 80RR117B. (39) Granite xenolith in granite 80RR079B. (40) Fine-grained tonalite 80RR122B. (41) Fine-grained quartz diorite 80RR151A. (42) Fine-grained granodiorite 80RR152A.

	1	2	3	4	5	6	7	8	9	10	11	12	13	14	15	16	17	18	19	20	21
Plagioclase	35.7	41.7	39.2	41.9	37.4	37.8	35.4	38.6	41.1	34.5	19.8	30.7	43.3	45.3	51.5	47.3	44.9	43.0	45.0	43.1	38.7
Quartz	25.6	30.9	33.7	28.2	29.5	35.1	25.6	30.0	29.8	26.5	44.5	38.5	27.6	29.4	29.7	29.4	44.0	31.8	33.5	31.7	30.9
K-spar	31.7	24.3	24.8	24.2	25.9	23.2	22.3	24.3	25.2	29.4	35.0	18.5	25.3	16.7	9.8	18.5	5.2	18.1	17.0	19.6	17.8
Biotite	6.1	2.5	2.0	4.7	6.9	2.8	6.7	3.6	2.4	5.7	0.2	9.1	3.3	8.2	8.2	4.8	5.4	6.7	3.1	4.1	2.5
Muscovite	0.3	0.6	0.3	0.6	0.2	0.9	9.7	3.6	1.3	3.7	0.4	3.0	0.3	0.4	0.8			0.2	1.2	1.0	9.9
Accessories	0.6	tr	tr	0.4	0.2	0.2	0.2	tr	tr	0.2	tr	0.2	tr	tr	tr	tr	0.5	tr	0.2	0.5	tr
	100.0	100.0	100.0	100.0	100.1	100.0	99.9	100.1	99.8	100.0	99.9	100.0	99.8	100.0	100.0	100.0	100.0	99.8	100.0	100.0	99.8

	22	23	24	25	26	27	28	29	30	31	32	33	34	35	36	37	38	39	40	41	42
Plagioclase	40.3	39.8	48.2	32.0	46.2	44.0	51.3	52.2	42.7	45.9	45.1	46.1	36.1	39.8	28.1	30.3	59.9	39.7	37.3	53.9	42.2
Quartz	33.5	32.1	30.2	48.6	27.0	27.3	34.5	30.5	32.3	30.6	34.9	38.3	39.3	5.3	31.0	27.3	18.5	30.9	29.4	5.7	12.6
K-spar	19.9	19.7	13.3	7.8	19.4	19.6	9.5	12.0	20.8	18.9	13.8	14.3	17.6		34.6	32.6	5.9	23.3			5.6
Biotite	3.1	6.0	7.7	0.7	7.2	2.5	4.2	4.2	3.8	4.3	4.2	1.1	3.1	20.1	5.6	7.3	15.7	6.1	32.8	25.4	30.9
Muscovite	3.1	2.4	0.4	11.0		6.4	0.4	1.1	0.4		2.0	0.2	3.9		0.6	1.8					
Hornblende														26.1						10.5	7.4
Accessories	tr	tr	tr	tr	0.2	0.2	tr	tr	tr	0.2	tr	tr	tr	8.7	tr	0.7	tr	tr	0.5	4.4	1.3
	99.9	100.0	99.8	100.1	100.0	100.0	99.9	100.0	100.0	99.9	100.0	100.0	100.0	100.0	99.9	100.0	100.0	100.0	100.0	99.9	100.0

untwinned, where composition is close to An_{20}. In several granodiorites, plagioclase is in flattened, 2x4 mm to 2x6 mm grains that are aggregates of strain-free, 0.8 mm subgrains. In three granodiorites, plagioclase occurs in strings of 1.5 mm equant grains to give the appearance of rodding in the foliation. In five granodiorites, 0.5 mm-wide blastomylonite zones involving strain-free, 0.2 mm granoblastic quartz grains, and biotite and muscovite in 0.2 mm reconstituted grains, anastomose around feldspar grains for the most part, but locally break and recrystallize plagioclase of the same composition in 0.3 mm granoblasts; yet these zones remain broadly parallel to the secondary foliation. In one rock, the matrix plagioclase is An_{25} and the blastomylonite plagioclase in An_{22}; in most rocks, the compositions are more or less identical.

Quartz (19% to 50% in the mode) occurs in 1.5 to 4 mm grains in the massive granodiorite, broken to 0.5 to 0.7 mm, strain-free subgrains in all but two rocks. In twelve foliated granodiorites, quartz occurs in flattened, 1x4 to 2x6 mm grain aggregates of strain-free, 0.7 mm subgrains, some of them platy. In four granodiorites, quartz is cut by 1 mm-wide blastomylonite zones in which quartz occurs in 0.05 to 0.2 mm, strain-free, granoblastic grains; in one of them a conjugate pair of blastomylonite zones occurs, containing quartz and feldspar as well as fine-grained muscovite and biotite. In a few of the rocks, subgrain boundaries are sutured a bit and the subgrains have a little undulatory extinction.

K-feldspar (5% to 25% in the mode) occurs in 0.7 to 5 mm grains in the massive granodiorite. The K-feldspar is roughly one-third microcline, one-third submicroscopically twinned microcline, and one-third orthoclase; only one of these varieties was found in any particular rock. The three varieties appear to be randomly distributed. The larger K-feldspar grains contain many inclusions of plagioclase and biotite, but little to no quartz. K-feldspar is in flattened grains (e.g., 4x8 mm) in seven rocks, broken in 0.5 to 1 mm, strain-free subgrains. The subgrains are free of inclusions, perhaps due to differential clearing under strain. Microcline in one granodiorite is cut by blastomylonite zones in which microcline occurs in 0.07 mm, strain-free, granoblastic grains.

Biotite (0.7% to 11% in the mode) occurs in 0.5 to 2 mm grains, lepidoblastic in about a third of the rocks, and randomly oriented in the rest. In one rock, trains of 0.5 mm grains are lepidoblastic over distances of 2 to 3 mm, but these lepidoblastic arrays stand in different orientations, producing an axial symmetry. A little alteration to pennine-epidote-sphene occurs. In blastomylonitic shears in three rocks, biotite is reduced to 0.1 mm, lepidoblastic flakes. Along late mylonitic shears, biotite is altered to very fine-grained sericite. Muscovite (zero to 15%, absent in four rocks) is like biotite in its occurrence. In one rock, it is rich in fibrolite inclusions. Accessory minerals given in their approximate order of decreasing abundance include zircon, magnetite, apatite, thorite, epidote, allanite, baddeleyite, beta-zoisite, and monazite.

Quartz monzonite.

One quartz monzonite was found, in the McConnell Mountain quadrangle; its petrographic elements are like those of the granite and the granodiorite. The mode is given in table 8, mode 60. It appears to grade into surrounding granite and granodiorite.

Quartz diorite.

A concordant sheet of biotite-hornblende quartz diorite occurs in the Elk Summit area of the Cedar Peak quadrangle (table 10, mode 35). It is the source of the abundant black sands in several creeks in its vicinity. It was injected along the secondary foliation in the gneissic granitic rocks and then metamorphosed. Plagioclase (An_{45}) in 2.5 mm grains is unzoned, prismatic, and subhedral. Quartz is interstitial in 0.5 mm grains, more or less broken in 0.2 mm strain-free subgrains. Biotite is in 2 mm flakes which partly include and replace green hornblende, itself in 1.5 mm grains. Accessories include magnetite and apatite.

Xenoliths.

Xenoliths are scarce in the central sector. A zone of calc-silicate gneiss about 0.5 km wide occurs in the McConnell Mountain area (table 8, mode 68), in the ridge south of McConnell Mountain. At Barren Ridge, a zone of blocky tonalite xenoliths occurs, with internal foliation in the blocks oriented at various angles to the flow foliation in the enclosing granitic rock. Aplite dikes cutting the tonalite blocks are ptygmatically folded about axial planes parallel to the external flow foliation, indicative of ductile strain in the blocks during late-stage deformation of the granitic rocks. Xenoliths of biotite quartzite, marble, amphibolite, granite, granite gneiss, and granodiorite were also seen. Some xenoliths are found within irregular zones elongate along 290° az.

The mode for a tonalite xenolith is given in table 8, mode 66. Plagioclase (An_{38}) is in prismatic, unzoned, 2 mm grains, cut by an early set of extension fractures, perpendicular to the flow foliation, filled with quartz and biotite. Other, presumably later extension fractures are filled with epidote. Many grains are cataclastically bent or broken. Quartz occurs in 1 mm aggregates of 0.1 mm cataclastic subgrains with intricately microsutured quartz-quartz boundaries. Cataclastic shears pervade the rock, but affect principally quartz and biotite; plagioclase is little affected, as discussed above. Biotite is crudely lepidoblastic in folia that swirl around plagioclase grains, in 1 mm flakes, reduced to 0.2 mm flakes along cataclastic shears. Accessory minerals include magnetite, apatite, thorite, sphene, and allanite.

A quartz gabbro xenolith occurs within the tonalite xenolith described above; its mode is given in table 8, mode 67. Plagioclase occurs in two phases, both An_{55}. The first is prismatic, unzoned phenocrysts 2 to 4 mm long. The second is anhedral, 0.2 mm grains somewhat myrmekitically intergrown with quartz. Quartz is in 0.1 mm grains. Biotite is minor in 0.5 mm flakes, and green hornblende is abundant in 0.7 mm grains; some of these have 120° triple junctions.

Two samples of calc-silicate gneiss were studied. One from rubble (table 8, mode 68) has quartz, diopside, and granoblastic plagioclase (An_{83}), all of 0.3 mm diameter, with accessory sphene. The other (table 8, mode 69) is from a rotated, 3 m block in the granitic rock; average grain size is about 0.3 mm. Minerals present include phlogopite, diopside, plagioclase (An_{70}), garnet, a colorless, optically positive amphibole, sphene, and apatite.

A quartzite xenolith contains quartz, biotite, and muscovite. Average grain size is about 2 mm in a typical fabric due to secondary strain (flattened quartz, strain-free subgrains). Accessory minerals include magnetite, zircon, and epidote.

A 5 m block of amphibolite in the granite was studied (table 8, mode 70). Hornblende (1.5 mm) is poikiloblastic with 0.03 mm quartz inclusions. Quartz is interstitial in 0.5 mm grains, with some deformation lamellae. Plagioclase (An_{77}) is in 0.5 mm, granoblastic grains.

A xenolith of biotite-plagioclase-actinolite schist (table 9, mode 58) contains plagioclase (An_{65}), minor quartz, and accessory sphene and apatite. This rock might be metamorphosed diorite or a member of the calc-silicate clan; the calcic plagioclase would seem to support the latter notion. The rock is lineated along 50°, 280° az, the trend of the secondary lineation.

Granite gneiss (table 9, mode 60) occurs as a 1x25 m xenolith oriented parallel to the secondary foliation and seemingly stretched therein. The average grain size for all the main minerals is 0.5 mm. Plagioclase (An_{18}) is xenoblastic and unzoned; a few relict grains are prismatic and have vestiges of normal zoning. Quartz is free of subgrains, perhaps due to its small size. Microcline is submicroscopically twinned and somewhat microperthitic. Biotite and muscovite occur in random to lepidoblastic arrays in different parts of the slide. Accessory minerals include zircon, magnetite, apatite, and thorite. Microcline and muscovite are both much higher in the mode than in any of the Bitterroot granite.

A granite xenolith (table 10, mode 39) was found in the granite. Plagioclase occurs in 2 mm, prismatic grains, euhedral to subhedral, with normal zoning from cores of An_{28} to rims of An_{25}. Quartz is 1 mm grains, and microcline is in submicroscopically twinned 1 mm grains. Biotite is randomly oriented in 1 mm flakes; no muscovite is present. Accessories include zircon, magnetite, and epidote.

Fine-grained dikes.

The granitic rocks, including gneissic variants, are cut at four places by fine-grained granite sheets and dikes; modes were measured for three of them (table 8, mode 61; and table 10, modes 36 and 37). One of these is cut by pegmatite and aplite. The aplite is schistose with secondary foliation across its contacts, whereas the enclosing gneiss shows no schistosity (but it does have a secondary fabric). A granitic dike is foliated parallel to its walls, and another is cut across by secondary foliation parallel to that in the enclosing granitic gneiss. Average grain size in all of them is about 0.5 mm. Plagioclase in the fine-grained granite dikes (28% to 33%) in the mode) ranges in composition from An_{22} to An_{28}. It occurs in unzoned, prismatic, subhedral grains for the most part, although a few relict, normally zoned grains occur with cores An_{35} and rims An_{28}. Quartz (27% to 31% in the mode) occurs in 0.5 to 0.7 mm, irregular grains, partly with 0.3 mm, strain-free subgrains. Microcline (32% to 36% in the mode), submicroscopically twinned in 0.5 to 1 mm grains, includes both plagioclase and quartz; a few 0.5 mm, strain-free granoblastic subgrains occur in the larger grains. Biotite occurs in 0.5 mm, lepidoblastic flakes and muscovite in 0.3 mm lepidoblastic flakes. Accessories include magnetite, zircon, and apatite.

Four fine-grained granodiorite dikes were encountered; modes were measured for three of them (table 8, modes 62 and 63; and table 9, mode 48). Plagioclase (44% to 54% in the mode) ranges in composition from An_{25} to An_{28}, in irregular, granoblastic, unzoned grains; only a few grains contain relicts of normal zoning. Quartz occurs in 0.5x2 mm, flattened grain aggregates of 0.3 mm, strain-free subgrains. Orthoclase occurs in flattened 0.5x1 mm grains, partly in 0.4 mm, strain-free subgrains. Biotite and muscovite are lepidoblastic in 0.5 mm grains. Accessories are magnetite and zircon. One of the dikes is schistose across its contacts along 080° az, 44° NW; the slab shows rodding near 40° 315° az. Some of the rod-shapes seen in the slab are shown in thin section to consist of trains of equant feldspar grains 0.5 to 1 mm across and up to 6 mm long, within which individual granoblastic grains are 0.1 to 0.5 mm in diameter. Plagioclase in An_{25}. K-feldspar is submicroscopically twinned microcline. Quartz occurs in 0.5x2 mm rods, aggregates of individual granoblastic grains 0.1 to 0.5 mm in diameter. Biotite and muscovite are streaked out parallel to the quartz and feldspar rods. In another granodiorite of comparable mineralogy, a directed fabric expressed by mica developed, but granoblastic quartz and feldspar show no signs of rodding. Yet another granodiorite has a largely igneous texture free of the effects of secondary strain. Plagioclase (zoned, cores An_{24} to rims An_{20}) occurs in euhedral, prismatic, 1 mm grains. Microcline, submicroscopically twinned and with abundant Carlsbad twins, occurs in euhedral, 1 mm prisms that enclose some quartz. Some grains in the rock are of orthoclase. Quartz is in 0.7 mm grains mostly free of subgrains. Biotite and muscovite are in 0.3 mm grains. Accessories include zircon, apatite, and magnetite.

Pegmatite suite.

Four granodioritic aplites were studied (table 8, mode 65; and table 9, modes 54 to 56). They have a secondary strain fabric and mineralogy virtually identical to those of schistose granitic aplite described above. Granodioritic alaskite was sampled at two places. A mode is given in table 10, mode 33. Plagioclase is stubby prismatic in 1 mm grains, and many grains contain relicts of normal zoning, from cores of An_{27} to rims of An_{20}, myrmekitic against K-feldspar. Quarts occurs in 0.7 mm grains, reduced to 0.5 mm grains along blastomylonitic shears. Zircon is the sole accessory mineral seen.

Two pegmatites studied have modes estimated in the granite field. All grains are more than several centimeters in diameter. Under the microscope, plagioclase (An_{17}) is seen to consist of 2 mm strain-free subgrains, quartz of 0.5 mm, strain-free subgrains, and microcline of 0.5 mm, strain-free subgrains. Biotite and muscovite occur in trace amounts in 0.5 mm flakes. Some microcline is cut by extension fractures filled with muscovite.

One trondhjemitic alaskite was studied (table 9, mode 57); it is intruded into granodiorite. Plagioclase (An_{15}) occurs in 4 mm, unzoned prisms partly in strain-free, 0.5 mm subgrains. Quartz is in 2 mm anhedrons mostly broken in strain-free, 0.7 mm subgrains, and partly in smaller subgrains in blastomylonitic zones. Biotite and muscovite occur in 0.5 mm grains. Trace amounts of garnet occur in 0.3 mm grains.

Blastomylonite.

Two outcrops with zones of blastomylonite up to 10 cm thick were seen (fig. 58). These are megascopic analogs of the many blastomylonite shears about 0.5 mm thick seen in thin section. One is foliated with fine-grained, streaky biotite lineation, and the other lineated with fine-grained, streaky biotite lineation, but not foliated. Thin-section study shows the tiny, strain-free grains characteristic of blastomylonite.

Mylonite.

Two thin, low-angle mylonitic shears (less than 1 mm thick) were seen, with streaky lineation on annealed slickensides and microgouging (fig. 59). These are the outcrop analogs of at least some of the several 0.1 mm mylonitic shears seen in thin section. Much undulatory extinction and bending of mineral grains is due to this feature.

Mylonitic shear joints.

Several non-mineralized shear joints of northeast trend were mapped; they contain thin, lineated mylonite zones (fig. 60). They cut the thin, low-angle mylonites, but their petrography looks like that of the low-angle mylonites; it was not possible to separate their effects in thin section.

Mineralized shear joints.

Next youngest are shear joints with slickensides patterned by chlorite and minor epidote (fig. 61). These shear joints trend ENE and their slickensides plunge at varied angles both to the NE and to the SW. In a few cases, the joints developed by reactivation of earlier fractures, as shown by chlorite overprinting mullions or lineated tourmaline of different rake. Thin section study shows that very fine-grained microbreccia occurs along the mineralized shear joints.

The eastern sector

Structure.

Granitic rocks.

The eastern sector, entirely within the field of secondary strain, is underlain by granite, granodiorite, and minor tonalite and anorthosite, based on modes from thin sections, stained slabs, and field count of phenocrysts in coarsely porphyritic rocks. Parts of the following 7 1/2 ′ quadrangles were mapped: Jeanette Mountain, Idaho; Blodgett Mountain and Tenmile Lake, Idaho-Montana; Printz Ridge and Ward Mountain, Montana. Few contacts were found, as the various rock types look much alike in the field. One dark-colored tonalite changes to quartz diorite to the west along its strike, in the Cedar Ridge quadrangle of the western sector; its contacts are sharply defined where exposed. Granite and granodiorite occur in roughly equal amounts and are more or less intermixed, as elsewhere in the pluton. About 20% of the rock is porphyritic, more than in the areas to the west. The various textural types are commingled in seemingly random fashion. Porphyritic zones become so in gradual fashion, with no sharply defined contacts. At one point, foliated granite contains bands of porphyritic, foliated granite up to 10 cm wide parallel to the foliation. These bands are lenticular and discontinuous, up to 3 m long. Porphyritic granite and granodiorite occur only in the higher elevations in the Tenmile Lake quadrangle and not in the valley bottoms. This suggests at least a local elevation control of the development of porphyritic rocks.

Foliation.

Most of the rock in the eastern sector is foliated. Foliation is expressed by parallel biotite grains, flattened or rodded quartz and feldspar grains, parallel schlieren, feldspar prisms partly parallel to flow planes, parallel slabby xenoliths of biotite quartzite and fine-grained schist derived from biotite diorite, amphibolite, or fine-grained biotite tonalite, and by biotite-rich bands.

Foliation relations are more complex in the eastern sector than in the two sectors to the west, described above, and require description in three subareas, A, B, and C. Subarea A is defined as the area covered by the Jeanette Mountain quadrangle, the west half of the Blodgett Mountain quadrangle, the Tenmile Lake quadrangle, and the Ward Mountain quadrangle, and consists of a continuation of the WNW trends from the western and central sectors (fig. 63). The data display markedly axial symmetry. Much of the foliation appears to be of medium-grained, secondary character. It cuts in places across folded schlieren of various trends that appear to reflect an early, primary flow foliation; it also cuts some pegmatite and distorts it. In places, it seems to parallel earlier primary foliation, defined by slabby xenoliths and schlieren. Lineation plunge averages near horizontal through this subarea, in contrast to the average of about 30° to the NW, seen in the central and western sectors. This is due to a lineation (and foliation) arch across the area, from westerly plunges on the west to easterly plunges on the east. Lineation includes axes of passive-flow folds in schlieren, streaked-out biotite, the long axes of oriented feldspar phenocrysts, and the long axes of flattened quartz and feldspar grains. It is clear from the outcrop data that both primary and secondary foliation are included in figure 63. The two structures look much alike in the field; most commonly, only one was present and could not then be assigned with confidence to one or the other set. However, the angular differences between the two sets are small for the most part, and the averaged values are probably representative both for primary and secondary foliation.

Feldspar phenocrysts in shallow-dipping foliation are rotated both clockwise and counterclockwise as seen in sections looking NNE. At one point, half a dozen anorthosite orbicules are strung out like rotated beads along a single flow lamina in gneissic granite. Calc-silicate gneiss xenoliths are separated by 6 m intervals along a single lamina in the flow foliation at another place. Although the granitic rocks are mostly foliated and lineated in the area, there are yet a few places where the rocks are strongly lineated but yet not foliated through zones more than a few meters thick. Further, quartzite sheet xenoliths and related migmatites, measured from meter to kilometer scales in screens in a few places, have orthogonal crossing relation; one sheet stands vertical in the foliation and another stands perpendicular to it dipping at low angles; they intersect in the lineation, which in the examples measured plunges at low angles toward 290° az. The symmetry is axial.

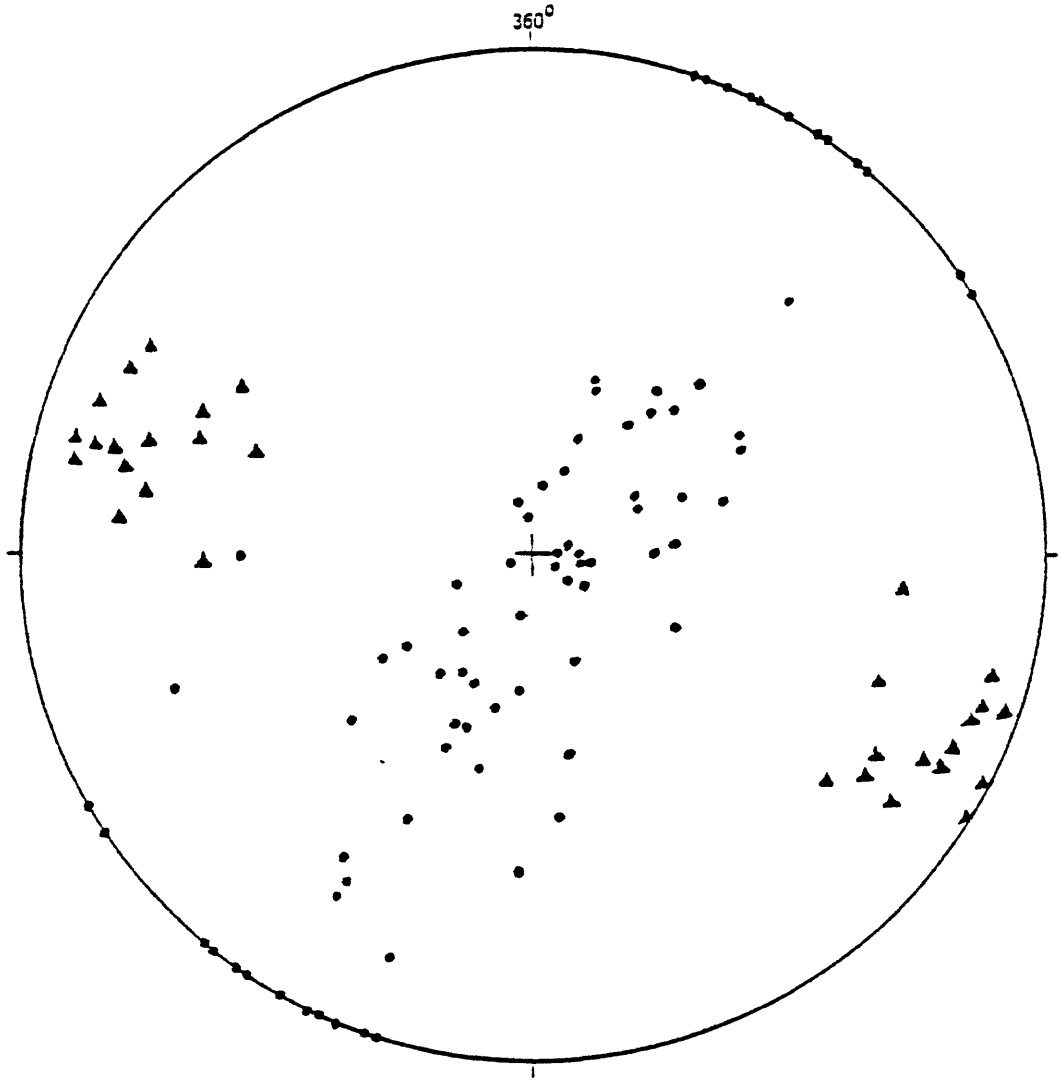

Figure 63.--Poles to flow foliation (●) and linear features (▲) in granitic gneiss of the western and southern parts of the eastern sector (Subarea A), Bitterroot lobe of the Idaho batholith, west of Hamilton, Mont. Data are plotted on lower hemisphere of Wulff stereonet.

In the ridge south of Roaring Lion Creek in the Tenmile Lake quadrangle, sheets of tonalite up to 20 cm thick occur as discontinuous layers along the primary flow foliation in the gneissic granitic rock and are themselves of gneissic character. They pass laterally into biotite schlieren with a kind of "popcorn" texture due to the idiomorphic habit of the small amounts of remaining feldspar. Some of the layers are folded with the flow foliation. The tonalite layers show gradual transition to granite through zones about 5 mm thick. Tonalite is also seen as 5 to 10 cm laminae of lit-par-lit character in biotite quartzite sheet xenoliths.

Three steep, northeast-trending ductile shears that concentrate biotite cut across the main foliation(s).

In an expression of crossing relations involved in the eastward transition to foliation orientation in Subarea B, a biotite-quartzite stringer oriented in the primary flow foliation has the form of an isoclinal fold more than 30 m in length along its 020° az-trending axial plane. This structure is cut across by 300° az-trending, secondary foliation and is refolded in the foliation, with the development of a secondary crossing foliation in the fold limbs, parallel to the 300° az trend. A related feature is shown by a slabby, 10-cm-thick, biotite-quartzite xenolith that extends for more than 25 m in a 101° az trend along the relict primary flow direction. Streaky biotite lineation in it is oriented 20°, 290° az, in the general direction of the steep secondary foliation.

Foliation Subarea B of the eastern sector occurs principally in the east half of the Blodgett Mountain quadrangle and in the western half of the Printz Ridge quadrangle. Foliation in Subarea B trends NNE and dips steeply (fig. 64). Angular relations between primary and secondary foliation in Subarea B are comparable to those in Subarea A, but extensive flattening and mineral rodding are absent. Lineation is rare, expressed mostly by small fold axes in the gneiss. Some swirling of the foliation is evident; for example, at one outcrop near Castle Crag, the foliation trend changes from 275° az to 070° az within a few meters; the small folds are part of a conical fold set due perhaps to secondary deformation of primary flow foliation. The rocks near Castle Crag, in the northern part of Subarea B, are more complex than those in adjoining areas. Both granite and granodiorite occur as early phases, apparently emplaced at the same time and recrystallized equally in he field of secondary strain. A younger granite injected along the foliation remains unaffected by the secondary strain; it may equate to or post-date the fine-grained granite sheets of neighboring areas, not otherwise seen in Subarea B. Migmatite zones of northeasterly trend, up to 2.5 km thick, occur in the Castle Crag area, involving biotite granodiorite as the major paleosome together with a few xenoliths of biotite quartzite and amphibolite. The migmatite has experienced strong secondary strain, and biotite-quartzite xenoliths were flow folded about steep axial planes, as were aplite and pegmatite dikes. Pegmatite was also stretched and boudined. Abundant are flow-folded, biotite granite-granodiorite migmatites. The granodiorite occurs also partly as flow bands along the primary flow foliation in the granite. Tonalite enters as a minor component involved in migmatitic, lit-par-lit banding both within the granite and the granodiorite. One of the larger amphibolite xenoliths contains small xenoliths of hornblende granite and pink-weathering, fine-grained diorite. The northeast trends die out quickly to the south, in areas that were sparsely mapped or bypassed in reconnaissance mapping. If the small structures recapitulate the large ones, then a major, steep-plunging fold hinge on the primary flow foliation may exist in the vicinity of he southern margins of the Blodgett Mountain and Printz Ridge quadrangles, overprinted and perhaps destroyed in strong secondary foliation development to the south.

Foliation Subarea C of the eastern sector occurs in the eastern parts of the Printz Ridge and Ward Mountain quadrangles, the most easterly extent of this mapping. This subarea is part of the Bitterroot frontal gneiss zone. Foliation dips at shallow angles to the east (fig. 65); in prior work, the view has been advanced of an east-dipping gneiss sheet inclined at about 30°. The data gathered for this report represent an inclined axial symmetry of tilted domical character. Foliation is expressed by oriented biotite flakes and by flattened quartz and feldspar grains. In the transitions from Subareas A and B (not studied in detail), the foliation becomes stronger, feldspar grains are generally flattened in the foliation, and the rocks become strongly lineated in places, on the same general trend as that in the rocks to the west. The lineation is expressed by elongate biotite grains, trains of small biotite flakes, rodded quartz and feldspar grains, and minor fold axes in biotite-quartzite xenoliths. Some zones more than a few hundred meters thick are lineated but not foliated.

The remaining structural features to be discussed are common to Subareas A and C, but are largely or completely lacking in Subarea B. Feldspar prisms, some of them coarse-grained to porphyritic in the medium-grained matrix, lie with their prism faces parallel to low-angle foliation for the most part, as seen in the rock faces exposing the *a*-*c* section (kinematic axes, on the assumption that rodded quartz and feldspar grains represent the direction of extension and therefore the slip line). Viewed along the *a*-direction (in the *b*-*c* section), the feldspar prism cross-sections are oriented in all possible directions relative to the foliation, in an axial symmetry, but not all the feldspars seen in the *a*-*c* section of the outcrop face have their *c*-axes and thus prism faces parallel to the foliation. At a particularly favorable exposure, all the large feldspar grains, whose *c*-axes are roughly alined in the ESE direction, were counted in a 37x39 cm^2 area. Of 23 large grains present, looking NNE, seven show counterclockwise rotation, one shows clockwise rotation, and 15 are not rotated. At another place where flattened feldspars are well exposed, only three feldspar grains show any rotation, all counterclockwise looking NNE. None of these rotations is large, most of them being less than 25° from the foliation plane.

The secondary flow foliation continued to form in less intense fashion following the pegmatite stage, and some of the later features are now considered. A fairly common relation is depicted in figure 66. Non-penetrative shear zones and surfaces a few millimeters thick are coated with lineated biotite; both steep- and shallow-dipping surfaces contain lineation of approximately the same orientation; the shears are clearly of axial symmetry. The shears cut across the earlier foliation, which is itself a part of a broader axial symmetry (see fig. 63). Both sets of axial symmetry are developed on the same axis, trending in the 110°-290° az sector. In places, these shears become more penetrative and converge in character with the more penetrative, early secondary foliation. Some of the later secondary shears reduce feldspar phenocrysts to flaser structures fairly penetratively, but with

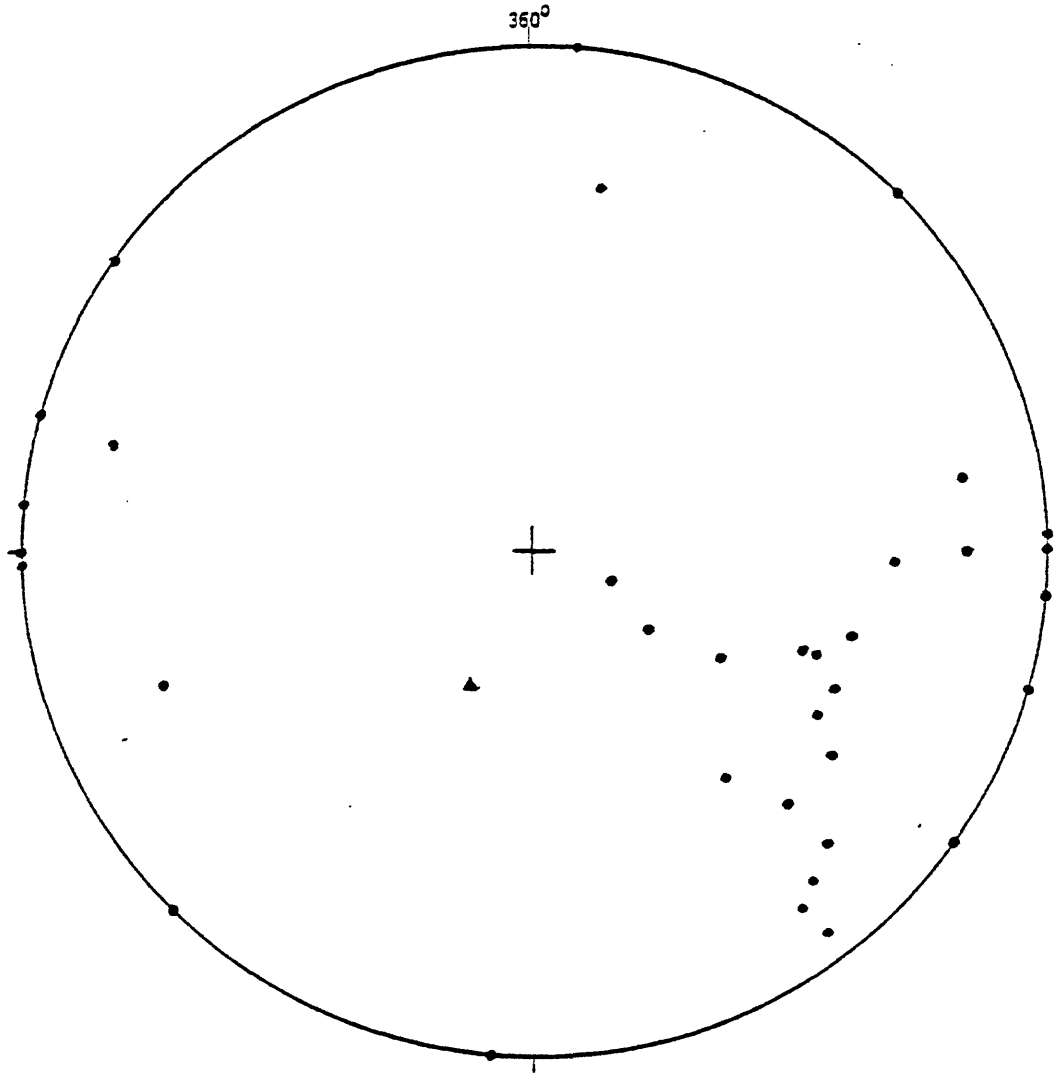

Figure 64.--Poles to foliation (●) and a flow fold axis (▲) in granitic gneiss in Subarea B, of northeast-trending gneiss in the Bitterroot lobe of the Idaho batholith. Data are plotted on lower hemisphere of Wulff stereonet.

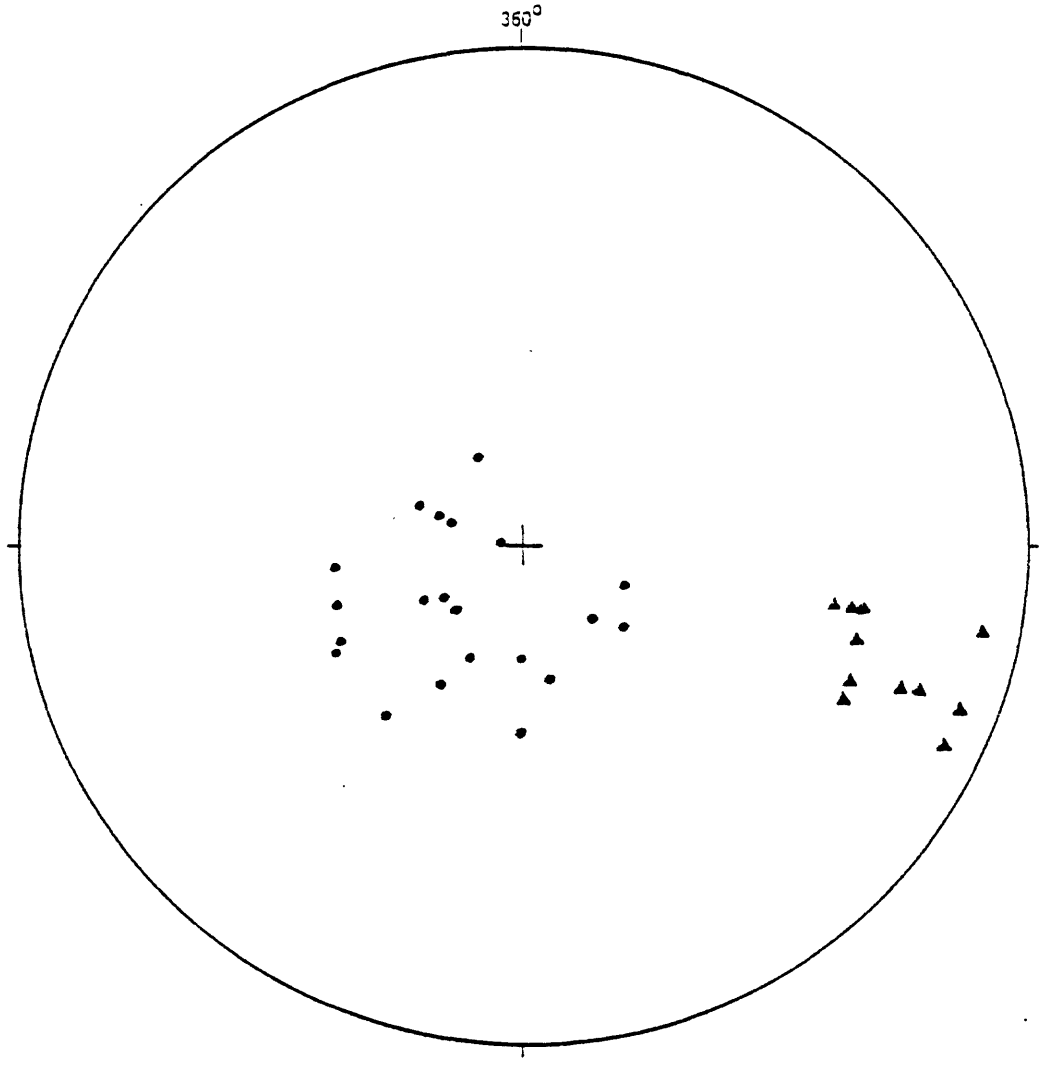

Figure 65.--Poles to gneissic foliation (●) and mineral lineation (▲) in the gneiss of Subarea C of the eastern sector (Bitterroot gneissic front) of the Bitterroot lobe of the Idaho batholith, west of Hamilton, Mont. Data are plotted on lower hemisphere of Wulff stereonet.

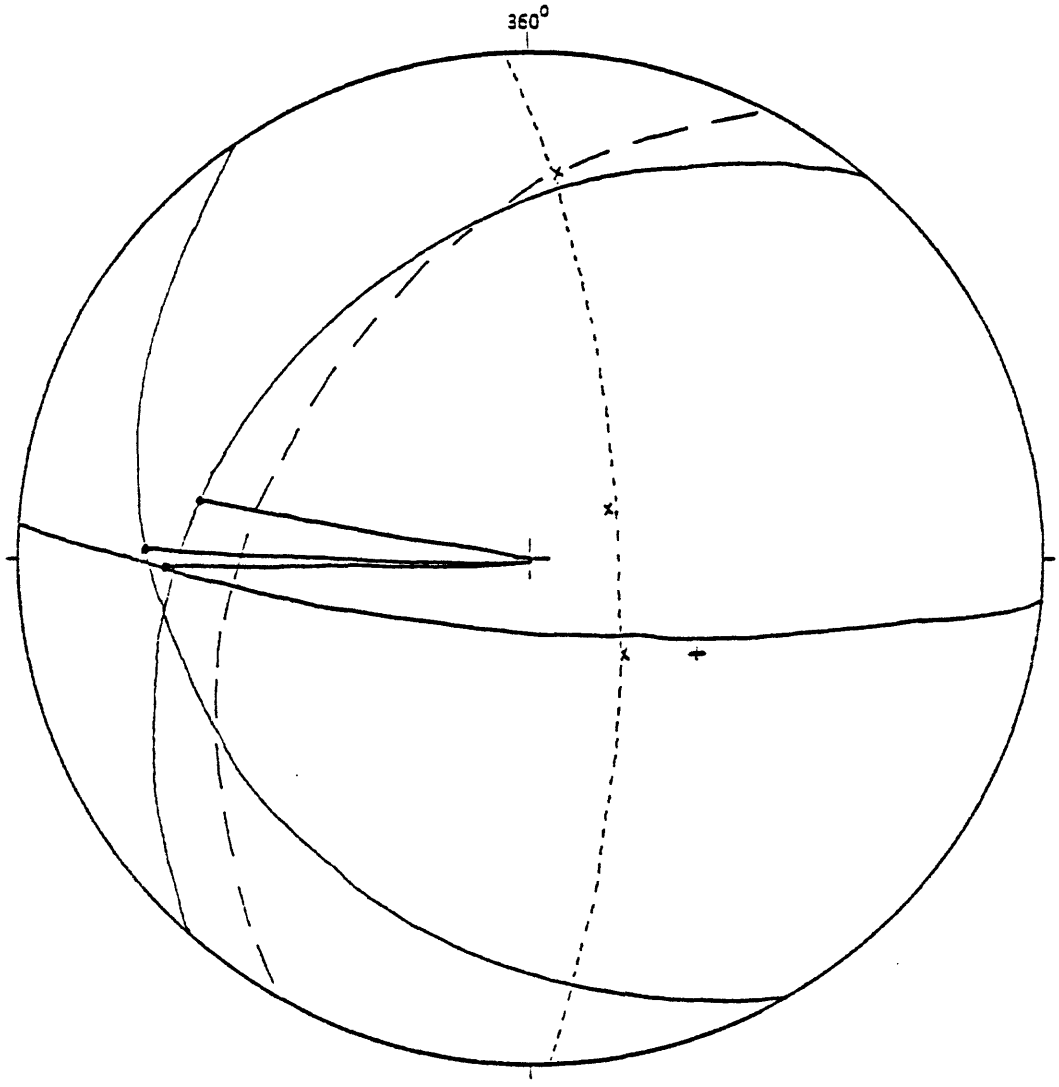

Figure 66.—Late-stage, secondary foliation relations in the eastern sector of the Bitterroot lobe of the Idaho batholith, west of Hamilton, Mont. Primary foliation is shown by the coarse-dashed arc, and its pole by (+). Three solid-line arcs show a family of late, secondary shear surfaces coated with lineated biotite (●). The fine-dashed arc is a girdle containing the poles (X) to the late shears. The pole to the girdle is approximately defined by the average of the biotite lineations. Data are plotted on lower hemisphere of Wulff stereonet.

varied intensity through gradational zones. The phenocrysts, in low-angle secondary foliation, are distorted in flattened, somewhat lenticular rods, which parallel streaky biotite and rodded quartz grains generally oriented at low plunges toward 290° az. At a typical place, 30 grains were measured, 10 in each of three orthogonal faces: a-c, b-c, and a-b (kinematic axes). The average dimensions of the flattened rods are c - 6.7 mm, b - 8.6 mm, and a -13.6 mm, for an axial ratio of 1.0:1.3:2.0. Most of the undeformed phenocrysts are stubby prismatic and not in linear array, so that stretching seems clearly indicated in rod formation. This is borne out by the occurrence of some thin, quartz-filled extension fractures in the rodded feldspar grains, standing in the b-c plane.

Anorthosite I.

A few blocks of anorthositic orbiculite were seen in the granite talus, but not found in place. A few such orbicules were observed strung out and rotated along primary flow foliation planes in the granite. Anorthosite was found in place at two localities; because of its physical resemblance to granodiorite, it was not recognized as anorthosite in the field.

Schlieren.

Biotite-rich schlieren are seen in several associations: (1) primary flow concentrations in granitic rock; (2) secondary flow concentrations in granitic rock; (3) thin, trailing ends of lit-par-lit bands of granodiorite in granite; and (4) thin, trailing ends of lit-par-lit bands of tonalite in granitic rocks.

Ductile shears.

A few thin, NE-trending, ductile shears with biotite concentrated in them transect both the primary and the secondary foliation.

Xenoliths.

Xenoliths include biotite quartzite, andesine quartzite, calc-silicate gneiss, biotite granodiorite, biotite-granodiorite gneiss, tonalite gneiss and schist, quartz diorite, quartz-diorite gneiss, biotite diorite schist, and amphibolite; they are considerably more plentiful in the eastern sector than in the central sector.

Fine-grained dikes.

Several dikes of fine-grained biotite granite occur in Subareas A and C, with some variation in their features. Two are 70 to 85 cm thick, injected as sheets along the secondary foliation in the enclosing gneissic granitic rocks, extending for more than 55 m along the strike before going under cover. One is cut by aplite dikes which are passively flow-folded in it along a fine-grained schistosity parallel to the dike walls and the external foliation. Another, a 20-cm dike, oriented 015° az, 33° NW, and schistose parallel to its walls, cuts massive granite. The same outcrop contains a 10 cm, 290° az, 60° NE dike schistose parallel to its walls, cut by aplite dikes. These two dikes intersect in a line oriented 30°, 310° az, which defines the slip direction for contemporaneous shear in the two dikes. At another place, fine-grained granite is in concordant sheets up to 5 m thick, lenticles and boudin-like pods, all cut by non-schistose pegmatite and aplite dikes. Lineated biotite in it trends 18°, 285° az. At yet another place, it cuts early foliation (293° az, 90°) in a dike oriented 028° az, 40° NW, with an internal flow or secondary flow foliation parallel to is walls. Minor faulting occurred during the emplacement of the fine-grained intrusions, as shown by one example, which also shows something of the sequence of injection of rock types. Dike 1, of fine-grained biotite tonalite, is oriented 345° az, 64° SW, and is 15 cm thick. It is offset right laterally 1.5 m along a shear oriented 055° az, 90°, which is injected by dike 2 (which shows no sign of shearing) of fine-grained biotite granite.

An outcrop on the ridge south of Roaring Line Creek (in the Tenmile Lake quadrangle) shows a particularly good exposure of fine-grained biotite granobiotite. At this outcrop, a primary flow foliation shown by relict biotite schlieren is cut and partly obliterated by secondary flow foliation. Fine-grained biotite granodiorite intrudes along and across the secondary flow foliation and is sheared by it in such a way that two dikes of fine-grained biotite granodiorite (oriented near 285° az, 47° NE, parallel to the secondary foliation, and 080° az, 09° SE) are both foliated parallel to their walls and both contain a stretched biotite lineation oriented near 06°, 100° az. Further, the line of intersection of the two dikes is parallel to the stretched biotite lineation. The fine-grained biotite granodiorite dikes are cut by NE-trending alaskite dikes which bend right-laterally as they cross the fine-grained biotite-granodiorite dikes; the alaskite is sheared in the secondary flow foliation and is schistose parallel to the secondary flow foliation. One steep, fine-grained granodiorite dike averages 6 cm thick over a strike length of 200 m and goes under rubble at both ends. At one point, it sent an offshoot as a 30 cm-thick dike into a 015° az, 90° fracture that is approximately perpendicular to the stretching lineation.

Pegmatite suite.

Filled primary fractures are represented by scarce aplite and pegmatite dikes 4 to 18 cm thick. Some are cut by foliation parallel to that in the enclosing gneissic granitic rock, but others are massive and unaffected. A 3 cm, biotite-patterned, ductile shear oriented 275° az, 90°, cuts the main foliation and offsets a pegmatite dike 10 cm left-laterally.

Blastomylonite.

Blastomylonite is relatively scarce in the western part of the eastern sector, but is yet present in amounts larger than those of the central sector; it becomes still more abundant to the east. Blastomylonite orientations over the eastern sector are given in figure 67. In the western part, 5 to 8 cm thick, fine-grained blastomylonite zones inclined at low angles cut the earlier foliation, and are typically spaced at 0.5 m or larger intervals in the rock where they occur. As indicated above, blastomylonite is absent in the steep, NE-trending foliation of Subarea B. The blastomylonite contains a fine-grained, streaky lineation oriented in the 110° az - 290° az sector. Blastomylonite is seen in relatively few outcrops, but generally a few 1 to 2 mm shears are seen per thin section in two-thirds of the thin sections studied. Distribution over the western part of the sector seems to be more or less random. Commonly associated with blastomylonite of the eastern sector, and different from blastomylonite of the central sector, is reconstituted quartz in medium-grained lenticules (2 to 4 mm) and some longer ribbons; reconstituted quartz encloses fine-grained mica relicts from former blastomylonite zones where

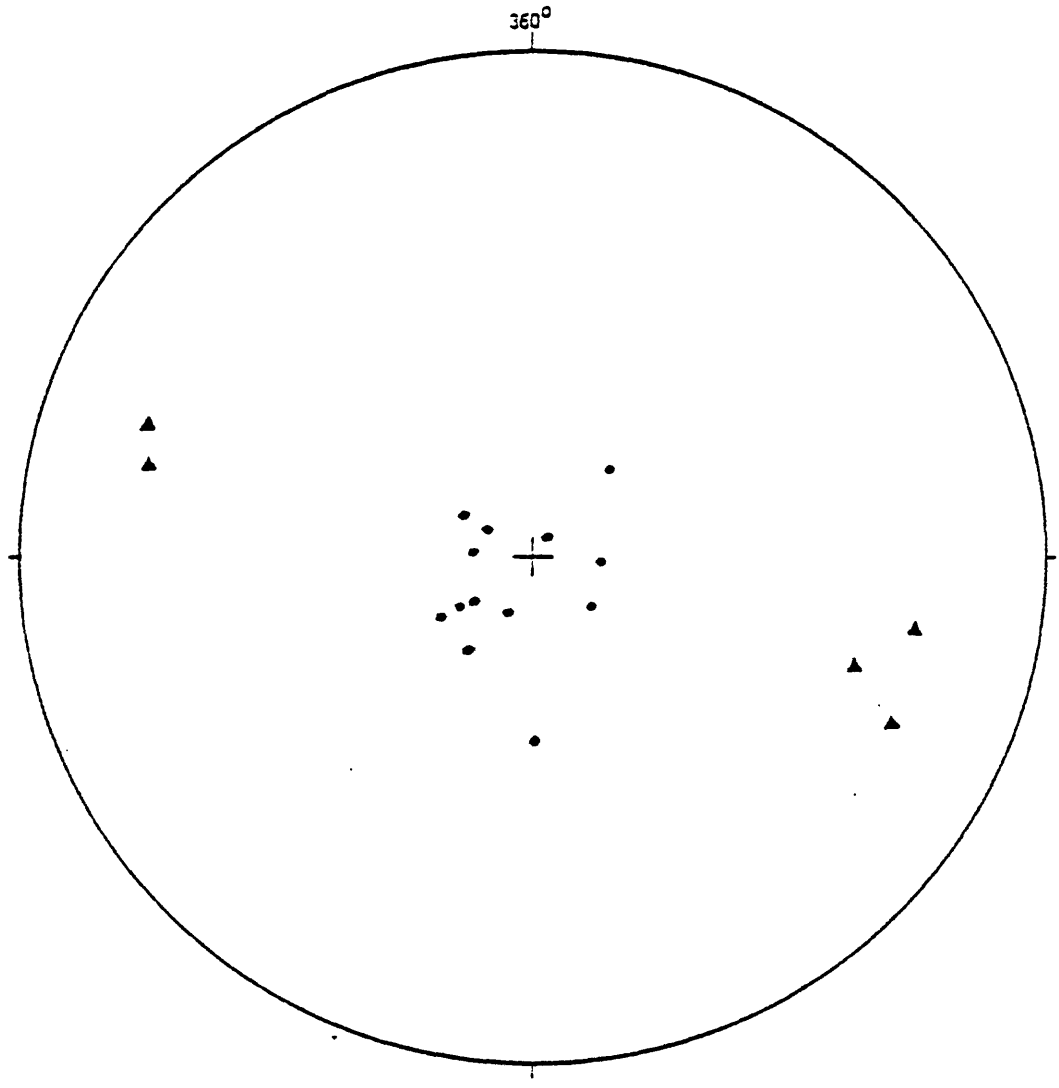

Figure 67.--Poles to blastomylonite foliation (●) and fine, streaky biotite lineation (▲) in blastomylonite in the eastern sector of the Bitterroot lobe of the Idaho batholith, west of Hamilton, Mont. Data are plotted on lower hemisphere of Wulff stereonet.

they transected original quartz grains. The common appearance of the phenomenon is that blastomylonite zones stop at relatively large quartz grains. This quartz reconstitution is called the "quartz-ribbon" event, and evidently occurred in late- or post-blastomylonite time; it characterizes blastomylonite fabric throughout the eastern sector. Some thicker blastomylonite zones, thicknesses measured in centimeters, extend for distances measured in kilometers as low-angle shears or ductile thrust faults; in the central part of the sector, in the Tenmile Lake quadrangle, several such shears were mapped, separated vertically by approximately 300 m intervals. In the eastern part of the sector, density of blastomylonite development increases considerably. Blastomylonite shear zones cut the gneiss of the eastern part (Bitterroot frontal gneiss zone) along dips somewhat shallower than those of the gneiss; thus, arching of the secondary foliation and, therefore, doming had already begun in pre-blastomylonite time. The shear zones range from 1 to 50 cm thick and are spaced vertically at 45 to 85 cm intervals. The lineation trends expressed by fine-grained, streaked-out mica are comparable to those of the gneissic granite. Stretching in this episode produced quartz-filled fractures whose geometry indicates that tops moved to the southeast.

Mylonite.

A few thin (fraction of a millimeter) mylonitic shears occur in the western and central parts of the eastern sector (but not in Subarea B); they stand at shallow to steep dip angles and are lineated with streaky sericite and are microgrooved on polished surfaces along trends near 110° az. The mylonitic shears become relatively numerous in the eastern part, in and near the gneissic Bitterroot front. The shears occur in sheeted zones 2 to 5 cm thick and spaced at 8 to 100 cm apart. Westward, toward the center of the eastern sector, they become scarcer, so that one may be seen in a 100 m section of gneiss. General orientation data are give in figure 68. Some mylonitic shears transport to the west, based on shear steps in the shear surfaces, and some transport to the east. This is due to the fact that they belong to conjugate shear pairs; an example is given in figure 69 and analyzed in the caption. A steeply oriented axis of maximum principal stress is deduced. Showing unexpected complexity, however, but rare on the whole, is another kind of shear pair, slickensided in a direction near the line of intersection of the two planes (movement in a younger stress field?). Some mylonite zones are crossed by shears internal to the zones, at angles of 15° to 30° to the bounding shear surfaces. These are taken to be Riedel shears; the sense of shear transport at such places, derived from the Riedel shears, is the same as that shown independently by shear steps. The steep shears seem clearly due to steeply inclined stress; the shallow-dipping mylonitic shears are perhaps similar in their mechanics to the blastomylonitic shears, although they cut across them at small angles and are clearly later.

Mineralized shear joints.

Next are high-angle shear joints (015° az trend), patterned with chlorite and slickensided obliquely or along their dips (fig. 70). Both right- and left-lateral oblique slip have occurred in different places, based both on shear steps and on offset features together or singly.

Secondary fractures.

The orientations of secondary joints other than those patterned with chlorite are give in figure 71. A good bit of scatter occurs, but the 015° az trend is fairly pronounced.

One E-W fault, oriented 270° az, 70° N, was mapped in the Castle Crag area. Slickensides plunge down the dip, and related extension joints are oriented 270° az, 85° S. The fault gouge is a few cm of brown, clay-like material.

Petrography.

Granite.

In spite of the structural variations noted above, the basic petrography of the rocks throughout the eastern sector is very similar, so that the various rock types can be described collectively.

Granite (table 11, modes 1 to 3; table 12, modes 1 to 13; table 13, modes 1 to 20; table 14, modes 1 to 9; and table 15 modes 1 to 11) looks very much the same over the entire sector and contains from 17% to 46% plagioclase (An_{18} to An_{33}). Grains are equant (2 to 4 mm), euhedral to subhedral, to sublenticular in flattened grains up to 4 mm long parallel to the foliation. Most grains are unzoned, but a few relicts of normal zoning occur, cores An_{29} to rims of An_{22}. Much of the plagioclase is myrmekitic adjacent to K-feldspar grains, and some of it is untwinned. Subordinate are 1 mm, strain-free subgrains. Plagioclase in some rocks is cut by a few extension fractures up to 0.4 mm wide, filled with quartz-microcline-muscovite-pennine, in various combinations. In the subordinated lineated gneiss (foliation absent), plagioclase occurs in stringers of equant, unzoned grains up to 2 mm diameter, giving the appearance of drawn-out rods as seen in the sawed slab. Rodding seen in the plagioclase of one granite is developed on grains 3x8 mm or longer, segmented in several parts by extension fractures 0.2 to 0.3 mm thick, filled with pennine-muscovite-microcline-magnetite-allanite-quartz. Considering the mobility of microcline and quartz, the rodding may have developed before the granite was completely crystallized. Along restricted shear zones up to 0.3 mm wide in the western part of the sector, plagioclase is reduced to 0.1 mm irregular grains, along with 0.3 mm biotite and muscovite flakes and 0.1 mm, irregular grains of quartz. Many of these small grains show more or less undulatory extinction, and some mica flakes are bent. Yet many are not, and many quartz grains are granoblastic and strain free. This may be a condition of blastomylonite development in which strain outlasted recrystallization, or it may be a situation in which there was some late mylonitic shear. In the central and eastern parts of the eastern sector, some plagioclase is cut by blastomylonitic shear zones up to 2 mm thick in which plagioclase has been broken and recrystallized to 0.3 mm, granoblastic, strain-free grains (An_{23} in one example where matrix plagioclase has a composition of An_{28}; in other rocks, matrix and blastomylonite plagioclase have the same composition). Such effects are seen in about half the thin sections, and range from minor up to half the volume of the gneiss in which it is found. Many 120° triple junctions are seen among the quartz and plagioclase grains. In some of the gneiss, blastomylonite zones pass laterally into curved, single-grain quartz ribbons up to 0.5x2 mm in size. Blastomylonite zones nearly wrap some of the feldspar grains, and large, platy quartz grains do the same; the platy quartz grains are perhaps in part recrystallized quartz masses derived from original large quartz grains, and in part quartz masses formed by segregation effects, formerly reduced to fine grain size in blastomylonitic shear, a view reinforced by inclusions of blastomylonitic mica within them.

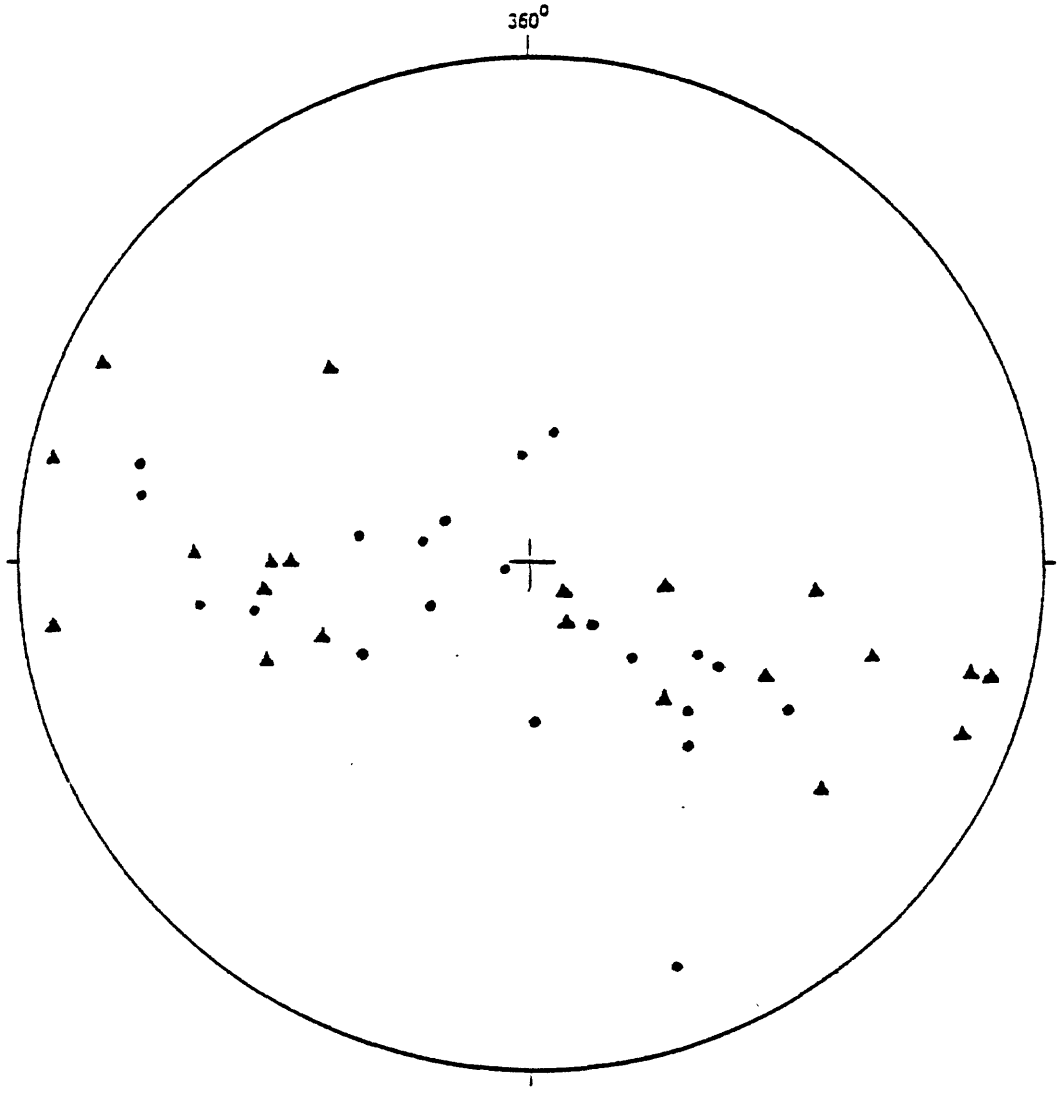

Figure 68.--Poles to mylonitic shears (●) and lineation (▲) due to fine streaking and grooving in mylonitic shears in the Bitterroot gneissic front in the eastern sector (Subarea C) of the Bitterroot lobe of the Idaho batholith, west of Hamilton, Mont. Data are plotted on lower hemisphere of Wulff stereonet.

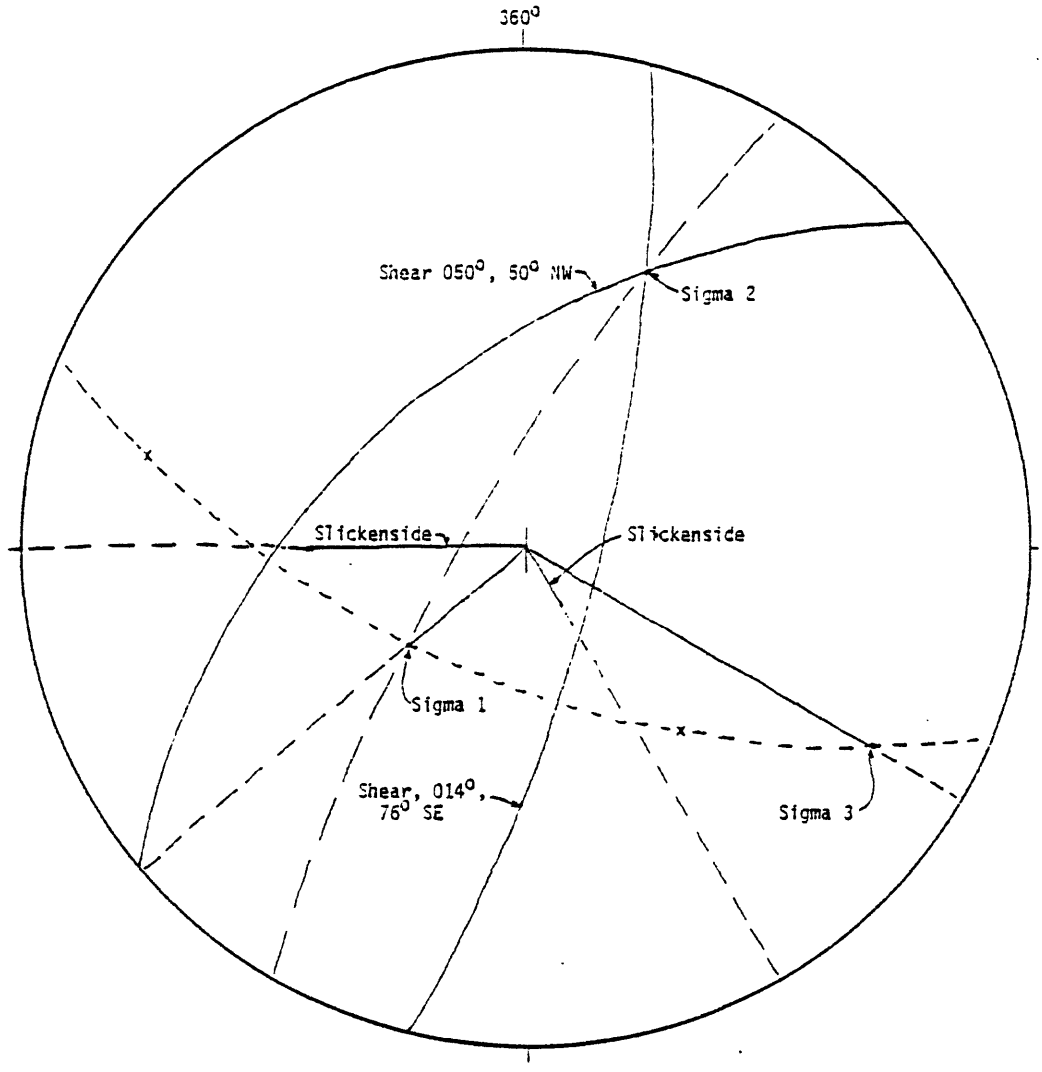

Figure 69.--Conjugate pair of mylonite shears measured at a single outcrop in the eastern sector (Printz Ridge quadrangle) of the Bitterroot lobe of the Idaho batholith, west of Hamilton, Mont. Shears are shown by the two solid arcs. Poles to shears (X). The angle between the shears is 66°. Slickenside grooving in the 050° az shear is oriented 40°, 270° az, and in the 014° az shear, 75°, 150° az. Measurement error is responsible for the failure of the measured slickensides to coincide with their theoretical orientations shown by the points of intersection of the fine-dashed arc with the two solid arcs. The axis of maximum principal stress (sigma 1) for this array is oriented 56°, 230° az. The axis of least principal stress (sigma 3) is oriented 13°, 120° az, near the average lineation trend for the eastern sector. The two sets of slickensides lie approximately in the sigma 1-sigma 3 plane, consistent with largely normal dip-slip movement in the two mylonite shears (normal-left lateral in the 050° az shear, and normal-right lateral in the 014° az shear). Data are plotted on lower hemisphere of Wulff stereonet.

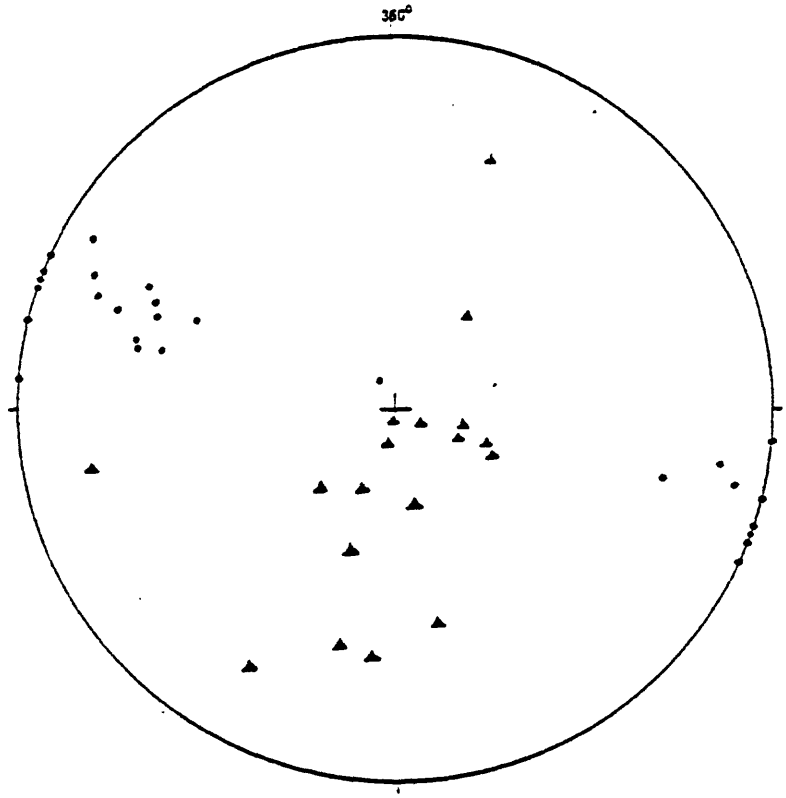

Figure 70.--Poles to chlorite-coated shear joints (●) and lineation (▲) defined by chlorite=patterned slickensides in the shear joints in the eastern sector of the Bitterroot lobe of the Idaho batholith, west of Hamilton, Mont. Data are plotted on lower hemisphere of Wulff stereonet.

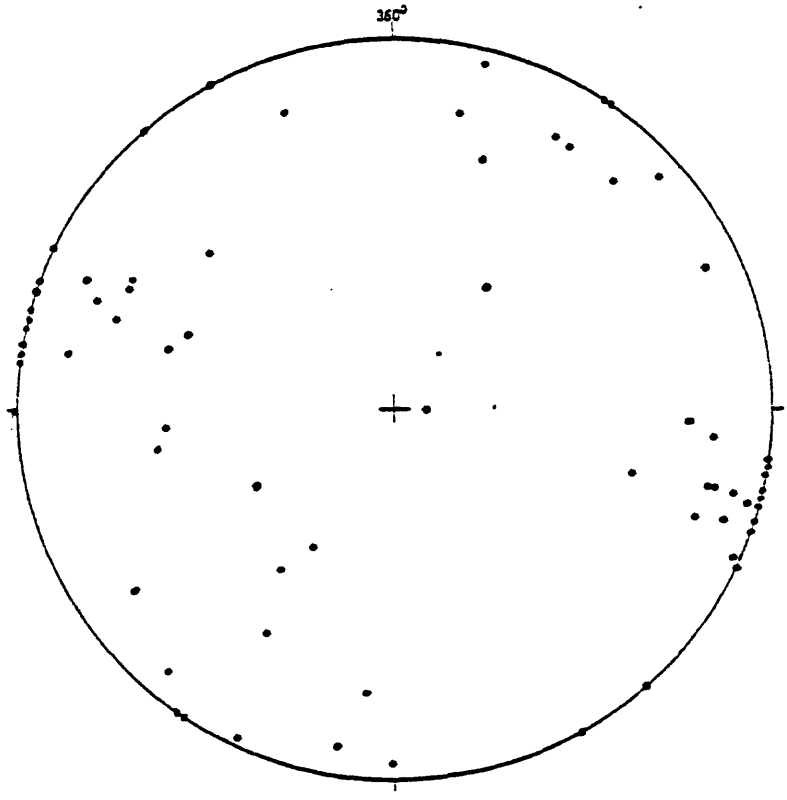

Figure 71.--Poles to secondary joints (●) in the eastern sector of the Bitterroot lobe of the Idaho batholith, west of Hamilton, Mont. Data are plotted on lower hemisphere of Wulff stereonet.

Table 11.--Modes in the Jeanette Mountain quadrangle (HL6)

(1) Granite 80RR233B. (2) Granite 80RR238A. (3) Granite 80RR316A. (4) Granodiorite 80RR096A. (5) Granodiorite 80RR099A. (6) Granodiorite 80RR103A. (7) Granodiorite 80RR235A. (8) Granodiorite 80RR235E. (9) Granodiorite 80RR236A. (10) Granodiorite 80RR241A. (11) Granodiorite 80RR289A. (12) Granodiorite 80RR290A. (13) Tonalite 80RR240A. (14) Granitic aplite 80RR101A. (15) Granitic aplite 80RR315A. (16) Fine grained tonalite 80RR235B. (17) Tonalite 80RR241B.

	1	2	3	4	5	6	7	8	9	10	11	12	13	14	15	16	17
Plagioclase	40.8	41.2	38.3	37.4	49.3	45.5	50.2	48.2	46.8	55.4	45.7	40.7	64.1	41.9	32.4	56.3	47.0
Quartz	31.1	30.1	24.9	40.8	30.1	34.7	21.0	26.1	30.8	21.0	31.9	32.2	26.3	28.0	29.0	21.3	14.8
K-spar	24.0	23.0	26.2	13.4	15.2	12.5	25.1	20.0	16.7	17.9	17.8	16.9	4.2	28.2	29.7		
Biotite	2.2	3.0	3.7	7.7	4.6	4.7	1.2	4.5	4.1	5.0	6.3	6.5	5.4	1.9	3.7	22.0	19.3
Muscovite	1.9	2.6	6.7	0.7	0.8	2.6	2.5	1.2	1.2	0.7	1.9	3.3			5.2		
Hornblende																	14.8
Accessories	tr	tr	0.2	tr	tr	tr	tr	tr	0.2	tr	0.2	0.4	tr	tr	tr	0.4	4.2
	100.0	99.9	100.0	100.0	100.0	100.0	100.0	100.0	99.8	100.0	100.0	100.0	100.0	100.0	100.0	100.0	100.1

Table 12.--Modes in the Blodgett Mountain quadrangle (HM6)

(1) Granite 80RR013A. (2) Granite 80RR014A. (3) Granite 80RR046B. (4) Granite 80RR248A. (5) Granite 80RR280A. (6) Granite 80RR285A. (7) Granite 80RR287A. (8) Granite 80RR309A. (9) Granite 80RR309E. (10) Granite 80RR311A. (11) Granite 80RR314A. (12) Granite 80RR330A. (13) Granite 80RR334A. (14) Granodiorite 80RR010A. (15) Granodiorite 80RR012A. (16) Granodiorite 80RR040A. (17) Granodiorite 80RR042A. (18) Granodiorite 80RR043A. (19) Granodiorite 80RR044A. (20) Granodiorite 80RR047A. (21) Granodiorite 80RR229B. (22) Granodiorite 80RR232A. (23) Granodiorite 80RR286A. (24) Granodiorite 80RR288A. (25) Granodiorite 80RR307A. (26) Granodiorite 80RR308B. (27) Granodiorite 80RR330B. (28) Granodiorite 80RR336A. (29) Granodiorite 80RR339A. (30) Anorthosite 80RR045A. (31) Orbicular anorthosite 80RR046A. (32) Quartz anorthosite 80RR231B. (33) Quartz anorthosite 80RR232H. (34) Anorthosite 80RR282A. (35) Fine-grained granite 80RR307B. (36) Fine-grained granodiorite 80RR281A. (37) Fine-grained granodiorite 80RR287B. (38) Fine-grained tonalite 80RR232B. (39) Fine-grained tonalite 80RR280B. (40) Fine-grained tonalite 80RR282E. (41) Calc-silicate granofels 80RR313A. (42) Tonalite gneiss xenolith 80RR040B in granite. (43) Tonalite gneiss xenolith 80RR312A in granite. (44) Amphibolite xenolith 80RR330E in granite.

	1	2	3	4	5	6	7	8	9	10	11	12	13	14	15	16	17	18	19	20	21	22
Plagioclase	28.9	22.6	17.3	40.2	40.1	38.5	32.9	43.5	28.2	40.9	39.9	38.9	44.7	48.5	37.6	45.5	43.2	44.6	43.4	54.1	46.3	47.8
Quartz	28.0	39.0	25.6	29.3	33.9	26.5	32.7	27.5	31.6	28.7	29.6	26.6	26.5	31.5	39.4	30.0	32.4	26.0	34.9	22.6	28.5	36.1
K-spar	30.7	33.0	51.6	25.1	22.8	27.0	31.2	23.6	30.6	25.0	25.7	33.5	25.3	13.8	16.6	20.0	21.4	22.9	16.3	17.6	19.6	11.0
Biotite	9.3	3.9	4.2	4.0	2.5	3.7	2.7	4.3	5.8	3.7	4.0	0.9	3.5	5.4	4.6	4.1	2.9	5.6	4.5	2.4	4.7	4.3
Muscovite	3.1	1.5	1.3	1.1	0.7	4.2	0.4	0.9	3.9	1.6	0.3			0.9	1.8	0.4		0.9	0.9	2.9	0.8	0.6
Sillimanite																						
Accessories	tr	tr	tr	0.3	tr	tr	tr	0.2	tr	tr	0.5	tr	tr	tr	tr	tr	tr	tr	tr	0.3	tr	tr
	100.0	100.0	100.0	100.0	100.0	100.0	99.9	100.0	100.1	99.9	100.0	99.9	100.0	100.1	100.0	100.0	99.9	100.0	100.0	99.9	99.9	99.8

	23	24	25	26	27	28	29	30	31	32	33	34	35	36	37	38	39	40	41	42	43	44
Plagioclase	46.7	50.0	50.6	51.2	51.1	42.8	44.2	82.2	89.7	83.6	85.4	87.2	41.8	46.7	62.0	65.7	52.8	60.8	33.3	45.3	39.2	61.0
Quartz	31.1	26.8	32.5	30.2	25.9	29.7	29.2	tr	2.6	9.5	10.1		27.4	23.7	18.4	24.5	29.0	22.7	27.9	19.2	28.1	6.4
K-spar	16.9	17.2	12.1	15.5	11.5	18.3	20.9			1.5	1.0	7.8	26.7	19.4	7.3	3.7	4.0	4.3				
Biotite	3.8	5.6	4.1	3.1	11.3	5.6	4.6	1.9	7.7	4.6	3.0	4.0	3.2	10.0	11.4	5.4	13.1	11.2		28.1	28.9	4.9
Muscovite	1.4	0.3	0.6			3.1	1.2	12.0		0.8	0.5	0.8	1.0		0.8	0.6	0.4					
Sillimanite								3.9														
Calcite																						
Actinolite																			36.2			
Garnet																			0.4			
Hornblende																				6.5		27.3
Accessories	tr	tr	tr	tr	0.2	0.4	tr	tr	tr	tr	tr	0.3	tr	0.2	tr	tr	0.8	1.0	2.1	1.0	3.7	0.4
	99.9	99.9	99.9	100.0	100.0	99.9	100.1	99.9	100.0	100.0	100.0	100.1	100.1	100.0	99.9	99.9	100.1	100.0	99.9	100.1	99.9	100.0

Table 13.--Modes in the Tenmile Lake quadrangle (HM7)

(1) Granite 80RR048A. (2) Granite 80RR048E. (3) Granite 80RR048G. (4) Granite 80RR051A. (5) Granite 80RR159A. (6) Granite 80RR161A. (7) Granite 80RR162A. (8) Granite 80RR165A. (9) Granite 80RR166A. (10) Granite 80RR249A. (11) Granite 80RR318A. (12) Granite 80RR320A. (13) Granite 80RR322A. (14) Granite 80RR323A. (15) Granite 80RR324A. (16) Granite 80RR325F. (17) Granite 80RR327A. (18) Granite 80RR328A. (19) Granite 80RR340A. (20) Granite 80RR343A. (21) Granodiorite 80RR049A. (22) Granodiorite 80RR055A. (23) Granodiorite 80RR155A. (24) Granodiorite 80RR157A. (25) Granodiorite 80RR163A. (26) Granodiorite 80RR317A. (27) Granodiorite 80RR341A. (28) Granodiorite 80RR344A. (29) Granodiorite 80RR345A. (30) Granodiorite 80RR346A. (31) Granodiorite 80RR347A. (32) Fine-grained granodiorite 80RR348A. (33) Tonalite 80RR340E. (34) Granitic alaskite 80RR048F. (35) Fine-grained granodiorite 80RR325A. (36) Blastomylonitic granodiorite 80RR325B. (37) Biotite tonalite 80RR325E. (38) Calc-silicate gneiss 80RR318E. (39) Tonalite gneiss xenolith 80RR323B. (40) Anorthosite 80RR340F.

	1	2	3	4	5	6	7	8	9	10	11	12	13	14	15	16	17	18	19	20
Plagioclase	27.6	33.6	33.4	37.6	42.2	45.5	28.4	36.3	37.4	33.6	34.6	32.7	42.5	32.6	38.9	39.1	45.0	42.0	39.2	41.3
Quartz	29.9	39.3	21.6	36.6	27.3	23.3	31.4	27.2	31.9	35.4	28.7	30.4	24.6	21.7	24.6	32.3	25.6	28.5	25.1	26.1
K-spar	31.8	21.8	40.2	24.2	24.7	26.1	35.9	29.2	26.4	28.9	31.8	33.8	28.5	36.2	33.7	22.7	24.6	26.3	31.7	28.1
Biotite	8.9	4.0	4.5	1.3	4.4	4.9	3.9	5.2	3.6	1.1	3.8	2.4	2.8	6.0	2.4	5.1	4.5	3.2	3.3	4.3
Muscovite	1.7	1.0	0.2	0.4	0.9		0.2	1.6	0.5	0.9	0.7	0.6	1.1	2.5		0.6			0.4	0.2
Accessories	0.2	0.2	tr	tr	0.5	0.2	0.2	0.4	0.2	tr	0.4	0.2	0.5	0.8	0.2	0.2	0.3	tr	0.4	tr
	100.1	99.9	99.9	100.1	100.0	100.0	100.0	99.9	100.0	99.9	100.0	100.1	100.0	99.8	99.8	100.0	100.0	100.0	100.1	100.0

	21	22	23	24	25	26	27	28	29	30	31	32	33	34	35	36	37	38	39	40
Plagioclase	47.4	43.7	50.0	52.9	48.0	43.3	49.2	46.4	55.6	52.0	42.9	34.1	64.5	29.6	47.2	45.2	63.4	15.2	57.2	87.2
Quartz	27.5	25.8	22.6	24.7	32.6	34.1	22.4	24.2	19.6	20.7	30.3	31.8	24.5	33.8	24.5	30.3	16.2	65.4	21.0	
K-spar	21.0	23.4	22.2	15.3	14.6	16.7	22.0	24.4	18.6	21.6	22.6	15.0	4.0	29.2	24.5	21.8	1.0			7.8
Biotite	4.1	6.6	3.5	6.1	4.6	5.4	4.9	4.4	5.2	3.6	2.3	17.3	6.9	0.5	3.8	2.3	17.6		20.6	4.0
Muscovite			0.4		0.2		1.1	0.2	0.4	1.6	1.0	1.8		6.9		0.4	1.0		0.9	0.8
Tremolite																		18.6		
Accessories	tr	0.4	1.2	0.9	tr	0.5	0.4	0.4	0.4	0.4	0.9	tr	tr	tr	tr	tr	0.7	0.8	0.3	0.3
	100.0	99.9	99.9	99.9	100.0	100.0	100.0	100.0	99.8	99.9	100.0	100.0	99.9	100.0	100.0	100.0	99.9	100.0	100.0	100.1

Table 14.--Modes in the Printz Ridge quadrangle (HN6)

(1) Granite 80RR019A. (2) Granite 80RR021A. (3) Granite 80RR024A. (4) Granite 80RR028A. (5) Granite 80RR031A. (6) Granite 80RR036A. (7) Granite 80RR039A. (8) Granite 80RR328E. (9) Granite 80RR329A. (10) Granodiorite 80RR017A. (11) Granodiorite 80RR022A. (12) Granodiorite 80RR023A. (13) Granodiorite 80RR025A. (14) Granodiorite 80RR026A. (15) Granodiorite 80RR029A. (16) Granodiorite 80RR030A. (17) Granodiorite 80RR030E. (18) Granodiorite 80RR031E. (19) Granodiorite 80RR032A. (20) Granodiorite 80RR035A. (21) Granodioritic alaskite 80RR035B. (22) Granodiorite 80RR038A. (23) Granodiorite 80RR225A. (24) Granodiorite 80RR227A. (25) Granodiorite 80RR228B. (26) Granodiorite 80RR328A. (27) Quartz diorite 80RR018A. (28) Quartz diorite 80RR020A. (29) Fine-grained biotite granodiorite 80RR028A. (30) Granodiorite xenolith in granite 80RR030B. (31) Granodiorite gneiss xenolith 80RR036B in granite. (32) Tonalite gneiss xenolith 80RR031B in granite. (33) Tonalite gneiss 80RR036E. (34) Tonalite gneiss xenolith 80RR037A in granite. (35) Quartz diorite xenoliths 80RR017B in granite. (36) Quartz-biotite-bytownite schist xenolith in granodiorite 80RR328B.

	1	2	3	4	5	6	7	8	9	10	11	12	13	14	15	16	17	18
Plagioclase	30.3	34.6	39.8	34.4	32.8	30.8	32.9	36.3	45.0	49.4	47.5	41.3	43.6	44.2	46.7	34.8	41.4	36.1
Quartz	30.6	40.7	28.4	39.6	38.9	35.6	35.4	29.4	24.3	30.1	30.9	38.7	16.5	26.6	28.9	39.3	33.3	35.5
K-spar	37.1	21.0	24.9	19.4	20.1	27.1	24.5	30.6	22.2	15.6	9.5	15.1	6.6	23.4	14.6	18.6	16.7	19.1
Biotite	2.0	3.6	4.3	4.0	5.2	6.1	4.1	3.6	5.7	4.3	8.3	2.8	20.2	5.2	5.1	2.8	5.7	6.1
Muscovite			2.2	2.6	2.6	0.2	3.1		2.9	0.6	3.5	2.1		0.6	4.7	4.3	2.3	3.2
Hornblende													9.4					
Accessories	tr	tr	0.4	tr	0.4	0.2	tr	tr	tr	tr	0.2	tr	3.7	tr	tr	0.2	0.5	tr
	100.0	99.9	100.0	100.0	100.0	100.0	100.0	99.9	100.0	100.0	99.9	100.0	100.0	100.0	100.0	100.0	99.9	100.0

	19	20	21	22	23	24	25	26	27	28	29	30	31	32	33	34	35	36
Plagioclase	48.4	53.7	32.2	50.3	45.2	49.1	41.3	49.1	54.1	63.9	41.6	41.3	41.7	52.2	67.3	58.7	49.8	50.4
Quartz	29.8	20.6	48.9	22.1	31.6	32.6	27.6	29.1	9.6	6.1	34.4	26.4	35.8	14.4	22.8	34.3	9.9	14.6
K-spar	13.1	19.0	10.1	17.0	11.1	9.2	22.0	12.2		0.7	5.9	20.0	10.0		5.1	2.3		0.4
Biotite	4.5	5.0	2.9	8.0	7.0	6.2	6.2	8.7	19.2	27.2	18.1	8.5	12.5	25.8	4.6	4.6	28.1	34.0
Muscovite	3.8	1.4	5.8	2.3	4.7	2.7	2.7					3.0			0.2			
Hornblende									14.5					7.6			10.3	
Accessories	0.2	0.2	tr	0.3	0.4	0.2	0.2	0.9	2.7	2.0	tr	0.8	tr	tr	tr	tr	2.0	0.8
	99.8	99.9	99.9	100.0	100.0	100.0	100.0	100.0	100.1	99.9	100.0	100.0	100.0	100.0	100.0	99.9	100.1	100.2

Table 15.--Modes in the Ward Mountain quadrangle (HN7)

(1) Granite 80RR009A. (2) Granite 80RR033A. (3) Granite 80RR060A. (4) Granite 80RR066A. (5) Granite 80RR107A. (6) Granite 80RR109A. (7) Granite 80RR126B. (8) Granite 80RR127A. (9) Granite 80RR127B. (10) Granite 80RR129A. (11) Granite 80RR223A. (12) Granodiorite 80RR005A. (13) Granodiorite 80RR006A. (14) Granodiorite 80RR007A. (15) Granodiorite 80RR008A. (16) Granodiorite 80RR059A. (17) Granodiorite 80RR126A. (18) Granodiorite 80RR127F. (19) Granodiorite 80RR222A. (20) Granodiorite 80RR224A. (21) Granodiorite 80RR252A. (22) Tonalite 80RR128A. (23) Granodioritic gneiss xenolith 80RR008B in granodiorite. (24) Fine-grained granite 80RR222B. (25) Quartz diorite gneiss xenolith 80RR005B in granodiorite. (26) Quartz-diorite schist xenolith 80RR033B in granite. (27) Quartz-diorite xenolith 80RR106A in granite. (28) Plagioclase-biotite quartzite xenolith in granodiorite.

	1	2	3	4	5	6	7	8	9	10	11	12	13	14	15	16	17	18	19	20	21	22	23	24	25	26	27	28
Plagioclase	26.9	33.6	37.8	37.7	40.6	39.4	33.9	40.3	32.4	26.3	36.3	44.7	42.8	41.9	51.7	43.5	49.4	50.4	42.2	44.9	49.2	64.5	36.7	40.4	46.7	52.5	49.5	18.0
Quartz	41.7	38.3	26.4	26.5	21.0	30.1	35.2	31.4	31.8	40.6	24.6	31.4	29.9	29.0	27.0	32.7	24.8	30.2	32.4	31.4	29.8	25.9	30.0	24.8	27.5	7.1	21.0	52.0
K-spar	23.0	19.4	31.5	31.7	31.1	22.2	23.0	22.4	24.0	28.6	35.1	18.0	15.6	9.5	13.6	19.2	20.6	13.9	15.1	20.0	17.7	4.6	5.6	27.5				4.0
Biotite	7.2	5.4	3.6	3.0	5.5	4.8	2.1	4.5	10.7	4.3	2.5	5.9	11.4	13.7	6.1	3.6	3.1	4.5	4.4	2.7	2.3	3.5	26.2	5.7	24.0	30.4	22.8	22.0
Muscovite	0.8	3.3	0.3	0.2	1.2	2.8	5.2	1.2	0.3		1.0				1.1	1.0	1.1	1.0	5.3	0.2	1.0	1.3		1.1				4.0
Hornblende														3.7											tr	8.8	4.8	
Accessories	0.2	tr	0.3	0.9	0.7	0.6	0.7	0.2	0.8	0.2	0.4	tr	0.3	2.1	0.4	tr	0.9	tr	0.4	0.7	tr	0.2	1.5	0.4	1.8	1.2	1.9	tr
	99.8	100.0	99.9	100.0	100.1	99.9	100.1	100.0	100.0	100.0	99.9	100.0	100.0	99.9	99.9	100.0	99.9	100.0	99.8	99.9	100.0	100.0	100.0	99.9	100.0	100.0	100.0	100.0

Quartz, 21% to 41% of the mode, occurs partly in equant, 1 to 4 mm grains, and partly in flattened, 1x3 to 2x6 mm grains; most of the quartz grains are aggregates of 0.3 to 0.7 mm, strain-free subgrains. Some of the grain aggregates in the western part of the eastern sector are deformed in 1x4 mm rods in a strong lineation; rods are flattened so that their ends have a tapered appearance. Some of the large, flattened quartz grains have few or no subgrains; their association with blastomylonite zones makes it clear that they have been annealed late in the blastomylonite event. Contained with some of the large, platy quartz grains are inclusions of 0.2 mm, lepidoblastic biotite flakes, apparently remnants from blastomylonitic shear. Blastomylonite zones contain 0.3 mm, strain-free quartz where commingled with feldspar and mica of like size. Blastomylonite zones terminate at large quartz grains, and only the 0.2 mm biotite inclusions in quartz mark the former course of blastomylonite zones. Some of the large quartz grains in the eastern part of the eastern sector (Bitterroot gneissic front) are drawn out in ribbons 0.5 mm wide and more than 24 mm long, of "flattened" single grains 0.5x1 mm in size in curving trains along the course of former blastomylonite zones. Some segregation of quartz would seem to be involved.

In a few rocks, quartz and other minerals are cut by 0.4 mm zones of strong cataclastic shear, filled with flattened 0.05 mm grains of quartz and feldspar, sutured and with strong undulatory extinction. These are due to the mylonitic shears seen at the outcrops.

K-feldspar (19% to 52% in the mode) occurs in 1 to 5 mm grains; in part of the gneiss, it is in flattened 1.4 to 5.16 mm lenticles. In the western and central parts of the eastern subarea the K-feldspar is partly orthoclase, partly submicroscopically twinned microcline, and partly microcline. In the eastern part, it is entirely microcline. The variety of K-feldspar is independent of the degree of flattening. K-feldspar is partly in 0.5 mm, strain-free subgrains, more common in flattened grains than otherwise. Most K-feldspar grains include plagioclase, but none of them include quartz. Flattening and rodding become more pronounced in the Bitterroot frontal gneiss zone (Subarea C), than in the areas to the west. In a typical situation, the grains occur in 2x3x6 mm rods, lineated in the 290 az direction. Some of these rods contain quartz-filled extension fractures perpendicular to their long axes. In some of the rocks, microcline is cut by zones of blastomylonitic shear and reduced to strain-free, 0.3 mm, granoblastic grains.

Biotite occurs in 0.5 to 1 mm grains, from 1% to 9% of the mode, more or less lepidoblastic, except that it is randomly oriented in about half the rocks of the western part of the eastern sector. Minor pennine alteration is ubiquitous. Biotite is reduced to 0.2 mm flakes in blastomylonite zones. Some grains are broken in polygonal arcs in curving blastomylonite zones, others are still bent in curved arcs, and still others show partial polygonal arcs, with some grain segments still bent and others annealed to strain-free crystal segments tangential to the arc. Muscovite occurs in 0.5 to 2 mm grains, from zero to 7% in the mode and absent in several rocks. Its occurrence is much like that of biotite. Accessory minerals listed roughly in their order of decreasing abundance include zircon, magnetite, apatite, thorite, allanite, baddeleyite, epidote, and monazite. Magnetite is far less abundant than in rocks of the western and central sectors.

Granodiorite.

Granodiorite (table 11, modes 4 to 12; table 12, modes 14 to 29; table 13, modes 21 to to 31; table 14, modes 10 to 20 and 22 to 26; and table 15, modes 12 to 21) contains from 36% to 56% plagioclase (An_{20} to An_{36}) in the mode, in unzoned, equant, subhedral, stubby, 1.5 to 4 mm prismatic to lenticular grains up to 2x4 mm parallel to foliation. Relicts of normal zoning are rare; calcic cores up to An_{40} are found in a few grains. Untwinned grains are common in rocks with more-sodic plagioclase. In a number of rocks, plagioclase is myrmekitic or has developed albite rims against K-feldspar. Some plagioclase grains include biotite or fine, fibrolitic sillimanite. Some grains are cut by extension fractures at a high angle to the external foliation, filled with quartz-K-feldspar-biotite-pennine, in various combinations. Part of the plagioclase has been converted to 0.5 mm, pavement-like, strain-free subgrains. Some of the large, lenticular grains are free of subgrains; perhaps they adjusted to flattening without breaking in subgrains, possibly due to favorable orientations that allowed cleavage-plane slip to predominate. In some of the more gneissic granodiorite, strings of equant plagioclase grains lend an aspect of seeming feldspar rodding. Plagioclase in a number of rocks is cut by 2 mm-wide blastomylonitic shear zones in which 0.4 mm, granoblastic strain-free plagioclase grains occur, of the same composition as larger grains in the rock. Some plagioclase is cut by thin (0.1 mm) mylonitic shears coated with sericite and very fine biotite and in which quartz shows undulatory extinction in 0.04 mm grains. These shears curve about very irregularly in curves with wave length-amplitude of about 0.7 mm. This is probably responsible for microgrooving seen on mylonitic shears in the outcrop. They cut across earlier shears of blastomylonitic character.

Quartz (16% to 41% in the mode) occurs in equant, 1 to 4 mm grains in some rocks, but is mostly in 1x2 to 1x4 mm, flattened grains. Most quartz is broken in 0.5 to 0.7 mm, strain-free subgrains; some of it is largely free of subgrains. The quartz in a few rocks occurs in 1x4 mm rods of quartz in a strong lineation. Some rods also contain 0.7 mm, strain-free subgrains. Blastomylonite shears cut quartz in many of the rocks, up to 2 mm thick, in which 0.2 to 0.4 mm, strain-free grains occur, of commingled quartz, feldspar and mica. In certain of the rocks, these zones terminate at large (up to 1x4 mm) tabular grains of quartz, single grains free of subgrains, in which tiny inclusions of blastomylonitic mica yet persist. Some of the quartz is in ribbons or rods more than 10 mm long, of several platy grains of quartz. Rodding appears to be most pronounced near ductile shears or thrusts also of blastomylonitic character. Quartz in some of the rocks is cut by 0.1 mm mylonite zones in which quartz occurs in 0.04 mm, strained particles.

K-feldspar (6% to 25% in the mode) occurs partly as equant, 1 to 5 mm grains, and partly in flattened 2x4 to 6x10 mm grains. K-feldspar occurs partly as orthoclase, partly as submicroscopically twinned microcline, and partly as microcline, except that only microcline occurs in the gneiss near to and in the Bitterroot front. Microcline generally includes plagioclase but not quartz. Some 0.7 mm, strain-free subgrains are found in equant K-feldspar, but are more strongly developed in flattened grains. The microcline in one rock is cut by quartz-filled extension fractures. Blastomylonitic shears reduce K-feldspar to 0.2 to 0.3 mm, strain-free grains in several rocks.

Biotite (1% to 20% in the mode) occurs in 0.3 to 1 mm grains, crudely lepidoblastic in part of the rock and randomly oriented in the rest. Minor pennine alteration is ubiquitous. Fibrolite inclusions occur in the biotite of one granodiorite. In blastomylonite zones, the biotite is near 0.2 mm, and in later mylonite zones, 0.02 mm. Muscovite (zero to 6.7%; absent in several rocks) occurs in 0.5 to 1 mm grains. Its occurrence is much like that for biotite; fibrolite inclusions occur in muscovite of a few rocks. The accessory minerals seen, in their approximate order of decreasing abundance, include zircon, apatite, thorite, magnetite, monazite, baddeleyite, allanite, and sphene. Magnetite is far less abundant than in the western areas, and total accessories are less. But the picture is still more complicated in detail; averages of all the modes for both granite and granodiorite show 0.6% accessories in the western sector, 0.1% accessories in the central sector, and 0.4% in the eastern sector.

Among the granodioritic rocks is a blastomylonite developed from granodiorite (table 13, mode 27). It is in a zone of ductile shear 8 cm thick that is well exposed in a cirque headwall. It erodes at a different rate than the massive granitic gneiss, thereby producing a step in the topography. By means of such steps combined with sporadic exposure of blastomylonitic rock, ductile shears on three principal surfaces spaced at about 300 m intervals vertically were mapped in the Tenmile Lake quadrangle, extending over distances of several kilometers. These ductile shear surfaces dip west at shallow angles and contain a fine streaky lineation trending about 285° az.

The average grain size of rock within the ductile shear zone is near 0.3 mm. All quartz and feldspar grains are granoblastic and strain-free. Plagioclase is unzoned, near An_{22}. Microcline is submicroscopically twinned, and quartz occurs partly in 0.2 mm grains and partly in 0.3x5 mm ribbons; individual quartz grains in the ribbons are 0.3x1 mm. Micas are lepidoblastic; accessories include zircon, apatite, magnetite, and allanite.

Tonalite.

Tonalite occurs in several ways in the eastern sector. One tonalite, near Big Sand Creek in the Jeanette Mountain quadrangle, is light-colored and could not be distinguished from granite or granodiorite in the field; its mode is in table 11 (mode 13). Plagioclase (An_{22}) is in unzoned grains, partly broken in 0.3 mm granoblastic grains in diffuse 0.5 mm thick blastomylonite zones. The subgrains show some sutured boundaries and undulatory extinction. Microcline occurs in 0.5 mm grains, broken to 0.2 mm grains in blastomylonite zones. Biotite is in 1.5 mm flakes, locally lepidoblastic in 0.3 mm flakes in blastomylonite zones, and partly altered to pennine throughout. Accessories seen are zircon and apatite.

Another dark tonalite in the Jeanette Mountain quadrangle (table 11, mode 17) is in a 30 m-thick, concordant sheet at Diablo Mountain, metamorphosed in about the same degree as the enclosing gneiss, and cut by pegmatite, aplite, and quartz dikes like those in the granite. It is rather heavy and is likely the source for the heavy black minerals in Duck Creek to the north and in other creeks in the area. This tonalite turns into quartz diorite farther west, where the intrusive unit is thicker.

Plagioclase (An_{45}) in the tonalite is in 2 mm, unzoned, subhedral subparallel to foliation, reduced to 0.2 mm, granoblastic (An_{37}) in blastomylonite zones. Hornblende (0.7 mm) and biotite (0.4 mm) are reduced to 0.1 mm grains in blastomylonite zones. Quartz occurs in 0.2 mm, strain-free grains in the matrix. Accessories seen include magnetite (abundant), zircon, and sphene; there is a little alteration of magnetite to hematite. The accessory mineral content (4.2%) is high for rocks in the central and eastern batholith.

Along the arete between upper Roaring Lion Creek and upper Tenmile Creek, in the Tenmile Lake quadrangle, minor tonalite occurs in 1 cm to 20 cm sheets and discontinuous lenses along the primary flow foliation in the granitic rocks. These sheets extend for many meters, passing laterally into biotite schlieren with a distinctive kind of "popcorn" texture due to blocky feldspar grains, not seen in schlieren of other origins. Secondary flow foliation crosses the primary flow foliation at various angles, affecting both granite and interlaminated tonalite. Two rocks from the tonalite bands were studied (table 13, modes 33 and 37).

Plagioclase in the tonalite (64% in the mode) occurs in 2 mm, unzoned, subhedral, equant grains (An_{22} to An_{26}). K-feldspar and quartz are both subordinated; biotite constitutes 7% to 17% in the mode. Accessories include magnetite, zircon, and apatite.

Tonalite was sampled at one point along lower Roaring Lion Creek, the only occurrence found in the Ward Mountain quadrangle; the stained slab shows flattened feldspar, not readily apparent in thin section. Plagioclase (An_{25}) occurs in 3 mm, equant grains, unzoned and partly broken in 1 mm, strain-free, granoblastic subgrains. Some crystals are cut by extension fractures up to 0.2 mm thick, filled with quartz-muscovite-pennine. Blastomylonite zones up to 1 mm thick contain 0.3 mm, granoblastic, strain-free grains of plagioclase. Quartz occurs in irregular, 2 mm patches much segmented in strain-free, 0.7 mm subgrains. Microcline occurs in 21 mm grains, segmented in 0.5 mm, strain-free subgrains. Biotite and muscovite occur in 0.5 mm flakes; biotite is a bit altered to pennine. Magnetite is the only accessory seen.

Quartz diorite.

One or more small bodies of more or less primary flow-foliated quartz diorite are exposed in the north valley wall of Mill Creek, southeast of Castle Crag, in the Printz Ridge quadrangle. Two specimens were studied (table 14 modes 27 and 28). Plagioclase (An_{35}) occurs in 2 mm, mostly unzoned, prismatic grains; a few relicts of normal zoning persist. Quartz is minor in 0.5 mm grains free of any subgrains. Biotite is important in both rocks, and hornblende in one of them, in 1 mm grains. Accessories include magnetite, apatite, and sphene.

Anorthosite I.

Anorthosite (table 12, modes 30 to 33) was found at three locations in the Blodgett Mountain quadrangle; the rock resembles granodiorite closely in physical appearance and was not recognized as anorthosite until analyzed in the laboratory. Its relations to the granite and granodiorite are not known--whether xenoliths or synplutonic intrusions, or later intrusion. We suspect synplutonic emplacement.

Plagioclase in the anorthosite occurs in 4 to 8 mm grains, unzoned of composition An_{27} to An_{29}. These grains are partly converted to granoblastic, pavement-textured grains 0.5 to 1 mm in diameter. Quartz occurs in irregular 2 mm grains and contains a few strain-free subgrains 0.5 mm in diameter. Microcline occurs in one of the anorthosites in 1 mm aggregates of 0.5 mm subgrains with approximately 120° triple junctions. Biotite occurs in 0.5 mm flakes, with a bit of pennine alteration. Muscovite occurs as 2 mm grains in a schlieren zone in one anorthosite; sillimanite is abundant in the schlieren zone. One anorthosite contains no muscovite. A little zircon was seen in one anorthosite; no accessory minerals were seen in the others.

Xenoliths.

The following types of xenoliths were sampled: granodioritic gneiss, biotite-quartz-diorite gneiss, hornblende-quartz-diorite gneiss, quartzite, tonalite gneiss, and calc-silicate gneiss. Modes are given in table 13, modes 32, 38, and 39; and in table 15, modes 25 to 28. The petrography closely resembles that given above for comparable rocks.

Fine-grained dikes.

Dikes of fine-grained granite intrude the granitic rocks all across the eastern sector, except in Subarea B, both along and across the secondary foliation; two modes are given, in table 12, mode 35, and table 15, mode 24. Plagioclase (An_{23} to An_{25}) occurs in 0.3 to 0.5 mm, mostly unzoned, equant to prismatic grains. One rock has mostly zoned plagioclase (cores An_{28} to rims An_{20}). Quartz occurs as irregular, 0.5 mm grains to platy 0.3x0.5 mm, flattened grains, parallel to foliation, some with and some without subgrains. Microcline, submicroscopically twinned, is in irregular, 0.5 mm grains to 0.5x2 mm, flattened grains, parallel to foliation, and partly of 0.3 mm, strain-free subgrains. Biotite and muscovite (absent in some rocks) are lepidoblastic in 0.3 to 0.5 mm grains. Accessory minerals seen include zircon, apatite, magnetite, and sphene.

Dikes of fine-grained granodiorite intrude the granitic rocks all across the eastern sector, except in Subarea B, both along and across the foliation (table 12, modes 36 and 37; table 13, mode 35; and table 14, mode 29). One fine-grained granodiorite dike cuts the foliation of the granitic gneiss. Flow foliation is parallel to its walls and highly discordant to the foliation of the enclosing gneiss; the fine-grained granodiorite contains xenoliths of the gneissic granite. Both intrusive units are cut by vertical, northeast-trending shears with nearly horizontal, chlorite-patterned slickensides. Still younger is a 0.7 mm-thick microbreccia. In another dike, foliation in the granitic gneiss cuts across and overprints the fabric of the fine-grained granodiorite. Plagioclase (An_{10} to An_{27}) occurs in 0.5 to 1.5 mm, stubby prismatic, mostly unzoned crystals; some with relict normal zoning and many with 0.5 mm, platy granoblastic, strain-free subgrains, or in 0.7x1.5 mm, flattened aggregates of 0.5 mm, strain-free subgrains. Quartz and orthoclase (microcline in some of the rocks) occur in 0.4x0.8 mm flattened grains parallel to the foliation. Biotite partly altered to pennine and muscovite (in one rock only) occur in 0.3 mm, lepidoblastic grains. Accessories seen include apatite, zircon, allanite, and epidote.

Fine-grained tonalite dikes were seen at several places in the eastern sector (table 11, mode 16; and table 12, modes 38 and 39). Plagioclase (An_{29} to An_{31}) in the tonalite occurs in 0.7 mm, unzoned, equant grains, some with relict normal zoning. Many grains contain 0.5 mm, platy granoblastic, strain-free subgrains. Quartz and microcline are in 0.5 mm grains partly broken in 0.2 mm, strain-free subgrains; some are in flattened 0.5x1.5 mm, flattened aggregates of 0.5 mm subgrains. Some of the flattened grains are single optical elements or grains, free of subgrains, probably a part of the "quartz ribbon" structure. Biotite and muscovite are lepidoblastic in 0.3 to 0.5 mm grains. Accessory minerals seen are zircon, apatite, allanite, and magnetite.

Pegmatite suite.

The fine-grained granite to tonalite dikes are cut by various members of the pegmatite suite, including granitic aplite (table 11, modes 14 and 15) and alaskite (table 13, mode 34). One granitic aplite contains plagioclase (An_{31}) in 0.7 mm, prismatic grains, normally zoned from cores of An_{31} to rims of An_{20}. Quartz occurs in 0.7 mm grains with few subgrains. Microcline (submicroscopically twinned) and orthoclase both occur in the rock. Biotite and muscovite occur in 0.5 mm flakes in a weak preferred orientation. Accessories include zircon and apatite. Another aplite has been deformed and the light minerals flattened (2:1) and lineated (rodded). The average grain size is 0.5 mm. Plagioclase (An_{23}) is unzoned, subhedral, equant to flattened, and mostly untwinned. Microcline is very finely, almost submicroscopically, twinned. Quartz occurs in 0.5x1 mm ovoids, partly of smaller, strain-free subgrains. Biotite is in 0.3 mm lepidoblastic grains partly altered to pennine. Zircon is the sole accessory mineral seen.

Anorthosite II.

A 16 m volcanic neck in the Blodgett Mountain quadrangle contains miarolitic intrusive rock identified as anorthosite (table 12, mode 34). The plagioclase (An_{37}) is in stubby, prismatic, unzoned grains with mild sericite and clay alteration. A few 0.3 mm grains of quartz occur. A little sanidine, intimately intergrown with plagioclase in 0.3 mm grains, occurs about miarolitic cavities. Biotite occurs in 0.5 mm grains. The pipe is cut by a fine-grained, low-angle, blastomylonite shear zone 10 m thick. The shear zone is filled with 0.5 mm, pavement-textured, unzoned, strain-free, plagioclase grains (An_{37}), with clay and sericite alteration.

In the Tenmile Lake quadrangle, a 1 m anorthosite dike (table 13, mode 40) was injected into the gneiss along a 035° az, 65° SE fracture, altering the rock strongly for 5 to 10 cm on each wall so that a kind of cavernous weathering results. Plagioclase (An_{36}) is major, in 3 mm, unzoned grains strongly altered to sericite and clay. Minor sanidine and biotite occur as well as traces of muscovite.

GENERAL STRUCTURE

A compilation of average flow directions in the granitic rocks of the project area is given in figure 72. The flow trends include those both for primary and secondary flow features, as well as for blastomylonite where it has developed. The flow trends form a fan-shaped array opening out to the southeast, within the field of secondary strain, and stand more or less perpendicular to fractures that

appear to have originated as tensional openings roughly at right angles to the flow lines. Flow lines plunge northwesterly at about 30° over most of the area, but become horizontal near the Bitterroot arch, and then plunge at about 30° to the southeast in the Bitterroot gneissic front. This diagram is generalized to omit the local complications of Subarea B in the eastern sector.

Subarea B is compiled in figure 73, which shows the complications in foliation trends near the Bitterroot gneissic front.

The structure section given in figure 74 shows the disposition of secondary flow lineation across the mapped interval. As shown earlier, the intensity of the strain fabric becomes less to the west, and structurally higher in the pluton as shown in the section. The mylonite zone at the eastern margin of the pluton is removed by erosion at its western edge and is not certainly seen again farther west. If it continued farther west, it must have become highly discordant to the secondary flow lineation.

If the arch shown in the section is due wholly to upwarp of the secondary flow lineation, then the batholith thickness would have been 30 km or more prior to arching. The question of the former situation of the mylonite zone to the west becomes a major one.

A mylonite zone about 30 m thick trends north-south and dips shallowly to the west in the Jeanette Mountain quadrangle (fig. 74, quadrangle 7). Further, more detailed mapping should investigate the possibility that this mylonite is the westward continuation of the frontal mylonite. The structural position seems about right. In that case, the mylonite zone appears to be dying out to the west, within the igneous mass.

Evaluating other work in terms of the cross-section given in figure 74, it is notable that Wiswall's proposed base of the batholith (1979) lies to the south of the cross-section, along the trend of the arch. Therefore, the proposal appears to be consistent with the regional structure. On the other hand, the work done by Toth (1981) proposing that the Bear Creek pluton and Cub Creek pluton are exposed at a position near the roof of the batholith seems unlikely; Toth's rocks lie south of the cross section just west of the axis of the arch and therefore deep within the pluton, near its base.

The area affected by secondary strain, that is to say affected by metamorphic core complex processes, is a pie-shaped block, shown in figure 75. Its boundaries are known only approximately, extrapolated between a few known points both on the north and the south.

TERTIARY HYPABYSSAL ROCKS

Tertiary dikes are uncommon to rare; both andesite and quartz latite were seen. The dikes average a 360° az strike and near-vertical dips. We see them as intrusions into tensional openings created in a field of generally horizontal stress oriented 360° az (fig. 76).

Andesite to quartz latite

One andesite(?) dike experienced shear in microbrecciation to mylonitization, so that an ill-defined schistosity developed on 0.3 mm grains of tremolite, biotite, plagioclase, and sericite.

Eight andesite dikes of northeasterly trend were mapped in the western sector; they are free of cataclastic effects. Their average grain size is about 0.4 mm, and they contain brown to green hornblende, plagioclase (An_{35} to An_{55}) and in some of them minor biotite. Three dacite to quartz-latite dikes, also in the western sector, were mapped, trending from NNE to NW. Plagioclase phenocrysts up to 4 mm long have a composition of An_{45}, are partly glomeroporphyritic, and associate with 0.5 mm clusters of biotite and ferrohastingsite. Oscillatory normal zoning is present with up to twelve oscillatory cycles shown. Matrix minerals average about 0.2 mm diameter in roughly equal parts of biotite, plagioclase, K-feldspar, and quartz. All appear to be free of any cataclastic effects.

Rhyolite

Two rhyolite dikes of NW trend were mapped in the western sector. Plagioclase phenocrysts (An_{60}) up to 0.7 mm long, and 0.5 mm biotite and quartz phenocrysts occur in a matrix of 0.02 mm grains of K-feldspar micrographically intergrown with quartz and intermixed plagioclase. No effects of cataclastic strain were seen.

A swarm of NW- to NE-trending rhyolite dikes occurs in the southern part of the central sector (southern McConnell Mountain quadrangle). Two rocks were studied in thin section. Phenocrysts of quartz, sanidine, plagioclase (An_{25}) and biotite are 1 to 2 mm in size. The matrix is a holocrystalline, homogeneous aggregate of 0.03 mm grains of sanidine, quartz, and plagioclase.

TERTIARY (?) GRANODIORITE AND QUARTZ DIORITE

A small swarm of Tertiary (?) granodiorite to quartz-diorite dikes (table 10, modes 41 and 42) occurs in the central sector (Maple Lake Ridge area of the Cedar Ridge quadrangle). Plagioclase occurs in 0.5 mm grains in the granodiorite but is absent in the quartz diorite. Biotite and green hornblende in 0.5 mm grains are parallel to dike-wall rock contacts and define flow directions; muscovite is absent. Accessories include sphene, apatite, allanite, and magnetite. The rocks are free of any cataclastic effects.

PETROLOGY AND STRUCTURE OF THE WALL ROCKS

The calc-silicate gneiss displays a fabric of flow foliation containing steeply plunging, lineated diopside, hornblende, biotite clots and streaks, and quartz rods. Although the fabric relations are not entirely clear as to the relative times of growth of these minerals, there appears to be no problem with the concept of a single recrystallization event apparently required by the single lineation direction of

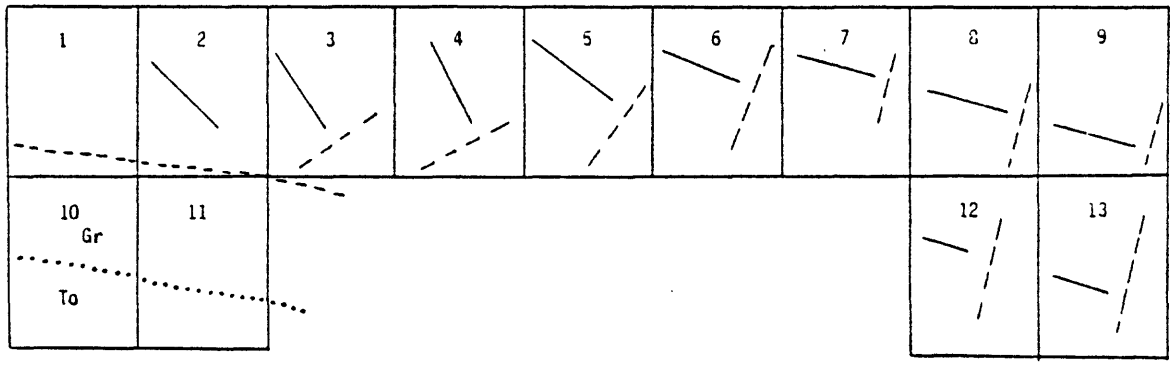

Figure 72.--Average flow directions (shown by solid lines) in granitic rocks in several 7½' quadrangles across the central Bitterroot lobe of the Idaho batholith, west of Hamilton, Mont. The long-dashed lines show the trend of chlorite-coated, microbrecciated shear joints in the several quadrangles, believed to be tension fractures developed initially perpendicular to flow lines and reactivated in younger stress. The dotted line shows the generalized contact between older tonalite (To) of the Bitterroot lobe and granitic rock (Gr). The short-dashed line shows the southern margin of the field of secondary strain. Key to quadrangle names: L. Huckleberry Butte, 2. Greenside Butte, 3. Fish Lake, 4. McConnell Mountain, 5. Hungry Rock, 6. Cedar Ridge, 7. Jeanette Mountain, 8. Blodgett Mountain, 9. Printz Ridge, 10. Chimney Peak, 11. Fenn Mountain, 12. Tenmile lake, 13. Ward Mountain.

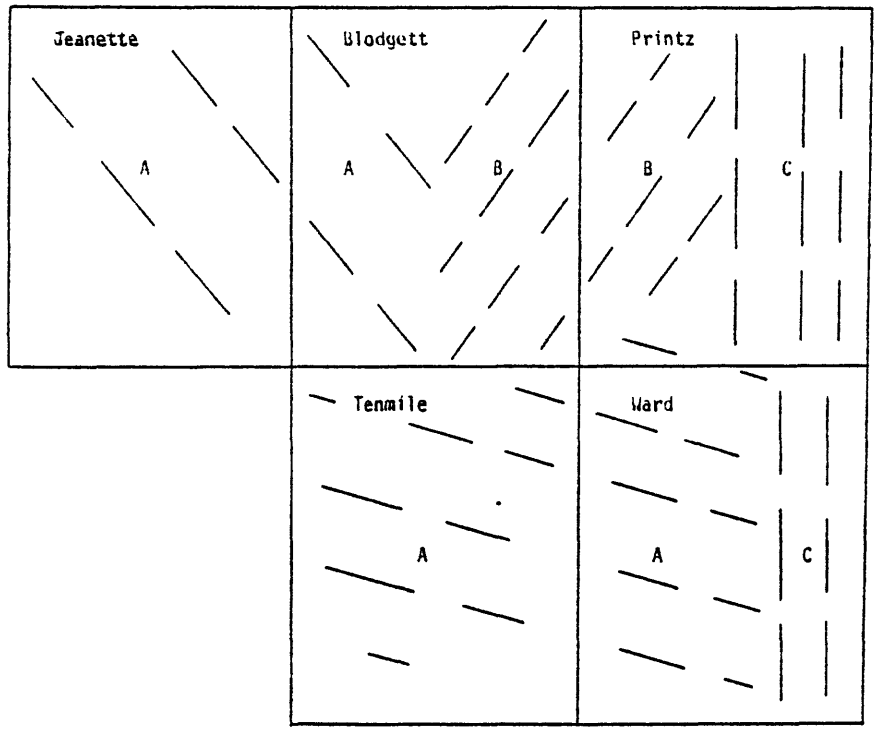

Figure 73.--Foliation trends (dashed lines) in Subareas A, B, and C of the eastern sector, Bitterroot lobe of the Idaho batholith. The trend differences in Subarea A are due to different folia in the axial flow system, all developed in flow along the 290° axis; the lineation trend is the same throughout.

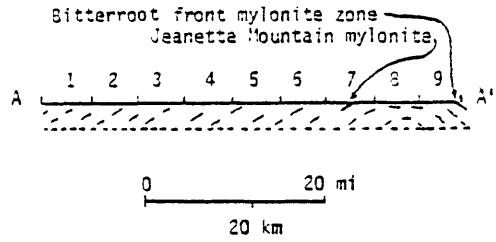

Figure 74.--Diagrammatic structure cross section (85 km long) across the Bitterroot lobe of the Idaho batholith, showing the disposition of secondary flow lineation trending about 290°-110° az, approximately parallel to the plane of the section. Relief is generalized except at the Bitterroot front, where the slope on the mylonite zone is shown approximately. The base of the section is at about 6 km below the surface; data are extrapolated from surface exposures. The base of the batholith likely lies shallower than 6 km below the surface within the arch under the eastern part of the section. Numbers on the section refer to 7½ quadrangles as follows: (1) Huckleberry Butte, (2) Greenside Butte, (3) Fish Lake, (4) McConnell Mountain, (5) Hungry Rock, (6) Cedar Ridge, (7) Jeanette Mountain, (8) Blodgett Mountain, (9) Printz Ridge.

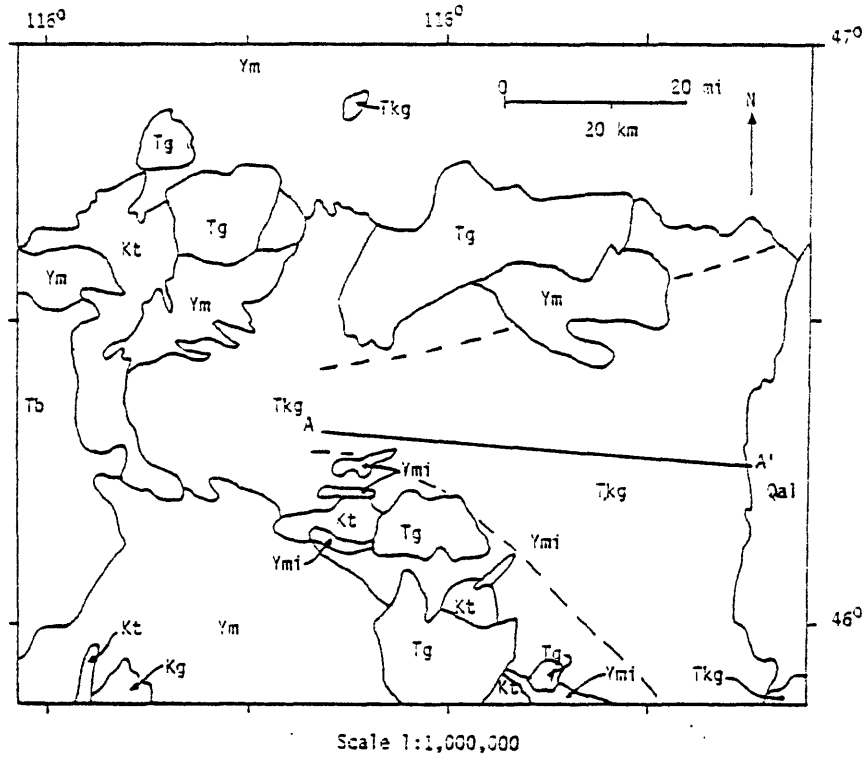

Qal ALLUVIUM (QUATERNARY)
Tb BASALT (MIOCENE)
Tg EPIZONAL GRANITE (EOCENE
Tkg MESOZONAL GRANITIC ROCKS OF THE BITTERROOT LOBE
Kt MESOZONAL TONALITE, DIORITE, AND QUARTZ DIORITE
Kg GRANITIC ROCKS OF THE ATLANTA LOBE OF THE IDAHO BATHOLITH
Ymi MIGMATITE (PROTEROZOIC Y?)
Ym METAMORPHIC ROCK (PROTEROZOIC Y?)

Figure 75.--Generalized geologic map of the Bitterroot lobe of the Idaho batholith, adapted from a project map by M. I. Toth. The dashed lines show the approximate boundaries of the pie-shaped field of secondary strain, that area affected by metamorphic-core-complex phenomena. A-A' is the line of section in Figure 74.

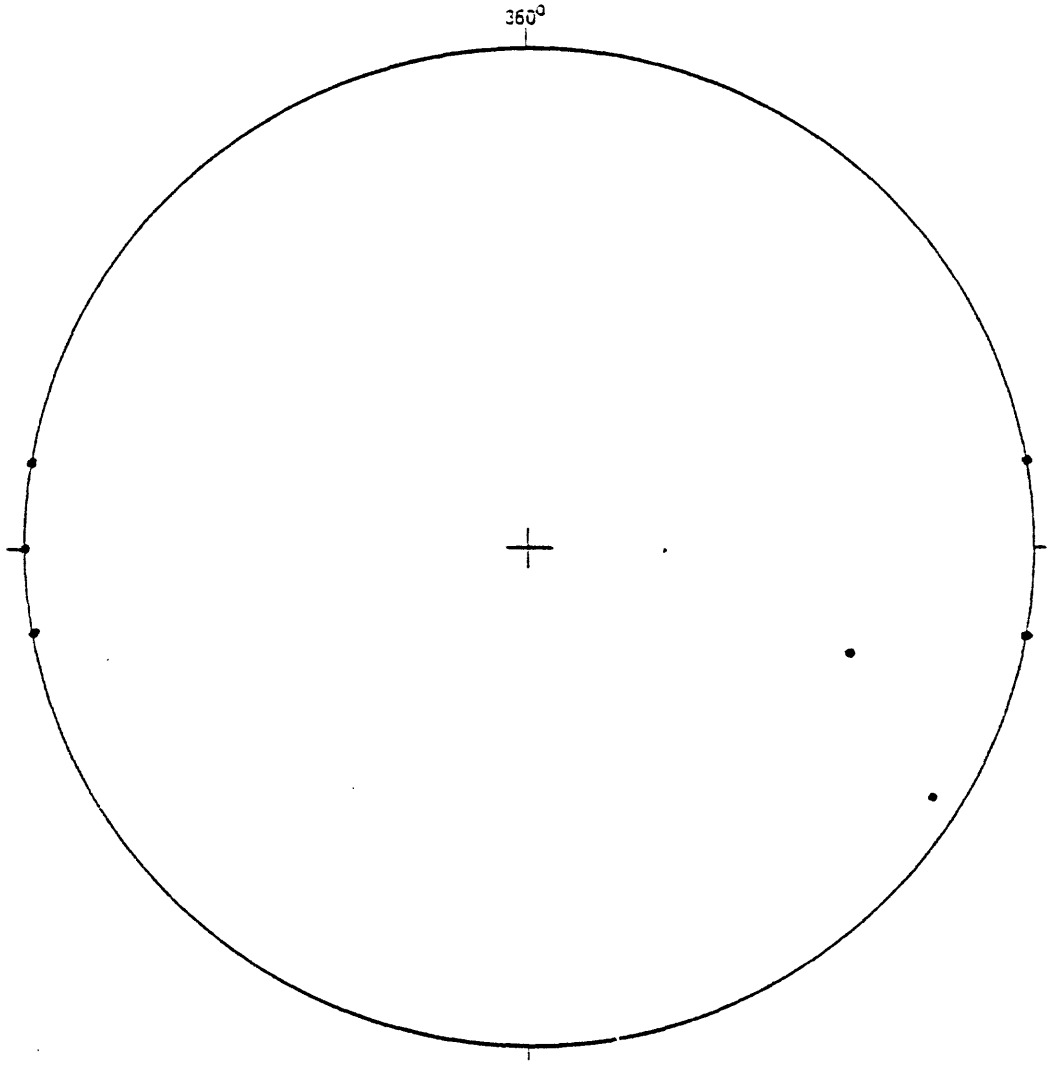

Figure 76.--Poles to hypabyssal dikes in the Fenn Mountain area, western sector of the Bitterroot lobe of the Idaho batholith, west of Hamilton, Mont. Poles plotted on lower hemisphere of Wulff stereonet.

all the minerals present. Any pre-existing metamorphic fabric has apparently been completely destroyed in the latest event.

During the deformation associated with the metamorphism, minor passive-flow folds developed. Their axes plunge steeply and their axial planes parallel the foliation of the enclosing gneiss. The shear sense in these small folds is both clockwise and counterclockwise, more or less randomly through the outcrops. This suggests an orthorhombic symmetry with flattening perpendicular to the A-B plane (foliation).

The parallelism of the mineral lineation and the minor fold axes suggests a common origin. One possibility is that all the linear elements were generated in a horizontal attitude in the flow plane perpendicular to kinematic a, taken as the near-vertical flow direction imposed on the wall rocks of the batholith by the upward-moving magma. In this case, the lineation was rotated toward kinematic a in continuing flow. A second possibility is that the linear elements were generated directly in the kinematic a direction during flow. Available evidence does not permit a choice between these two possibilities. The approach to an axial-orthorhombic symmetry may favor the latter one.

The foliation has been warped into various orientations after the development of the minor folds, perhaps in a field of dying stress. The same steep axes prevail that characterize the minor folds and mineral lineations. Because the stress field must have been the one related throughout to rise of the magma, with some lateral spreading in the upper levels perhaps, we suppose that the vertical folds somehow relate to the vertical flow process and are generated in that vertical flow; salt-stock structure provides an excellent analog. The generation of these late-stage vertical folds supports the latter hypothesis above, that the linear elements were generated directly in the kinematic a direction during flow.

The structure in the tonalitic gneiss resembles strongly that in the calc-silicate gneiss. Thus, the two rocks have been subjected to the same structural history. This requires that the tonalitic gneiss be injected before or during the metamorphism that produced the steeply plunging minor folds and mineral lineation in the rocks. But the fabric does not look metamorphic; rather, it has the appearance of an "intense" sort of primary flow foliation. The feldspar retains much of its igneous form, but in a flow foliation. Zoning is mostly absent, although a few prisms show normal zoning. The texture is closer to hypidiomorphic granular than to crystalloblastic. Therefore, the tonalitic gneiss is a synkinematic intrusion.

The structure in the tonalitic gneiss differs from that in the calc-silicate gneiss only in that the axial planes of the minor folds in the tonalitic gneiss have axial symmetry. This might be accounted for by the assumption that the deformation was less viscous in character in the tonalitic gneiss so that some rotation by swirling of the minor folds was possible.

Lit-par-lit stringers of microcline-free trondhjemite lie along the foliation in the tonalitic gneiss and the calc-silicate gneiss. The similarity of the trondhjemite in the two units suggests that all trondhjemite is of the same age, source, and mode of emplacement. The process is considered to be magmatic injection of late-stage alaskitic material, with more-sodic plagioclase than in the parent tonalite. This appears to be approximately the same age and type of material as that injected in alaskite sheets in the tonalite of the batholith; then came continued folding of the foliation in passive-flow folds with steep axes and axial symmetry consistent with vertical flow. Elongate biotite clots and streaks grew in stretching parallel to the fold axes. The total fabric suggests a single-stage event involving metamorphic recrystallization and igneous injection during near vertical flow. Locally, some late-stage rotation during continuing flow gave rise to crossing flow directions.

Quartzite is exposed along and south of the Selway River. The D_1 fold set in the quartzite is sharply isoclinal as suggested by two small outcrops in which minor folds assigned to D_1 have axial-plane foliation. The varied plunge of the D_1 axes, from near the strike line to the dip line suggests, in the method of Hansen (1971), that younger shear in the plane of foliation has rotated D_1 folds toward the slip line of a younger deformation, D_2. Pegmatite was injected into the D_1 structure at some point in its development; the relation of pegmatite to D_2 structure suggests that the time of pegmatite injection was during D_2. Thus, it is possible that the pegmatite in the D_1 structure was injected during D_2 reactivation. In this case, the D_1 event could pre-date intrusion. Alternatively, the pegmatite injection may be truly synkinematic in D_1. In that case, the D_1 folds represent an early stage of deformation accompanying intrusion, and any older structures have been obliterated.

Folds assigned to D_3 appear to be the youngest in the section; they are of concentric character and of relatively shallow though varied plunge. Moreover, they clearly deform a set of lineations assigned to D_2, the axes of the conical folds and the mineral lineations parallel to them. Only in certain areas can small conical and concentric folds be seen; however, the gross character of the structure leaves little doubt of the relatively large scale of the D_3 fold event in this part of the section. Similarly, large conical folds are probably present.

In order to analyze D_2 structures, it is best to consider them after removal of the D_3 overprint. When the D_3 folding is removed, one sees a near-vertical sequence of metaquartzite along the Selway River. Conical folds with mineral lineation parallel to their axes plunge down the dip of the near-vertical sequence.

In the Elk City area (Reid, 1959), the isoclinal D_1 fold set, with axial-plane foliation, was recumbent prior to younger deformation. Perhaps the D_1 fold set of that region extended into the Fog Mountain-Selway River area, which is only about 30 mi northeast of the Elk City area. Near the batholith, the isoclinally folded rocks have been tilted steeply from an initially recumbent position, as the batholith rose diapirically into and through superjacent rocks. This resulted in a strain axis not parallel to the layering, the general requirement for the generation of conical folds (Stauffer, 1964). Moreover, because the slip line is near vertical in this case, the axis of the conical folds generated will also be near vertical, plunging down the dip of the vertical foliation. The active folding of injected pegmatite in conical folds supports the proposed contemporaneity of batholith intrusion and D_2 folding, although the pegmatite continued to be injected after some conical folds had already developed.

In the rocks west of the batholith and within its tectonic mantle, the diapiric rise of the batholith has imposed such vertically plunging folds on its wall rocks. Perhaps the somewhat random sense of rotation of the minor folds is to be expected in this structural environment. The helical or screwlike character of the axes of the conical folds is attributable to unstable, vertical, viscous flow during D_2, in which a rotational component was imparted to the vertically flowing rocks.

Small, horizontal D_2 folds may represent original attitudes of the folds, as suggested earlier; alternatively, they may suggest that extension flow occurred in two directions in the A-B plane. Folds of both near-horizontal and near-vertical plunge are present. The latter idea is supported by the existence of lozenge-shaped boudins, doubly extended, of pegmatite, measured in centimeters, some of which display separations in the A-B plane up to 1.5 m. Large strains are suggested.

The near-axial symmetry of the rocks supports the notion of major vertical flow. Sillimanite and muscovite grew parallel to D_2 fold axes in this flow, but partly grew after the cessation of fold development, as exemplified by the growth of vertically lineated sillimanite in late shear fractures. Reid and others (1979) discussed evidence showing that the wall rocks flowed vertically downward along the wall of the rising batholith.

The D_3 folds are viewed as a major drag-fold set imposed by the batholith on its wall rocks late in its rise. The result is that the conical folds are now draped over the hinges of the concentric folds of D_3 age, roughly at right angles to their axes. The complex geometry implicit in this structural array is no doubt responsible for the wide scatter of poles to foliation in the Selway River quartzite.

Next to be considered are rocks south of the Selway River, both in the southern Fog Mountain quadrangle, and in the Vermillion Peak area, which lies south of the Fog Mountain quadrangle. In the Vermillion Peak section, three fold sets emerge: D_1 - tight, originally recumbent isoclinal folds with axial-plane schistosity, original trend or trends not known; D_2 - tight folds that deform the S_1 schistosity of D_1 and develop a second axial-plane schistosity (S_2); and D_3 - open kink or crenulation folds with steeply dipping axial planes. In a way, this structural sequence correlates to that in the biotite quartzite some kilometers to the northwest along the Selway River. The D_1 folds at both places are similar in style though different in orientation. Those at the selway River plunge 0° to 90° in a near-vertical foliation, whereas those in the Vermillion Peak area plunge at shallow angles and in various trends. The D_2 folds in the two areas may be different. Those at the Selway River are conical and plunge at angles near 90°. Those of the Vermillion Peak area plunge in various directions at angles up to 65°, but mostly shallow. If those two fold sets formed at the same time, the conditions of deformation were different.

The D_3 crenulation folds dominate the structure of the Vermillion Peak area, whereas comparable D_3 folds at the Selway River section are subordinate and develop at only a few places. The mesoscopic folds seen in the outcrops are clearly minor folds on a major fold structure, as shown in cross-section analysis.

Amphibolite, tonalite, and pegmatite were all injected into the foliation and were involved in the D_1 and subsequent folds and the associated metamorphism. The D_1 folds may pre-date the time of igneous activity. If that is so, then they have been injected by igneous material later, probably in D_2, and have been reactivated in componental movements along the schistosity caused by D_2 movements. Structures that seem to suggest synkinematic D_1 injection would then be due to synkinematic D_2 injection. Alternatively, all three sets of folds may be due to movement associated with igneous emplacement, in which case pre-igneous structure that may have existed has been destroyed.

It is important to note that biotite and muscovite lineation parallels the axes of all three fold sets. This permits the inference that all three fold sets developed during a single phase of metamorphism. Given the abundant igneous injection into the rocks and the metamorphism of much of that igneous material, it seems clear that the thermal and mechanical energy for metamorphism is due to the emplacement of the Idaho batholith. Quartz veins developed in D_3 perhaps represent an episode of silicification due to late-stage igneous and hydrothermal activity in the cooling batholith.

Structure in the southern Fog Mountain quadrangle, lying between the Vermillion Peak area and the Selway River section, is complex. Foliation trends are widely scattered. D_1 and D_2 fold axes and associated mineral lineation have widely scattered orientations with a few very steep plunges like those in the Selway River section. D_3 axial trends are similar to those in the Vermillion Peak area. The structural pattern may thus be viewed as a transitional one, particularly the transition from the near-vertical conical folds of the Selway River section to the shallow-plunging, probably cylindrical folds of the Vermillion Peak area. Such a transition might produce the complexities of the southern Fog Mountain area, which otherwise defy interpretation.

Finally, we need to seek a reason for the above-described structural transition. The rocks in the Selway River section have been interpreted above as lying in the wall of the batholith, their steep dips and plunges as due to downward flow of the country rock along the batholith margin. The relatively shallow dips and plunges that characterize most of the rocks in the Vermillion Peak area might correspondingly be explained as due to a situation on the roof of the batholith. The intervening rocks of the southern Fog Mountain area then are those that were bent over the shoulder of the intrusion. The 30° southeasterly plunge exposes progressively higher rocks to the southeast.

PETROLOGY AND STRUCTURE OF THE TONALITE

Flow foliation in the tonalite intrusive unit near the batholith contact in the Chimney Peak area dips about 70° west. Flow lineation in the intrusive unit plunges about 70° in the plane of the foliation and is taken as representing the direction of flow parallel to the contact. The steep flow represented within the intrusion has no doubt been responsible for the production of the steep flow structures described above in the wall rock adjacent to the batholith, through a mechanism of fractional drag on the walls and the resulting passive flow in the strongly heated walls of the intrusion. Metamorphic rock in the migmatite screens in the batholith behaved similarly. The partly axial symmetry of flow elements in the several units supports the idea of diapiric intrusion. The solid-state flow in

the metamorphic rocks resulted in recrystallization so strong as to destroy virtually all fabric elements of any older metamorphic event. Shallow-dipping sheets of trondhjemite and granite alaskite stand nearly perpendicular to the inferred batholith contact and to the direction of flow lineation. Thus, the lineation is seen as a stretching lineation, and the shallow-dipping sheets represent primary tensional joints perpendicular to the direction of stretching (cf. Balk, 1937). Sheets of the same sort occur in the wall rock of the batholith, which has therefore also been stretched in the same way during batholith emplacement.

The alaskitic materials have invaded the primary joints as they formed. The varied dike composition, trondhjemite and granite, suggests more than one intrusive episode; the requirement for simultaneous emplacement may demand synmagmatic emplacement of different magmas. The following mechanism (oral communication, W. R. Greenwood, 1978) may be applicable to explain alaskite formation. Early primary joints developed as soon as the rock had cooled enough to sustain fractures. A mixture of quartz and plagioclase in the grain interstices was available to enter the early joints. Later or continued fractures tapped an interstitial fluid richer in quartz so that quartz cores could develop in the sheets. Latest fractures found only quartz available in the interstitial liquid, so that sheets of pure quartz could develop. For the trondhjemite, the alaskitic material is largely of local derivation from the immediate host rock, derived through time from whatever residual magmatic fluid was available to enter the en echelon primary fracture at the time each particular fracture developed. The observed data would be more difficult to understand if one were to try to explain them on the basis of a central store of pegmatitic magma at some remote location, perhaps near the center of the intrusion.

The granite alaskite implies a more complex history, as it must have been derived from a granite emplaced synplutonically with the tonalite. Such granite is not found, but may be represented by granite xenoliths found in the younger granite described below. From that earlier, synplutonic granite, granitic alaskite migrated into the neighboring tonalite and was emplaced at the same time as the trondhjemite.

In most thin sections of the biotite tonalite, the plagioclase is euhedral and unzoned. Anorthite content of the plagioclase shows no systematic variation. A bit of normal zoning appears in a few grains. Thus, it seems that the magma either crystallized slowly at an approximation to equilibrium conditions, or that the plagioclase grains were somehow annealed later. The plagioclase grains, predominant among the rock constituents, are free of strain phenomena; there was apparently little late-stage magma movement leading to protoclasis, or alternatively, very little cataclasis due to external tectonic activity while the rocks were still hot.

The rocks in the Fenn Mountain area are strongly flow foliated. With Balk (1937), we assume that flow foliation formed in a simple shear regime by flow steeply upward more or less parallel to the batholith walls. Planes of laminar flow, tantamount to planes of shear, segregated minerals of different flow response into laminae of different composition; some layers are plagioclase-rich and others are rich in dark minerals.

The foregoing general formulation is adequate for a beginning understanding of the flow foliation, but not adequate to explain a number of details. Consider the complex folds in the flow foliation arrayed about a more or less vertical axis. The folds are not clearly either cylindrical or conical, although both kinds are seen, but the pattern is inescapably reminiscent of that within salt stocks (i.e., it has axial symmetry); flow mechanics comparable to those within salt stocks may be envisioned. Moreover, just as within the wall rock of the batholith, a twisting or torsional component to the vertically directed flow was probably present, leading to the complexly twisted or curved axes of some of the steep folds whose axes plunge near vertically. In other cases, the foliation is folded in rectilinear folds, cylindrical and of steep plunge. Associated minor folds show randomly both clockwise and counterclockwise rotation through individual small outcrops, suggesting that the folding was not systematic.

Flow lineation in the biotite tonalite plunges steeply to the southwest. Too few lineations were found to lend statistical validity to the estimate of the average plunge of the flow line, which is shown on the diagram (fig. 30) at about 60°, 220° az. This is 10° less than that found in the Chimney Peak area to the west and may represent a slight flattening of the flow structures verging toward the roof of the pluton.

The biotite tonalite was cut by dikes of leucocratic biotite tonalite which solidified, were then sheared while hot, and were recrystallized as a fine-grained, biotite-plagioclase schist or blastomylonite with strong field resemblance to mylonite. The shearing pre-dated the pegmatite stage and suggests the operation of faulting in pre-pegmatite time, along trends parallel to the Trans-Idaho Discontinuity (Yates, 1968). Thus, that discontinuity may have been active during or after tonalite emplacement.

Coarse-grained alaskite and pegmatite occur in the biotite tonalite in two ways, similar to relations in border-zone tonalite to the west, both as shallow-dipping sheets and as steep dikes mostly cutting the flow foliation but partly parallel to it. The dikes are granodiorite to granite in composition and thus not derived from the tonalite. As above, they were most likely injected from a former, synplutonic granite body nearby, removed by younger intrusions. The pegmatite sheets are more or less perpendicular to the flow lineation, injected into primary joints perpendicular to the stretching direction represented by the flow lineation (cf. Balk, 1937, p. 31). Note that the tonalite had to be sufficiently crystallized that it could sustain fractures at the time of diking, and the fractures, extensional in character, represent stretching in consolidated rocks caused by the continuing rise of the entire intrusion.

At several places, exposures reveal the en echelon character of pegmatite sheets, consistent with an origin by extension. Some of the pegmatite contains zones of cataclastic shearing along which the cataclastically reduced grains are largely strain free, apparently recrystallized in an annealing stage. This may be understood as the result of shearing of the pegmatite along restricted zones when it was solidified but still hot. Such movement in the rock may have been caused by continuing rise of the deeper part of the batholith, resulting in shearing on steep- and shallow-dipping planes associated both with components of rising and of lateral spreading. This would be a kind of protoclasis. Alternatively,

the rocks may have been subjected to external tectonic activity when consolidated but still hot. The same kind of annealed fabric would result, but the shearing could be due to various kinds of faulting such as transcurrent faulting in the Trans-Idaho Discontinuity or flat thrusting.

The trends of the steep-dipping pegmatite are widely scattered, resulting in more or less axial symmetry to their pattern of distribution. This feature may relate somehow to the axial symmetry of the flow foliation. Perhaps more likely, it may indicate a radial spreading of this part of the batholith as it rose into higher crustal levels. Fractures of diverse orientation opened simultaneously to receive pegmatitic magma. The above discussion has brought suggestions of the operation both of magma tectonics and of external tectonics on the tonalite at a time when it was hot enough to recrystallize if sheared. Perhaps both processes operated simultaneously.

The age of the tonalitic rocks presents a problem. In earlier work, Reid and others (1973) found the tonalitic gneiss and related augen gneiss in the country rock of the batholith to be Precambrian, based on Pb^{207}/Pb^{206} zircon ages. Field work in this project led to the alternative idea that the tonalite gneiss might be an early precursor of the batholith, emplaced in the Cretaceous. The zircon ages might reflect the ages of parent rock from which the tonalite gneiss derived. K-Ar work on hornblende by R. Fleck (oral commun., 1979) has shown both the tonalite gneiss and the tonalite to be about 65 m.y. old. Thus, the tonalite gneiss and the tonalite were apparently intruded nearly simultaneously; the tonalite cuts the tonalite gneiss and is thus at least slightly younger. Bickford and others (1981, p. 453) found quartz diorite gneiss at the northeast contact of the batholith to be about 73 m.y. old.

MIGMATITE SCREENS OF THE SOUTHERN ZONE OF THE WESTERN SECTOR

The pelitic metamorphic rocks in the migmatite screens closely resemble those of the wall rock of the batholith. However, the wall-rock stratigraphy does not match well, if at all, with the form and trend of the migmatite screens. Moreover, the radioactivity of the migmatite screens is higher (Reid and others, 1979) than that of the batholith rocks intermixed with them and even higher than that of the wall rocks. Finally, Sr^{87}/Sr^{86} data persuaded R. Fleck (oral commun., 1979) that the migmatitic rocks are probably basement-derived.

The E-W trend of the migmatite screens also constitutes a problem. If the rocks are correlative to the wall rock, then a means to rotate them from the wall-rock orientation (northwest) would have to be found. The rising magma is unlikely to rotate rocks strongly from their original strike. Perhaps shear movement in the Trans-Idaho Discontinuity could be responsible. Alternatively, if the rocks are basement derivatives, their current trends might reflect original trends. The problem is far from solved. The idea of former roof rocks of an age different from that of the wall rock, though possible, seems unlikely. Finally, if the magma flowed to the east as it rose, the migmatite sheets would assume an easterly trend.

TERTIARY DIKES OF THE SOUTHERN ZONE OF THE WESTERN SECTOR

The tonalitic rocks of the Crags area are cut by dikes of andesite to quartz latite. The dikes dip steeply and average a 360° az trend. No cataclasis is seen in thin sections of these rocks, and they therefore post-date the mylonitization event. Attitudes of the dikes are given in figure 44. It is assumed that the dikes represent an episode of N-S compression and E-W extension.

JOINTS OF THE SOUTHERN ZONE OF THE WESTERN SECTOR

Joints in the Crags area are oriented more or less randomly, and bear no demonstrable relation to any regional fault system. Perhaps, as they are not mineralized, they represent the result of volumetric expansion accompanying erosional unloading and isostatic rise of the rocks. Alternatively, near a transform fault that has experienced alternate right-lateral and left-lateral movement, still a speculative matter in itself, complex arrays of joints might develop that would appear to be random in a composite plot.

PETROLOGY AND STRUCTURE OF THE GRANITIC ROCKS

Magmatic features

The granitic rocks of the Bitterroot lobe are clearly younger than the tonalite of the Crags area, inasmuch as there are xenoliths of tonalite in them near the contact, as on the northeast ridge of Stanley Butte for instance. The presence in the area of an older granite, of the same age as the tonalite and displaced by the granites there now, has been suggested earlier; this suggestion is reinforced by the presence of granite xenoliths in the granite. The granitic rocks are predominantly of granite and granodiorite, apparently more or less randomly commingled with each other and with smaller amounts of quartz monzonite, quartz monzodiorite, tonalite, and anorthosite. These rocks share many petrographic similarities, suggesting that they were emplaced synplutonically. Although magma mixing seems possible, the idea of complex multiple sources seems more likely, with little mixing of magma. Such features as trondhjemitic pegmatite intruded both in granite and granodiorite seem to support the idea of separate, simultaneous emplacement, and later pegmatite injection into diverse lithologies, drawing perhaps from the same source areas as did the principal rocks. The fine-grained dikes also inject other than their own lithologies, further suggestive of separate sources for the several magma types. Relict zoning in the plagioclase of granodiorite and tonalite shows plagioclase progressively more calcic, also suggestive of independent sources. The rocks are variably porphyritic, mostly in a random way; in one area (Tenmile Lake quadrangle), there is a suggestion of elevation control, phenocrysts in the rocks of the aretes but not of the valley bottoms.

Tonalite sheets along the primary flow foliation in the Tenmile Lake quadrangle appear to have been liquid at the time of formation; this suggests synplutonic emplacement, accompanied perhaps by some mixing with granite and granodiorite magma. Many tonalite sheets pass into thin, biotite-rich schlieren, with a distinctive texture doe to the retention of a small amount of euhedral feldspar within them. Much of the original quartz and plagioclase of the tonalite may have been absorbed into the granitic magma. Granodiorite in the Castle Crag area appears to occur in part in sheets parallel to flow foliation in granite; again, synplutonic injection seems likely.

The intrusive emplacement of anorthositic magma in the Bitterroot lobe granitic rocks requires special comment. Anorthosite is generally held to be exclusively of Precambrian age, and that would require the anorthosite here to be rafted hypoxenoliths. However, no evidence of rafted xenoliths was seen; therefore, it is believed that the conditions for generation of anorthosite magma were met in this area, and that small amounts of anorthosite were formed.

One difference in the granitic rock across the batholith is that K-feldspar includes quartz in the western and central sectors, but does not in the eastern sector. Perhaps cooling rates were different in the eastern sector, so that quartz began to crystallize somewhat later than it did in the two sectors to the west.

Another difference across the pluton is that microcline is the sole K-feldspar near the eastern and western margins, whereas orthoclase occurs in addition to microcline in the interior, in all the rocks. No reason for this has suggested itself; if the batholith cooled more slowly in its interior, then microcline should be the sole feldspar. Strain effects are not likely involved; some orthoclase grains were flattened and re-equilibrated as orthoclase.

The granitic rock of the western sector contains some relict crystalloblastic plagioclase, possibly incompletely melted material that has retained its metamorphic aspect in part. Some of the crystalloblastic plagioclase is enclosed by microcline and is clearly not a late-stage phenomenon. The source for the granitic rock then may be at least in part due to older granitic material partly melted at depth.

The more quartz-rich rock of the western sector may have gotten its quartz by assimilation from the quartzite of the migmatite screens.

Schlieren develop in several environments in the granitic rock of the Bitterroot lobe. Schlieren in both primary and secondary flow become concentrated due to segregation effects in differential flow. Schlieren also developed from various rocks both metasedimentary and metaigneous, as well as igneous, included in the magma. Here it seems that partial melting and assimilation of the low-melting components of the inclusions may occur--principally quartz and feldspar--resulting in an effective concentration of biotite. The resulting biotite concentrations, now schlieren, are more or less streaked out in continuing flow.

Suggested in Sr^{87}/Sr^{86} values found by R. Fleck (personal commun., 1979), the tonalite and granitic rocks seem to contain partly mantle-derived and partly crustal-derived material. As discussed above, the crustal contribution is probably anatectic material. This anatectic contribution perhaps did not melt and mix completely. Then, if the tonalite and granite magmas are each discrete entities formed in independent but simultaneous melting, the granodiorite as well as the variability in the modes found within each intrusive unit could be explained as the result of incomplete mixing. As above, multiple intrusive sources may be involved for each of the magma types encountered.

Feldspars are alined within flow foliation in parts of all intrusive units. It is not certain whether this represents the alinement of partly crystallized material or whether it represents incomplete melting and intrusion as a crystal mush. A mush of crystals incompletely melted would find difficulty in attaining any degree of mixing with adjacent synplutonic material. Alinements in the central and eastern sectors are increasingly due to a metamorphic overprint, and initial flow cannot be evaluated.

Steep flow lineation in the granitic rock near its contact with the older tonalite in the southern zone of the western sector shows near-vertical flow along a locally east-trending contact. Near-horizontal pegmatite sheets are consistent with vertical stretching along this contact. Features along this contact are taken as representative of the principal magma tectonics of the granitic rocks, modified and extensively obliterated to the north and to the east as discussed below.

Blastomylonite parallels the granitic rock contact in the Louse Point area of the southern zone. It seems clear that late movement occurred in the granite parallel to the contact when the granite was still hot. The rock was sheared mylonitically, but was annealed by the remanent heat. This is a kind of protoclasis. Alternatively, faulting may have occurred along the contact shortly after consolidation, with the same outcome; no evidence for faulting was seen however. The existence of a vertical lineation in the mylonite, consistent with late movement of the igneous rock up along the contact, supports most strongly the concept of a protoclastic process.

Migmatite screens in the northern zone of the western sector contain schistosity/foliation with the same geometry as that in the enclosing granitic rock, highly discordant to that of the granitic rock of the southern zone, near the contact. Too few data exist to define the slip line accurately, but the average of the lineation suggests an orientation near 30°, 320° az. The involvement of granitic sheets in migmatite folding shows active participation of the migmatite screens in the igneous flow process. The internal linear elements of the migmatite have either been rotated toward the slip line, or new linear elements have been generated in the solid-state flow.

Pegmatite/aplite dike orientations portray an ill-defined girdle. The pole to this girdle is oriented near 10°, 300° az, not far from the slip line for flow in granitic rock and migmatite screens. It appears that solid-state flow continued on about the same axis as the liquid-state flow, when the granitic rock had consolidated sufficiently to sustain shear. The few pegmatites found intersect in the slip line. Fractures generated in the solid-state, axial flow were injected by pegmatitic magma.

Blastomylonite schistosity averages 320° az, 40° SW on the few outcrops found, and the lineation, taken as the slip line, averages 30°, 290° az, similar to the orientation of the slip lines postulated above, but rotated counterclockwise with respect to them. Therefore, it appears that continuing movement in post-pegmatite time along the 290° az trend led to blastomylonite development. This trend is

discordant to that of blastomylonite near the granitic rock contact in the southern zone, but the two blastomylonites must be nearly the same age. The features of the northern zone are discussed later in this paper.

In connection with the petrology of the granitic rocks, it is useful to consider the tectonic mantle surrounding the batholith, as well as the orientation of structural elements within it. This mantle is the zone of rocks in which the fabric is reconstituted by shearing and recrystallization due to the mechanical and thermal activity of the rising pluton. Reconnaissance to the west of the map area suggests that the tectonic mantle is many km thick in the Lowell region. The mantle rocks within the study area, while retaining evidence of multiple folding, have an orthorhombic-axial metamorphic fabric produced in a single recrystallization. The fabric elements are arrayed about a single, major, near-vertical axis presumably related to the near-vertical flow processes of pluton emplacement. The discordant tectonic elements of the northern zone of the western sector, important to the east, were not seen in the wall rocks as they pass to the north of the map area.

Published mapping and studies north and northwest along the Idaho batholith trend are inadequate to show how far north and northwest the tectonic mantle extends. Depending on the plunge of the batholith roof, the mantle could extend for a considerable distance. The character of the rocks in the St. Joe area of northern Idaho (Reid and others, 1981) suggests that it does not extend that far north; therefore, its northern limits must be sought in the North Fork of the Clearwater River area, probably in the Kelly Fork district (Kell and Chase's (1976) area).

The fact that the tectonic mantle of the batholith in the Lowell area contains only vertical elements injected by igneous material during folding suggests that external folding was not involved. Further, the tonalite and granitic rocks of the southern zone contain only near-vertical flow elements and retain their principally igneous fabric. No external metamorphic overprint has occurred that might have developed through external metamorphic processes associated with folding and metamorphism.

However, some faulting occurred at the time of tonalite emplacement. The northwest trend of the batholith contact in the Crags area is likely fault controlled; it may well be a manifestation of the Trans-Idaho Discontinuity (Yates, 1968). Moreover, the tonalite body was cut by a few northwest-trending fault fractures filled with late-stage trondhjemite (sheared and recrystallized while still hot by movement along the faults) and then was cut by post-kinematic trondhjemitic alaskite almost certainly generated as pegmatitic magma in the tonalitic mass. Therefore, faulting occurred sporadically through the time of tonalite emplacement and consolidation. This faulting may continue during granitic rock emplacement, as a tear fault related to regional low-angle thrusting; the low-angle thrusting, as discussed below, may be responsible for the discordant structures of the granitic rocks of the northern zone of the western sector and related rocks to the east.

Migmatite screens

Migmatite screens are major only in the western sector. Migmatite screens were apparently involved in some strain, including rotation, during liquid flow, as they are more or less alined in the northwest-trending axial-flow pattern of the granitic rocks in the northern zone of the western sector, as well as alined in vertical flow in the southern zone near the contact between older tonalite and the granitic rock. Migmatite screens resemble the country rock in their content of calc-silicate gneiss, plagioclase quartzite (major), plagioclase-bearing schist, and scanty amphibolite. A major difference is in the content of granitic gneiss, not seen in the country rock. Actually, there are two kinds of concordant granitic rock in the migmatite. First is the granitic gneiss, crystalloblastic and in sheets of varied thickness. Second is the granite to granodiorite, hypidiomorphic granular and therefore unmetamorphosed, but with some primary flow foliation. The granitic gneiss must represent earlier granitic material injected in the migmatite and then metamorphosed with it, perhaps in the same metamorphism that recrystallized the metasedimentary rocks. The locus of that earlier granite event may have been similar to that of the event in which the granite of the Bitterroot lobe was emplaced.

Migmatite zones in the eastern sector (Castle Crag area) trend northeasterly parallel to local trends and are different in this northeast trend from others to the west; they are also different in that gneissic granodiorite is the principal paleosome rather than the biotite quartzite major in most of the other migmatite. Granodiorite occurs partly in blocks, partly lit-par-lit injected by granite, and partly as flow layers along the primary flow foliation in granite. This complex occurrence might be explained as synplutonic injection of granodiorite and granite, with the granodiorite attaining sufficient rigidity to break partly in blocks ahead of the granite. Tonalite occurs in minor amount in stringers along the flow foliation both in granodiorite and in granite; therefore, all three magmatic types may have been essentially synplutonic.

One amphibolite xenolith in the migmatite contains small xenoliths of hornblende granite and fine-grained, pink diorite, different from all the rocks seen in the area by this writer; some earlier plutonic cycle would seem to be represented.

Xenoliths

Xenoliths occur in considerable variety. They are scarce in the western sector, a little surprising in view of the large volumes of migmatite there, and increase in abundance toward the east. Many of the xenoliths are of metasedimentary material, probably derived from the roof, similar to that of the wall rock and the migmatite screens. Unexpectedly, considerable numbers of xenoliths of igneous material were encountered, including granite, granodiorite, granitic gneiss, granodioritic gneiss, metagabbro, tonalite, tonalite gneiss, tonalite schist, quartz-diorite schist, and amphibolite. The igneous xenoliths suggest earlier intrusive activity in the area, prior to the emplacement of the granitic rocks of the Bitterroot lobe. Those igneous rocks that were metamorphosed suggest dynamic metamorphism in the area prior to Bitterroot lobe emplacement. The fabrics of the metamorphic xenoliths have in some instances been reconstituted in some measure during their immersion in the magma and then in the ensuing

field of secondary strain. The massive igneous xenoliths suggest a variety of intrusions later than the dynamic metamorphism but earlier, of course, than the granitic rock of the Bitterroot lobe. The fabric of these rocks has been little affected by post-immersion events.

The anorthosite orbicules strung out along the foliation in the granitic gneiss of the Tenmile Lake quadrangle are xenoliths of a sort. It is judged that they derive from anorthositic magma in the area, during synplutonic emplacement.

Xenoliths become more numerous to the east, perhaps indicating rocks closer to the batholith roof.

Secondary foliation

Origin of unzoned plagioclase.

Unzoned plagioclase occurs over the whole area. It is possible that cooling under near-equilibrium conditions occurred, so that zoned plagioclase could equilibrate. Secondary strain may have aided this process, but unzoned plagioclase seems to develop about as well outside the field of secondary strain as within it. However, this idea needs testing farther away from the field of secondary strain.

Similarity of plagioclase composition in granite and granodiorite.

Plagioclase composition ranges from about An_{18} to An_{33} over the whole area, in a random way. Cores in relict zoned grains in granodiorite are somewhat more calcic than those in granite, suggesting that the granodiorite had the potential to form more calcic plagioclase. However, the secondary strain has affected the plagioclase of both rocks in the same P-T interval during solid-state strain. Thus, the plagioclase in both rocks was re-equilibrated to lie in the same range of compositions.

Fibrolite inclusions.

Fibrolitic sillimanite occurs as inclusions in a few igneous rocks in grains of mica or feldspar, and in migmatite and xenoliths as inclusions in the same minerals, and as independent grains and grain clusters. In the igneous rocks, it may be due to the presence of assimilated pelitic material. In general, it may have formed during the metamorphic event that generated the secondary foliation.

Generation of extension fractures.

Evidence of movement in the igneous rocks in the late-liquid stage, when the crystal meshwork was sufficiently established to undergo strain, is found in quartz-microcline-filled extension fractures in plagioclase. Quartz-filled extension fractures in microcline show the same thing near the end of the magmatic stage, as movement continued. Extension fractures developed later in the continuing, solid-state strain are filled with muscovite, quartz, and pennine. These fractures all stand more or less perpendicular to the mineral lineation, and are due to stretching along that lineation.

Origin of the secondary foliation.

The fabric elements of the northern-sector granitic rocks as well as those to the east, produced in secondary strain, are virtually identical in granite and in granodiorite as well as in the less common varieties of plutonic rock. This suggests that the several rocks are of the same age (synplutonic), inasmuch as they experienced the same post-consolidation, high-temperature strain event. Relict igneous fabric is rare; the granitic rock of the entire area is essentially a metamorphic unit.

The shallow plunge of linear elements in the secondary foliation of the granitic rocks of the northern zone of the western sector, compared to the steep plunge of linear elements in the older tonalite as well as the younger granitic rocks of the southern zone, shows that the rocks experienced dramatically different tectonic environments. Granite of the southern sector rose vertically along its contact, crystallized, and experienced no further activity. Secondary foliation, on the other hand, began to form in the northern-sector granitic rock before it was entirely solid, as shown by extension fractures in the feldspar filled with late-stage magmatic material. It continued to form after consolidation, forming gneissic foliation, flattening feldspar and quartz, and deforming the later fine-grained dikes as well as still-later pegmatite to aplite. The strain was principally axial in character on the west, becoming more orthorhombic to the east. Both quartz and mica show indications of axial symmetry in their distribution in thin section, sympathetic to the axial fabric symmetry brought out by structural geometric analysis of the outcrop data.

The diffuse zone defining the southern boundary of the secondary strain field in the granitic rock of the western sector is interpreted as the boundary of a broad zone of distributed shear. Flow foliation except near the contact in the western sector formed independently of the secondary strain field boundary; thus, a good part of it is of primary origin, formed in flow of axial symmetry. This axial-flow pattern continued during solid-state strain north of the secondary strain field boundary, as shown, for example, by the injection of some pegmatite and aplite into the secondary shear planes. The axis of flow plunges at a shallow angle to the NNW, indicating an inclined field of axial symmetry.

Deformed pegmatite shows that movement continued in the solid state, when the rocks were still hot. The effects of the solid-state movements are described as secondary strain fabric, a crystalloblastic feature. Quartz subgrains formed in secondary strain are in irregular, somewhat pavement-like arrays to more irregular arrays, with varied c-axis orientation rather different from that of the original grain. The fact that the subgrains are strain-free suggests annealing during or following secondary strain.

It appears that the principal petrographic criteria for secondary strain include anhedral to flattened quartz grains with strong, annealed subgrain development, filled extension fractures in the feldspar, flattened feldspar grains, and subgrain development in the feldspars, which is, however, not as strong as in quartz.

Considerable thermal reconstitution of many foliated xenoliths seems to have occurred during immersion in the magma, and some effects of secondary strain are seen in the form of lineation parallel to secondary lineation in the enclosing igneous rock. Whatever the history of the xenoliths was prior to the immersion in the batholith, their fabric has been modified during secondary strain.

Farther east, in the central and eastern sectors, secondary foliation becomes stronger and little or no effects of primary foliation are seen in the stained slabs or in thin section. Primary foliation either did not develop or has not been preserved in the foliation in many of the foliated rocks

sampled. Some primary foliation has been destroyed during secondary flow, and schlieren alone remain to mark the former primary foliation.

The increasing proportion of foliated rocks from west to east over the area may be due to close approach to a border zone of locally more intense strain lower and to the east, near the base of the pluton, along a zone due to thrusting. Strain-free subgrains in the plagioclase become more common to the east, deeper in the pluton, due to more intense deformation and concomitant annealing in that direction. Mica generally becomes oriented in the rock only under somewhat more intense strain that that in which quartz and feldspar first become flattened. This is perhaps due to the flattening nature of the strain. Considerably more strain may be required to reorient a mica in a field of flattening than in one of rotational strain. In many places in the eastern sector, feldspar grains are rotated out of parallelism with the foliation, largely counterclockwise looking north.

This results in a feldspar foliation that dips more steeply than the biotite foliation. Thin section analysis suggests that biotite grains lie on shear surfaces; therefore, as suggested above, the C and S surfaces of Berthé and others (1979) may be present. Analysis based on this assumption and based on exposures at three places shows that the upper rocks sheared southeast relative to the lower rocks during the generation of gneiss early in the tectonic sequence.

Thus, a root zone for thrusting may have cut through the pluton near its base, during the time of intrusion; alternately, perhaps the pluton spread laterally along a thrust zone and was subsequently cut by the thrust in continuing movement. The thickness of the pluton would require that this happened near the base of the crust.

The granitic rock of the eastern sector is less porphyritic than that of the western sectors. This may be partly a function of the milling-down in secondary strain of K-feldspar phenocrysts.

As shown in figure 73, the flow lines in the Bitterroot lobe have been important in the generation of structures in the late liquid stage and in the post-consolidation stage of the batholith. The granitic rock apparently rose into or crossed a structural discontinuity in which subsequent movement deformed it during igneous flow and then along similar lines in solid-state flow. The flow was extensional, a concept supported by curving extension fractures perpendicular to the flow lines (later reactivated as chlorite-patterned shears). This suggests thinning during deformation. The fact that the gneissic foliation in the granitic rock dies out quickly to the north (yet north of this map area) so that it is not seen along U.S. Highway 12, is consistent with the 30° northwesterly plunge of the flow lineation and with the concept of involvement in a thrust. As discussed above, this thick intrusion may have been cut near its base by the root zone of a thrust. The intensity of the strain died out slowly upward in the intrusion, through a zone more than 30 km thick.

The strong lineation and widespread flattening of the rock in the eastern sector, also involving some rodding, may be explained as due to flattening near the base of the pluton. The batholith would be spreading in an ESE direction under its roof and along the basal thrust to produce the lineation.

Migmatite involvement in the flow foliation.

Migmatite screens in the granitic rock within the secondary strain field were apparently involved in some rotation during liquid flow, as they are more or less alined in the axial flow system. Migmatite strain in the solid-state flow resulted in many flow folds of northwesterly trend, as well as mineral lineation, parallel to the secondary lineation of the enclosing granitic rock. It appears that secondary strain resulted in the retention of strong schistosity in the migmatite; otherwise, it might have been hornfelsed in considerable degree in thermal metamorphism.

Development of Subarea B of the eastern sector.

Flattened mineral grains are rather scarce and much less strongly developed in the rocks of Subarea B than in adjoining areas (see fig. 73). It appears that the primary flow foliation has been deformed in a gigantic fold during early flow, due perhaps to impingement of an eastward-moving sheet of granite upon an eastern buttress or wall—the eastern batholith contact. At a later stage in consolidation, when magma could still move as a partly solidified mush, the flow continued and became of secondary character with strain along directions only at small angles to the earlier flow, so that the two flow foliation sets have much the same geometry. Tangential compression seems to have predominated and flattening was much subdued; such little flattening as occurred parallels the steep axial planes of the folds and is not related to the low-angle flattening of adjacent strain fields, apparently due to vertical stress.

The Bitterroot gneissic front.

Near the eastern margin of the eastern sector, the dips become shallow and the trends change to those of a domical symmetry (see figs. 65 and 73), cutting abruptly across the trends of Subareas A and B. The near-domical symmetry suggested by figure 65 may be of only local significance, but it raises the possibility of a series of coalescent marginal domes concealed in the tilted foliation along the eastern side of the Bitterroot lobe. This domical symmetry combined with the east-trending lineation is a feature common to the metamorphic core complexes of the western Cordillera (e.g., Davis and Coney, 1979); Hyndman (1980) discussed a metamorphic core complex interpretation applied to the Bitterroot lobe. As discussed above, the possibility of thrusting in this area suggests a way for the lineation to form other than that envisioned by Davis and Coney; during the time that this paper was in preparation, a paper by Mattauer and others (1983) appeared, proposing a thrusting model for the metamorphic core complexes.

The foliation in the gneiss of the Bitterroot frontal zone is stronger than that seen in the gneissic granite to the west, opening the possibility that the foliation is of a different age, perhaps younger than that to the west. This possibility is supported in age dating work by Bickford and others (1981, p. 453) showing "cataclastic granite" to have an age in the range 49 to 46 m.y. However, because the foliation had formed already in pre-pegmatite time, as shown by the injection of pegmatite sheets along it, and continued to be deformed in post-pegmatite time, as shown by the development of secondary fabric in the pegmatite, and because its fabric is shown petrographically to be identical to that of gneiss farther west, only a bit more intense, the gneiss foliation would seem generally to be of the same age as the granitic rock foliation farther west; the granitic rock shows many of the same relations. But it must be admitted that these data are only suggestive and not conclusive.

To the west, the dips change from easterly to westerly over an arch that is perhaps partly of coalescent, small-dome character, and over a narrow transition zone give way either to the steep, northeast trends of the giant fold or to the northwest trends of axial symmetry. This geometry may mirror the joint constraints of deep shear zone and eastern contact.

No evidence for sliding-off of supracrustal rock is seen in the data. Chase and Hyndman (1977) and Hyndman (1980) have suggested that the Sapphire block slid off the Bitterroot lobe. It appears to us that the structure section (fig. 74) cannot be interpreted in that way.

Origin of the secondary lineation.

Flow foliation planes lie in various orientations, and their poles define crude girdles whose poles lie in the northwest trend. It is clear that all the flow planes must share a common flow or slip line of axial symmetry, defined by northwest-plunging girdle poles. Secondary mineral rodding due to axial strain developed where strain was relatively intense. At a number of places in the eastern sector, lineated gneiss free of foliation formed in this way.

Secondary lineation plunges west in the western Blodgett Mountain quadrangle. At one point, a younger blastomylonite lineation plunges to the east. The trends are about the same, but the slip line "rotated" through 55° between the two events. Thus, a considerable stress reorientation is suggested between the two events, which must have been rather close together in time. Given the rapid uplift shown by Garmezy and Sutter (1983), the two events may have happened in rather different crustal levels.

Late-stage secondary foliation.

Secondary strain continued in post-pegmatite time, mostly in the eastern sector, with less intensity and probably under lower temperature if not lower pressure. But in the transitional stage to less-ductile yielding, the strain still was able to develop discrete shears of millimeter to centimeter scale within which medium-grained biotite was concentrated, recrystallized, and lineated. These shears have partly the character of thin, ductile thrust faults and related tear faults, and partly are of lenticular form, with curving shears lineated along the dip line (in the slip direction), but striking at right angles to the slip direction and perhaps to be interpreted as C and S surfaces (cf. Berthé and others, 1979). These late-stage secondary shears are not so penetrative as the main-stage secondary foliation, but in some places their operations are sufficiently strong to produce shearing reduction of feldspar phenocrysts to flaser structure. Feldspar in the flasered zones is converted to flattened rods with axial ratios of 1:1.3:2. The long axes parallel the slip line operative in secondary flow, and the a-b plane of the flattened rods lies in the low-angle foliation.

Combined flow symmetries.

The symmetry of the flow in the western and central sectors, high in the pluton, is largely axial. In the eastern sector, deep in the pluton, flattening becomes important, and the symmetry is axial-orthorhombic; both flattening and rodding appear to be important. Right-lateral bending of alaskite dikes in the secondary foliation suggests also the entry of a component of monoclinic strain, and the fabric shows elements of combined axial-orthorhombic-monoclinic symmetry. The changes in symmetry combined with increase in foliation intensity, all to the east and deeper in the pluton, betoken the approach to a detachment or narrowing ductile thrust zone of some sort.

Tonalite to quartz diorite intrusions

The thick sheet of biotite-hornblende quartz diorite along the secondary flow foliation in the Elk Summit area (central sector) was injected soon after the granitic rock consolidated, clearly before the time of pegmatite formation, as it is cut by dikes of the granitic pegmatite suite. Like the granitic rock, this unit is more or less completely metamorphosed due to secondary strain under high remanent igneous temperature; it is foliated in its outer parts and more massive internally, but crystalloblastic throughout. This body is co-extensive with the dark tonalite at Diablo Mountain; like the main intrusion of granitic rock, it has varied composition. Tonalite dikes in the Bailey Mountain area of the central sector, cut by pegmatite dikes, may be of the same age as the quartz diorite.

Fine-grained dikes

Dikes and sheets of fine-grained granite, granodiorite, and tonalite were emplaced in the central and eastern sectors, but were not seen in the western sector. They are most abundant in the eastern sector, except that none were seen in Subarea B. Their distribution is thus asymmetrical; perhaps it correlates somehow with asymmetry of strain. The fine-grained sheets were emplaced during secondary strain into planes of secondary shear and generally metamorphosed in continuing movement. Fine-grained dikes were emplaced at the same time and also metamorphosed. Faults trending 055° az operated right laterally in the eastern sector during the time of fine-grained dike emplacement and were locally injected by fine-grained dikes, suggesting easterly compression creating faults across the field of secondary strain. Perhaps the fine-grained igneous rocks rose from the same sources as the main-stage batholithic rocks; deep, still unconsolidated, batholithic material constitutes an alternative source. Some fine-grained dikes were injected in extensional fractures perpendicular to the stretching lineation of the secondary strain field, showing in yet another way the extensional character of the secondary strain.

Ductile faults

Ductile faults were seen only in the eastern half of the Bitterroot lobe. These faults, of northeast trend, cut the earlier foliation and concentrated biotite in pre-pegmatite time; their relations to the fine-grained dikes are not clear, as no intersections were seen. Where lineation is present (streaky biotite or trains of biotite grains), it stands at a low angle indicative of strike-slip movement. A few offsets of earlier structure show right-lateral shear, indicative of east-trending stress; thus these faults are comparable in age to those that controlled some of the fine-grained

dikes. Comparable shears of ENE trend formed later than pegmatite but earlier than aplite and are thus broadly coeval with the emplacement of the pegmatite suite; they show left-lateral movement. Therefore a more northerly stress axis is indicated, a substantial change in trend from that operative in immediately pre-pegmatite time.

Pegmatite suite

Pegmatite is rare in the western and eastern sectors; the few dikes mapped show a complex pattern not clearly related in all instances to other structural elements and perhaps due therefore to random cooling fractures. Some dikes were injected along secondary foliation planes.

In the central sector, the primary fractures show a crude axial symmetry about the same axis as that which controls the orientation of the flow foliation. Therefore, many dikes of the pegmatite suite invaded secondary foliation planes. Aplite is generally later than pegmatite. This suggests a "dewatering" of the pegmatite magma through time.

Pegmatite suite rock is cut by secondary foliation in some places but not others, suggesting that the cessation of movement along the secondary foliation did not occur at the same time at all places.

Anorthosite II

The miarolitic andesine anorthosite pipe in the Blodgett Mountain quadrangle and the miarolitic andesine anorthosite dike in the Tenmile Lake quadrangle are both due to the late-stage emplacement of anorthosite magma. These features may bear the same relation to Anorthosite I as the fine-grained granitic dikes do to the granitic rocks of the Bitterroot lobe. As the anorthosite is medium-grained, it was emplaced either as a crystal mush largely crystallized at a deeper level prior to emplacement, or at a deep level in rocks of high temperature in which crystallization occurred slowly. Like the fine-grained granitic dikes, the andesine anorthosite is cut by blastomylonitic shears, themselves developed while the country rock was hot. The anorthosite bears a strong physical resemblance to the anorthosite I rock of the Blodgett Mountain quadrangle and may very well be a late product of the magma chamber(s) that gave rise to anorthosite I.

Blastomylonite

Blastomylonite is rare in the western sector and becomes more common in the central sector to abundant in the eastern sector. Thus, its development reflects that of the secondary-strain foliation. Petrographic features of the blastomylonite suggest simultaneous shear and recrystallization along zones of restricted shear. In some places, crystallization outlasted deformation, and the fabric is strongly annealed. In others, deformation outlasted crystallization somewhat, and polygonal arcs are only imperfectly developed. Some blastomylonitic shears in the western sector parallel secondary foliation and thus mirror the axial symmetry of the secondary strain event. Therefore, they may represent late, renewed strain in that event. Temperature had fallen a bit in some places by blastomylonite time, as some blastomylonite plagioclase is slightly more sodic than plagioclase equilibrated in the secondary strain event. In most places, however, both kinds of plagioclase have the same composition, reflecting little or no change in temperature between the two events. Generally, the blastomylonite seems to have formed little later than the secondary foliation. Biotite also formed stably in blastomylonite, although reduced in grain size due to shear.

In the central sector, blastomylonite shears have axial symmetry (fig. 58) about an axis that plunges toward the northwest parallel to the strain axis of the secondary strain event. The two sets of structural features formed sequentially in response to the same stress field; they evidently have shared a common slip line defined by that axis, which is also the girdle pole. Rodding developed in some blastomylonite due to relatively intense axial strain. Blastomylonite in low-angle arrays that strike more or less perpendicular to the trend of the girdle axis have the character of small, ductile thrust faults, described above, at one of which the upper halves of two phenocrysts were thrust 5 cm to the southeast; therefore, the strain has an element of monoclinic symmetry. The steeper shears function somewhat as small, ductile tear faults relative to the thrusts.

Further thoughts are based on conjugate blastomylonite shears seen in thin section and on a pair of conjugate shears found at one outcrop (see fig. 58). The two conjugate shears contain blastomylonite and thus developed at the same time as the rest of the blastomylonite. The bisectrix of the acute angle between them gives the orientation of the maximum principal stress that effected their development, an axis inclined at a moderate angle to the northwest. The conjugate shears raise the idea of a somewhat more-brittle shear; yet the poles to blastomylonite shears are not distributed in accord with the distribution expected for a unique orientation of two conjugate shear sets. Therefore, we examined the possibility of a uniaxial stress configuration, consistent with axial strain, in which yielding was somewhat more brittle than elsewhere in the field of blastomylonitic strain. In this case, the locus of shears would be in planes tangent to a 60° cone whose axis in the maximum principal stress, and the poles would plot in a small circle 120° from the maximum principal stress axis. The dashed-line arcs in figure 58 portray this condition. It will be seen that some of the poles lie on or near the small-circle arcs and may therefore belong to the postulated less-ductile shears due to uniaxial stress along an inclined axis. Others lie in intermediate positions consistent with a large-circle girdle developed in more-ductile yielding.

Blastomylonite zones in the eastern sector are more abundant than in the other sectors, although they were not found in Subarea B. They occur throughout the sector otherwise and resemble those of the other sectors in all but two respects. First, in thin section they terminate at large, lenticular grains of quartz or quartz ribbons, although some of their fine-grained mica continues as inclusion trains in the large quartz grains; it seems clear that large quartz grains transected by blastomylonite have recrystallized in late- or post-blastomylonite time in a "quartz-ribbon" event. This might be related to

somewhat higher temperature due to more intense shear. Second, the blastomylonite occurs mostly along low-angle shears in its megascopic manifestations, but partly also on steeply dipping shears; therefore, the blastomylonite appears to form in low-angle, ductile thrust faults more abundantly than to the west, with a few associated ductile tear faults. The thrusts, though having ductile shear zones averaging 8 cm thick, extend for distances along their strike measured in kilometers. Their generally westward dip, except where arched over the Bitterroot front, is consistent with a thrust mechanism. Scanty evidence in the central sector suggests that the movement on any one thrust has been small, measured in centimeters; this is consistent with their small thickness. Quartz ribbons are in part due to segregation during the blastomylonite event and are most strongly developed in and near major blastomylonite shears.

The blastomylonite of the eastern sector, standing at low angles, has a major element of flattening in its strain pattern; thus, the total symmetry is combined axial-monoclinic-orthorhombic, like that of the secondary foliation. Like the strain pattern in the secondary foliation, in which tops moved east, in the blastomylonitic shears the tops moved to the east, consistent with the regional sense of transport in the Laramide thrust faults. The blastomylonite may well be due to continued slip on Laramide thrust surfaces. From a rheological point of view, the blastomylonite may represent a continuation of movement responsible for the secondary foliation, under somewhat less ductile conditions, perhaps involving considerable reduction in pressure. Arching along the Bitterroot front began in pre-blastomylonite time and continued in post-blastomylonite time.

An alternative view on the generation of blastomylonite might hold that it developed during the Sapphire block slide (for example, see Chase and Hyndman, 1977). The generally west dip of the blastomylonites except across the Bitterroot arch seems incompatible with a view of eastward gravity sliding.

Mylonite

Mylonite is rare in the western and central sectors, occurring in only a few, low-angle shears. Tops moved east, based on shear steps on the few shear surfaces seen. Lineation trends WNW, like that in the blastomylonite and secondary gneiss.

Mylonite in the Jeanette Mountain quadrangle (western part of the eastern sector) has linear trends like those of the mylonite to the west, but the tops moved west here, again based on shear steps on the shear surfaces. Farther east, the mylonite is abundant and developed in conjugate shears about a near-vertical axis of maximum principal stress.

The change in stress response, from thrusting farther west to high-angle shears in the east, all developing mylonite of the same petrographic and outcrop character, is ascribed to the late-stage arching of gneiss in the Bitterroot frontal zone; arching associated with active uplift brought about a change in the effective stress orientation across the top of the arch.

Mineralized joints

Mineralized shear joints in the western sector have an average ENE trend, varied dips, and largely strike-slip movement. Chlorite alteration and some pyrite introduction occur in these joints. In the central sector, these joints swing to a NE trend, and the movement is mostly oblique slip in character. In the eastern sector, these joint swing to a NNE trend and show partly dip-slip, partly oblique-slip movement.

Injection of fractures of the same trends by fine-grained granitic dikes, perpendicular to the stretching lineation of secondary strain, as well as the presence in some fractures of lineated tourmaline of the pegmatite stage, suggest that all these fractures were initiated as tension fractures perpendicular to the fan of stretching lineation of secondary strain. Reactivation at a later time combined with reflection of stress into the fractures, created complex movements along them and brought about the chloritic alteration.

Tertiary (?) dikes

Porphyry dikes are free of cataclasis, suggesting that cataclastic deformation had ceased prior to their injection. Post-dike strain is largely brittle in character, producing, therefore, some post-dike fault movement along and across the dikes, in which breccia and gouge formed.

The porphyry dikes are relatively few in number and occur only in the western and central sectors. They were apparently injected in extensional fractures of NE and NW trend, a different stress regime from that of earlier events.

Secondary joints and faults

One E-W, normal fault occurs in the Castle Crag area. Such faults and their related extension joints may control the very straight, E-W valleys east of the Bitterroot crest.

The latest structures in the region are a number of secondary joints apparently younger than the porphyry dikes. They no doubt comprise both shear and extension joints, although weathering has generally removed evidence to that point. Overall, their orientation is mostly random, although some subareas show preferred NW and NE trends. In the eastern sector, the secondary joints reflect the 015° az trend, a strong shear-joint set. The random joints important in many of the subareas may reflect random breaking in expansion upon erosional unloading of the area.

REFERENCES CITED

Anderson, A. L., 1952, Multiple emplacement of the Idaho batholith: Journal of Geology, v. 60, p. 255-259.

Armstrong, R. L., 1974, Magmatism, orogenic timing, and orogenic diachronism in the Cordillera from Mexico to Canada: Nature, v. 247, p. 348-351.

_____1975a, Precambrian (1500 m.y. old) rocks of central Idaho-the Salmon River arch and its role in Cordilleran sedimentation and tectonics: American Journal of Science, v. 275-A, p. 437-467.

_____1975b, The geochronometry of Idaho: Isochron West, no. 14, p. 1-288.

Balk, Robert, 1937, Structural behavior of igneous rocks: Geological Society of America Memoir 5, 177 p.

Bell, T. H., and Etheridge, M. A., 1973, Microstructure of mylonites and their descriptive terminology: Lithos, v. 6, p. 337-348.

Berg, R. B., 1969, Petrology of anorthosite of the Bitterroot Range, Montana, in Origin of anorthosite and related rocks: New York State Museum and Science Service Memoir 18, p. 387-398.

Berthé, D., Choukrone, P., and Jegouzo, P., 1979, Orthogneiss, mylonite, and non-coaxial deformation of granites: The example of the South Armorican Shear Zone: Journal of Structural Geology, v. 1, p. 31-42.

Bickford, M. E., Chase, R. B., Nelson, B. K., Shuster, R. D., and Arruda, E. C., 1981, U-Pb studies of zircon cores and overgrowths, and monazite: Implications for age and petrogenesis of the northeastern Idaho batholith: Journal of Geology, v. 89, p. 433-457.

Bittner-Gaber, E., 1983, Geology of selected migmatite zones within the Bitterroot lobe of the Idaho batholith, Idaho and Montana: Unpublished Ph.D. thesis, University of Idaho, Moscow, Idaho, 173 p.

Bradley, M. D., 1981, Geology of northeastern Selway-Bitterroot Wilderness Area, Idaho and Montana: Unpublished M.S. thesis, University of Idaho, Moscow, Idaho, 51 p.

Chase R. B., 1968, Petrology of the northeast contact zone of the Idaho batholith, northern Bitterroot Range, Montana: Unpublished Ph.D. thesis, University of Montana, Missoula, Montana, 158 p.

Chase, R. B., Bickford, M. E., and Tripp, W. E., 1978, Rb-Sr and U-Pb isotope studies of the northeastern Idaho batholith and border zone: Geological Society of America Bulletin, v. 89, p. 1325-1334.

Chase, R. B., and Hyndman, D. W., 1977, Mylonite detachment zone, eastern flank of the Idaho batholith: Field Guide no. 1, Rocky Mountain Section, Geological Society of America, Department of Geology, University of Montana, Missoula, Montana, 31 p.

Cheney, J. T., 1975, Kyanite, sillimanite, phlogopite, cordierite layers in the Bass Creek anorthosite, Bitterroot Range, Montana: Northwest Geology, v. 4, p. 77-82.

Davis, G. H., and Coney, P. J., 1979, Geological development of the Cordilleran metamorphic core complexes: Geology, v. 7, p. 120-124.

Garmezy, Lawrence, and Sutter, J. F., 1983, Mylonitization coincident with uplift in an extensional setting, Bitterroot Range, Montana-Idaho: Geological Society of America Abstract with Programs, v. 15, no. 6, p. 578.

Greenwood, W. R., and Morrison, D. A., 1973, Reconnaissance geology of the Selway-Bitterroot Wilderness Area: Idaho Bureau of Mines and Geology Pamphlet 154, 30 p.

Glossary of Geology, 1972, American Geological Institute, Washington, D.C., 805 p.

Goodge, J. W., 1983, Fold reorientation and quartz microfabric in the Okanogan dome mylonite zone, Washington: Kinematic and tectonic implications: Unpublished M.S. thesis, University of Montana, Missoula, Montana, 65 p.

Hansen, E., 1971, Strain facies: Springer-Verlag, 207 p.

Hyndman, D. W., 1980, Bitterroot dome-Sapphire tectonic block, an example of a plutonic-core gneiss-dome complex with its detached suprastructure, in Crittenden, M. D., Jr., Coney, P. J., and Davis, G. H., eds., Cordilleran metamorphic core complexes, Geological Society of American Memoir 153, p. 427-443.

Johnson, B. R., 1975, Migmatites along the northern border of the Idaho batholith: Unpublished Ph.D. thesis, University of Montana, Missoula, Montana, 120 p.

Kell, R. E., and Chase, R. B., 1976, Multiphase deformation and polymetamorphism along the north-central border zone of the Idaho batholith, Kelly Fork district, Clearwater County, Idaho: Geological Society of America Abstracts with Programs, v. 8, no. 4, p. 485-486.

Langton, C. M., 1935, Geology of the northeast part of the Idaho batholith and adjacent region in Montana: Journal of Geology, v. 43, p. 27-60.

Larsen, E. S., and Schmidt, R. G., 1958, A reconnaissance of the Idaho batholith and comparison with the southern California batholith: U.S. Geological Survey Bulletin 1070-A, p. 1-33.

Leischner, L. M., 1959, Border zone petrology of the Idaho batholith in the vicinity of Lolo Hot Springs, Montana: Geological Society of America Bulletin, v. 70, p. 1782.

Lindgren, Waldemar, 1904, A geological reconnaissance across the Bitterroot Range and Clearwater Mountains in Montana and Idaho: U.S. Geological Survey Professional Paper 27, 123 P.

Mattauer, Maurice, Collot, Bernard, and Van den Driessche, Jean, 1983, alpine model for the internal metamorphic zones of the North American Cordillera: Geology, v. 11, no. 1, p. 11-15.

Morrison, D. A., 1968, Reconnaissance geology of the Lochsa area, Idaho County, Idaho: Unpublished Ph.D. thesis, University of Idaho, Moscow, Idaho, 126 p.

Nold, J. L., 1974, Geology of the northeastern border zone of the Idaho batholith, Montana and Idaho: Northwest Geology, v. 3, p. 47-52.

Reid, R. R., 1959, Reconnaissance geology of the Elk City region, Idaho: Idaho Bureau of Mines and Geology, Pamphlet 120, 74 p.

Reid, R. R., Bittner, E., Greenwood, W. R., Ludington, S. D., Lund, Karen, Motzer, W. E., and Toth, M. I., 1979, Geologic section and road log across the Idaho batholith: Idaho Bureau of Mines and Geology Inf. Circle 34, 20 p.

Reid, R. R., Greenwood, W. R., and Nord, G. L., Jr., 1981, Metamorphic petrology and structure of the St. Joe area, Idaho: Geological Society of America Bulletin, v. 92, pt. II, p. 94-205.

Reid, R. R., Morrison, D. A., and Greenwood, W. R., 1973, The Clearwater orogenic zone: a relict of Proterozoic orogeny in central and northern Idaho, in Belt Symposium, University of Idaho, Moscow, Idaho, p. 10-56.
Ross, C. P., 1928, Mesozoic and Tertiary granitic rocks in Idaho: Journal of Geology, v. 36, p. 673-693.
_____1952, The eastern front of the Bitterroot Range, Montana: U.S. Geological Survey Bulletin 974-E., p. 135-175.
_____1965, The Idaho batholith: Geological Society of America Special Paper no. 82, p. 343.
Ryder, R. T., and Scholten, R., 1973, Syntectonic conglomerates in southwestern Montana: Their nature, origin, and tectonic significance: Geological Society of America Bulletin, v. 84, p. 773-796.
Stauffer, M. R., 1964, The geometry of conical folds: New Zealand Journal of Geology and Geophysics, v. 7, p. 340-347.
Streckeisen, E., 1973, Plutonic rocks: Classification and nomenclature recommended by the IUGS Subcommission on the Systematics of Igneous Rocks: Geotimes (Oct.), p. 26-30.
Toth, M. I., 1981, Petrology and structure of the east-central Bitterroot lobe of the Idaho batholith: Geological Society of America Abstracts with Programs, v. 13, no. 4, p. 228.
_____1983, Reconnaissance geologic map of the Selway-Bitterroot Wilderness, Idaho County, Idaho and Missoula and Ravalli Counties, Montana: U.S. Geological Survey Miscellaneous Field Studies Map MF-1495-B, scale 1:62,500.
Toth, M. I., Coxe, B. W., Zilka, N. T., and Hamilton, M. M., 1983, Mineral resource potential map of the Selway-Bitterroot Wilderness, Idaho County, Idaho and Missoula and Ravalli Counties, Montana: U.S. Geological Survey Miscellaneous Field Studies Map MF-1495-A, scale 1:62,500.
Williams, L. D., 1977, Petrology of a section across the Bitterroot lobe of the Idaho batholith: Unpublished Ph.D. thesis, University of Montana, Missoula, Montana.
Wiswall, C. G., 1979, The base of the Idaho batholith: Geological Society of America Abstracts with Programs, v. 11, p. 305.
Yates, R. G., 1958, The trans-Idaho discontinuity: International Geologic Congress, 23rd, Prague, Proceedings, v. 1, p. 117-123.